ANALYSIS OF THE BEHAVIOR OF GEOTEXTILE REINFORCED SLOPES WITH DIFFERENT KINDS OF FOUNDATIONS, BACKFILLS AND INCLINATIONS WITH FINITE ELEMENTS METHOD

by

Serhat Dosay

B.S., Civil Engineering, İstanbul University, 1998

Submitted to the Institute for Graduate Studies in
Science and Engineering in partial fulfillment of
the requirements for the degree of
Master of Science

Graduate Program in Civil Engineering

Boğaziçi University

2006

ACKNOWLEDGEMENTS

I would like to express my sincere gratitude to Professor Erol Güler for his invaluable guidance and help during the preparation for his dissertation. I would like to mention his patience and determination even in heavy snow when İstanbul was stuck last winter, while we were discussing about the topics.

As I started to prepare this thesis in 2001, I'm very happy for coming to an end. I would also like to thank Professor Emre Otay for his assistance to all M.S. students who were trying to finish their theses like me.

I also want to thank to my wife, my friends for their regardless help and patience during the preparation of this thesis.

ABSTRACT

ANALYSIS OF THE BEHAVIOUR OF GEOTEXTILE REINFORCED SLOPES WITH DIFFERENT KINDS OF FOUNDATIONS, BACKFILLS AND INCLINATIONS WITH FINITE ELEMENTS METHOD

Geotextiles have developed into common materials on many retaining wall and embankment projects throughout the world. This widespread acceptance of geotextiles is a result of thousands of successful installations, many comprehensive research studies, and proven economical benefits derived from their use.

In this project, eighteen different analyses of geotextile reinforced slopes with the combination of three kinds of foundation, two kinds of backfill material and three kinds of inclination, were conducted by means of finite elements program PLAXIS. In the analyses, a model similar to the study of San, Leshchinsky and Matsui (1994) is used. In this program, six node triangular elements and two dimensional plain strain model is considered. The backfill material is modeled by Hardening soil model and the foundation is modeled by Mohr-Coulomb model. The stage construction method of Plaxis is used in the model and 50 cm layers were considered during stage construction. Also Phi-c reduction procedure was carried out for the safety analysis. The effects of using different parameters in the structure were determined.

ÖZET

SONLU ELEMANLAR METODU İLE FARKLI TEMEL, DOLGU VE EĞİMLERDE GEOTEKSTİL DONATILI ŞEVLERİN DAVRANIŞININ ANALİZİ

Geotekstiller tüm dünyadaki istinat duvarı ve bent projelerinde ortak bir malzeme olarak gelişme göstermişlerdir. Geotekstillerin bu yaygın kullanımı, binlerce başarılı uygulama, birçok araştırma ve kanıtlanmış ekonomik faydalarının ortaya çıkması ile gerçekleşmiştir. Bu projede üç tip temel, iki tip dolgu ve üç farklı eğimin kombinasyonu olmak üzere onsekiz değişik geotekstil donatılı şev modelinin sonlu elemanlar programı PLAXIS ile analizi gerçekleştirilmiştir. Analizlerde San, Leshchinsky ve Matsui (1994)'nin yaptığı çalışmada kullandıkları modellerden yola çıkılmıştır. Modelleme sırasında altı düğüm noktalı üçgen elemanlar ve iki boyutlu düzlem şekil değiştirme durumunun geçerli olduğu düşünülmüştür.

Dolgu malzemesi Hardening- Soil, temel malzemesi ise Mohr-Coulomb modeline göre dizayn edilmiştir. Plaxis programında inşaat aşamasının daha iyi modellemek amacıyla geotekstillerin 50 cm. Aralıklarla yerleştirildiği kademeli inşaat yöntemi kullanılmıştır. Ayrıca güvenlik için Phi-c azaltma analizleri yapılmıştır. Tüm bu değişik parametrelerin yapının davranışını nasıl etkiledikleri incelenmiştir.

TABLE OF CONTENTS

LIST OF FIGURES

LIST OF TABLES

LIST OF SYMBOLS

A_o	Effective ground acceleration coefficient
c	Cohesion
c_{up}	Undrained peak cohesion
C_i	Soil – geosynthetic interaction coefficient
C_{ds}	Direct sliding coefficient
C_h	Horizontal equivalent earthquake coefficient
e	Pore ratio
E	Modulus of elasticity
E_{50}	Secant modulus
F_s	Factor of safety
FS_s	Factor of safety against sliding
FS_{ot}	Factor of safety against overturning
H_o	Backfill height
I	Structural coefficient
k	Permeability
k_v	Vertical seismic acceleration coefficient
k_h	Horizontal seismic acceleration coefficient
K_o	Coefficient of earth pressure at rest
K_a	Active earth pressure
K_{ad}	Dynamic active stress coefficient
K_{as}	Active earth pressure at rest
L_{ds}	Required reinforcement length by direct shear analyses
L_c	Reinforcement length
L_o	Overlap length
L_e	Required embedment length
M_d	Driving moment
M_r	Resisting moment
n	Porosity
[N]	Matrix of contour functions

P	Concentrated load
P_a	Active earth load
P_s	Surcharge load
q	Surcharge load on ground surface
r_s	Strain softening function
S_h	Horizontal spacing of reinforcement
S_v	Vertical spacing of reinforcement
t_j	Tensile strength of geotextile
$t_{j,all}$	Required total geotextile tensile strength for internal stability
T_a	Allowable stress in the geotextile
T_i	Allowable geotextile tensile strength
T_{maks}	Maximum tensile force in the geotextile
T_{ult}	Ultimate tensile strength of geotextile
u_x	Lateral displacement
$\{u\}$	Displacement vector

ß	Slope inclination angle
ψ	Expansion angle
Ø	Angle of shearing resistance of soil
$Ø_p$	Peak friction angle
δ	Angle of shearing friction between soil and geotextile
γ	Unit weight of soil
υ	Poisson ratio
ν_{ur}	Unload – reload Poisson ratio
σ_a	Active earth pressure
σ_{av}	Average lateral earth pressure
σ_{hl}	Pressure due to live load
σ_{hq}	Pressure due to surcharge load
σ_v	Vertical earth pressure

1. INTRODUCTION

Lost in the pages of history, the initial attempts to reinforce soils with dissimilar materials possess properties that would enhance the behavior of the soil itself. It seems reasonable to assume that it was attempted to stabilize swamps and marshy soils using tree trunks, small bushes, and the like. These soft soils would accept the fibrous material until a mass was formed that had adequate properties for the intended purpose. It also seems reasonable to accept that continued use of such a facility was possible due to the properly stabilized nature of the now-reinforced soil (probably by a trial-and-error procedure), or impossible due to a number of factors, among which were:

- Insufficient reinforcement materials for the loads to be carried
- Pumping of the soft soil up through the reinforcement material
- Degradation of the fibrous material with time, leading back to the original unsuitable conditions

Such stabilization attempts were undoubtedly continued with the development of a more systematic approaching which timbers of nearly uniform size and length were lashed together to make a mattresses surface. Such split-log “corduroy” roads over peat bogs date back to 3000 B.C.

Historical Perspective

The ancient Mesopotamians used soil reinforcement for construction of religious ziggurats in the Fertile Crescent. This technology lay dormant for thousands of years until Henri Vidal, while on vacation along the coast of France, discovered that he could build small sand walls by layering pine needles in the sand. This observation quickly led to a series of patents, including patent 3,421,326, issued on Jan.14, 1969, which protected Vidal’s work in the United States. Throughout its 17-year life, this patent was vigorously defended, which limited the understanding and development of earth-reinforced walls by U.S. engineers.

The first reinforced-earth wall was constructed in France in 1966. In 1972, the first U.S. wall of this kind was constructed over a major landslide on U.S.Hwy.39, in the foothills above Los Angeles. These walls were built with metal strips for their reinforcement and with “select” gravel backfill.

In the mid-1970s, Bob Holtz, under B.Broms at the Swedish Royal Institute of Technology, studied how to use geotextiles to replace steel-reinforcing strips, while the Dick Bell-J.E. Steward team studied the same in the Pacific Northwest. As with the commercial walls of this period, research focused on the use of granular backfill.

The proceedings of the 1978 American Society for Civil Engineers (ASCE) Symposium on Earth Reinforcement provides a good summary of the early years of soil reinforcement (B.Broms 1978). Unfortunately, many wall designers of the 1990s don’t reference work that predates theirs, so this technology’s true age may not be appreciated by the novice.

With the expiration of Vidal’s patent in 1986, the full commercial potential of soil reinforcement was possible. This ushered in the current are of geogrids and segmental block walls.

2. GEOTEXTILE REINFORCED SOILS

Geosynthetics are not only used in reinforcement of soils but also used for different purposes in Civil Engineering applications. After a brief definition of these materials and application areas, soil reinforcement property of geotextiles will be explained in details.

2.1. Geosynthetics

It's called that the general area "geosynthetics" recognizing that the materials are used in soil and are synthetic (usually made from hydrocarbons). The specific families of geosynthetics on which will be focused are the following:

- Geotextiles
- Geogrids
- Geomembranes
- Geocomposites

As the main point of this thesis is geotextile reinforced slopes and retaining walls, you will find more information about geotextiles. Moreover, it's going to be explained that the geotextiles and geogrids in the point of different application techniques in slope and retaining wall design.

2.1.1. Geotextiles

2.1.1.1 Description and Properties of Geotextiles

Geotextiles are one of the newest products in geotechnical engineering that has an only 35 years past. But in these 35 years, an incredible development brought this product one of the favorite construction materials in geotechnical engineering.

Their rise in growth during the past 10 years has been nothing short of awesome. They are indeed textiles in a traditional sense, but consist of synthetic fibers rather than natural ones like cotton, wool and silk. Thus biodegradation is not a problem.

Most of the polymers are the product of hydrocarbons. Polypropylene is the most used polymer which is the cheapest raw material. Polyester is the secondary raw material that is used. As it is less resistant to alkali metals which have high pH values, there are many positive sides for efficient use.

The fibers are made into a flexible, porous fabric by standard weaving machinery or are matted together in a random or nonwoven, manner. Some are also knit. The major point is that they are porous to water flow across their manufactured plane and also within their plane, but to a widely varying degree. There are at least 80 specific application areas for geotextiles that have been developed; however, the fabric always performs at least one of five discrete functions:

1. Separation
2. Reinforcement
3. Filtration
4. Drainage
5. Moisture barrier (when impregnated)

Geotextile separation is the introduction of a flexible synthetic barrier placed between dissimilar materials such that the integrity and functioning of both materials can remain intact or be improved. When placing stone on oil there are two simultaneous mechanisms that tend to occur; one is that the soil fines attempt to enter into the voids of the stone, thereby ruining its drainage capability; the other is that the stone attempts to intrude into the soil, thereby ruining the stone's strength. When this occurs we have a situation that has been called "sacrificial stone," which is all too often the case without the use of a proper geotextile.

Geotextile reinforcement is the synergistic effect on system strength created by the introduction of a geotextile into a soil or other disjointed and separated material. Geotextiles being a type of tensile strength material can nicely complement those materials weak in tension. Thus low strength soils are prime target for geotextile reinforcement.

Filtration is the equilibrium fabric-to-soil system which allows for free water flow (but not soil loss), across the plane of the fabric over an indefinitely long time period. The geotextile function of filtration involves the movement of water through the fabric itself. At the same time, the fabric serves the purpose of retaining the soil on its upstream side. Both adequate permeability and soil retention are required simultaneously. A third factor is also involved, that being the long-term-soil-to-fabric compatibility that will deteriorate during the lifetime of the system.

Drainage is the equilibrium fabric-to-soil system which allows for free water flow (but not soil loss) in the plane of the fabric over an indefinitely long time period. All fabrics can provide such a function but to widely varying degrees. For example, a thin woven fabric, by virtue of the fibers crossing over and under another, transmits water within the spaces created at these crossover points but to a very modest degree. Conversely, the thick, needled nonwoven fabrics have considerable void space in their structure available for water transmission. It will be noted that there is a considerable overlap with the preceding section on filtration and except for the consideration of direct of flow, the soil retention and long-term compatibility concepts remain the same.

A moisture barrier can be created by rendering the fabric relatively impermeable to both cross-plane and in-plane flow. One is in essence creating a geomembrane, albeit one with a fabric structure rather than a sheet of plastic or rubber. The impermeability referred to here is generally obtained by spraying bituminous, rubber-bitumen, or polymeric mixes into a properly deployed geotextile-thus the creation of an in-situ moisture barrier. While the permeability referred to is obviously not zero (on an absolute basis, nothing has zero permeability), it is very low compared to that of the original geotextile. Quite possibly its permeability is now in the range 10^{-6} to 10^{-8} cm/sec. This is comparable to the permeability coefficient of many fine-grained soils in the clay family.

Within this function of moisture barrier, we obviously refer to the impedance of the flow of water but also to the movement of vapor across the barrier. Numerous situations where the soil on one side of the barrier must be kept free of moisture and water vapor fall into this category.

The procedure was outlined as identifying the geotextiles' primary function and designing accordingly. Where geotextiles are used for a single function, this can indeed be done. However, geotextiles often serve multiple or combined functions. Some examples are;

1. Prevention of crack reflection in asphalt pavement overlays, where both reinforcement and moisture barrier functions are involved.
2. Beneath railroad ballast, where separation, reinforcement, filtration, and drainage can all be involved.
3. In use of fabrics for flexible forming systems to contain grout, where separation, reinforcement and filtration are involved.

In these situations the primary, secondary, tertiary, and so on, functions must all be satisfied. They must all satisfy the required factor of safety. If the situation is properly assessed, the calculated factors of safety will be seen to increase progressively as one proceeds through the primary, secondary, tertiary, and so on, functions. If not, it only means that the critical functions were not properly estimated to begin with. Thus the minimum factor of safety will always indicate the primary function; the next highest value of factor of safety will indicate the secondary function, and so on. This approach, of course, assumes that a reasonably accurate quantitive analysis can be developed for each of the functions described.

2.1.1.2 Test Methods

As we study for design methods, the main point is to get the required property value (e.g., a required fabric strength or modulus, etc.). This numerical value must then be compared to the actual value that the candidate geotextile possesses. Thus it is necessary to have the properties of all commercially available fabrics at hand. In other words, what is needed is the "data base" from which one can select a fabric together with its relevant properties for comparison to the values required. Factor of safety (FS) then results, which is;

$$FS = \frac{\text{Candidate fabric property}}{\text{Required property}}$$

for the function under investigation and its application. When a favorable comparison is made to the required factor of safety , an acceptable design is concluded.

The “data base” referred to is the focus of this particular section. It by no means is complete for existing fabrics, let alone for new and yet-to-be-developed fabrics. Further more, many of the test methods are not even standardized as far as their test procedures are concerned. Since this is a known industry-wide problem, standards groups all over the world are actively involved in proposing, evaluating, round-robin testing, modifying and finalizing geotextile standards. Although such a process is very time consuming to bring to a conclusion, there are some tests that can be borrowed (in whole or in part) from other areas. For geotextile standards there is an obvious overlap with textiles (clothing textiles, industrial textiles, etc.) where many standards already exist. The overall textile industry is, of course, a large and mature one (currently sales are 40billion dollar per year) and one that has a direct interest and involvement in geotextiles. In fact, the manufacturing methods are one and the same; only the applications are different. Thus it should come as no surprise that many physical and mechanical test methods are partially, or completely, taken form existing textile standards. The different tests between textiles and geotextiles are those which involve hydraulic, endurance, and environmental properties. These are generally new tests oriented completely toward geotextiles. In the United States, the American Society for Testing and Materials has a specific standards committee for geotextiles (D35); however, the activity is indeed worldwide, as the following list indicates. One goal of the Standards and Specifications Committee of the International Geotextile Society (IGS) is to collect, compare and provide information on specific standards for geotextiles.

1. International Organization for Standardization (ISO) (International)
2. Permanent International Association of Road Congresses (PIARC) (International)
3. European Disposables and Nonwovens Association (EDANA) (International)
4. Permanent International Association of Navigation Congresses (International)
5. Ministery of Public Works (Belgium)
6. Canadian General Specification Board (Canada)
7. British Standards Institution of Civil Engineers (England)
8. The Institution of Civil Engineers (England)
9. Transport and Road Research Laboratory (TRRL) (England)
10. Technical Research Centre of Finland (Finland)
11. Comité Français des Géotextiles et Géomembranes (France)
12. L’Association Français de Normalisation (AFNOR) (France)

13.Réunion Internationale des Laboratories dé Essais et de Recherche sur les Matériaux et les Constructions (RILEM) (France)

14.German Standards Committee for Geotextiles (Germany)

15.Franzius Institut (für Wasserbau und Küstingenieurswesen der Universitat Hannover) (Germany)

16.Bundesanstalt für Wasserbau (Germany)

17.Deutsche Gesellschaft für Erd-und Grundbau (Germany)

18.Nederlands Normalisatie Instiut (NNI) (Holland)

19.CNR—Consiglio Nazionale Richerche (Italy)

20.ENEL/CRIS (Italy)

21.Unitex (Italy)

22.Korea Highway Corporation (Korea)

23.Norwegian Road Research Laboratory (NRRL) (Norway)

24.Joao de Matos Rosa (Portugal)

25.The Swedish National Road Administration (Sweden)

26.Swedish Geotechnical Institute (Sweden)

27.Schweizerisches Verband der Geotextilfachleute (Switzerland)

28.SA Bureau of Standards (South Africa)

29.American Society for Testing and Materials (ASTM) (United States)

30.U.S. Army Corps of Engineers-Waterways Experiment Station (United States)

31.Department of Transportation and Public Facilities (United States)

At this point in time, however, a unified document on geotextile standards and/or test methods is not available. Thus it is necessary in this section to give insight into test methods in use or at least currently favored for the testing of geotextiles. Reference will be made, whenever possible, to the existing ASTM Standard or to the proposed test method being considered by committee D35 on Geotextiles. The section will be subdivided into the following categories:

- Physical properties
- Mechanical properties
- Hydraulic properties
- Endurance properties
- Environmental properties

2.1.1.2.1 Physical Properties

The properties discussed here all refer to the fabric in its manufactured or as-received condition.

2.1.1.2.1.1 Specific Gravity

The specific gravity of the fibers from which geotextiles are made is actually the specific gravity of the polymeric feed stock. As customary, specific gravity is defined as the ratio of the substance's unit volume weight to that of water at 4 centigrade degree. Some typical values of the specific gravity of commonly used materials (mostly polymers) made into geotextiles are the following:

- Polypropylene:0.91
- Polyester:1.22 to 1.38
- Nylon:1.05 to 1.14
- Polyethylene:0.92 to 0.95
- Polyvinyl alcohol:1.26 to 1.32
- Glass:2.54

Note that the specific gravity of some of the materials is less than 1.0, which has a negative connotation when working with geotextiles under water (i.e., some of them will float).

2.1.1.2.1.2 Mass per Unit Area (Weight)

Mass per unit area is the proper term meant when most people state or asks for the "weight" of the fabric in question. It is also sometimes called "basis weight" but this is equally incorrect since neither weight nor basis weight co notates anything about area. Fabric mass per unit area is given in units of ounces per square yard (oz/yd') or grams per square meter (g/m'). The current ASTM test for this property is designated D1910. Unfortunately still other values are listed in the literature, such as ounces per linear yard (or grams per linear meter) for a fabric of given width. Sometimes the latter value is given inversely as linear yards per pound (or meters per kilogram). The point to make is that one must clearly state what value is being communicated.

Test wise, the mass(weight)should be measured to the nearest 0.01 per cent of the total specimen mass, and length and width should be measured under zero fabric tension. The range of typical values for most geotextiles is from 4 to 20 oz/yd^2 (135 to 680 g/m^2). Note that 1.0 oz/yd^2 is equal to 33.9 g/m^2, which is a conversion factor that is often used. Since fabric cost (and in general mechanical properties) is directly related to mass per unit area (weight), it is a very important property.

2.1.1.2.1.3 Thickness

Thickness of geotextiles is sometimes mentioned in specifications but is really more of a descriptive property than an index-or design-oriented property. It is measured as the distance between the upper and lower surfaces of the fabric, measured at a specified pressure. The thickness of commonly used geotextiles range from 10 to 300 mils.

2.1.1.2.2 Mechanical Properties

The properties to be discussed here are indicative of the fabric's resistance to mechanical stresses mobilized from applied loads and /or installation conditions.

2.1.1.2.2.1 Compressibility

Compressibility of a fabric is its thickness at varying applied normal pressures. For most geotextiles the compressibility is relatively low and of little direct consequence as far as design is concerned (e.g., with woven fabrics and with nonwoven heat-set and heavily calendared fabrics). For nonwoven needled or bulky resin bonded fabrics, however, compressibility is very important. This is because such fabrics are often used to convey water within the plane of their structure (i.e.; a hydraulic property to be described later called transmissivity. Figure 2.1 illustrates the compressibility of several geotextile types, where the influence of load on thickness is clearly seen. The slope of the initial portion of the curve is the compressibility modulus (or its inverse value the compressibility coefficient), which is an informative mechanical property.

2.1.1.2.2.2 Tensile Strength

Perhaps the single most important geotextile property is its tensile strength. Invariably all fabric applications rely on this property either as the primary function (as in reinforcement applications) or as a secondary function (as in separation, filtration, or drainage). The concept of the test is to place the fabric within a set of clamps or jaws, place this assembly in a testing machine, and elongate it in tension until failure occurs. Unlike soils, fabric failures are generally easy to identify. During the extension process, it is a customary to measure both load and deformation in such a way that a stress versus strain curve can be generated. From the "stress" (usually given as load per unit width) versus strain curve (calculated as deformation divided by original specimen width), four values are obtained:

1. Maximum tensile stress (referred to as the fabric's strength)
2. Strain at failure (often given as maximum elongation)
3. Toughness (work done per unit volume before failure, usually taken as the area under the stress-strain curve)
4. Modulus or stiffness (which is the slope of the initial portion of the stress versus strain curve)

Typical responses of geotextiles made from different manufacturing processes are given in Figure 2.1. Note that the vertical axis is in units of force per unit width of fabric (i.e., lb/in.) and is not a bona fide stress unit. To get stress units this value would have to be divided by the fabric's thickness. This is not conventionally done since the thickness varies greatly under load and during the extension process. This, of course, has implications in the toughness and modulus values as well since them, too, would have to be divided by thickness to obtain conventional engineering units.

There are several features of the tensile test which require further discussion since they have implications for subsequent design procedures, the major ones being the modulus and the specimen size. Regarding the modulus, several choices are available for measuring the initial sloe of the curve. These are the following:

Initial tangent modulus: This is straightforward for many woven fabrics in both their warp and weft directions and for some bonded nonwovens. Here the initial slope is quite linear and (as in conventional soil testing) a reasonably accurate modulus value can be obtained.

Offset tangent modulus: This concept is sometimes used when the initial slope is very low and is typical of needled nonwovens (recall Figure 2.1). To obtain the value one avoids the initial portion of the curve and essentially shifts the y-axis to the right where it meets the downward extension of the linear portion of the response curve.

Secant modulus: To avoid the somewhat arbitrariness of the above-mentioned methods, one could legislate the procedure of obtaining a value (e.g. a secant modulus at 10 per cent strain). Here one draws a line from the origin to the curve at 10 per cent strain and measures its slope.

Regarding the specimen size (length, width, and aspect ratio, i.e., length-to-width ratio), much has been written and investigation continues. ASTM Standards D1682 and D751 allow for a number of variations and ongoing efforts promise still further changes. Figure 2.2 illustrates the currently most popular specimen sizes. The reason for the necessity of wide-width specimens is that fabrics (particularly nonwovens) tend to have a severe Poisson's ratio effect under tensile stresses (i.e., they rope-up, giving artificially high values).

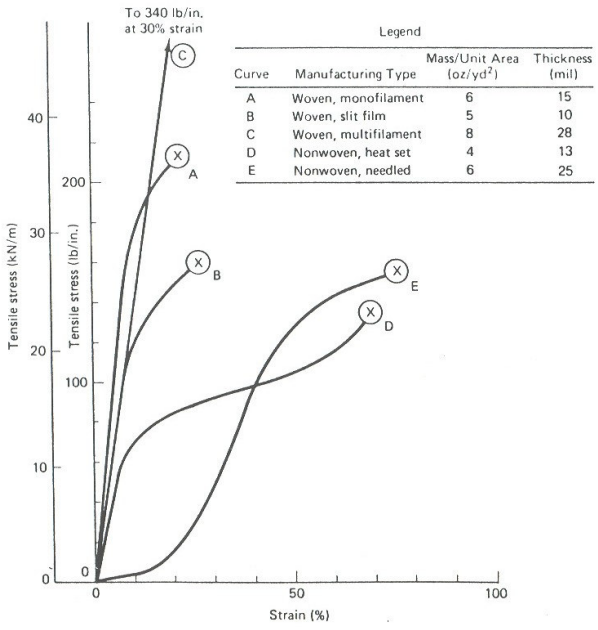

Figure 2.1 Tensile test response of various geotextiles manufactured by different processes (all polypropylene fabrics; specimens were 8 in. Wide by 4 in. High)

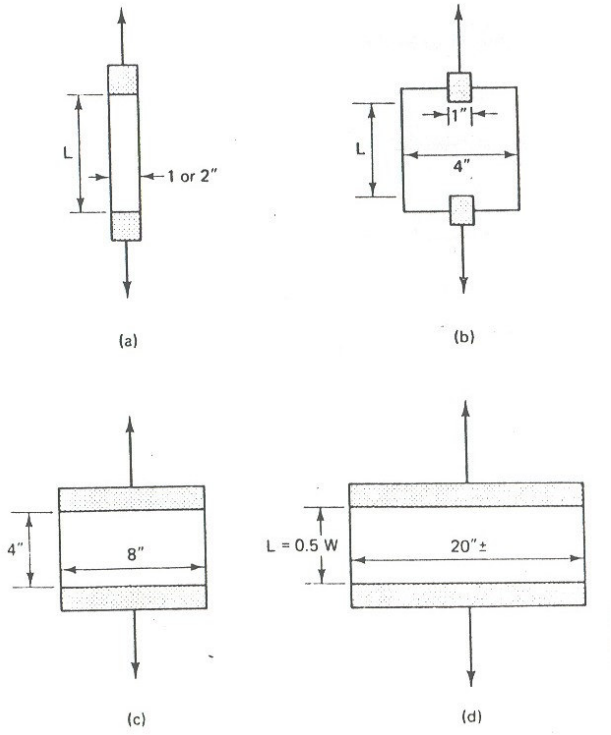

Figure 2.2 Various tensile test specimen sizes used to obtain fabric strength properties. (a) Narrow strip; (b) Grab; (c)ASTM wide width; (d) Very wide width.

Thus the tendency for performance (i.e., design related) tests is to use wide-width specimens. These are not intended for index tests, however and the grab specimen should be continued to be used in this regard (i.e., as a manufacturer and user quality control indicator). There are no universal relationships between the different test specimen sizes or shapes and therefore the choice of specimen size depends on the intended use of the data. Proper identification of the specimen size on test data is always necessary.

Regarding other features of tensile testing of fabrics (effect of fabric conditioning, load rate, load method, etc.), ASTM or other applicable standards should be consulted. Before finishing the topic, however it should be cautioned that all these tests are performed without soil adjacent to them (i.e., in isolation). With a soil covering, which obviously is how they are eventually used, results can be quite different. Mc Gown, et al.(5) has interesting test methods and results in this regard.

2.1.1.2.2.3 Fatigue Strength

Fatigue strength or fatigue resistance is defined as the ability of the fabric to with-stand repetitive loading before undergoing failure. The tensile test specimen, usually of a wide-width variety since this is primarily a performance test, is stressed longitudinally at a constant rate of extension to a predetermined length and then back to zero load. This cycling is repeated until failure occurs. The resulting cyclic stress versus strain response (i.e., the hysteresis loops) can be used to calculate a cyclic modulus which becomes evident after a number of load cycles are applied. Most important, however is the number of cycles required to bring the fabric to failure and the stress that was applied. This stress is usually expressed as a fraction of the quasi-statically applied failure stress (strength) described in the preceding section. As expected, the lower the stress level, the larger the number of cycles required before failure. The response is usually strongly exponential.

Although many variables remain to be defined (primarily, the decision as to what deformation to apply during testing), the test does simulate in-situ conditions better than most static tests.

2.1.1.2.2.4 Burst Strength

There are two test methods to load fabrics out of plane, thereby stressing them in tension until failure occurs. The most common is the Mullen burst test, which is covered in ASTM D774. In this test, an inflatable rubber membrane is used to distort the fabric into the shape of a hemisphere. Bursting of the fabric occurs when no further deformation is possible. The test is essentially an index which is widely used for quality control and cited in most specifications.

The alternative test uses a large rectangular test specimen and also deforms it by an underlying rubber membrane. Called a diaphragm test by Raumann (6), the central portion of the fabric (along the minor axis) is very close to plane strain conditions. As such, the pressure versus strain response yields a very accurate modulus. It is a difficult test to perform and is properly classified as a performance test.

2.1.1.2.2.5 Tear Test

Often during their installation, geotextiles are subjected to tearing stresses. While a test simulating such situations is important, it will be seen that the methods can also be used as index tests. There are three tear tests commonly used: trapezoidal, tongue and Elmendorf.

The trapezoidal tear test, ASTM D2263, now discontinued was originally devised for testing automotive fabrics. The trapezoidal tearing load is the force required to successfully break individual yarns (fibers) in a fabric. In this test, the fabric is inserted in a tensile testing machine on the bias so that the fibers are caused to tear progressively. An initial 5/8-in cut is made to start the process. The load actually stresses the individual fibers gripped in the clamps rather than stressing the fabric structure. The test was discontinued by ASTM in 1976 without replacement, although it is still commonly referenced.

The tongue tear test, ASTM D571, uses a 3-by 8-in. fabric specimen with a precut 3-in.-log initiation cut. The fabric is placed in a testing machine with the cut ends in the jaws of the machine. An increasing tensile force is applied to make the fabric tear along the initiation cut. The test configuration permits the yarns to “rope up” and works together to resist tear propagation. Thus tongue tear test results are usually much higher than results from trapezoidal tear tests.

The Elmendorf tear test is a covered in ASTM D1424 and covers a procedure for the determination of the average force required to propagate a single-rip tongue-type tear starting from a premade cut in a woven fabric. The cut is then continued by means of a falling-pendulum apparatus. The tearing force is the force required to continue the tear previously started in the specimen. The strength is calculated as the work done in tearing the specimen divided by twice the length of the tear. The test is often used in Europe to measure tear strength but has questionable validity for nonwoven fabrics.

2.1.1.2.2.6 Impact Tests

A number of tests have been developed to asses the impact resistance of fabrics since falling objects have been known to punch holes in geotextiles (e.g., sharp rock riprap, tools and other construction items). Often such tests have a weighted cone or dart falling freely from a known height above the fabric. The fabric is clamped firmly in an empty container

such as a CBR mold, which is commonly used in soil testing. The amount of cone penetration into the fabric is indicative of its resistance to impact stresses.

A different test and one that measures impact resistance directly in energy units (ft-lb or joules) has been developed for an Elmendorf tear apparatus. The impacting cone is attached to the pendulum arm of the Elmendorf tear tester and penetrates through the fabric specimen which is fixed on the end of the device. The test fixture holding the test specimen is called a Spencer impact attachment. Impact-resistances units are read directly from the system. Unfortunately, the limit of most commercially available systems is about 16 ft-lb, which is too low for many geotextiles. Thus it is necessary to use impact pendulum systems developed for other materials, for example, metals, which have energies of up to 240 ft-lb. Such devices are covered under ASTM A370 and ASTM D256. The specimen holder however, must be converted to hold fabrics rather than notched metal bars. The test is currently under review by ASTM.

2.1.1.2.2.7 Puncture Test

Rather than a dynamic test as just described for impact resistance, there is additional need for an assessment of geotextile resistance to objects such as rocks or sticks under quasi-static conditions. Such a test is described under ASTM D3787 with the puncturing ball changed to a blunt-ended metal rod. Current tests call for this rod to be 5/16in. in diameter. The fabric is firmly clamped in an empty cylinder of 1.75 in. inside diameter and the rod pushed through it via a compression testing machine. Resistance to puncture is measured in pounds force.

This test is a popular one used primarily as an index test, but has direct applicability to the field when properly modeled. It should be noted that there is a direct relationship between the puncture resistance value and the tensile strength of the fabric. This is because the fabric between the inner edge of the specimen holder and the outer edge of the puncturing rod is indeed in a pure state of axisymmetric tension. Although firm relationships have not been developed, they should be possible at least on a conceptual basis.

2.1.1.2.2.8 Soil-to-Fabric Friction Tests

In many design problems it is necessary to know the soil-to-fabric friction behavior. The most likely test setup is an adaptation of the direct shear test used in geotechnical engineering. The fabric is firmly fixed to one half of the test device with soil in the other half. After normal stress is applied, a shear force is mobilized until sliding occurs between the fabric and the soil with no further increase in required shear force. When the test is repeated at different normal stress, a trend is established from which the shear strength parameters can be obtained. Note that these soil-to-fabric shear strength parameters are related to-but not necessarily the same as the soil shear strength parameters. They (the soil parameters) are, however, the upper limits of the soil-to-fabric parameters.

2.1.1.2.2.9 Pullout (Anchorage) Tests

Geotextiles are often called on to provide anchorage for many applications within the reinforcement function. Such anchorage usually has the fabric sandwiched between soil on each side of it. The resistance can be modeled in the laboratory using a pullout machine.
The pullout resistance is obviously dependent on the normal force applied to the soil surrounding it, which mobilizes shear forces on both sides of the fabric.
Test results by Collios et al. (9) show a relationship of pullout test results to shear test results with some notable exceptions. If the soil particles are smaller than the fabric openings, efficiencies are higher; if not, they can be lower. In all cases, however, pullout test resistances are less than shear test resistances. This is due to the fact that the fabric is taut and exhibits large deformations. This in turn causes the soil particles to reorient themselves into a reduced-shear-strength situation at the soil-fabric interfaces, hence lower pullout resistance. The stress state mobilized in this test is a very complex one requiring additional research. (Figure 2.3)

2.1.1.3 Geotextile Applications

Geotextiles can be used in different areas in civil engineering. Geotextiles have not only primary functions but also secondary functions in use.

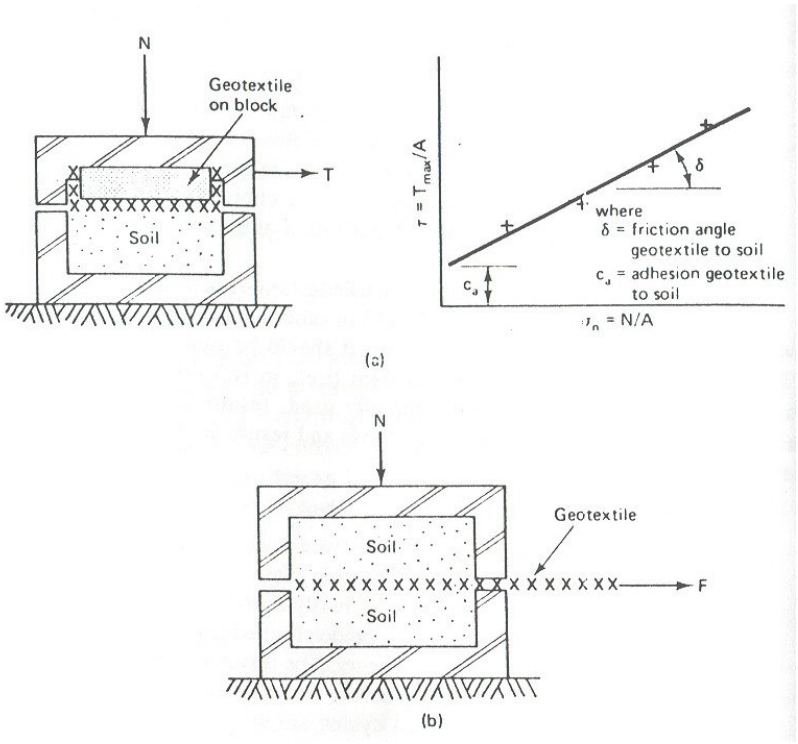

Figure 2.3 Schematic diagrams of test setups for friction and pullout evaluation of geotextiles in soils. (a) Soil to fabric friction test and results; (b) fabric pullout (anchorage) test.

Unpaved roads are the most popular applications of geotextiles. The geotextile is used on soft soil sub grades with stone aggregate placed directly above. No permanent surfacing is immediately placed on the stone. At most a smaller rock is placed for reasonable rid ability on the road's surface. At a later time, perhaps many years after settlement takes place and ruts are backfilled, permanent pavement is sometimes placed. However, there are many thousands of miles of unpaved secondary roads, haul roads, access roads, and like with no permanent surfacing on them.

In paved roads and airports, geotextiles are primarily used for separation of base and drainage layer. This is for preventing the fines to join soft soil of base.

However reinforcement is the primary function of geotextiles, stabilization is an other problem for civil engineers to be solved by the help of geotextiles as a secondary function. These problems are wall stabilization, embankment stabilization, foundation stabilization and in-situ stabilization which are the most important ones.

For filtration geotextiles are used; behind retaining walls, wrapping around under drains, beneath erosion control structures and as silt fences.

Regarding the flow capacity of geotextiles we can consider two general categories; gravity flow (chimney drains in dams, flow interceptors as in fin drains, pore water dissipaters behind retaining walls, beneath a geomembrane for water or air conveyance) and pressure flow (as vertical drains for rapid soil consolidation, in earth embankments and dams, beneath surcharge fills, within reinforced earth walls).

Geotextiles are often used in railroads beneath the stone ballast upon which the wooden or concrete tie system is placed. A critical aspect of the design is the depth at which the geotextile is placed beneath the bottom of tie. Geotextile use in railroads offers a number of benefits such as separation, reinforcement, filtration and drainage. Unfortunately, it cannot be categorically stated that one function dominates over the others in all cases. This application is indeed a multifunctional one which must be handled on a site-specific basis. Yet some functions (such as separation and filtration) are always present.

2.1.2. Geogrids

Geogrids represent a small, but rapidly growing, segment of the geosynthetics area. Rather than being a woven, nonwoven or knit textile (or even a textile like) fabric, geogrids are plastic formed into a very open netlike configuration. Often they are stretched in one or two directions for improved physical properties.

The basic polymer materials used in the manufacture of high-strength geogrids are either polypropylene or high-density polyethylene. Initially, they are of a heavy gauge and in sheet form. Holes are then punched into the sheeting on a regular pattern, and the sheet is then drawn uniaxially or biaxially. Drawing is done under controlled temperatures and strain rates so as to avoid fracture but to allow free flow of the molecules into an elongated and isotropic condition. The key variable process is the draw ratio, but other variables, such as molecular weight, molecular weight distribution, and degree of branching or cross-linking, are also important. Aside from market increases in modulus and strength, the creep sensitivity of the polymers is greatly reduced during the drawing process.

The main uses of geogrids are;

- Reinforcement of slopes,
- Reinforcement of soil retaining walls,

- Erosion control,
- Reinforcement of embankment fills and earth dams,
- Beneath aggregate in unpaved roads and railroad constructions,
- Drainage,
- As sheet anchors.

Geogrids are generally used for separation, reinforcement and drainage. They are not used in filtration or as a moisture barrier due to their large opening sizes. Also, when used as a drainage core, they are generally protected by a geotextile acting as a filter and thus become a geocomposite.

As in geotextiles, the properties of geogrids must be given by the manufacturer to make the best choice for the design. To obtain these properties we use the same test methods in geogrids like geotextiles.

Figure 2.4 Geogrid reinforced pavement construction

2.1.3. Geomembranes

Geomembranes are the second largest group of geosynthetics. Its main original uses were in the packaging and molding industries. The materials themselves are impervious thin sheets of rubber or plastic material used primarily for linings and covers of liquid or solid storage impoundments. Thus the primary function is always as a liquid or vapor barrier. The range of applications, however, is very great and at least 30 individual applications in civil engineering have been developed.

Most of the plastic geomembrane materials are polymer resins and thermoplastic materials which are ready to use after production in factories. Some of them are produced in the site by absorbing bitumen to the geotextile. But of course the properties of geogrids by these two production methods are not the same. The main uses of geomembranes are as follows;

- Liners for waste liquids,
- Liners for water conveyance canals,
- Liners for potable water,
- Liners for reserve water,
- Beneath asphalt overlays as a waterproofing layer,
- Flexible form where loss of material cannot be allowed,
- Liners for primary, secondary, and/or tertiary hazardous waste landfills,
- To control expansive soils,
- To prevent infiltration of water in sensitive areas,
- To form barrier tubes as dams,
- Waterproofing within tunnels.

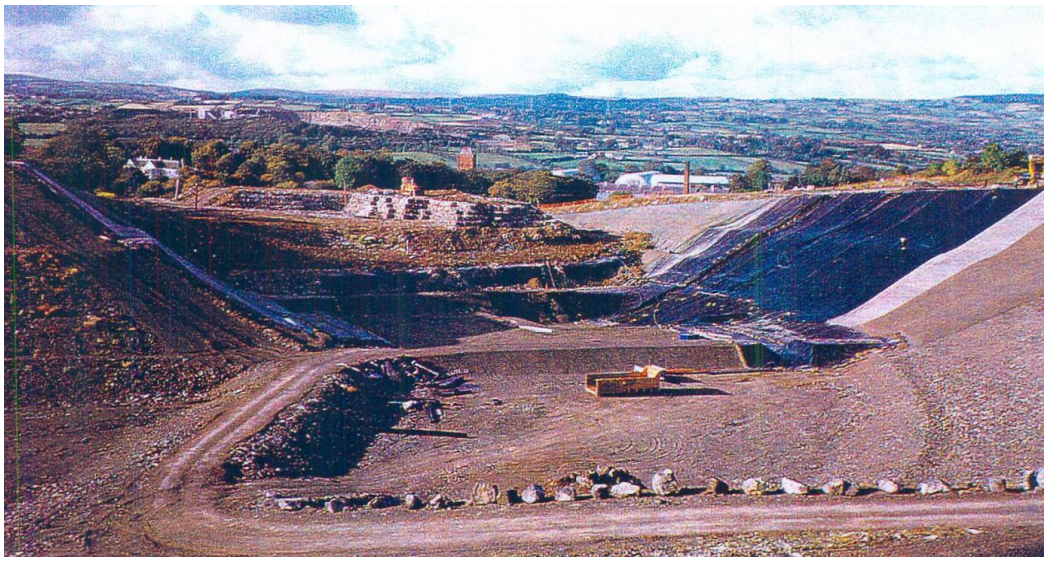

Figure 2.5 Geomembrane and Geotextile applications

2.1.4. Geocomposites

A geocomposite consists of a combination of geotextile and geogrid, or geogrid and geomembrane, or geotextile, geogrid and geomembrane, or any one of these three materials with another material.

The application areas are numerous and growing steadily. The major functions encompass the entire gambit of functions listed for the geosynthetics discussed previously;

- Separation,
- Reinforcement,
- Filtration,
- Drainage,
- Moisture barrier.

Geocomposites are difficult to produce and more expensive than other geosynthetic materials. As they are expensive its application areas are growing up.

2.2. Reinforced Earth

According to its original usage, the term “reinforced soil” refers to a soil which is strengthened by a material able to resist tensile stresses and which interacts with the soil through friction and/or adhesion. Subsequently, the meaning of soil reinforcement was broadened, and this term is now also used for other mechanical and structural methods of soil improvement, such as compressive reinforcement and reinforcement by confinement and encapsulation.

The primary purpose of reinforcing a soil mass is to improve its stability, increase its bearing capacity, and reduce settlements and lateral deformation. The broader definition of soil reinforcement also includes methods of erosion control and stress transfer via anchors and piles. The terminology is complicated by the fact that many of the materials used to improve engineering properties of soil, such as geotextiles, can fulfill multiple functions, e.g., provide structural strengthening, control groundwater flow or accelerate consolidation with their drainage capacity, prevent particle migration through filter action, and maintain separation of different soil layers during construction or under the influence of repeated external loading.

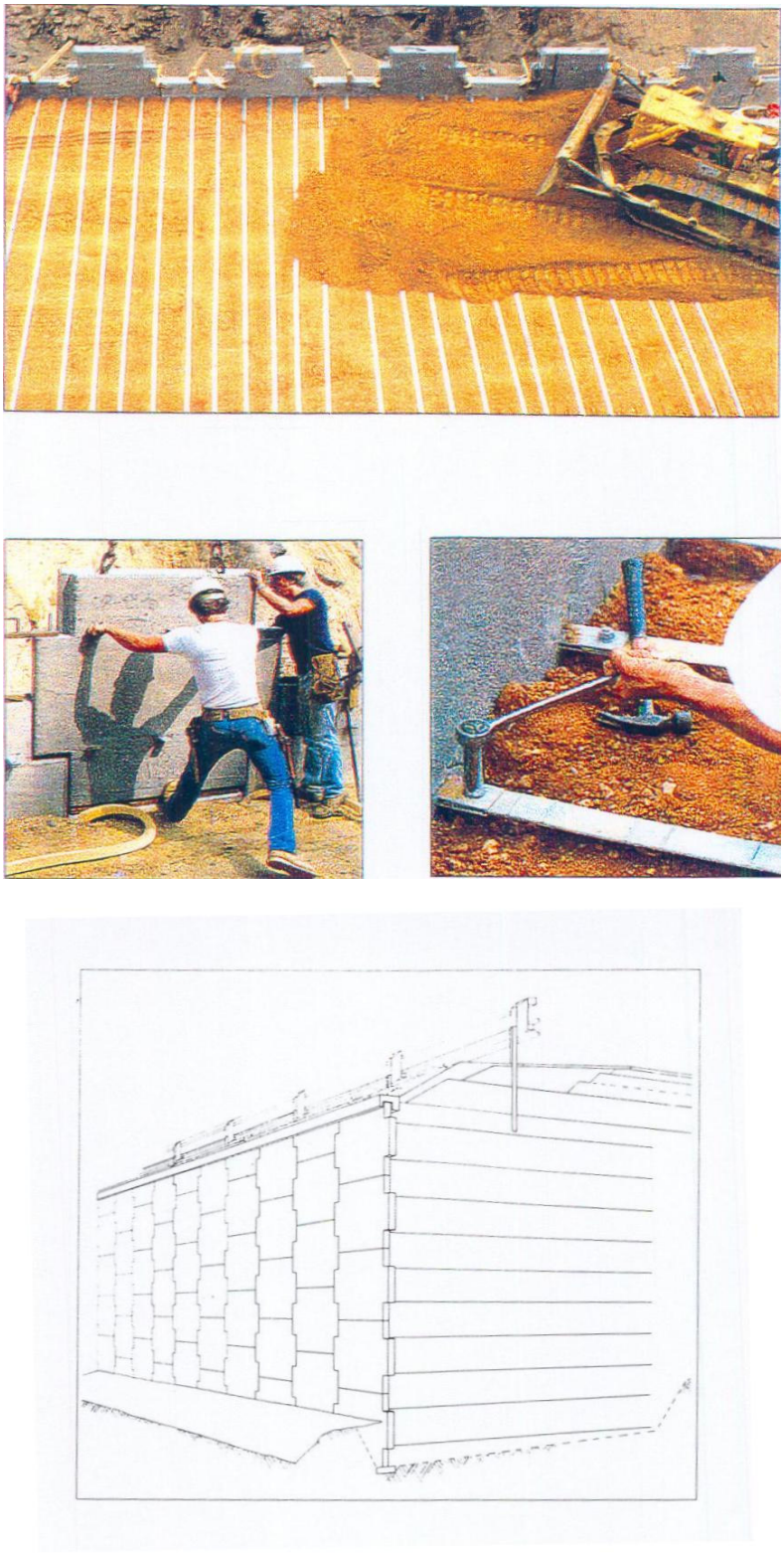

Figure 2.6 Reinforced earth applications

Soil reinforcement can be achieved even by relatively flexible, extendable, and sometimes compressible materials, such as nonwoven fabrics or large quantities of individual fibers. Also the actual strengthening of a soil mass may be a secondary effect, e.g., as achieved through accelerated consolidation. This is why the term “inclusions” rather than “reinforcement” is favored by some researchers working in this field.

Technical superiority of reinforced soil structures on difficult ground may have gained them attention and respect, but simple economics ensured their success.

Reinforced Earth has shown a most impressive versatility, and is used for retaining structures, bridge abutments, seawalls, dams and industrial bulk-storage facilities. In Reinforced Earth and newer related systems, prefabrication and elemental construction allow for adjustment to difficult topography and also permit the use of a relatively small unskilled and semiskilled labor force. A further advantage of reinforced soil structures is that they can adjust to large differential settlement; conventional alternatives may require sophisticated reinforced concrete structures supported on piles.

The biggest savings is achieved for high walls (> 5 m): A 20 to 60 per cent cost advantage has been reported for such structures. The higher number would relate to difficult foundation conditions where the competing designs may involve cantilever walls supported on piles.

For smaller walls , Reinforced earth or a similar technique may be more expensive than other retaining systems such as crib walls, gabions, or geotextile walls, the latter being the latest development. However, other factors may thebe dominate the choice among different soil-retaining systems, with or without involving soil reinforcement; aesthetics, resistance to erosion by seepage and surface sun off, durability, and susceptibility to vandalism.

The success of Reinforced earth in an urban environment has also been partly based on the reduced land requirements compared to what would possibly be cheaper in an unrestricted area, namely a simple embankment.

The total cost of a reinforced soil structure may be divided into three components:

- Cost of soil fill, including transport and placement,
- Cost of the reinforcement, including transport and installation,
- Cost of facing, including transport and erection.

According to Jones (1985), the cost of providing and installing reinforcement for walls increases with wall height and dominates total costs for high walls. The cost of

prefabricated face panels decreases with wall height, while the cost of soil fill is likely to increase, each representing 10 to 30 per cent of total costs.

Detailed breakdowns of costs will vary from site to site and country to country, but material costs are likely to be a multiple of the costs of labor or the cost of plant and operatives.

Increasing competition from newly developed soil-reinforcing systems, including those employing geosynthetics, promise even better economics; engineers must however now ensure that the current good safety record is not impaired.

2.2.1. Geotextile Reinforcement Applications

As is the case for other methods of ground modification for the purpose of reinforcing a soil mass, the objective of fabric inclusions generally is to increase the soil's stability (bearing capacity, slope stability, resistance to erosion) and reduce its deformation (settlement, lateral deformation). In order to provide stability the geosynthetic has to have adequate strength; to control deformation, it has to have suitable force-elongation characteristics measured in terms of a modulus (the slope of the force –elongation curve), or elongation under a particular load. In the following paragraphs geotextile applications with the primary purpose of reinforcement are enumerated and brief guidelines are given for selected design problems.

In many applications, geotextiles, like geogrids and geocomposites, serve more than one purpose, possibly including reinforcement, but in all cases a certain minimum strength is required. Even if just in order for the fabric to survive the effects of placement on an irregular ground surface and the loads imposed by equipment and personnel during installation. The terms survivability and workability have found acceptance for describing basic strength and stiffness characteristics required from geotextiles in a construction environment. In the United States these minimum requirements are usually expressed directly in terms of the grab tensile strength (ASTM D-1682) and related index test properties. In Australia, the "robustness" classification has been introduced by the Main Roads Department in Queensland; it rates a geotextile in terms of puncture strength and CBR plunger test results.

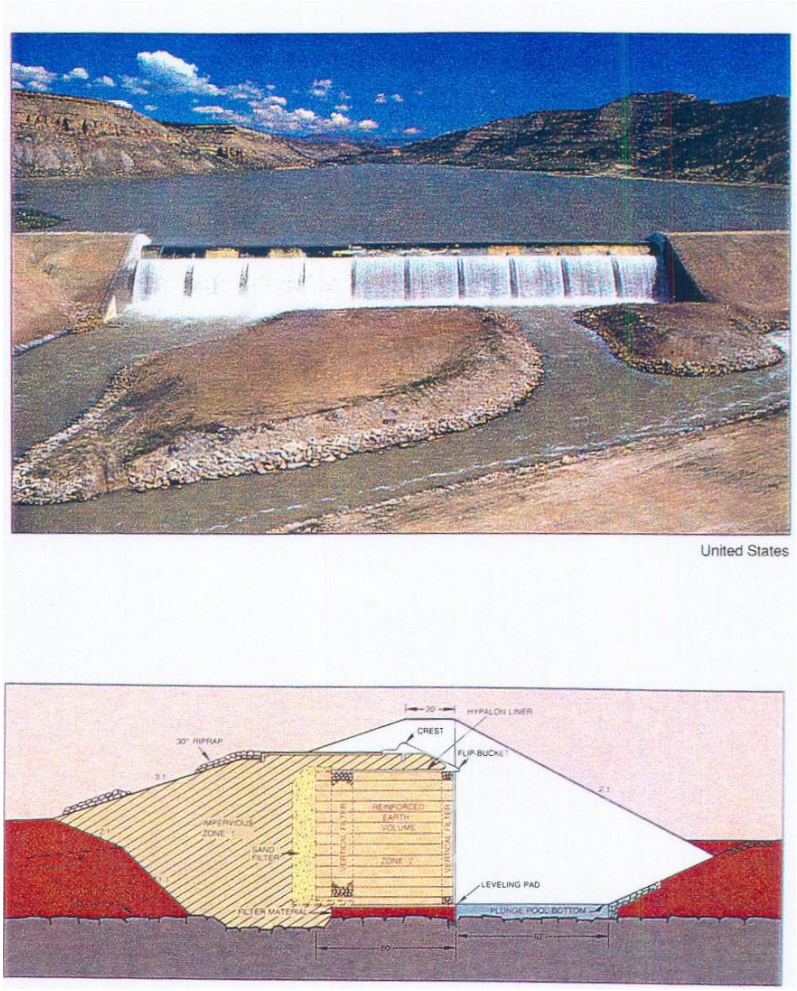

Figure 2.7 Geotextile reinforced dam application.

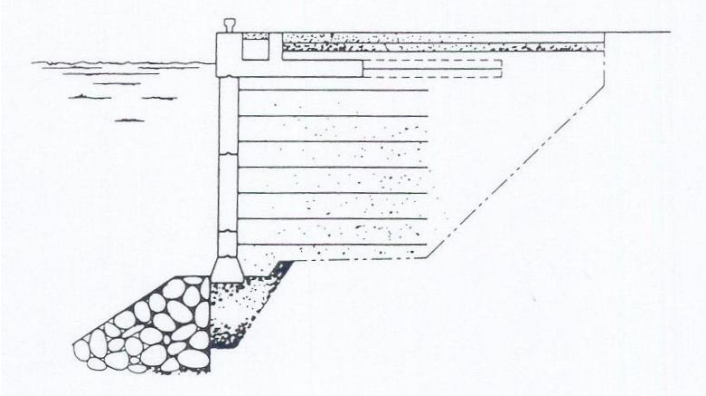

Figure 2.8 Geotextile reinforced retaining wall near the sea.

Survivability criteria have become synonymous with strength requirements for the separation function in most applications. A possible exception is the use of fabrics below railway ballast, where long-term abrasion under vibratory loads may place more severe conditions on the geotextile than construction stresses.

Koerner and Hausmann (1987) identified the following major applications where geotextile reinforcement is the primary function:

- Retaining walls,
- Slope stabilization,
- Embankments over very soft soils
- Foundations (improved bearing capacity),
- Unpaved road support.

Additionally, fabrics may be used in conjunction with other materials, such as polymeric grids and mats or even steel wires or meshes, forming "geocomposites". These types of construction elements are distinguished by extremely high strength and modulus values and have found application in the following tasks:

- Mattress and load support,
- Direct road support systems (surface mats),

Typical ranges of strength and modulus of geosynthetics used in the various categories of applications are given in Table 2.1. These values are not meant to be definite design guidelines but merely reflect the still-evolving practice of geotextile applications for reinforcement.

In reinforcement applications with predominantly single layers of geosynthetics (embankments, direct road support, mattresses, foundations and unpaved roads) it appears more likely that common rational design guideline will eventually develop, although the soil-reinforcement action may differ in detail. When looking at earth structures where multilayer reinforcement is standard (retaining walls, slope stabilization). Comparison based on wide-width tensile test results alone becomes somewhat questionable. Because the subcategories chosen in Table 2.1 do not reflect the vertical spacing options one might have with various-thickness-and thus various-strength and –modulus-fabrics and grids.

Geotextile applications(but not the use of composites)will be further discussed below.

Table 2.1 Typical geotextile wide-width strength and modulus in reinforcement applications.

Application area		Fabric strength, kN/m	Fabric modulus, kN/m
No.	Description		
1	Retaining Structures		
	Low height	13.1–17.5	35.0–52.4
	Moderate height	17.5–21.9	43.7–87.4
	High height	21.9–26.2	61.2–175
2	Slope Stabilization		
	Close spacing	13.1–21.9	26.2–61.2
	Moderate spacing	17.5–26.2	35.0–70.0
	Wide spacing	26.2–52.4	43.7–175
3	Unpaved Roads		
	CBR ≤ 4	13.1–21.9	52.4–87.4
	CBR ≤ 2	17.5–26.2	87.4–175
	CBR ≤ 1	21.9–52.4	175–525
4	Foundations (increase in bearing capacity)		
	Nominal	26.2–69.9	175–350
	Moderate	43.7–87.4	350–874
	Large	69.9–175	700–1750
5	Embankments over soft soils		
	Str. > 9.6 kPa*	87.4–262	874–1750
	Str. > 4.8 kPa	175–350	1750–3500
	Str. > 2.4 kPa	262–524	3500–6120
6	Mattress or load support (composites†)		
	Moderate	350–700	874–1750
	Heavy	700–1050	1750–4370
7	Direct road support (composites†)		
	Moderate	87.4–875	874–2620
	Heavy	875–2100	2620–7000

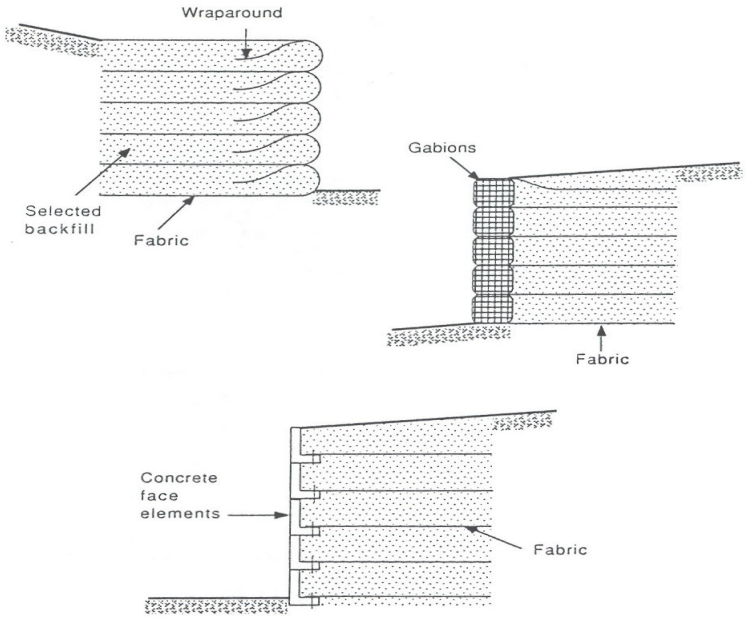

Figure 2.9 Alternative types of fabric walls

2.2.2. Retaining Walls

All kinds of fabrics have been successfully employed to build retaining walls-low-modulus nonwovens and high-modulus, high strength wovens. Typical geometric arrangements are shown in Figure 2.9.

Because of the difficulty of measuring stresses and strains in geotextiles, little internal performance data is available. Stability analysis of fabric-reinforced walls proceeds in similar way to that Reinforced Earth, mainly because a simple method taking into account the higher extensibility of fabrics (compared with steel) is not available. Besides ensuring external stability against global slope failure, bearing failure and sliding of the reinforced block of soil. Possible internal failure modes by rupture of the fabric (ties breaking) or slippage between fabric and soil (ties pullout) have to be assessed.

A Rankine analysis of stresses within the backfill or the Coulomb wedge-type analysis may be carried out. Procedures proposed vary with respect to the failure geometry (single wedge, double wedge, logarithmic failure surface, etc.), the magnitude of earth pressures acting (assuming an at-rest or active state of equilibrium), length of embedment effective against pullout, and minimum safety factors considered necessary. The effect of surcharge is evaluated in the same way as for conventional retaining walls. Seams and overlaps are not usually required, but where needed, they should be analyzed, because they represent weak links if under stress.

Protection of the wall face against degradation due to UV light and, to some degree, against vandalism can be provided by covering the fabric with Gunite, asphalt emulsion or other coatings.

Because of the lower stress-strain modulus of fabrics as compared to steel, geotextile walls likely deform more than reinforced earth walls and analysis of short-term and long-term strains (as discussed for geogrids) is deemed necessary. The actual parameters to be used in the analysis are, however, still subject to controversy, due to the nonlinear stress-strain behavior of fabrics and the effect of soil-fabric interaction.

Predicting deformations of reinforced soil walls requires knowledge of the tensile stress distribution in the fabric. Given the appropriate modulus of the fabric (this value may vary with stress level), the movement of the wall face can be calculated. Figure 2.10 illustrates various statically possible distributions of tension and shear stresses in the fabric.

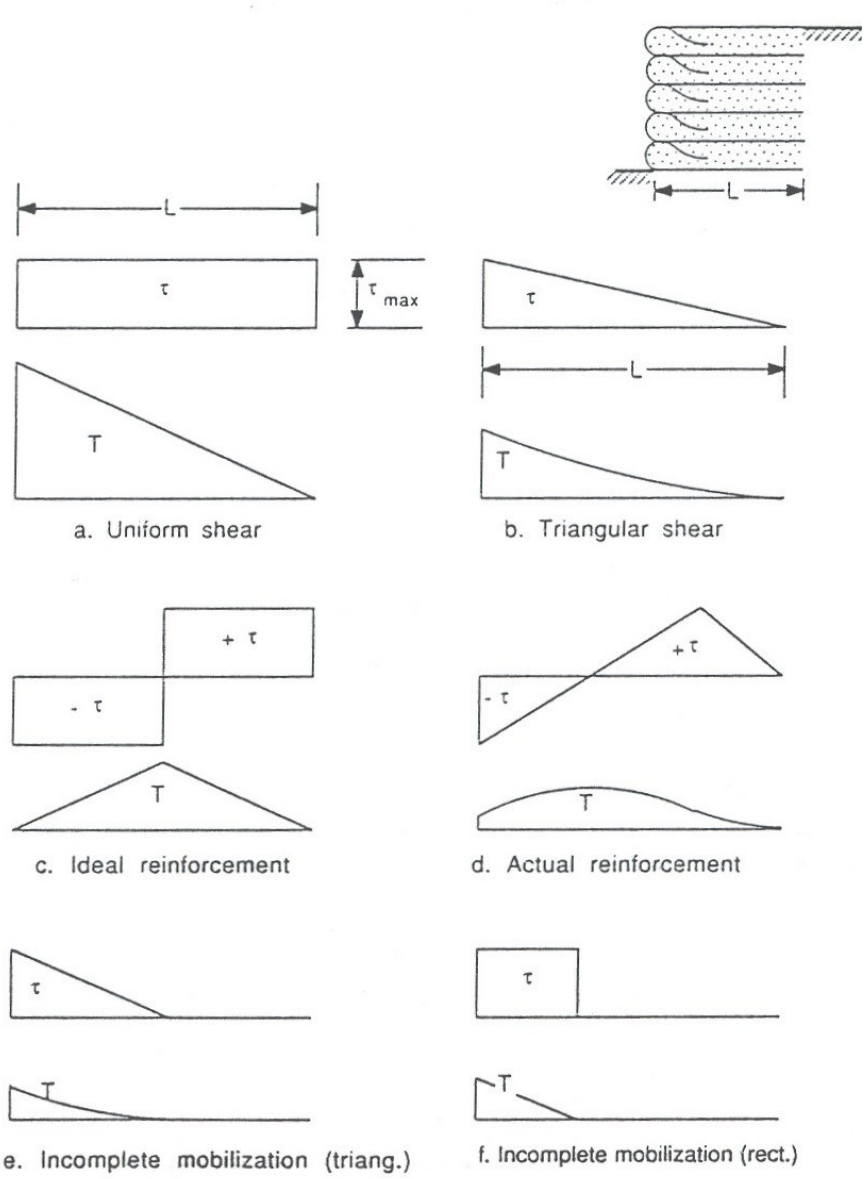

Figure 2.10 Statically possible distributions of tension and shear stresses in fabric wall reinforcement.

Field reports indicate that the deformation of geotextile walls is generally much less than expected. Because of the difficulties in measuring deformations of fabrics in situ. Not much information is currently available on actual fabric stresses and strains in retaining walls and other geotextile soil structures.

2.2.3. Slope Stabilization

The economic significance of damage due to slope mass movement is second only to the costs of controlling the effect of swelling and shrinking soils when it comes to ranking the significance of geotechnical hazards. Geotextiles offer a welcome additional technology for low-cost slope stabilization. They may be used to ;

- Prevent deep-seated failure by “tieback” action
- Contain surface soils in combination with soil nailing
- Protect slope surfaces against erosion
- Control sediment transport by wind and water

The stabilizing action of fabrics is perceived as similar to that of geogrids and other flexible reinforcement. The same methods of analysis are used to evaluate the stability of embankments and the global equilibrium of a reinforced soil retaining structure. Just as in geogrid and soil nailing applications, arguments may arise in respect to the direction of the tensile tieback force: “is the stabilizing force in line with the original orientation of the geotextile, or does the fabric aligns with the failure surface?”. Actual behavior may depend on the consistency of the soil and the stiffness of the fabric: lacking adequate knowledge of the failure mechanism, both cases should be analyzed and the more-conservative solution should be adopted for design.

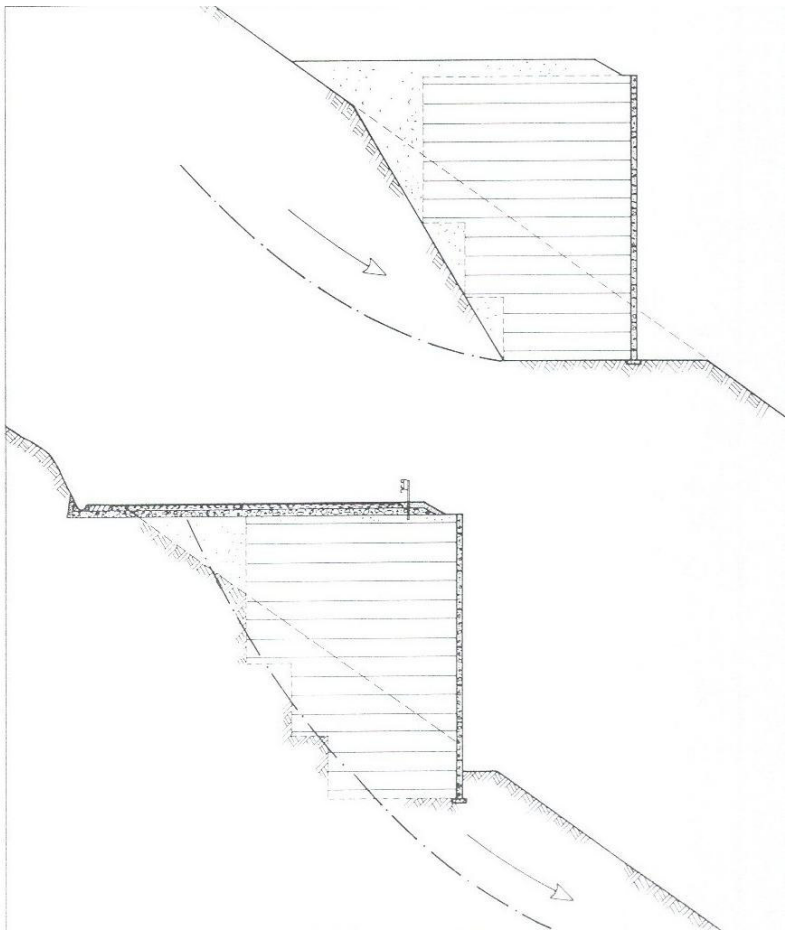

Figure 2.11 Slope stabilization models

Strength and flexibility as well as the permeability of fabrics are welcome properties in slope stabilization work. They facilitate traditional construction procedures such as benching and internal drainage and they enhance and protect the supporting effect of gabions and crib walls erected to inhibit or reduce slope movement.

2.2.4. Embankments

Depending on the construction material and the geological conditions in the foundation soil, conventional embankments can fail in a multitude of ways involving excessive settlement and lateral spreading, with or without single or multiple failure surfaces and surface bulging becoming apparent. A geotextile placed at the base of an embankment is

intended to interfere with the potential failure planes, provide restraint against lateral deformation, and possibly assist in load distribution on the soft subsoil.

Referring to Figure 2.12 the stability analysis of a reinforced embankment will have to take the following modes of failure or distortion into consideration:

(a) Block sliding on the geotextile: A vertical crack or other type of failure through the embankment isolates a block of soil which slides outward on the geotextile. A simple analysis would assume horizontal active earth pressures (and/or hydrostatic pressures in the case of water-filled cracks) pushing outward and soil fabric friction resisting this process. Uniform distribution of shear stresses would imply tensile forces in the geotextile which increase linearly toward the center of the embankment. For conditions as sketched in Figure 2.13 a we can calculate the resultant earth pressure E_a at the center of the embankment an the corresponding maximum tensile force T_{max} in the geotextile:

$$E_a = 0{,}5\gamma H^2 K_a$$

$$T_{\max} = \frac{\tau_r B}{2} = \frac{(\gamma H \tan\delta) B}{2}$$

American (largely the Corps of Engineers) practice suggests a minimum safety factor of 1.5 with respect to strength and a fabric strain limited to 10 per cent. The required fabric strength T_{req} and modulus E_{req} therefore are

$T_{req} = 1.5\ T_{max}$

$$E_{req} = \frac{T_{\max}}{\varepsilon_{\max}} = 10 T_{\max}$$

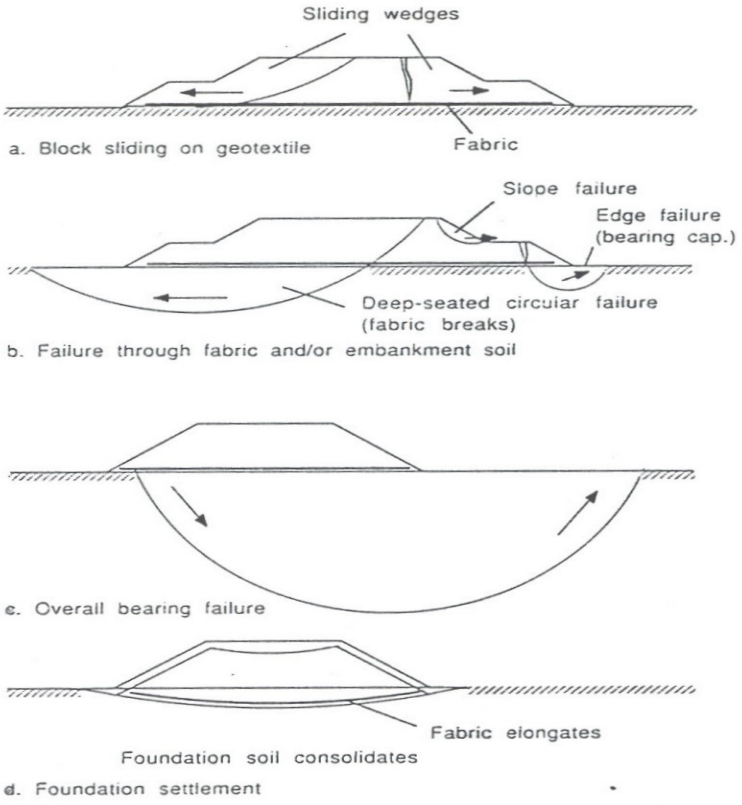

Figure 2.12 Embankment failure modes.

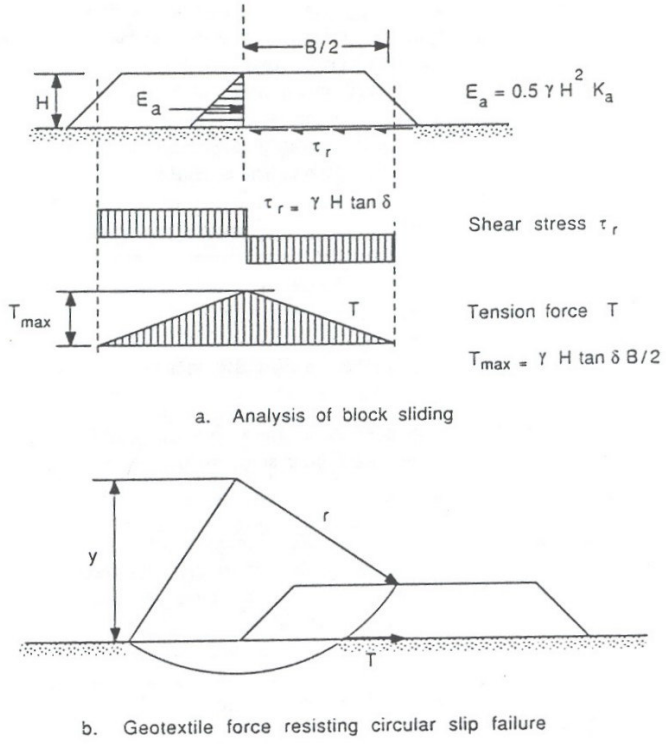

Figure 2.13 Analysis of geotextile-reinforced embankment.

(b) Failure along a slip surface: Typically assumed to be circular, either within the embankment or through the geotextile. The analysis proceeds along the usual steps with the fabric providing an additional stabilizing force T at the point of intersection with the failure surface (Figure 2.13 b). Opinions are again divided with respect to the calculation of the stabilizing moment due to the fabric:

$\Delta M = Tr$ or $\Delta M = Ty$

For circular failure surfaces and horizontal fabric layers, it is conservative to assume $\Delta M = Ty$ and to neglect any other possible effects on soil stresses.

(c) Overall bearing failure: Treated in the conventional manner according to Terzaghi's or Hansen's bearing capacity formula or similar formulas. The bearing capacity of an embankment foundation is essentially unaffected by a geotextile contained within or just below the embankment. Overall bearing capacity could only be improved if a mettresslile reinforced surface layer or larger extent than the base of the embankment would be provided.

Humphrey and Holtz (1986) reviewed the performance of 37 reinforced embankments, 11 of which failed by excessive deformation of fabric rupture. They observed that reinforced embankments could be built up to 2 m greater than conventional bearing capacity theory would indicate. They attributed this fact to limited thickness or an increase in strength with depth of the soft foundation soils, the effect of a dried surface crust, or dissipation of pore pressures during construction.

(d) Excessive settlement: Because of consolidation of the subsoil, the embankment might undergo large settlement resulting in excessive elongation of the fabric. Possibly resulting in eventual failure. A similar effect would arise from lateral squeezing of the foundation soil. The presence of the fabric may reduce differential settlement somewhat , but little reduction of the magnitude of total final settlement can be expected.

Because of the drainage effect of nonwoven fabrics, consolidation of the subsoil may be accelerated with a consequent gain in strength. Where deformation criteria require high-strength, high modulus woven fabrics, the drainage function may be provided by geocomposites.

In order to provide edge anchorage, the geotextile layer may be folded back similar to the wraparound in fabric walls. Alternatively the fabric may be anchored in trenches or weighed down by beams.

Additional geotextile reinforcement may also be placed within the embankment itself, rather than just below it. Narrower horizontal fabric strips along the side slopes (with wraparound) may enhance compaction at the edges, so overbuilding and cutting back is no longer necessary. Edge reinforcement also helps to reduce erosion and may assist in the establishment of vegetation.

Long-term creep of fabrics can be an issue in all reinforcement applications. A limited strain criteria related not only to the embankment performance but also to specific geotextile properties makes sense. Fortunately, foundation stability generally increases with time as consolidation of the soil takes place, thereby allowing some stress relaxation to occur.

2.2.5. Foundations

Geotextile-reinforced pads for structural footings are intended to provide improved bearing capacity and reduced by distributing the imposed loads over a wider area of weak subsoil. Little information is available on this application, except that relatively high-strength. high-modulus fabrics are preferred. The general approach is to provide an aggregate layer including geotextiles at one or more levels: in addition, the aggregate may be protected at its base (or all around) by a separation, drainage and filter fabric.

For heavy loads, composite reinforced structural layers may have to be designed, incorporating elements such as steel meshes or polymeric grids.

A different concept is employed where impermeable geomembranes are placed so as to isolate a bearing stratum of clay subject to swelling and shrinking during wet and dry seasons. This technique is referred to as Membrane Encapsulated Soil Layer (MESL) and has so far mainly been used in road construction [Lawson and Ingles (1982)].

Yet another approach is to use geotextiles for the confinement of soils, forming foundation beams, and piers.

2.2.6. Unpaved Roads

Unpaved roads present yet another application where the reinforcing action of geotextiles can be used to economic advantage. As in other designs of course, geotextiles in unpaved roads often fulfill additional basic functions such as separation, filtration and drainage.

Geotextiles are now a well-accepted construction material in the establishment of trafficable surfaces on soft clayey, silty and organic soils.

They may serve a temporary role in the development of a sealed-pavement structure, or they may be used for longer-term performance as an integral part of unpaved roads in country areas or as haul roads for civil and mining projects.

Both, nonwoven an woven fabrics are used in road construction. In recent years, experiments have also been carried out with other forms of geosynthetics [Khay et al. (1986)], such as polymer grids (e.g., Tensar), fiber reinforcement (e.g., Texsol) and geocells (e.g., Armater).

The aim of conventional unpaved road design is to provide adequate selected cover material in order to prevent bearing failure due to wheel loads and excessive rutting under traffic. Additional problems may be faced during construction, such as general shear failure of the subsoil due to the weight of the fill, impaired mobility of construction equipment, lack of suitable aggregate and excessive settlement.

In most situations the designer aims at finding a solution which will result in the lowest overall costs, taking into account initial construction costs, continuing maintenance costs and possibly costs related to production losses due to road colures.

Aspects of design for unpaved roads emphasized here are concerned with a rational assessment of the bearing capacity of the soil below the aggregate layer and an estimate of the surface deformation under static and repeated loading by vehicular traffic. The assessment of the overall stability and settlement of the fill during and after construction is expected to be treated as a separate problem according to standard soil mechanic principles.

3. LITERATURE REVIEW

In this section, some important studies about Geotextile reinforced structures will be introduced. Experiments on laboratory models are initially examined. Then, field tests to determine the in-situ performances of models for test fills are described. Finally, static and dynamic analysis methods of geotextile reinforced structures are mentioned.

3.1. Laboratory Models

In laboratories there are only centrifuge tests and small scaled laboratory models are being done to examine the performance of geotextile reinforced structures.

3.1.1. Centrifuge Tests

A centrifuge testing program was undertaken to investigate the failure mechanisms of geosynthetic reinforced soil slopes and to evaluate the assumptions in their design. Scaling laws were established so that factors of safety in the models would be identical to choose in prototype structures. Failure of the models was characterized by well-defined shear surfaces through the toe of the slopes, which is in good agreement with current design methods for reinforced slopes based on limit equilibrium. The moment of failure was defined by a sudden change in the rate of settlements at the crest of the slope. In contrast to the assumption in current design procedures that failure should initiate at the toe of a reinforced slope, failure initiated at midheight of the slopes. Model deformations were found to depend on the backfill properties, but were essentially independent of the tensile strength and spacing of the reinforcements. The test results showed that overlapping reinforcement layers contribute to stability as these failed by breakage instead of by pullout when intersected by the failure surfaces. The experimental results also indicate that stability of the reinforced slopes is governed by the peak shear strength of the backfill soil. A new distribution of maximum reinforcement forces with depth, which is consistent with the failure mechanism observed in the models, is proposed for geosynthetic reinforced soil slopes.

3.1.1.2 Static Centrifuge Tests

Limit equilibrium methods have been traditionally used to analyze the stability of slopes with and without reinforcements. As limit equilibrium predictions of the performance of geosynthetic reinforced slopes have not been fully validated against monitored failures, a centrifuge study was initiated to evaluate the assumptions and selection of parameters for design of these structures.

3.1.1.2.1 J. G. Zornberg, N. Sitar and J.K. Mitchell (1998)

Zornberg *et al.* (1998) evaluated the ability of limit equilibrium to predict the failure of the centrifuge models and consequently, the suitability of limit equilibrium for the design of geosynthetic reinforced slopes.

The principle of centrifuge modeling is based upon the requirement of similarity between the model and the prototype. If a model of the prototype structure is built with dimensions reduced by a factor 1/N, then an acceleration field of N times the acceleration of gravity g, will generate stresses by self-weight in the model that are the same as those in the prototype structure. Additional relationships can be determined either by analysis of governing differential equations or by dimensional analysis and the theory of models. All models were built with the same slope inclination (1H:2V) and the same total height. Vertical deformations are monitored by the transducer.

Failure in the models was characterized by well-defined shear surfaces through the toe of the slope, which is in good agreement with current design methods for reinforced slopes based on limit equilibrium.

Failure initiated at the midheight of the slopes, contradicting assumptions in current design methods that failure should develop from the toe of the reinforced slopes.

The location of the critical failure surfaces was found to be approximately the same for all models, which were built with different reinforcement spacings, reinforcement tensile strengths, and soil densities.

Settlements on top of the structure during centrifuge testing were observed to depend on the properties of the backfill soil, but to be essentially independent of the tensile strength and spacing of the reinforcements.

Important contribution to the stability of the models was provided by the overlapping layers, which failed by breakage instead of by pullout when intersected by the failure surfaces.

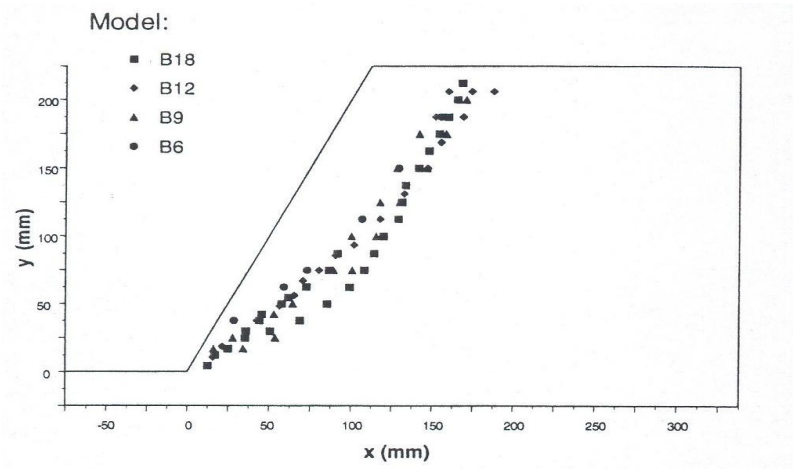

(a) Location of tears in reinforcements

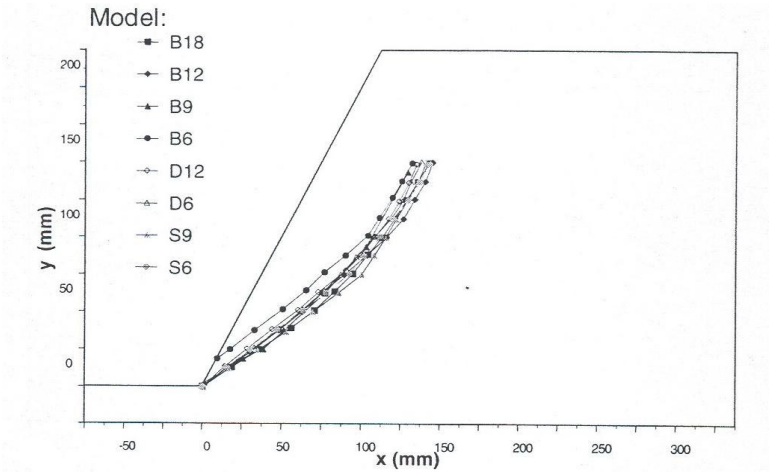

(b) Location of failure surface obtained from in-flight recorded images

Figure 3.1 Potential failure surface locations (Zornberg, 1998)

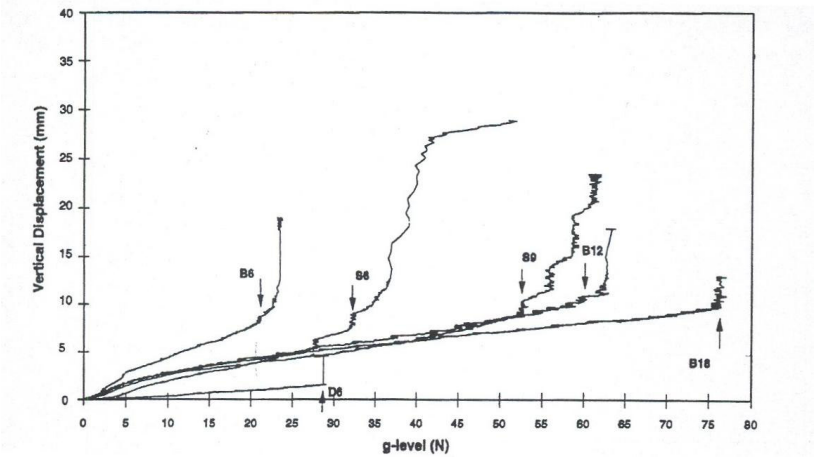

Figure 3.2 Vertical settlements on top of model slopes during centrifuge testing. (Zornberg, 1998)

The test results indicate that the stability of the reinforced slopes is governed by the peak shear strength and not by the critical state shear strength of the backfill soil.

A new distribution of reinforcement forces with depth, consistent with the failure mechanism observed in the slope models, is proposed for the design of geosynthetic reinforced soil slopes. Unlike the conventional triangular distribution of reinforcement tension with a maximum tension at the base of the slope, the location of the maximum reinforcement tension in the proposed distribution depends on the inclination of the reinforced slope. Considering the limited data in this experimental investigation, further research should be undertaken to validate the proposed distribution.

Finally, the results of this investigation show that centrifuge model testing is a useful tool investigate the stability of earth structures, particularly in the absence of prototype failure records.

3.1.1.2.2 A. Porbaha (1998)

An experimental investigation was carried out to study the traces of slip surfaces in geotextile reinforced cohesive soil retaining structures when the slope angle changes from vertical to the slope of 63.4° (1H:2V) using centrifuge modeling technique. The results indicate that as the length of the reinforcement increases from unreinforced to a length equal to 0.75 of the height, the slip surface moves toward the face of the reinforced structure, regardless of the slope angle. At all times, however, the slip surfaces were behind

the locations of failure surfaces of reinforced models. In addition, as the slope angle decreases from vertical to the slope of 63.4°, the slip surfaces have a tendency to move toward the face of the slope, regardless of the length of reinforcement. The locations and traces of the slip surfaces obtained from physical tests were consistent with those from limit equilibrium analyses.

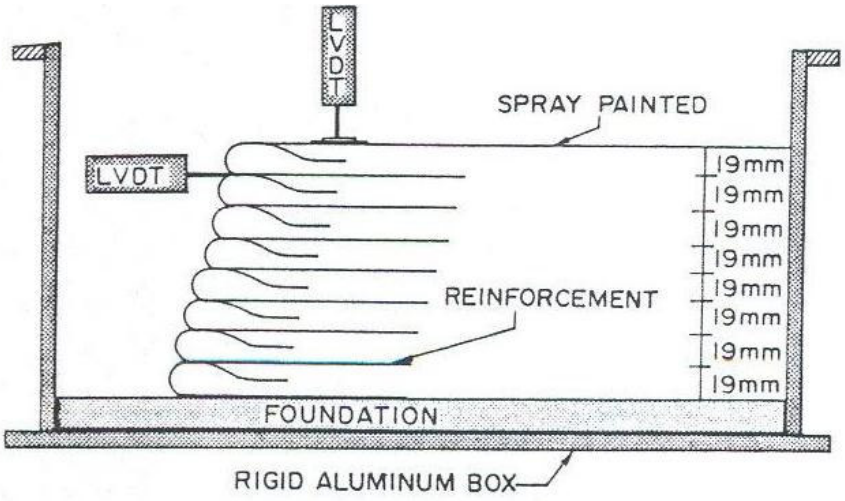

Figure 3.3 Profile of a typical model

Table 3.1 Physical geometry and prototype data

Model No.	Slope angle (deg.)	Reinforcement length (mm)	L/H Ratio	N_c (g)	N_f (g)	H_c (m)	H_f (m)
M-28	90	114	0.75	40	54	6.1	8.2
M-35	80.5(1H:6V)	114	0.75	48	73	7.3	11.1
M-47	71.6(1H:3V)	114	0.75	67	86	10.2	13.1
M-20	63.4(1H:2V)	114	0.75	92	102	14	15.5
M-49	90	100	0.67	36	49	5.5	7.4
M-37	80.5(1H:6V)	100	0.67	49	70	7.4	10.6
M-44	71.6(1H:3V)	100	0.67	63	83	9.6	12.6
M-42	63.4(1H:2V)	100	0.67	85	100	12.9	15.2
M-48	90	76	0.50	34	40	5.2	6.1
M-33	80.5(1H:6V)	76	0.50	44	56	6.7	8.5
M-43	71.6(1H:3V)	76	0.50	58	67	8.8	10.2
M-41	63.4(1H:2V)	76	0.50	73	77	11.1	11.7
M-34	90	0	0	34	35	5.2	5.3
M-29	80.5(1H:6V)	0	0	43	47	6.5	7.1
M-19	71.6(1H:3V)	0	0	52	58	7.9	8.8
M-21	63.4(1H:2V)	0	0	65	67	9.9	10.2

L/H = Length of reinforcement as a multiple of model height
N_c = Centrifugal acceleration @ tension crack (g)
N_f = Centrifugal acceleration @ failure (g)
H_c = Prototype equivalent height @ first tension crack (m)
H_f = Prototype equivalent height @ failure (m)

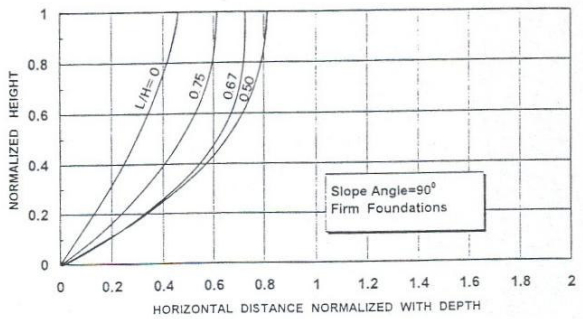

(a)

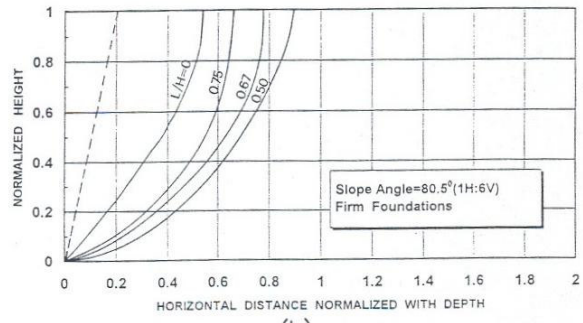

(b)

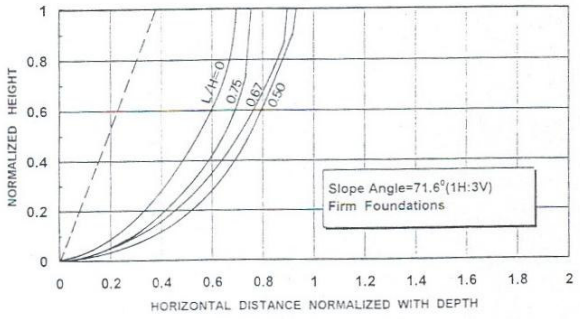

(c)

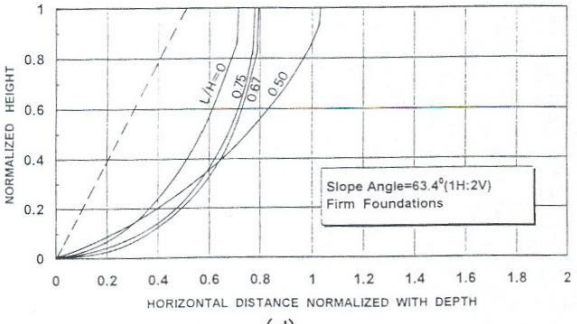

(d)

Figure 3.4 Failure surfaces obtained from experiments

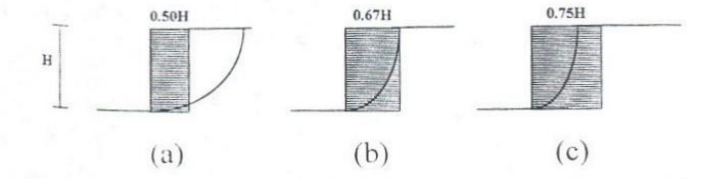

Figure 3.5 Effect of length of reinforcement on the location of failure surfaces

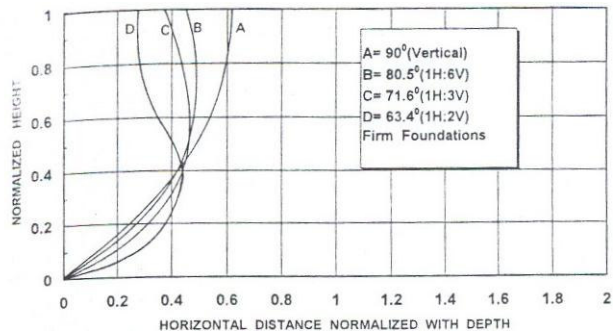

Figure 3.6 Traces of slip surfaces for different slope angles from centrifuge tests (Porbaha,1996)

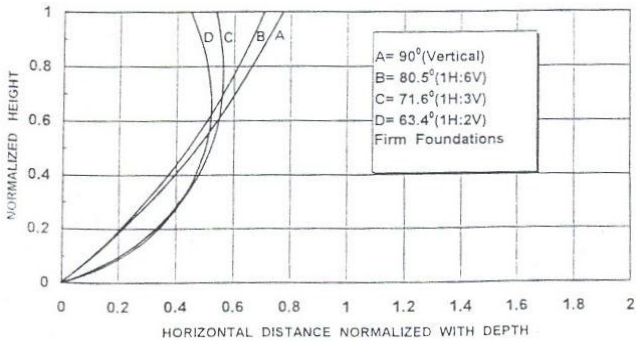

Figure 3.7 Traces of slip surfaces for different slope angles from limit equilibrium analyses (Porbaha,1996)

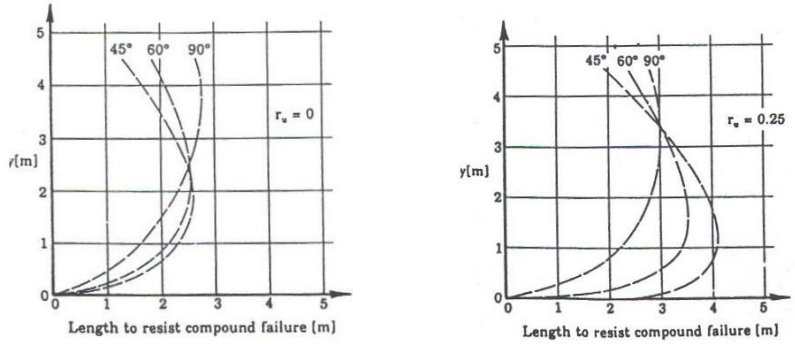

Figure 3.8 Traces of critical slip surfaces at various elevations (Leschinsky,1992)

3.1.1.2.3 S. M. Springman, S. Balachandran and C. Jommi (1997)

The dominant form of failure in a wall reinforced by extensible geotextiles is the deformation mode, since it is unlikely that ultimate failure will be critical. A reliable method for displacement prediction is thus the key factor in the analysis and design of reinforced soil structures. Centrifuge modeling was conducted on a series of small-scale, multi-layered reinforced walls, of prototype height 6-15 m, constructed in dry sand and subjected to a vertical surcharge load. Vertical and horizontal displacements of the wall were measures by transducers. Photographic records of markers placed within the fill allowed determination of deformation mechanisms. Two different model reinforcements were used in each of two walls, and all of these were instrumented to measure tension. Numerical back-analyses of these walls, provided insight into reinforced wall behavior, and validated the centrifuge model test data. Significant physical and numerical data are compared and discussed.

The centrifuge data showed a continuous form of deformation mechanism throughout the loading pattern. Constant shear strain and dilation were deduced, similar to the case of externally supported retaining walls.

Numerical analyses, performed with simple constitutive models with mean values for material parameters, lead to better understanding, of the deformation mechanism of reinforced soil walls, and highlight the role played by stress history in soil-reinforcement interaction. With equivalent model geometry and construction procedures, and separate discretization of soil and reinforcement, the experimental deformation mechanism was well reproduced. A homogeneous model which smeared the reinforcement into the whole soil mass showed noticeable differences in global deformation behavior (in spite of comparable values for total displacements) and did not appear to suit such widely spaced reinforced soil walls.

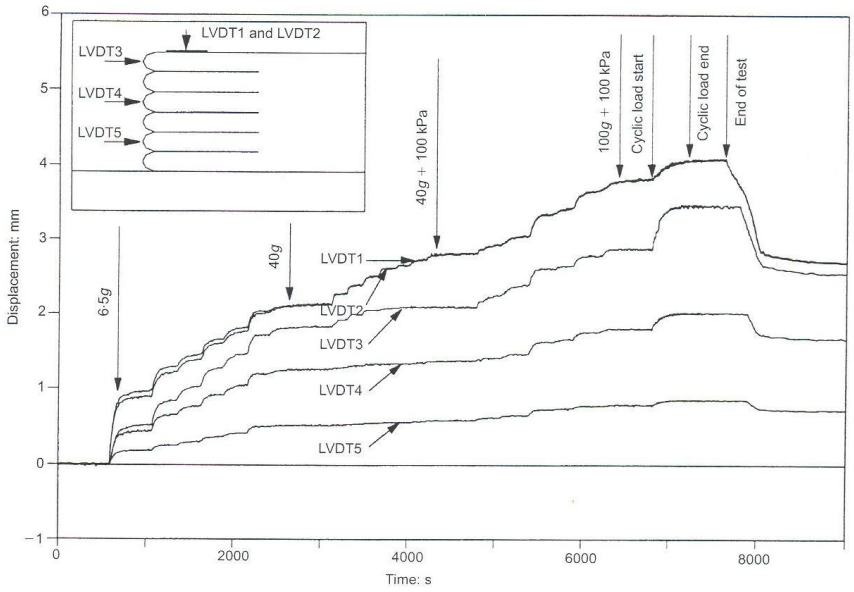

Figure 3.9 Horizontal and vertical LVDT measurements in test SB10 (bandage) at model scale (Springman *et al.*,1997)

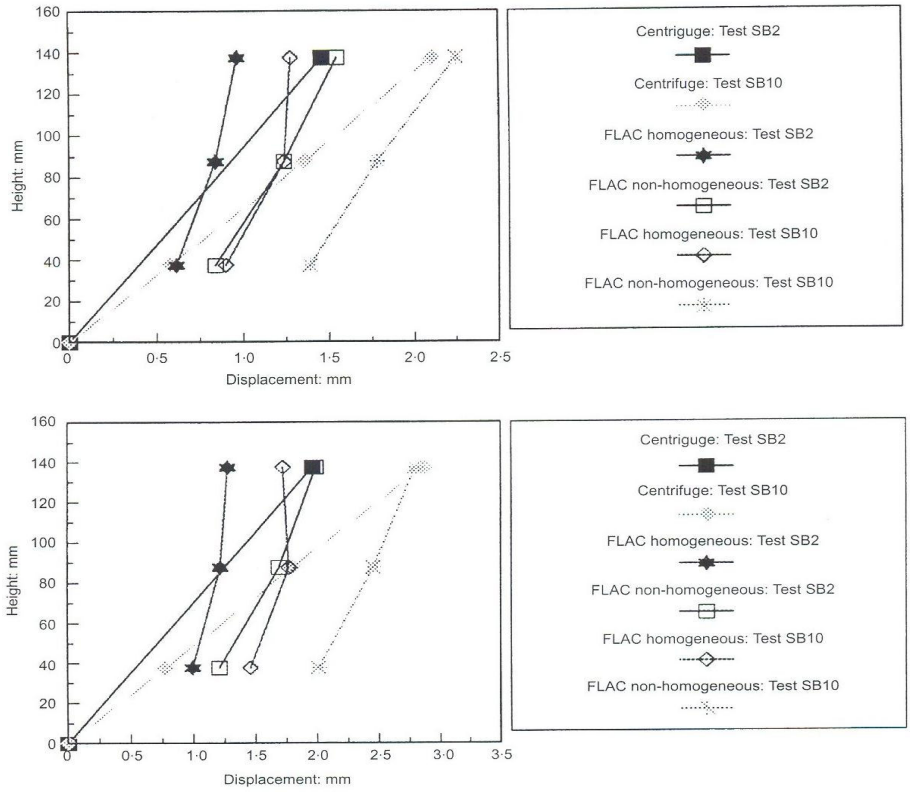

Figure 3.10 Comparison of numerical and centrifuge data for horizontal wall displacements at 40g + 100kPa and at 100g + 100kPa respectively. (Springman *et al.*,1997)

3.1.1.3 Field Models

Field models were constructed to examine the behavior of geotextile reinforced structures under real loads and effects with the help of position monitoring devices and electronic distance measuring apparatus which are placed inside the test fills or embankments. Several studies will be discussed in the following.

3.1.1.3.1 K. Rowe, C. T.Gnanendran, A. O.Landva and A. J. Valsangkar (1995)

The instrumentation, construction and field performance of a full-scale geotextile reinforced test embankment constructed on a soft compressible soil is presented. A relatively high-strength polyester woven geotextile was used as reinforcement. The construction sequence, the observed pore pressure response, and vertical and horizontal displacements are reported. The development and propagation of cracks in relation to the construction sequence and the manner in which the embankment failed are described. The field data suggest that the shear strength of the foundation soil was mobilized at a fill thickness between 5 and 5.7 m. However, due to the stabilizing effect of the geotextile reinforcement, the embankment did not fail until the geotextile reached its ultimate tensile strength and tore when the fill thickness reached 8.2 m. The failure of the embankment was of a viscoplastic nature and although additional fill could be placed after failure of the geotextile and embankment at 8.2 m, no additional gain in the net height could be maintained above the maximum of 6.6 m recorded when the fill thickness reached 8.2 m.

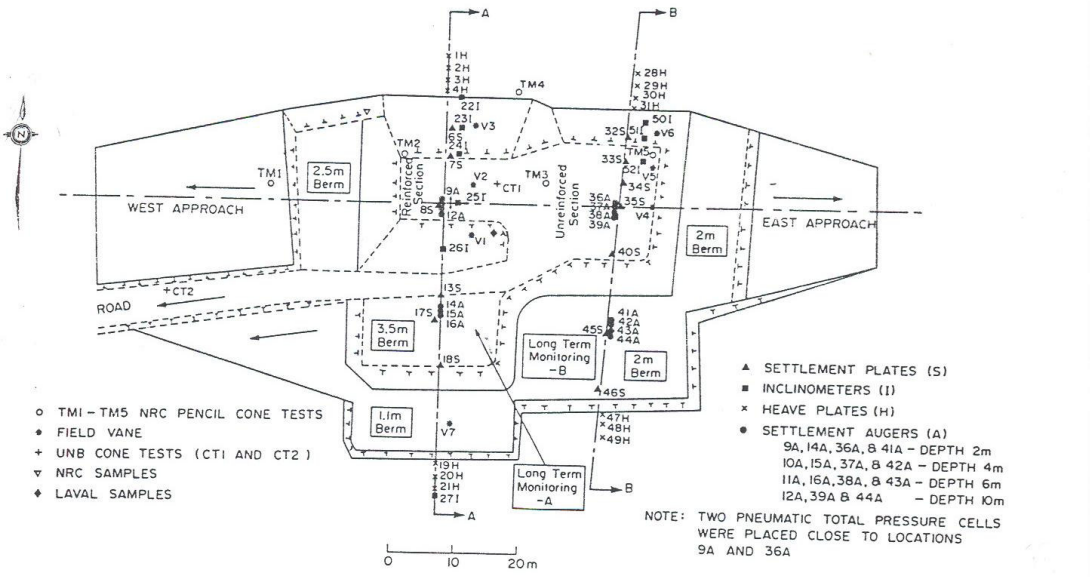

Figure 3.11 Layout of instrumentation plan

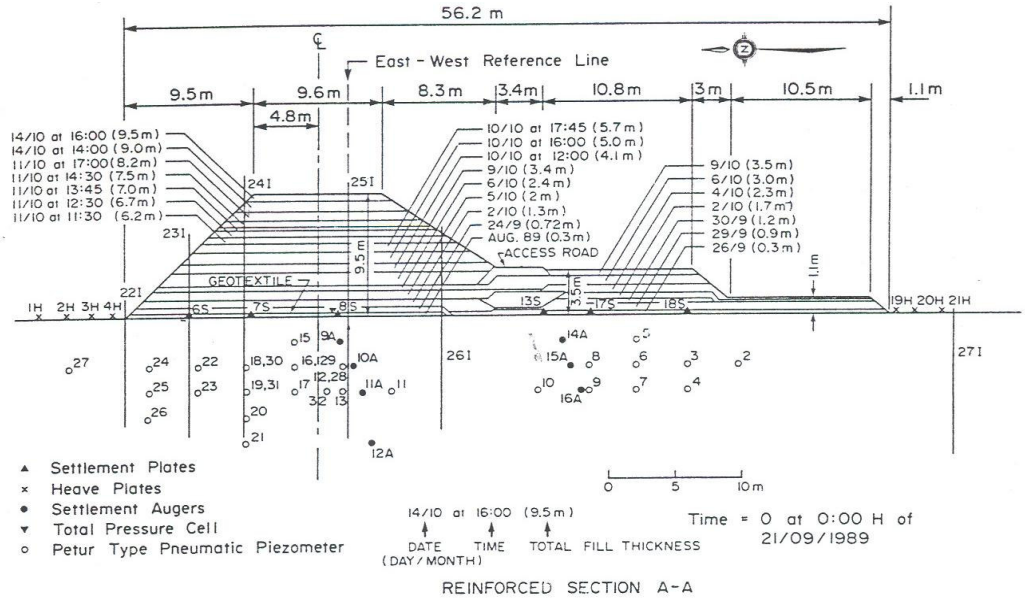

Figure 3.12 Layout of instrumentation and sequence of construction of reinforced embankment.

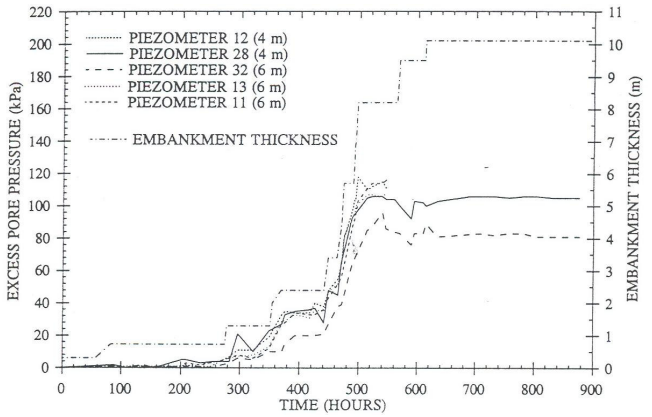

Figure 3.13 Variation of excess pore pressure with time for piezometers 12, 28, 32, 13 and 11.

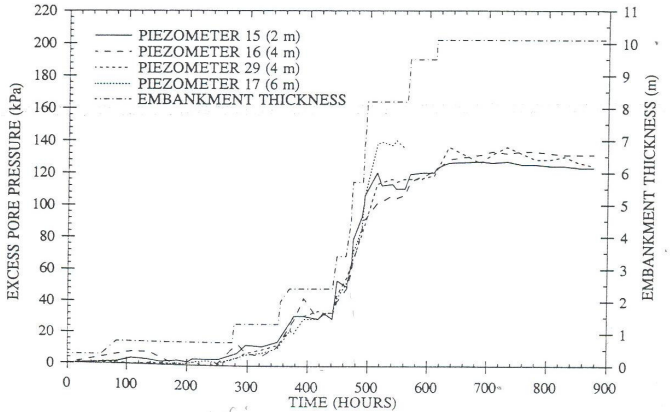

Figure 3.14 Variation of excess pore pressure with time for piezometers 15, 16, 29 and 17.

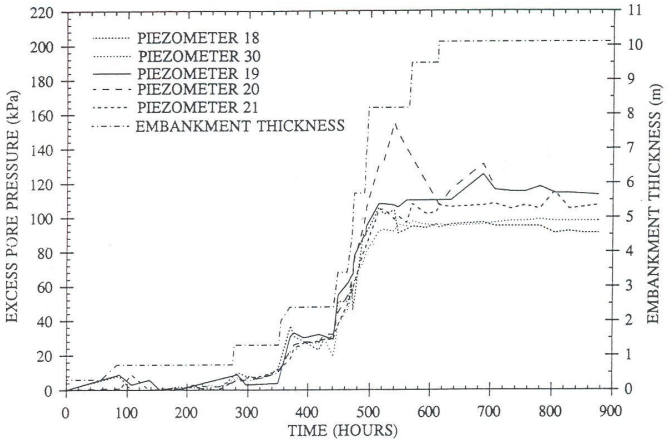

Figure 3.15 Variation of excess pore pressure with time for piezometers 18, 30, 19, 20 and 21.

3.1.1.3.2 Other Field Models

Actual projects that have been instrumented were of course, designed according to the current state of the art standards. These walls have been subjected to no more than design loadings.

Experimental walls, on the other hand, are generally intended for testing new designs or technologies. They are often loaded to failure.

The Triel wall, for example, built in 1975 by La Terre Armee S.A., France, was constructed to verify the behavior of high-adherence reinforcing strips, and to check the effects of vibrations.

Another experimental wall, erected in 1976 by the U.S. Army Corps of Engineers in Vicksburg, Mississippi, was built using non-standard metal facing panels of the military's design. It was then loaded to failure.

As part of the research into the durability of buried steel, Tierra Armada S.A., Spain, built a six-meter-high wall in Madrid in 1977 using thin reinforcing strips (0.6 mm). The structure was then inundated with brine to accelerate corrosion. Failure developed along a surface very similar to the line of maximum tensile force established by previous research. In addition, at the moment of failure the overall residual resistance of the reinforcements was very close to the sum of the theoretically predicted maximum tensile forces.

In 1978, the Public Works Research Institute (PWRI) of Japan built a six-meter-high experimental wall to study the effects of a sloping surcharge and the consequent role of the wall facing (Figure 3.16). When the reinforcing strips were unbolted from the outside, the face at first remained stable, confirming the hypothesis that it plays only a minor structural role. When the structure was loaded to failure, the break in the fill closely followed the theoretical line of maximum tensile stress, as shown in Figure 3.17.

Narrow Profile Walls in 1983, The Reinforced Earth Company and United States, built and instrumented a six-meter-high wall with short reinforcing strips at Millville, West Virginia. The structure has two cross-sections: one is rectangular, with reinforcing strips of 2.7 meters (L/H=0.45); the other is trapezoidal, with reinforcing strips of 1.8 to 3.0 meters (L/H=0.30 to 0.50) (Catalogue Reference)

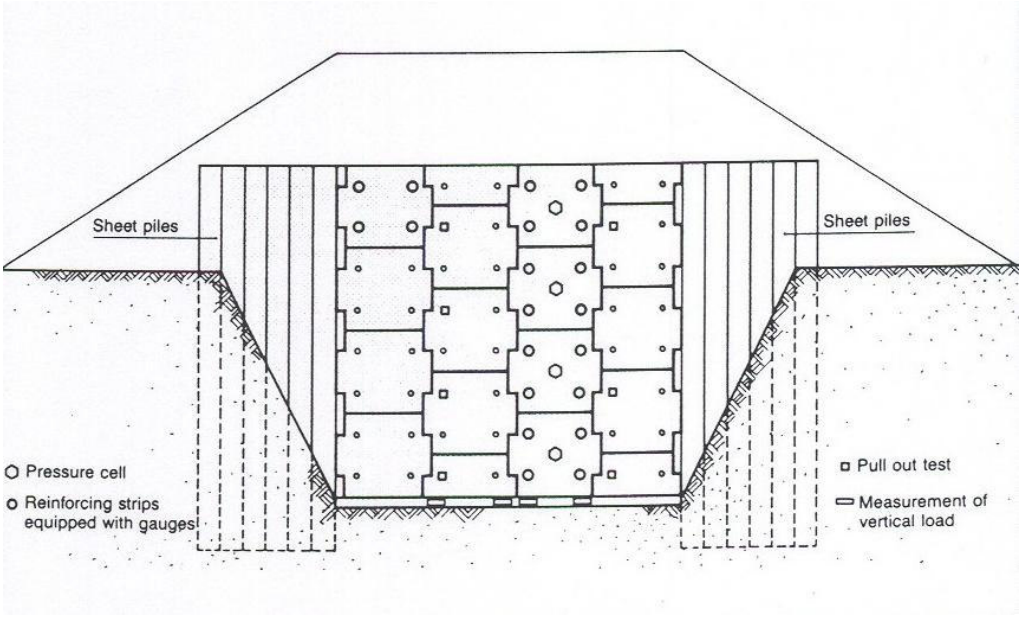

Figure 3.16 PWRI wall in Japan (Reinforced Earth, 1989)

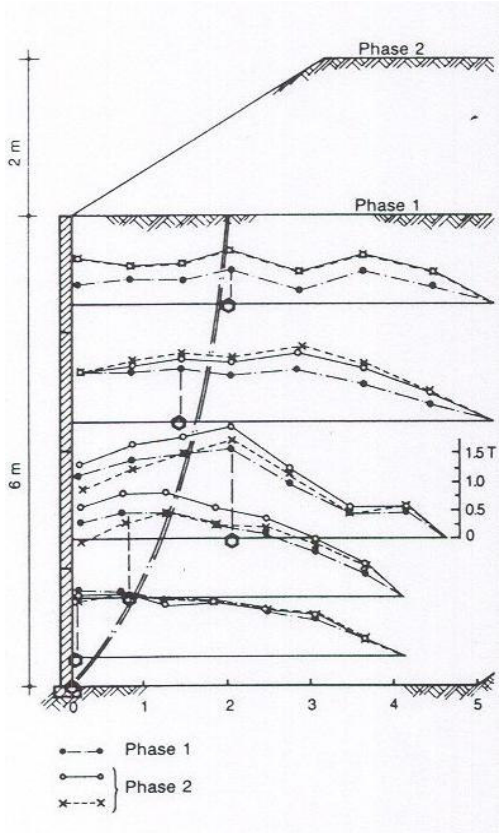

Figure 3.17 PWRI wall, Cross section and tensile forces.

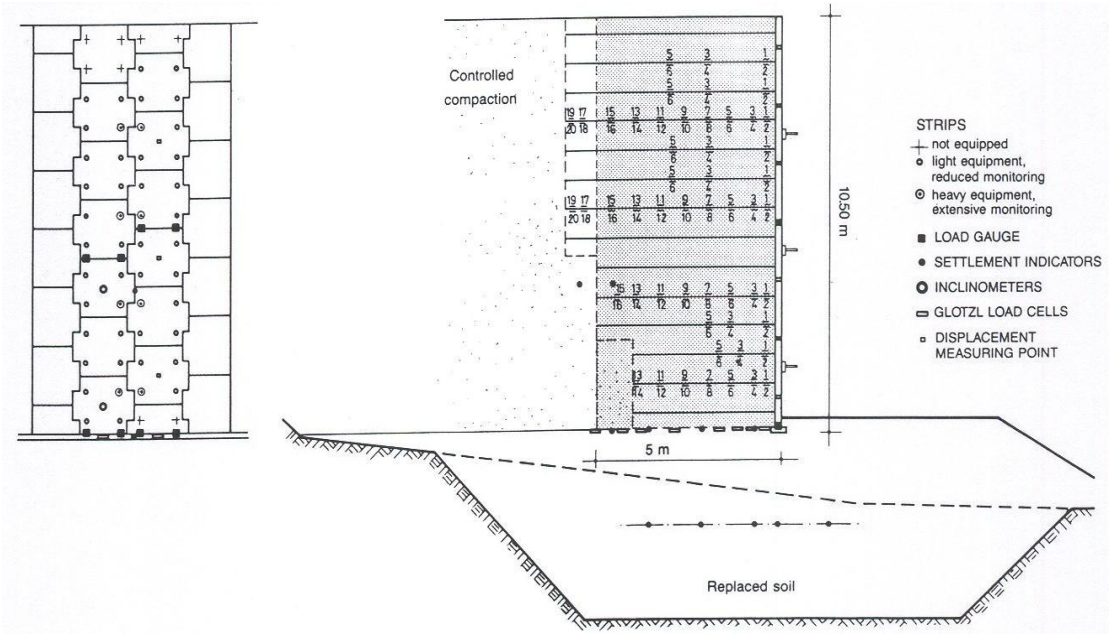

Figure 3.18 Instrumentation (Reinforced Earth, 1989)

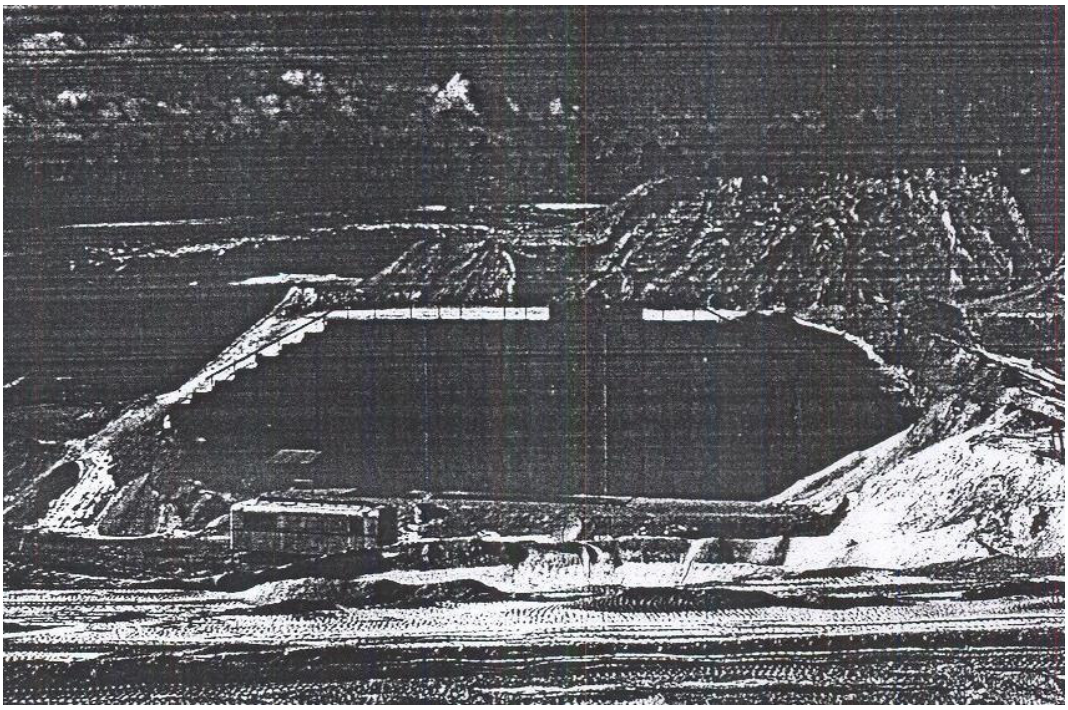

Figure 3.19 10.5 m high test wall in France. (Reinforced Earth, 1989)

An experimental wall of the same type, but with a height of 10.5 meters, was constructed in France near Fontainebleau by La Terre Armee S.A. and LCPC (1986/7). Building the wall, equipping it with complete instrumentation, and taking measurements cost about $360,000, of which 90 percent was provided by the Reinforced Earth Group.

As in Millville, the project included two separate sets of measurements (Figure 3.18). One set involves a rectangular cross-section and reinforcing strips of five meters ($L/H \tilde{=} 0.5$); the cross-section of the other set is trapezoidal, with reinforcements four to six meters in length ($L/H \tilde{=} 0.4$ to 0.6).

Deliberately built on relatively poor foundation soils and with fill of average quality, this experimental wall was designed to test practical construction conditions as well as the overall stability and design principles associated with a narrow profile structure.

3.2. Analysis Methods Used in Design of Reinforced Slopes

3.2.1. Static Analysis Methods

Past years many different methods were introduced to analyze the stability of geotextile reinforced slopes. But the following scientists' methods were more acceptable than others. These are Wright-Duncan, 1998, Schmertmann, 1987; Leshchinsky and Boedecker, 1989; Jewel,1990 and Sawicki-Lesniewska, 1989 ; Buhan,1989.

Nowadays it's seen that the studies did not give reliable results to use, in order to model the behavior of geotextile reinforced structures.

As it is known that the best method for analyzing is finite elements method, expensive and insufficient computers made difficult to spread this method in the past years. By the way scientists used limit equilibrium method to analyze the reinforced structures. As the computers became cheaper and faster, finite elements analysis methods and programmes were developed.

3.2.1.1 Limit Equilibrium Analysis.

Limit equilibrium methods have been traditionally used to analyze the stability of slopes with and without reinforcements. As limit equilibrium predictions of the performance of geosynthetic reinforced slopes have not been fully validated against monitored failures, a centrifuge study was initiated to evaluate the assumptions and selection of parameters for design of these structures.

The limit equilibrium method (Terzaghi, 1956) still remains the most widely used approach to obtain approximate solutions.

Limit equilibrium analysis of unreinforced structures includes assumptions that are also needed when analyzing reinforced soil slopes (e.g., the shape of the failure surface). Additional assumptions that are needed for the analysis of reinforced slopes include the inclination (e.g., horizontal, tangential) and distribution of the reinforcement tensile forces along the selected failure surface (e.g., linear, constant with depth).

The failure surfaces most widely used in the limit equilibrium analysis of reinforced soil slopes include the planar wedge (Schlosser and Vidal, 1969); the bilinear wedge surface

(Jewell, 1991); the logarithmic spiral (Leshchinsky and Boedeker, 1989); and the circular surface (Wright and Duncan, 1991).

3.2.1.1.1 J.G. Zornberg, N. Sitar and J.K. Mitchell (1998)

The purpose of Zornberg et al. (1998) is to further evaluate the results of the centrifuge testing program in order to investigate the validity of the limit equilibrium method as a basis for design of geosynthetic reinforced soil slopes. To this effect, an assessment of the strength properties under operational conditions of the backfill soil, the geotextile reinforcement, and the several interfaces in the slope models is initially presented. Then, different assumptions in the limit equilibrium analysis of geosynthetic reinforced soil slopes are evaluated, and a comparison between experimental results and limit equilibrium predictions is presented. Finally, normalization of the centrifuge test results and its implications on the design of geosynthetic reinforced soil structures are discussed.

Using the centrifuge modeling technique, a series of geotextile reinforced soil slope models was tested to failure in order to identify the possible failure mechanisms and to verify the ability of limit equilibrium methods to predict the experimental results. The variables considered in the centrifuge study were the reinforcement spacing, the reinforcement tensile strength, and the soil shear strength, which can all be taken into account using limit equilibrium analyses. A testing program was initially undertaken to evaluate the strength properties under operational conditions of the sand used as backfill material, the geotextile reinforcements, and the several interfaces in the slope models. The tensile strength of the model geotextiles was found to depend on the testing boundary conditions.

The effect of different modeling assumptions on the calculated factors of safety was investigated by performing parametric limit equilibrium studies. Based on the interpretation of experimental results on the performance of the reinforced slope models

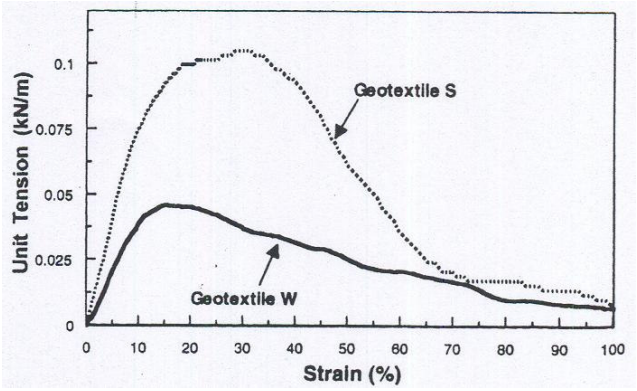

Figure 3.20 Typical wide-width tensile test results for geotextile reinforcements.

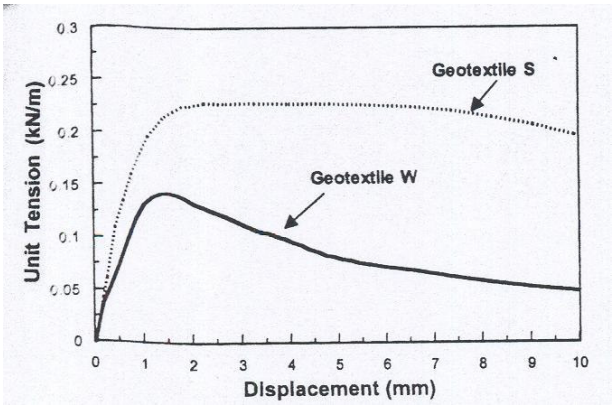

Figure 3.21 Typical tensile test results for model geotextiles observed using small gauge length setup.

at failure [see Zornberg et al.(1998)], the peak soil shear strength (instead of the critical state shear length)

And a uniform distribution of maximum reinforcement forces with depth, (instead of a conventional triangular distribution) was adopted in these analyses. The suitability of limit equilibrium methods for the analysis of geosynthetic reinforced slopes was then evaluated by comparing experimental results and analytical predictions. The following conclusions can be drawn from this evaluation:

•Very good agreement was obtained between the experimental *g*-levels at failure obtained for the centrifuge models and the results predicted by limit equilibrium.

•Equally good agreement was obtained between the locations of the failure surface obtained experimentally and the locations of the critical circular failure surface predicted by limit equilibrium.

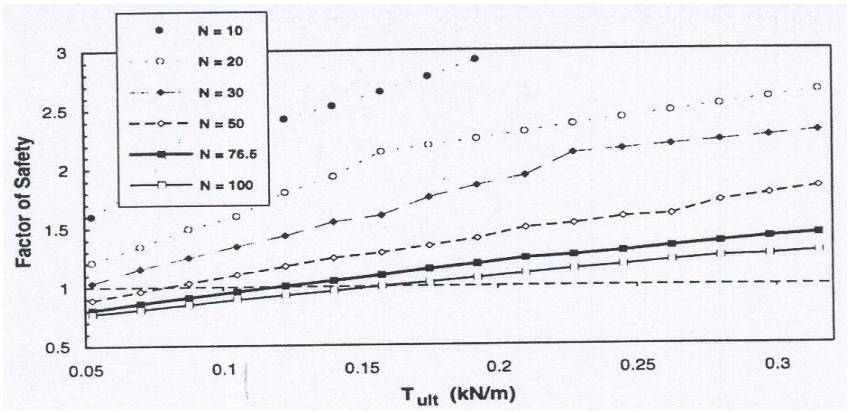

Figure 3.22 Effect of geotextile strength on calculated factor of safety for model B18

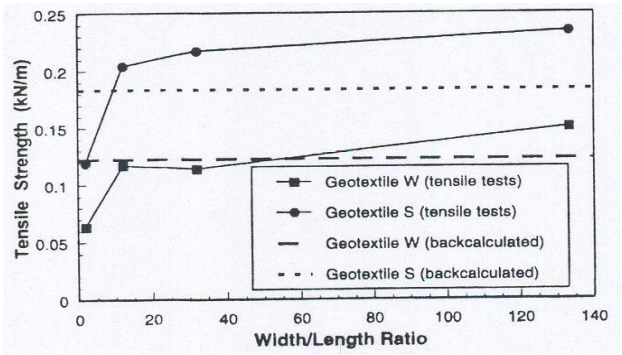

Figure 3.23 Tensile strength of model geotextiles as function of width/length ratio specimen.

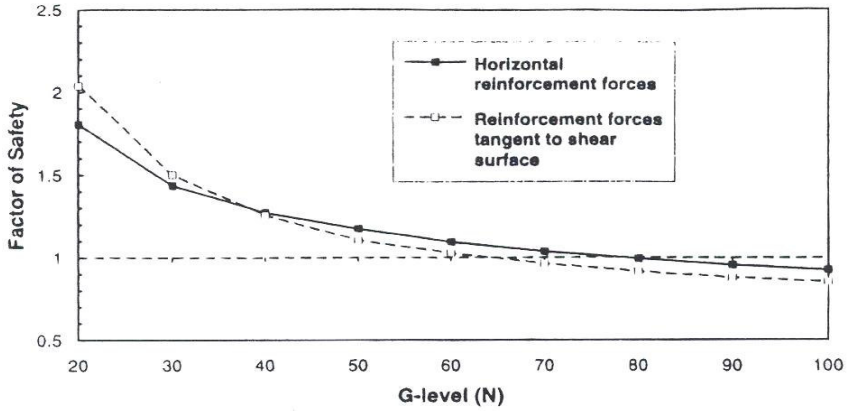

Figure 3.24 Calculated factors of safety for model B18 with increasing acceleration: Effect of orientation of reinforcement forces.

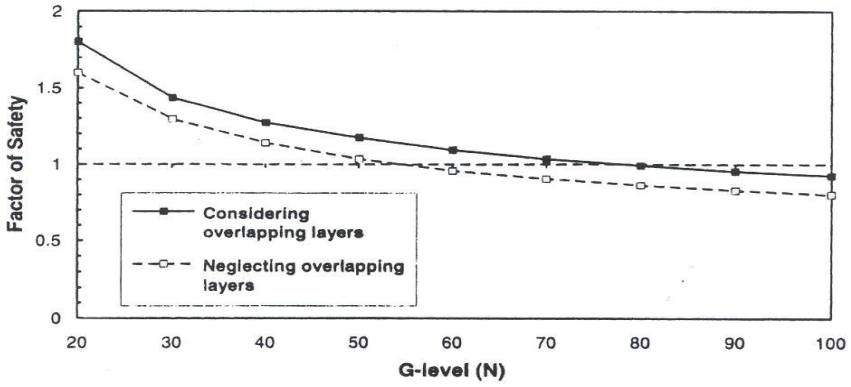

Figure 3.25 Calculated factors of safety for model B18 with increasing acceleration: Effect of geotextile overlaps.

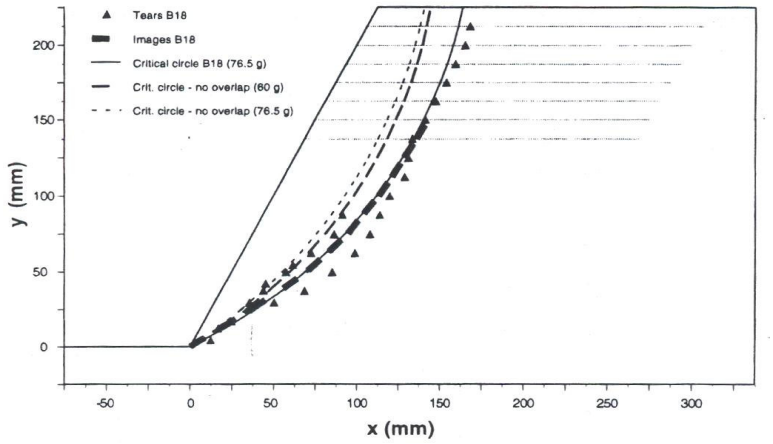

Figure 3.26 Effect of geotextile overlaps on predicted critical circles.

Table 3.2 Factors of safety calculated for model B18 Using Different Limit Equilibrium methods

Method (1)	Calculated factor of safety (2)
(*a*) Methods that satisfy all equilibrium equations	
Spencer (1967)	1.000
Morgenstern and Price (1965)	1.000
Sarma (1973)	1.000
Sarma (1979)	1.000
Janbu (1954)[a]	1.026
Correia (1988)	1.000
(*b*) Methods that do not satisfy all equilibrium equations	
Fellenius (1936)	0.780
Lowe and Karafiath (1960)	1.112
Bishop (1955)	1.000

[a]Janbu's method satisfies all equilibrium conditions except for the moment equilibrium of one slice.

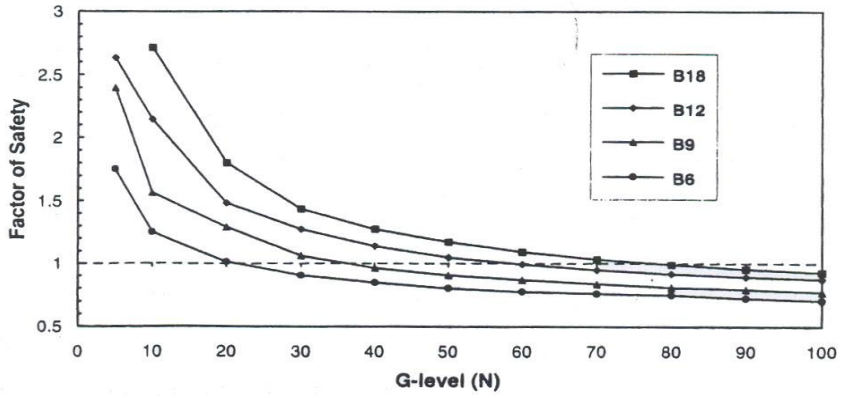

Figure 3.27 Calculated factors of safety with increasing g-level for models in B-series.

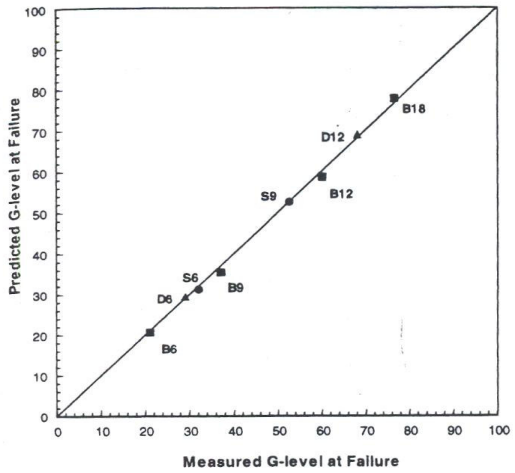

Figure 3.28 Predicted and measured g-levels causing failure for all centrifuge models.

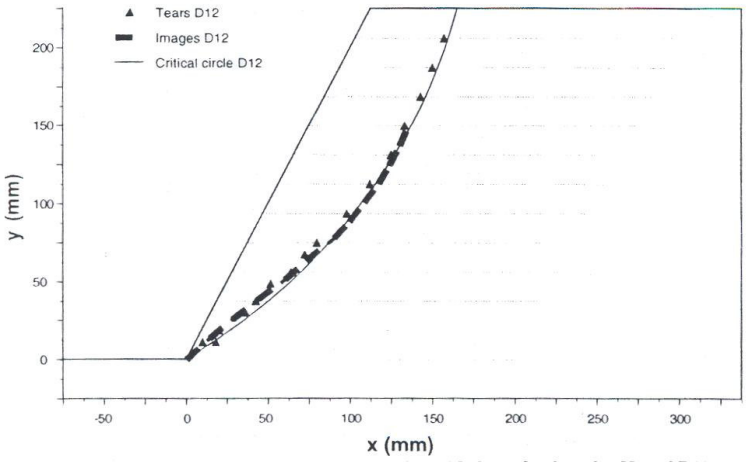

Figure 3.29 Predicted and measured location of failure surface for model D12

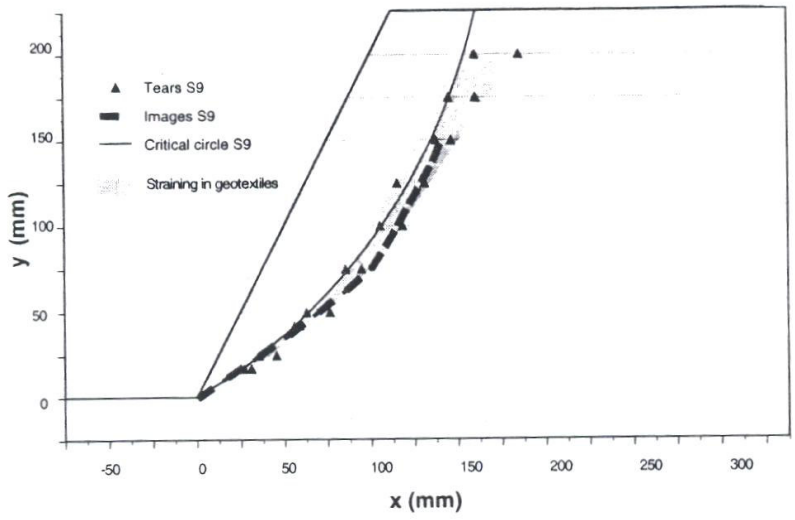

Figure 3.30 Predicted and measured location of failure surface for model S9

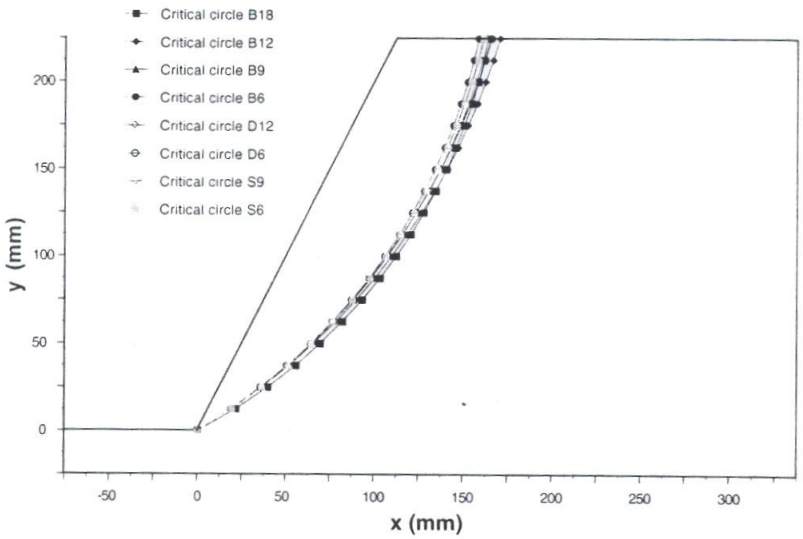

Figure 3.31 Critical circles predicted by Limit Equilibrium for all centrifuge models.

•Experimental observations and the good agreement between experimental and predicted results indicate that the orientation of the reinforcement forces should be considered horizontal in the analysis of reinforced soil slopes.

•Important contribution to the stability of the reinforced slope models was provided by the overlapping reinforcement layers.

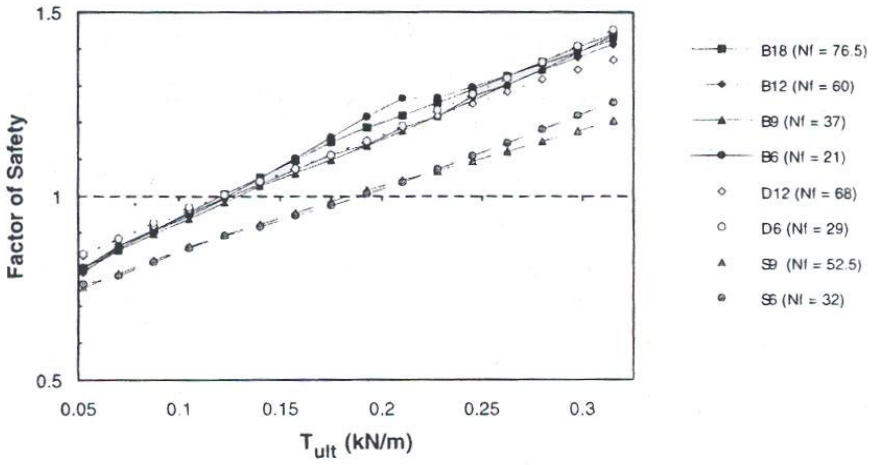

Figure 3.32 Effect of geotextile tensile strength on calculated factor of safety for all centrifuge models.

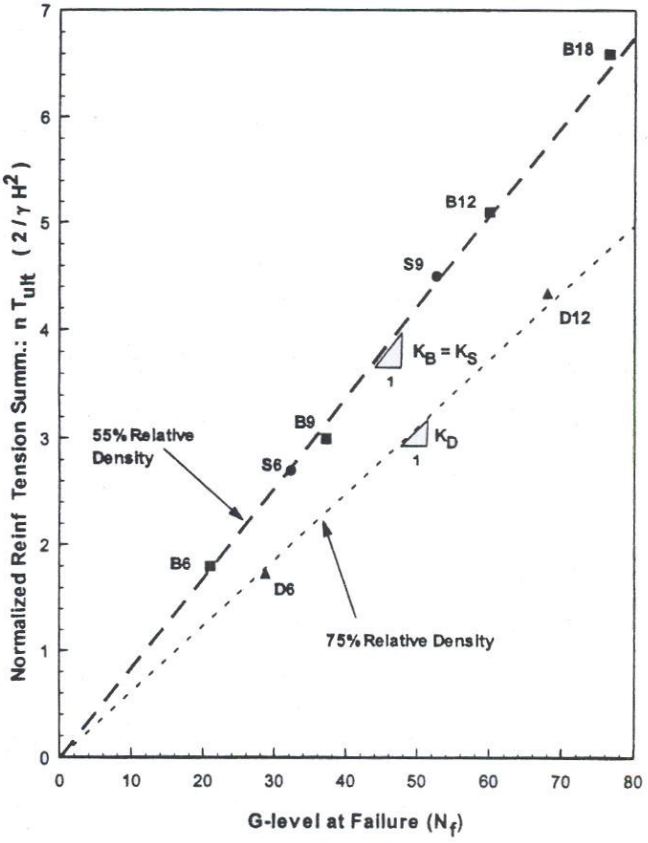

Figure 3.33 Normalized reinforcement tension summation values from centrifuge test results.

•Different rigorous limit equilibrium methodologies evaluated in this paper were found to provide equally good results.
•The centrifuge test results provided insight into the evaluation of in-soil tensile strength of geotextiles and suggest that in-soil improvement of geotextile mechanical properties is induced mainly by the restriction of lateral deformations.
•Consistency of the centrifuge results was observed by the fact that all centrifuge slope models built using the same backfill soil yielded a single Normalized Reinforcement Tension Summation coefficient. The normalization of the experimental results into dimensionless coefficients supports the use of charts for preliminary design of geosynthetic reinforced slopes.

Overall, centrifuge testing provided much needed evidence that limit equilibrium methodologies adequately predict the performance of geosynthetic reinforced soil structures at failure.

3.2.1.1.2 Robert Lo and Dai-Wei Xu (1992)

A new limit equilibrium analysis for assessing the stability of a reinforced embankment on soft clay against rotational undrained failure is presented. The analysis considers strain compatibility along the slip surface to deduce the tension mobilized in extensible reinforcement at collapse condition, and models strain softening of soils along the slip surface.
The configuration studied is shown in Figure3.34. The embankment material is assumed to be homogeneous and fail in a drained condition. The foundation clay is modeled by undrained failure and the strength parameters are; a non zero undrained cohesion and a zero friction angle. Adequate anchorage for the reinforcement is assumed. The slip surface consists of a circle through the foundation clay and a log-spiral through the embankment. The circle and the log-spiral have a common centre.
The reduction of friction angle of the embankment soil with strain softening is expressed by the equations which are modeled by a peak friction angle, $\emptyset_p$ and a strain softening function, r_s (Figure 3.34).

A new limit equilibrium analysis for assessing the stability of a reinforced embankment on soft clay against undrained rotational failure is presented. No statically assumption is

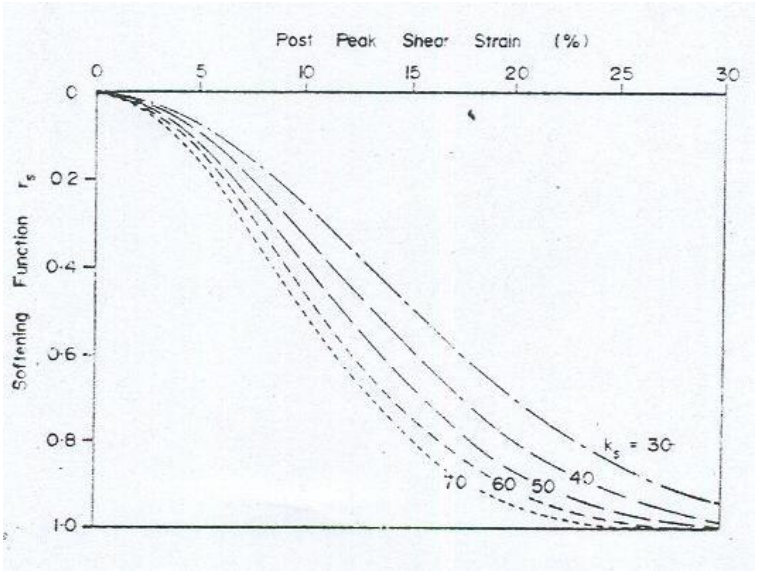

Figure 3.34 Strain softening function. (R.Lo and D.Xu, 1992)

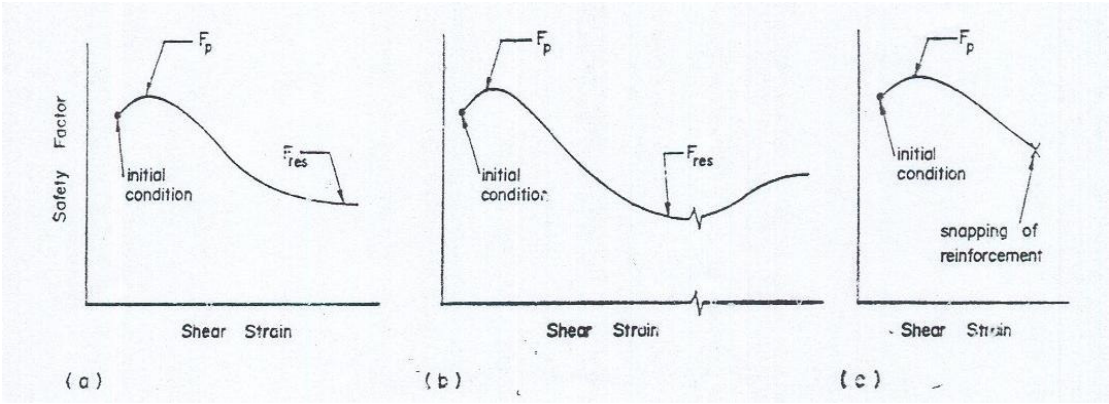

Figure 3.35 Safety factor versus shear strain of soil. (R.Lo and D.Xu, 1992)

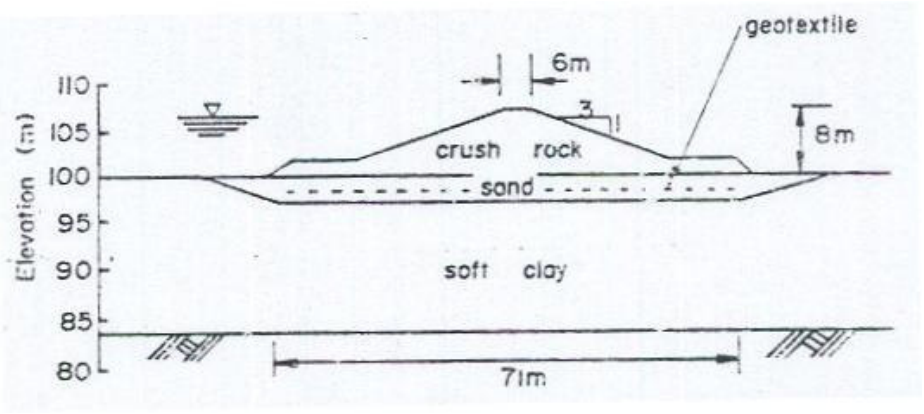

Figure 3.36 Breakwater at Red Bay in China. (R.Lo and D.Xu,1992)

involved in the limit equilibrium equation; and the critical slip surface is located by numerical optimization. The reinforcement force mobilized at collapse is established by considering strain compatibility along the slip surface. Strain softening of soils and influence of confinement on reinforcement properties are modeled. Non-uniform increase in undrained cohesion of the foundation clay during construction can also be considered. The analysis gives a safety factor versus soil strain curve instead of a unique value for the safety factor. A number of parameters for characterizing the safety factor curves are introduced.

Some parametric studies were conducted with the proposed analysis. This leads to the following findings;

(1) The use of residual strength parameters for soils in conjunction with full mobilization of reinforcement tensile strength may not necessarily lead to a conservative solution.

(2) The contribution of reinforcement to stability is significantly dependent on the stiffness of the reinforcement.

(3) Strain softening of soils leads to a significant reduction in the stabilizing effect of reinforcement. The reduction depends on the reinforcement stiffness.

(4) The soil strains required to mobilize peak strength parameters only have a slight effect on the stability.

(5) The stabilizing effect of reinforcement increases linearly with the quantity of reinforcement.

(6) The depth of the critical slip circle increases with *RE*, a measure of the reinforcement's contribution to stability. The depth versus *RE* relationship is essentially the same for all four series of analyses conducted.

(7) The increase in reinforcement strength and stiffness due to confinement may lead to a significant increase in the stability.

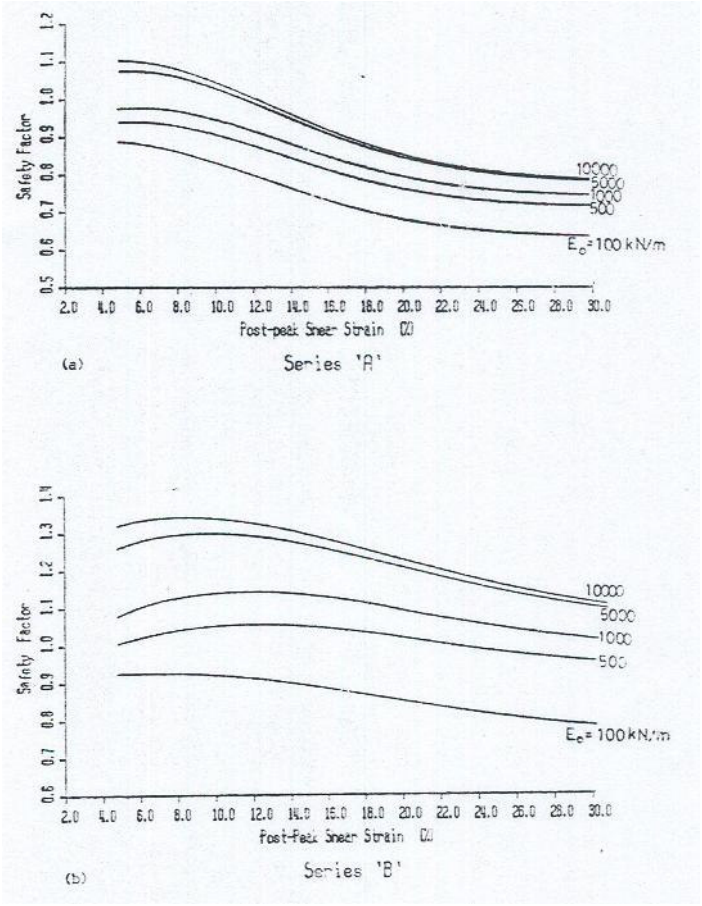

Figure 3.37 Safety factor curves : (a) Series A , (b) Series B (R.Lo and D.Xu,1992)

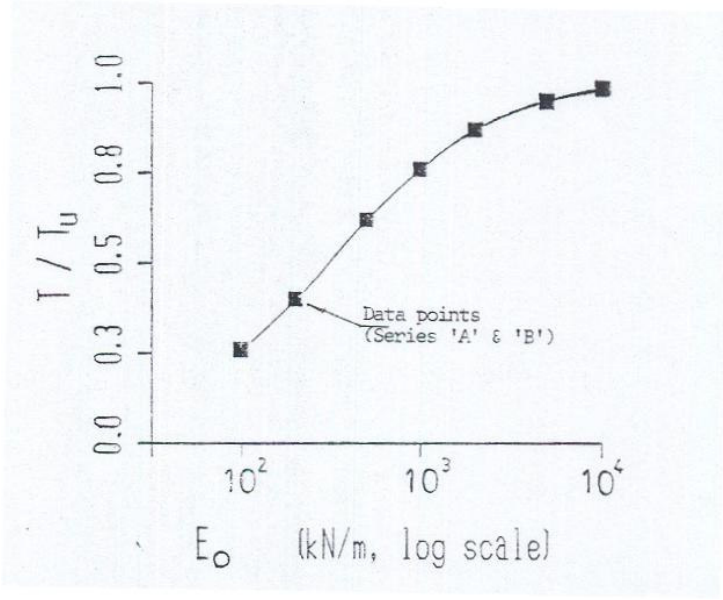

Figure 3.38 Tension force mobilized at F_{res} state. (R.Lo and D.Xu, 1992)

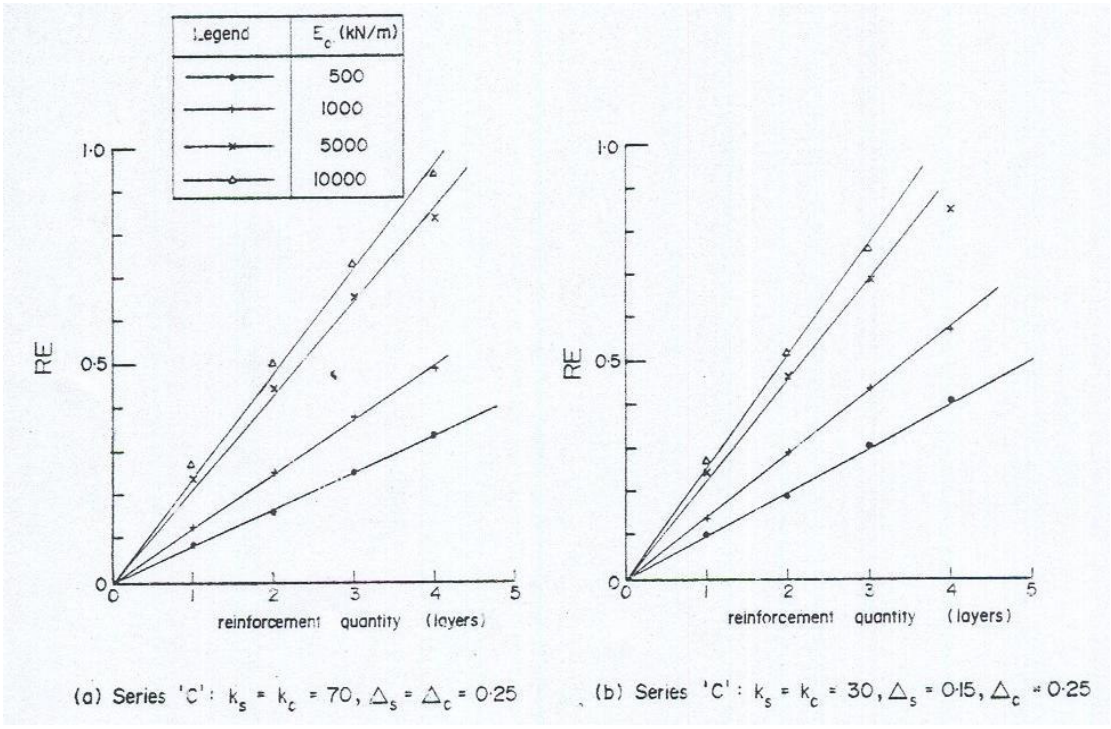

Figure 3.39 Influence of reinforcement quantity on R.E. (a) Series C , (b) Series D. (R.Lo and D.Xu, 1992)

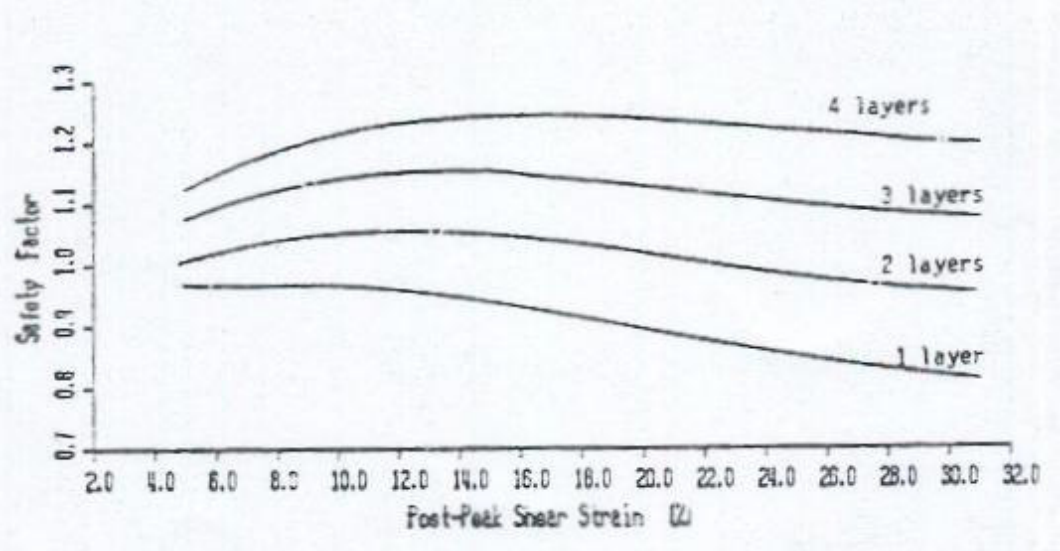

Figure 3.40 Influence of reinforcement quantity on shape of safety factor curve. (R.Lo and D.Xu, 1992)

3.2.1.1.3 J.Edirisinghe , N.Yagi, M.Enoki , R.Yatabe and G.Ohashi (1996)

In this study, scientists discussed the suitability of a method for analyzing stability of geotextile reinforced slopes by the Generalized Limit Equilibrium Method (GLEM) which is proposed by Enoki, (1991) before, for analyzing stability problems. In order to investigate the suitability of the proposed reinforcing mechanism and the proposed stability analysis method, a series of model tests were carried out on the bearing capacity of shallow foundations located at the crest of a reinforced slope. Finally the observations of model tests and the results of the analytical method were compared.

A series of direct shear tests were carried out in order to evaluate the role of geotextiles when the slip surface is fixed. The main objectives of these experiments were to determine the change of effectiveness of geotextiles considering various factors on strengthening the ambient of soil mass. Those factors included initial inclination with respect to the slip surface, the failure mode of the geotextiles.

After the analyses the final shape of the geotextiles are assumed to have one of the three shapes shown in Figure 3.41. Limit equilibrium analysis of geotextile reinforced slopes are done by using the block system in the GLEM method (Figure 3.42). Then energy equilibrium based analyses are done. In this method, non-circular or circular slip surfaces can be analyzed.

The main object of this series of experiments was to investigate the suitability of the proposed reinforced mechanism and present the method for suitability analysis. The apparatus used for the experiments is shown in Figure 3.43. Observations from model test were investigated analytically using the proposed method, GLEM and some conventional methods such as the Fellenius and simplified Janbu methods. The slip surfaces and bearing capacities obtained by these methods are shown in Figure 3.44 and Table.3.3

According to these observations, it can be concluded that the results from the proposed reinforcing mechanism with the proposed analytical method can give reasonable results in terms of slip surface and stresses compared to experimental observations.

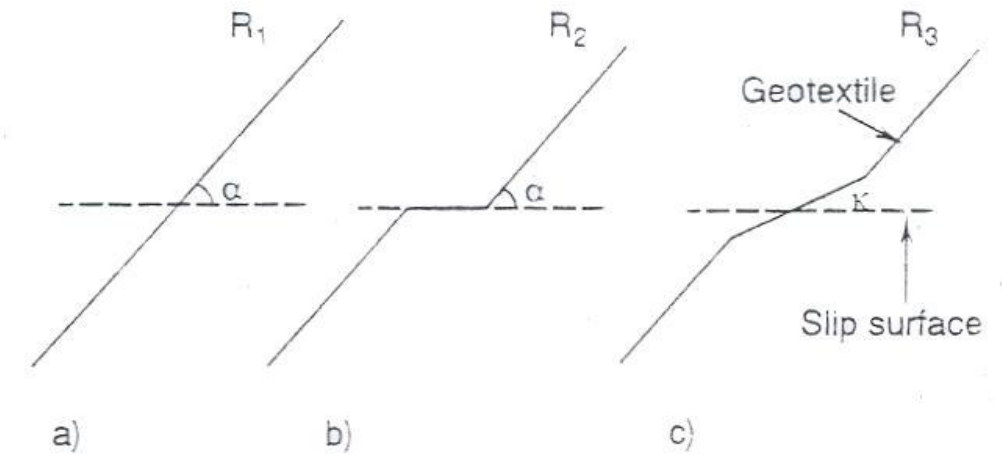

Figure 3.41 Configuration of the geotextiles after generation of the slip surface.
(Edirisinghe *et al.*, 1996)

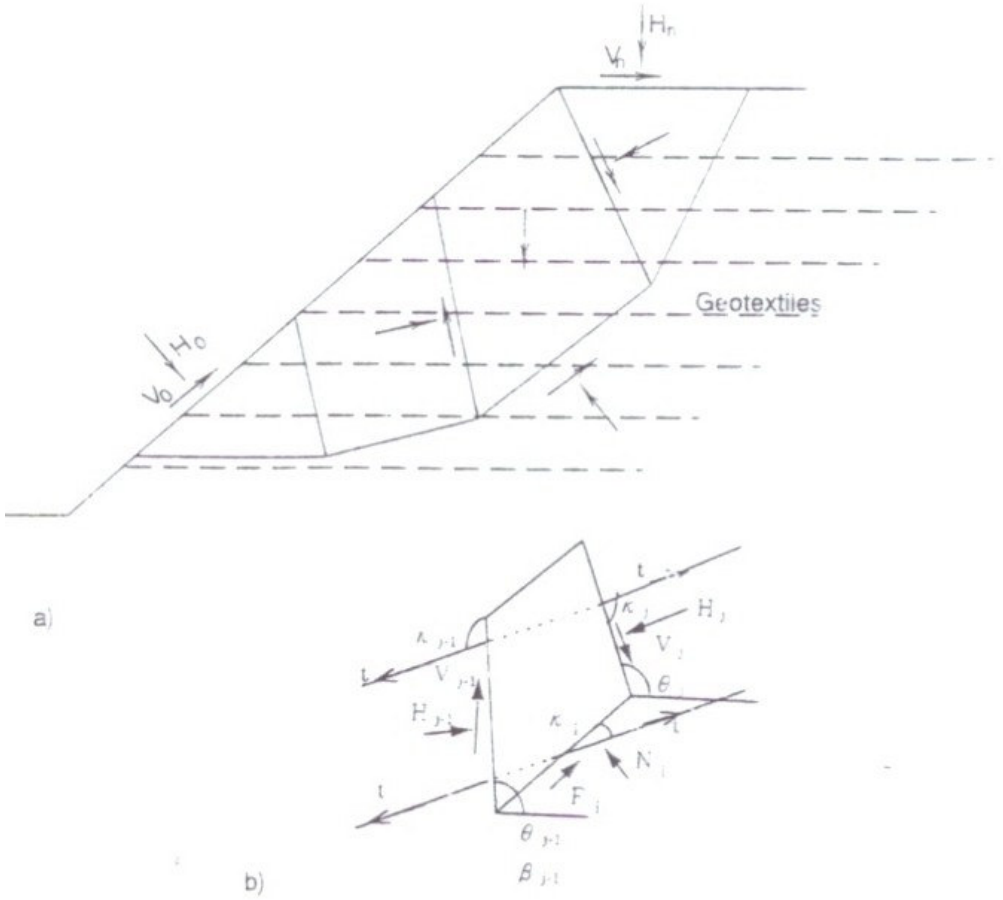

Figure 3.42 Block system used for analysis. (Edirisinghe *et al.*, 1996)

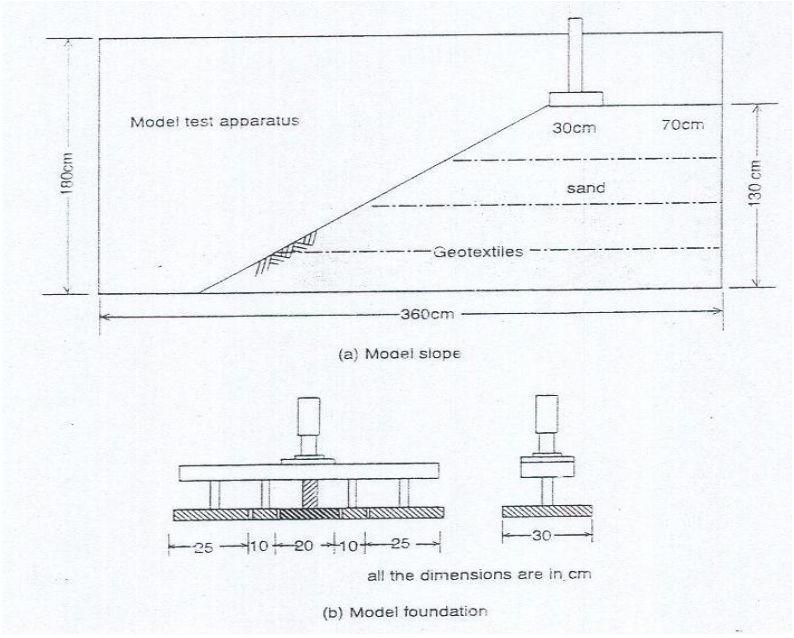

Figure 3.43 Model slope and model foundation. (Edirisinghe *et al.*, 1996)

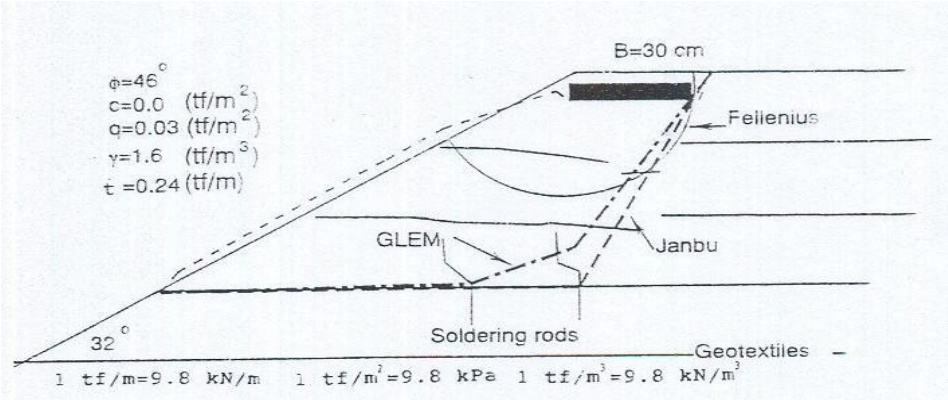

Figure 3.44 Comparison of slip surfaces for a bearing capacity problem of a reinforced slope. (Edirisinghe *et al.*, 1996)

Table 3.3 Comparison of bearing capacity determined experimentally and analytically. (Edirisinghe *et al.*, 1996)

	q_u (tf/m²)		
	R_1	R_2	R_3
GLEM	25.90	23.14	25.94
Janbu	10.37	8.98	10.62
Fellenius	11.93	10.58	13.05
Experiments	22.28		

1 tf/m²=9.8 kPa

3.2.1.2 Finite Elements Analyses.

Use of finite element method for geotechnical engineering began in 1966, when Clough and Woodward used it to determine stresses and movements in embankments, and Reyes and Deer described its application to analysis of underground openings in rock. Many research studies and practical applications have taken place in the intervening 35 years. During this period, considerable advances have been made in theory and practice, and the cost of computers has diminished to a small fraction of the cost 35 years ago.

Almost all geotechnical finite elements analyses are performed in steps that simulate a sequence of reveal events, such as the successive stages of excavation of a braced or unbraced cut, or placement of fill on an embankment. Performing the analyses in steps has two important advantages for geotechnical problems:

(1) The geometry can be changed from one step to the next to simulate excavation or fill placement, by removing elements or adding elements to the mesh.

(2) The properties of the soil can be changed from one step to the next to simulate the changes in behavior that result from changes in the stresses within the soil mass.

The amount of time and effort required for finite element analyses is very little, dynamic analyses are possible and easy to do. Also the cost of finite element analyses decreased last years because of the decrease in the cost of computers.

The finite element method complements field instrumentation studies very well because each stage in the analysis represents an actual condition during or following construction. By comparing the results of the finite elements analyses with measured behavior, the accuracy of the analyses can be assessed. If the calculated values are close enough to measured values to give confidence in the analytical results, the analyses can be used to infer information about aspects of the behavior that is not shown directly by the instrumentation. Finite element analyses thus extend the value of instrumentation studies by filling out the picture of behavior that ca be derived from the field measurements. Finite element analyses have also proved very useful for planning instrumentation studies by showing where instruments can be located to best advantage. In addition, the process of comparing calculated and measures results fits very well into the use of observational method, which offers one of the most reliable approaches for unusual and difficult problems.

3.2.1.2.1 K.San, D Leshchinsky, T.Matsui (1994)

In this study, comparisons between finite element and limit equilibrium reinforced slope stability analyses are conducted. First, reinforced slopes with dense and loose backfills, for three slope inclinations, are analyzed by the limit equilibrium analysis. Then finite element analysis of the reinforced slopes¸ designed by the limit equilibrium analysis is performed utilizing the Duncan and Chang et al. (1970) model. The backfill material properties correspond to data from triaxial tests, but the coefficient of earth pressure at–rest is chosen so that the limit equilibrium result of one arbitrary slope inclination will fit the finite element result. Finally, using the same parameters, finite element analysis for other slopes is performed and compared with the limit equilibrium analysis.

The design problem to be considered is a 5 m high granular slope with ten equally spaced horizontal reinforcement layers, as shown in Figure 3.45. The overall safety factor, F_s, is 1.0. Two types of backfills are considered, dense backfill with c=0.0 and Ø=35°, and loose backfill having a trace of cohesion with c=3.0 kPa and Ø=20°. For both backfills γ =20 kN/m³. The soil-geosynthetic interaction coefficients are C_i =0.8 and C_{ds}=1.0. C_i represents the ratio between Coulomb's shear strength of the interface of reinforcement-backfill and the shear strength of backfill; its value is typically determined from pullout test (Leshchinsky, 1992). C_{ds} is the direct sliding coefficient and it represents a similar relationship as C_i, however its value is established based on a direct shear test, presumably simulating the sliding of soil block over the reinforcement layer (Leshchinsky, 1992).

Three slope inclinations were studied (i equals 75°, 60° and 45°). The analysis was conducted using 'STRATA-SLOPE', a limit equilibrium slope stability analysis computer code (Leshchinsky et al. 1992). In this procedure, the reinforcement strength is determined based on internal stability considerations; reinforcement length is determined based on possible compound failure and direct sliding of the reinforced mass.

In assessing the internal stability, log spiral slip surfaces, passing through all reinforcing layers, are examined; the one rendering the maximum required reinforcement strength is considered the critical surface. Leshchinsky and Lambert, (1991) have demonstrated the adequacy of log spirals to represent critical slip surfaces in reinforced slopes.

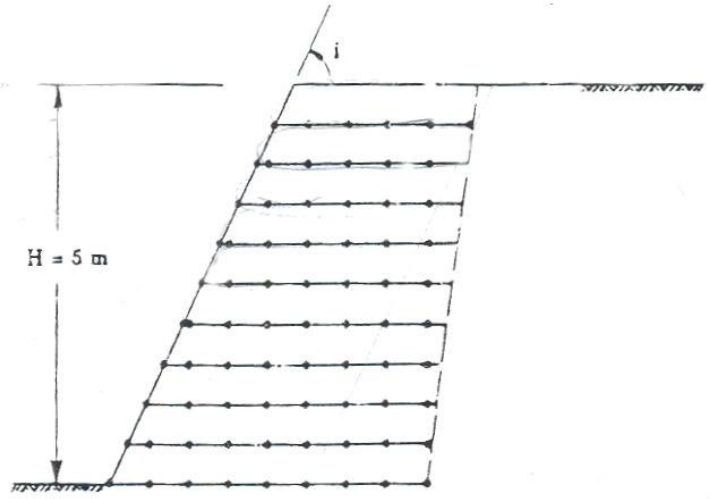

Figure 3.45 The slope to be considered

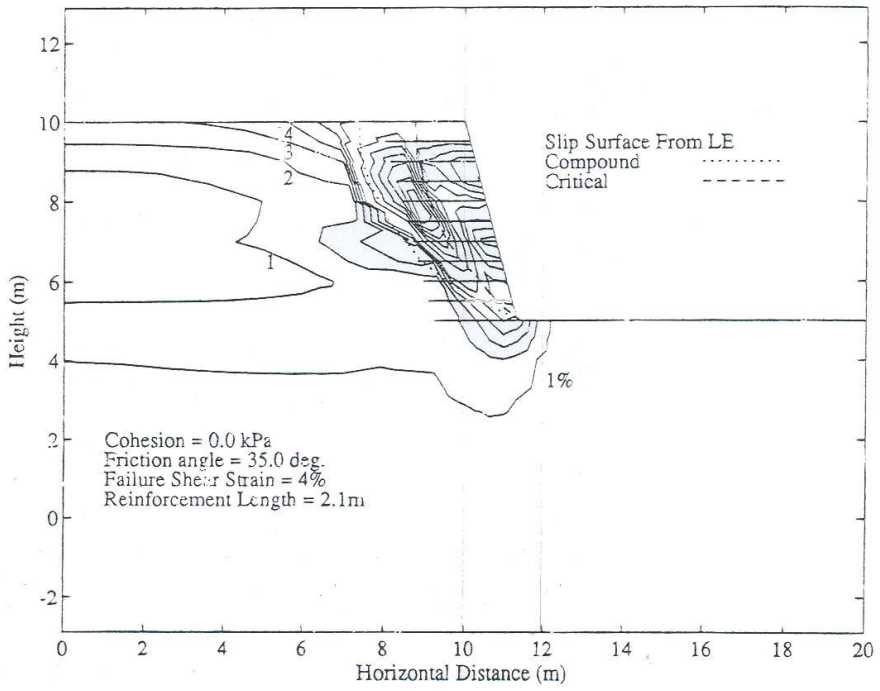

Figure 3.46 Failure pattern for 75º slope (dense granular backfill) (San *et al.*, 1994)

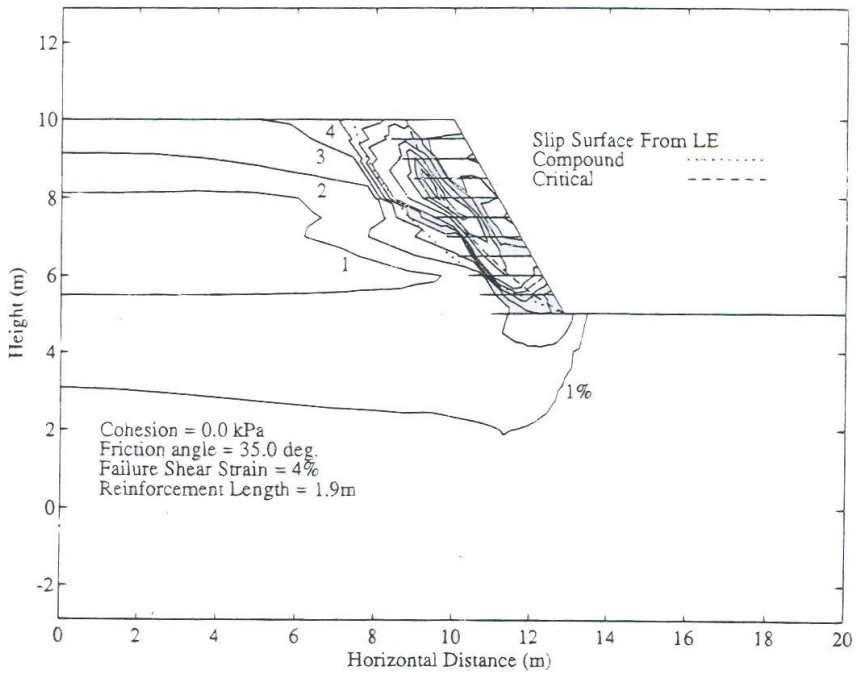

Figure 3.47 Failure pattern for 60º slope (dense granular backfill) (San *et al.*, 1994)

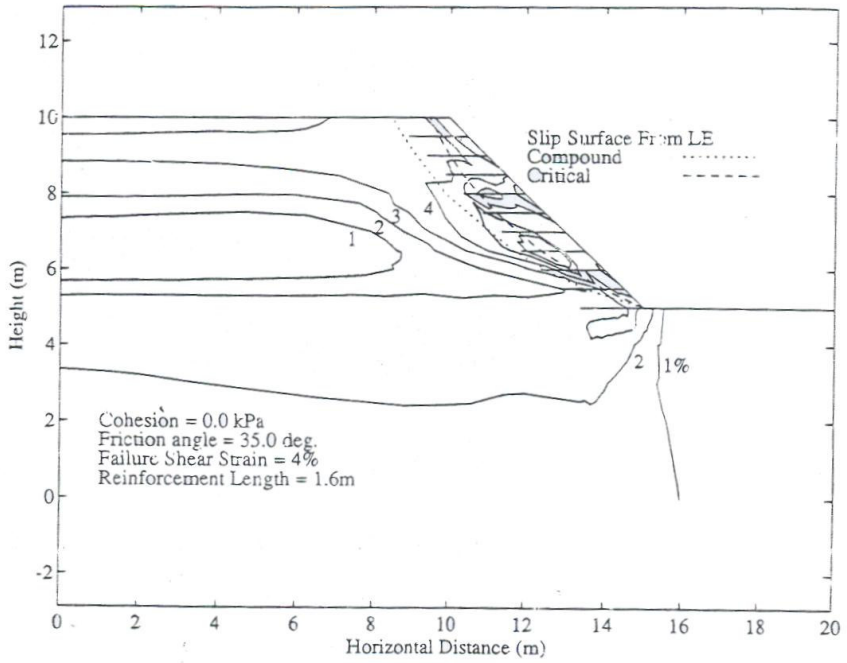

Figure 3.48 Failure pattern for 45º slope (dense granular backfill) (San *et al.*, 1994)

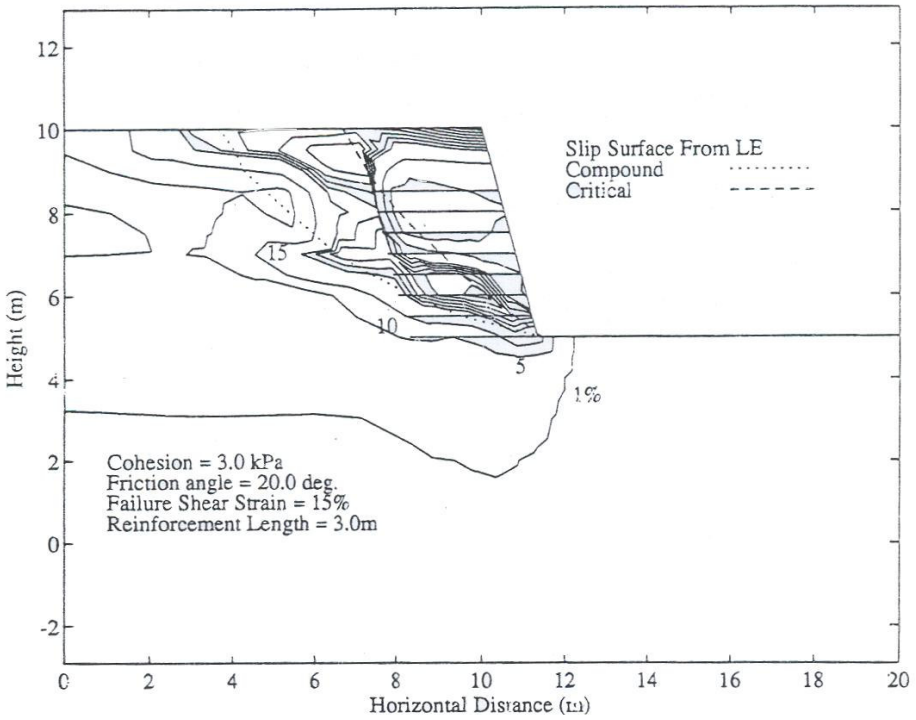

Figure 3.49 Failure pattern for 75º slope (loose backfill) (San *et al.*, 1994)

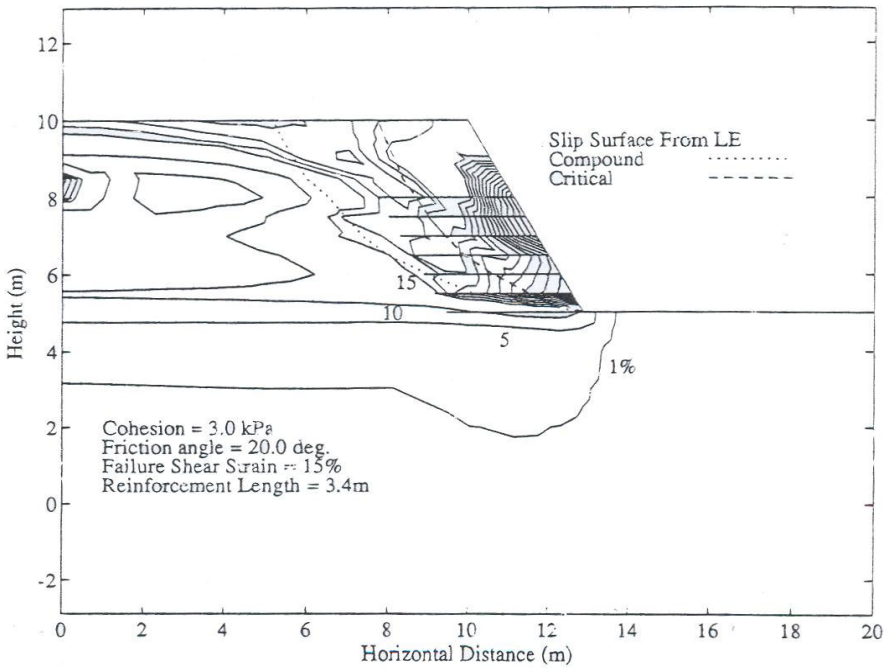

Figure 3.50 Failure pattern for 60º slope (loose backfill) (San *et al.*, 1994)

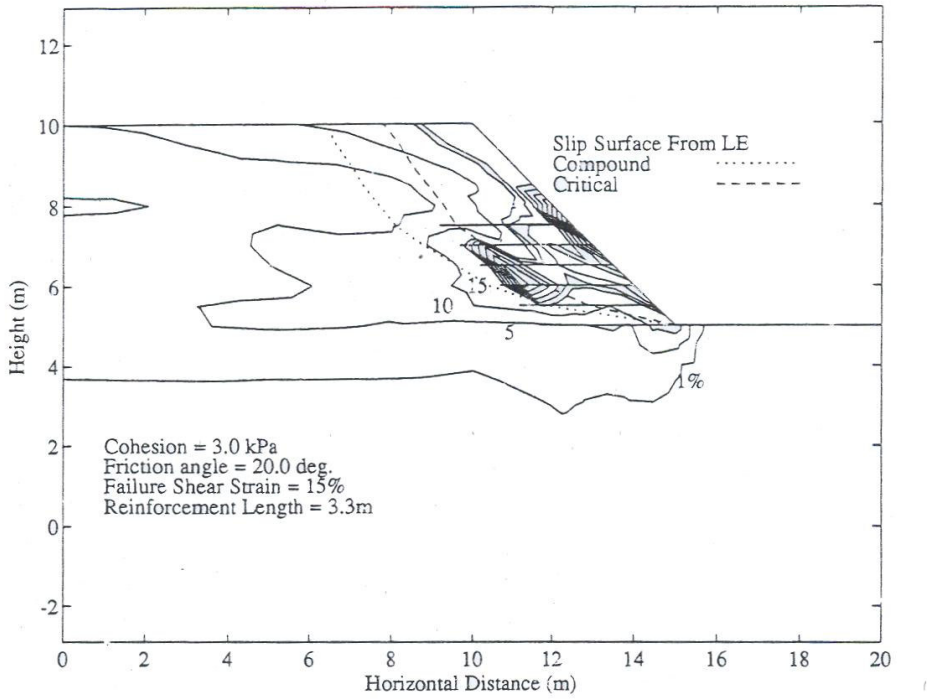

Figure 3.51 Failure pattern for 45º slope (loose backfill) (San *et al.*, 1994)

Table 3.4 Required reinforcement strength (kN/m) (Dense granular backfill)

i	Finite Element Method	Strata slope	Difference
75º	9.0	8.0	1.0
60º	6.0	5.0	1.0
45º	3.0	2.0	1.0

Table 3.5 Required reinforcement strength (kN/m) (Loose backfill)

i	Finite Element Method	Strata slope	Difference
75º	57.7	41.1	16.6
60º	19.2	23.9	4.7
45º	14.0	8.9	5.1

Table 3.6 Summation of required tensile resistance of all layers of reinforcement (kN/m)
(Dense granular backfill)

i	Finite Element Method	Strata slope	Difference
75º	9.0	8.0	1.0
60º	6.0	5.0	1.0
45º	3.0	2.0	1.0

Table 3.7 Summation of required tensile resistance of all layers of reinforcement (kN/m)
(Loose backfill)

i	Finite Element Method	Strata slope	Difference
75º	9.0	8.0	1.0
60º	6.0	5.0	1.0
45º	3.0	2.0	1.0

Furthermore, they have shown that the maximum height of a stable slope based on the log spiral limit equilibrium analysis procedure is very close to the measured value.

Referring to Fig.3.45, reinforcement length at the bottom is selected based on the direct sliding or compound failure; top reinforcement length is based on maximum length obtained from compound failure analysis. Length of intermediate layers is adjusted according to top and bottom layers. This practical layout results in overall reinforcement length that is somewhat longer than necessary based on compound failure.

The use of finite element method to analyze the stability of geotechnical problems needs an appropriate definition of failure. Definitions of failure commonly used in practice are mainly based on stress failure criterion. However, it appears that failure of a soil structure is more reasonably defined as a state of rapid increase of strains. Consequently, a strain based failure judgement method for finite element stability analysis has been proposed by Matsui and San, (1993). In the finite element analysis, failure is defined as the development of a full failure shear strain zone in the soil. The failure shear strain zone is the potential failure pattern in which the shear strain exceeds a cut off value (Matsui and

San, 1990), (Matsui and San, 1992b). The failure shear strain of soil can be obtained from the standard triaxial test.

The critical lengths of the reinforcement obtained from limit equilibrium analysis for a safety factor of F_s=1 are used as an input in the finite element analysis. The finite element analysis of the reinforced slope was performed by adding elements from the bottom to the top of the slope, and applying the gravity force to each element. The $K_0= \sigma_h/\sigma_v$ value was used to specify the initial stresses of the added elements. In the finite element analysis of the 60° slopes, for both dense and loose backfills, the value of K_0 was gradually reduced in subsequent runs from its empirical value (K_0=1-sinØ) until the failure of the slope occurred using the strain-based failure judgement method. It should be noted that the empirical value (K_0=1-sinØ) may not always satisfy the initial boundary conditions. The empirical values (K_0=1-sinØ) of the dense and loose backfills are 0.43 and 0.66 respectively. It was found the value of K_0, at failure for the dense and loose backfill walls are 0.40 and 0.62 respectively. Using these values of K_0, analyses of 75° and 45° slopes for both dense and loose backfills were conducted. The maximum reinforcement tensile force and the failure pattern of the reinforced slopes were then compared with the results obtained from limit equilibrium analysis. The required reinforcement strengths from finite element are quite close to those from limit equilibrium as shown in Table 3.4 and Table 3.5. The summation of required tensile resistance of all reinforcement layers for both backfills obtained from finite element are reasonably close to those obtained from limit equilibrium (Table 3.6 and Table 3.7). The comparisons of finite elements and limit equilibrium are shown in Figure 3.45 to Figure 3.51.

As the result of comparison between finite element and limit equilibrium analyses, it is found that good agreement between them for a range of slope inclinations could be achieved by adjusting slightly the empirical value of K_0. Using a consistent value of K_0, the results of finite element analysis agreed reasonably well with limit equilibrium results.

3.2.1.2.2 M.C.Alfaro, S.Hayashi, N.Miura and D.T.Bergado (1997)

This study focuses on the patterns of deformation of the wall and the soft clay foundation beneath the reinforced soil mass based from the results of full-scale field tests and finite elements analyses. The performances of two reinforced soil test wall-embankment systems

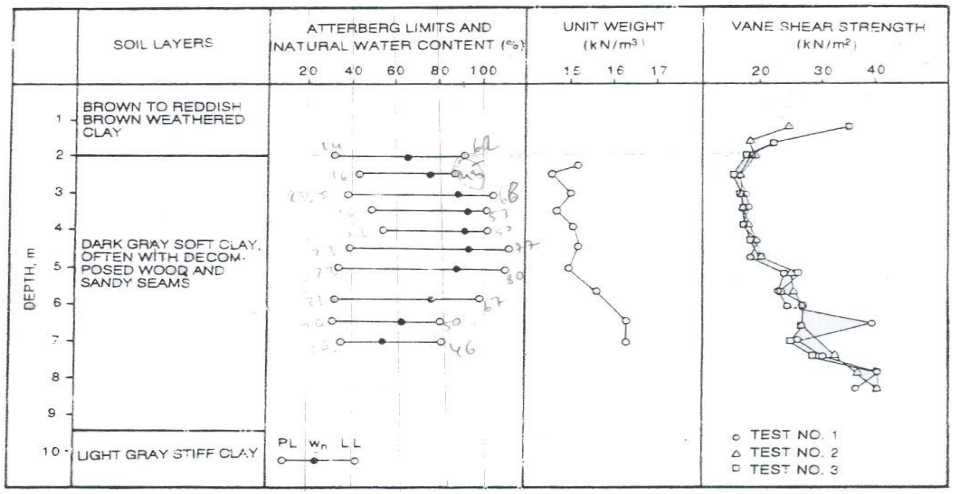

Figure 3.52 Subsoil profile and properties of the foundation at the site of test facilities. (Alfaro *et al.*, 1997)

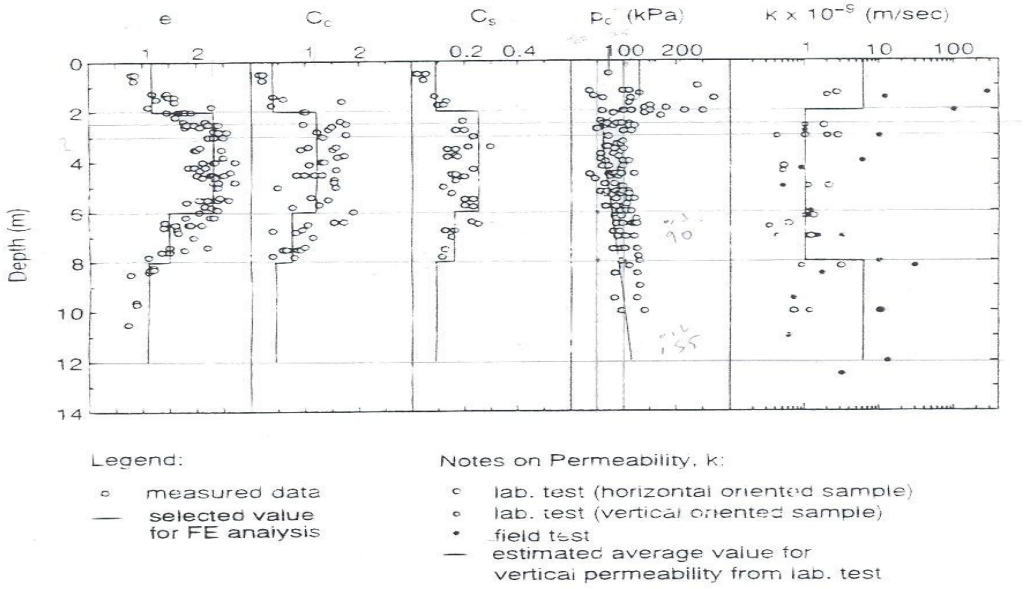

Figure 3.53 Variation of deformation parameters with depth of the foundation. (Alfaro *et al.*, 1997)

Table 3.8 Summary of soil properties for compacted weathered clay backfill.(Alfaro *et al.*,1997)

Soil	G_s	W_P (%)	W_L (%)	I_P (%)	Passing sieve no. 200 (0.075 mm) (%)	W_{OPT} (%)	$\gamma_{d\,max}$ (kN/m³)	Direct shear		Unconsolidated undrained TC	
								c (kPa)	ϕ (degrees)	c (kPa)	ϕ (degrees)
Weathered clay	2.67	21.0	45.0	24.0	22.0	22.0	16.3	129.0	30.7	118.0	30.7

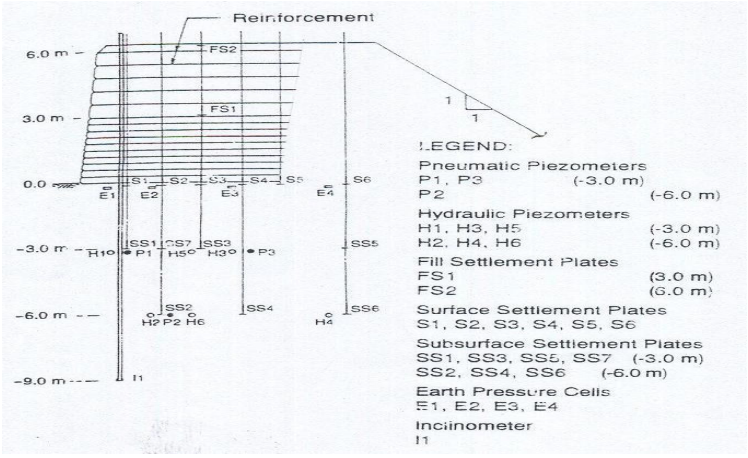

Figure 3.54 Cross-section of test facility II indicating key foundation instrumentations. (Alfaro *et al.*, 1997)

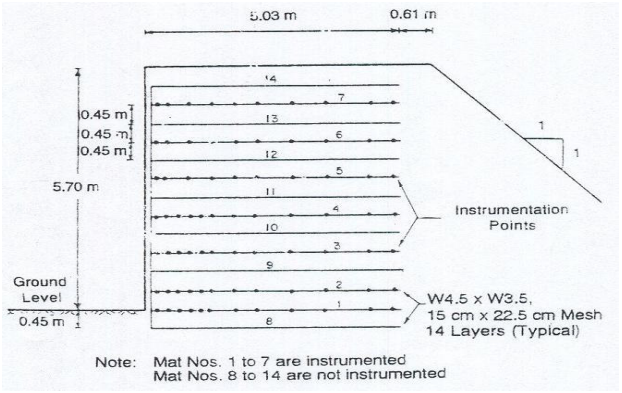

Figure 3.55 Cross-section of test facility I indicating reinforcement instrumentations. (Alfaro *et al.*, 1997)

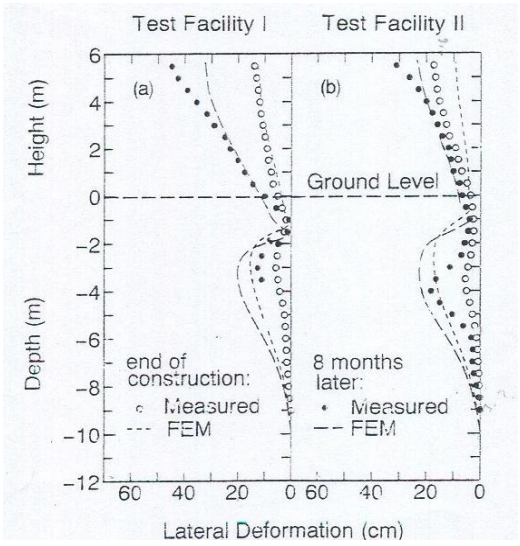

Figure 3.56 Measured and simulated lateral deformations. (Alfaro *et al.*, 1997)

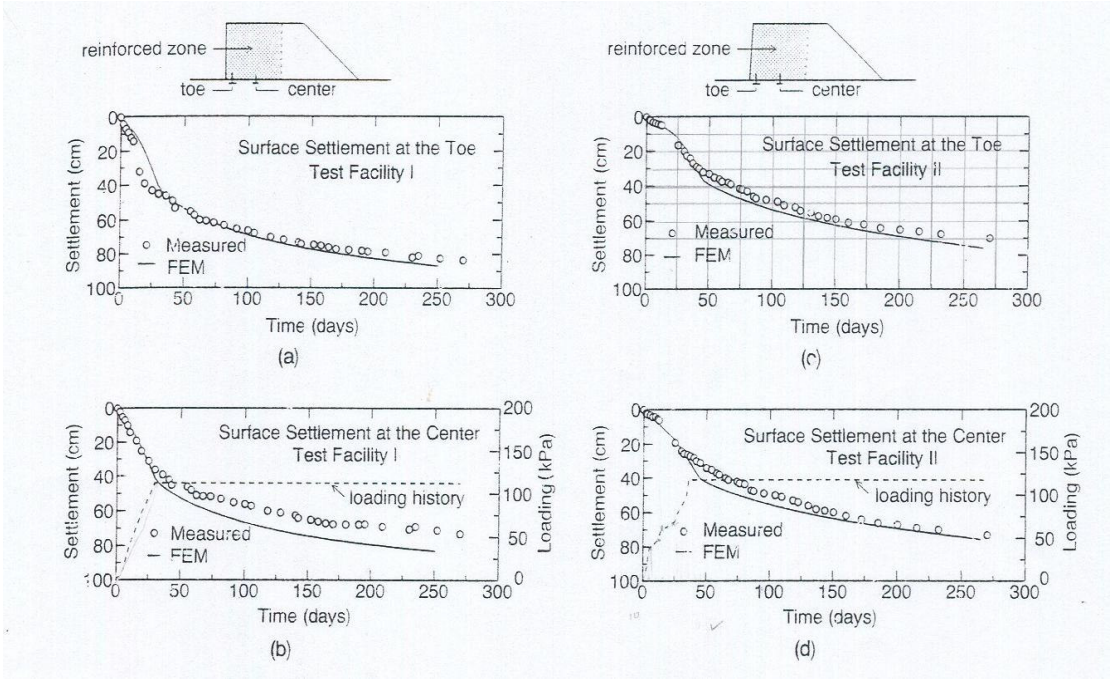

Figure 3.57 Measured and simulated rate of foundation settlements. (Alfaro *et al.*, 1997)

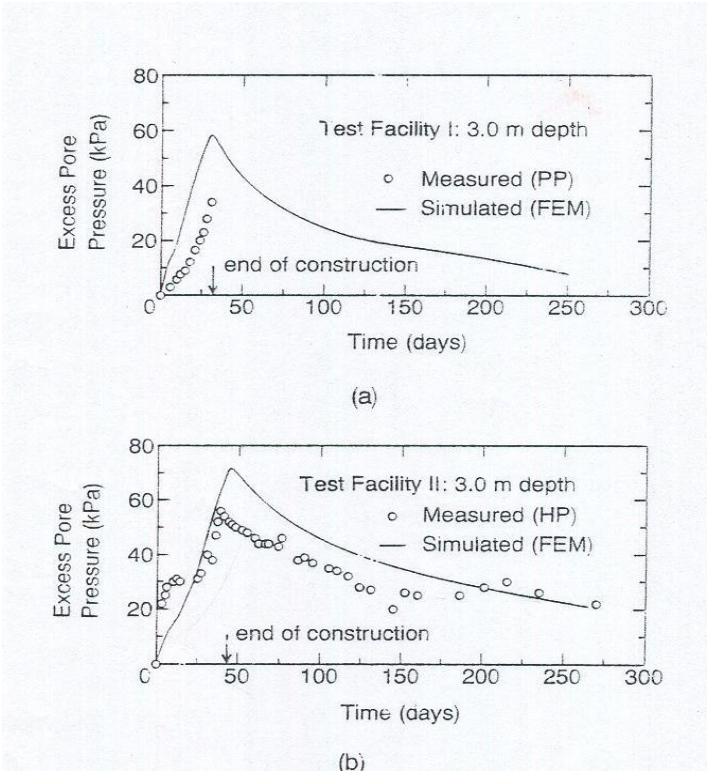

Figure 3.58 Measured and simulated excess pore water pressure dissipations with time. (Alfaro *et al.*, 1997)

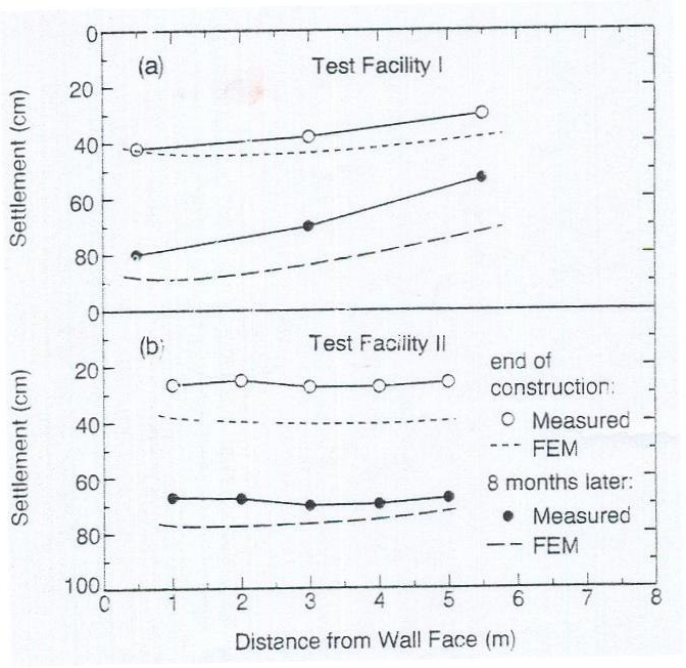

Figure 3.59 Measured and simulated settlement profile below the reinforced soil mass. (Alfaro *et al.*, 1997)

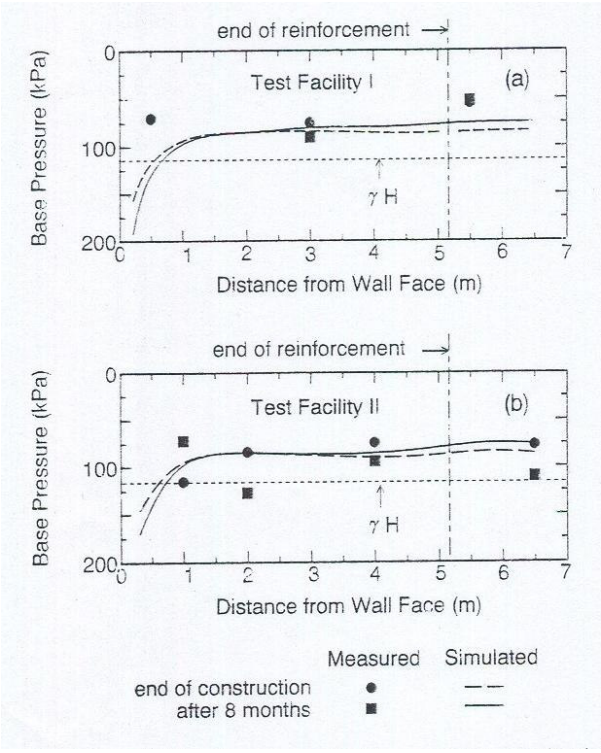

Figure 3.60 Measured and simulated vertical base pressure distributions. (Alfaro *et al.*, 1997)

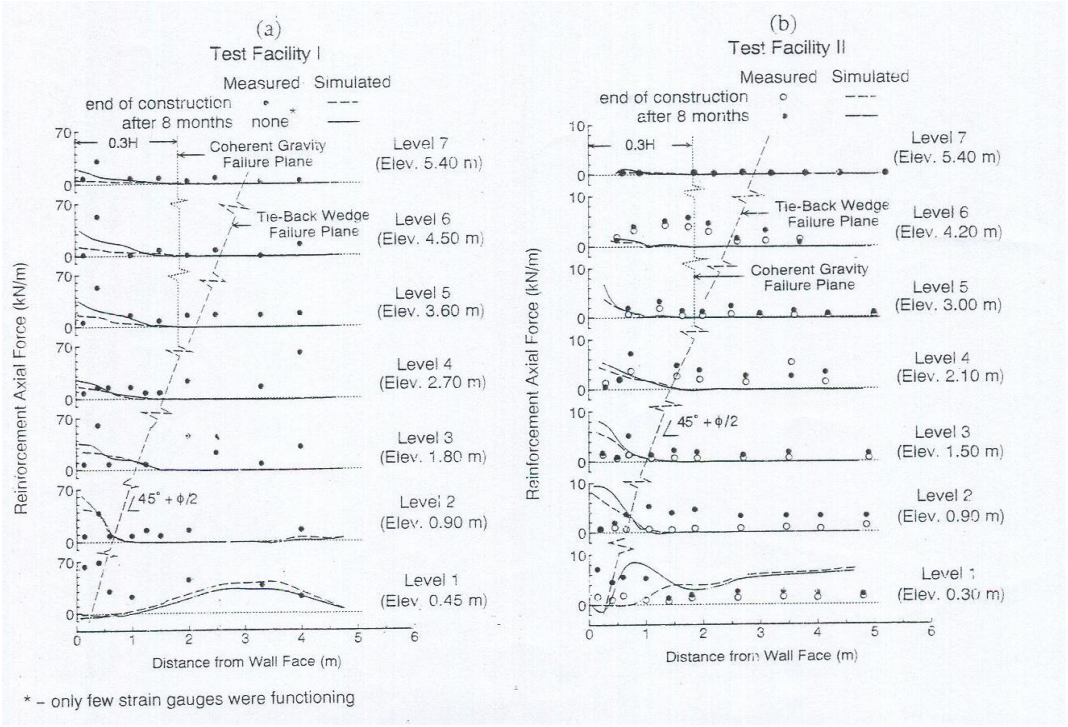

Figure 3.61 Comparison of S-wave velocity between empirical formula and test results. (Alfaro et al., 1997)

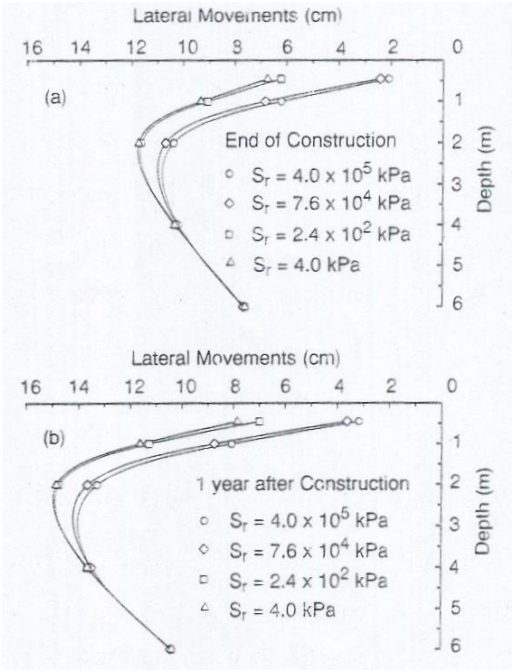

Figure 3.62 Computed lateral deformations at the foundation. (Alfaro *et al.*, 1997)

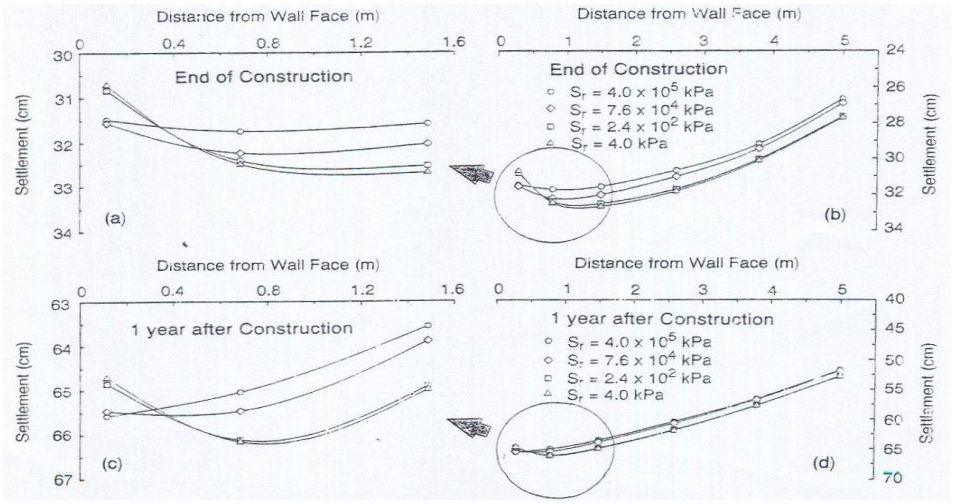

Figure 3.63 Computed settlement profiles below the reinforced soil mass. (Alfaro *et al.*,1997)

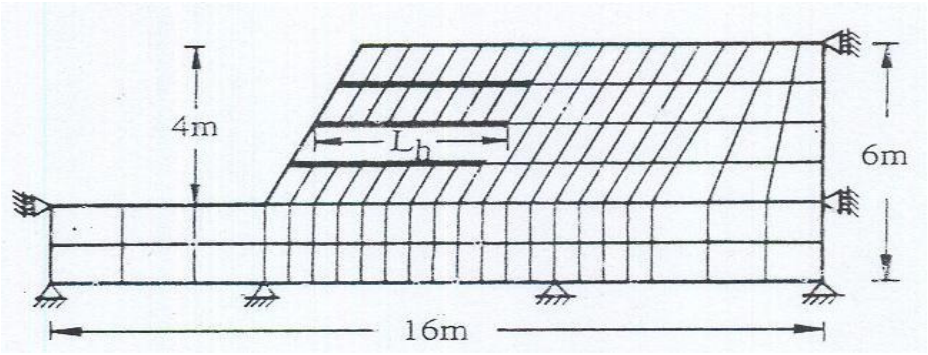

Figure 3.64 Finite element array for the reinforced slope stability problem. (Asaoka *et al.*, 1994)

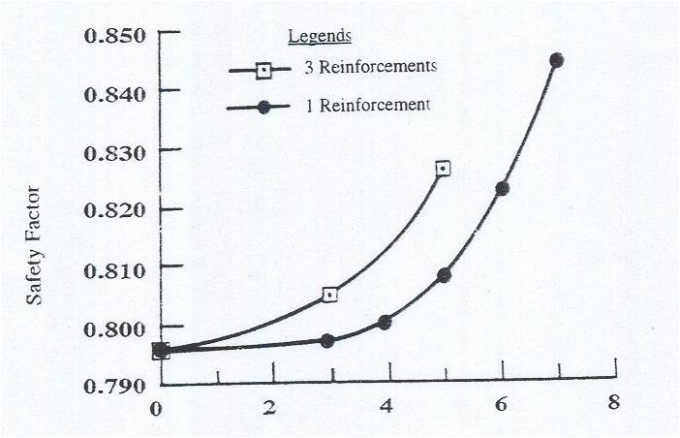

Figure 3.65 The computed factor of safety versus reinforcement length in slope stability problem with Mises material. (Asaoka *et al.*, 1994)

constructed on soft clay foundation with different reinforcement types but have the same backfill soils were used in the investigation. One test facility used steel grid reinforcements (higher stiffness or rigidity) and the other used polymer grid reinforcements (lower stiffness). Measurements from the instrumentations of these test facilities were compared with the results from numerical simulations based on a finite element solutions in which reasonable agreement were obtained. Parametric studies were then carried out to examine the effects of the stiffness of the reinforced soil system and the foundation on the overall deformation characteristics of reinforced soil wall. Results indicated that increasing the stiffness or rigidity of the reinforced soil system led to lower lateral spreading of the soft clay foundation owing to more lateral confinement of the underlying soil as compared with less stiff reinforced soil system tended to rotate more about the toe compared to that which has lesser system stiffness. Consequently, the pattern of foundation movements associated with system stiffness affected also the outward facing movement of the reinforced soil wall. It was found that the increase in reinforced soil system stiffness does not necessarily result to the reduction of the outward lateral wall deformation.

3.2.1.2.3 A.Asaoka, T.Kodaka, and G.Pokharel (1994)

The development of internal force in the reinforcement material as well as in the panel facing and their effect in the limiting equilibrium state of soil mass has been studied using rigid plastic finite element method. This research computes the axial force in reinforcing material as well as bearing capacity/factor of safety, velocity vectors and stress distribution simultaneously. Meanwhile, the mechanism of soil reinforcement is modeled by no length change condition that should be a kind of constraint condition imposed upon the plastic flow of soil skeleton at limiting equilibrium state. The computed factor of safety shows that the reinforcement is more effective in c-Ø material than purely cohesive soil. The effect of rigidity of panel facing is also clearly explained with the help of the axial and shear force developed in the facing.

As a result of this study, rigid-plastic finite element method is suitable for investigating the behavior of geotextile reinforced structures. The analyses also shows that effects of the reinforcement have contrast behavior on the safety factor of the problem under the same boundary conditions depending on soil type.

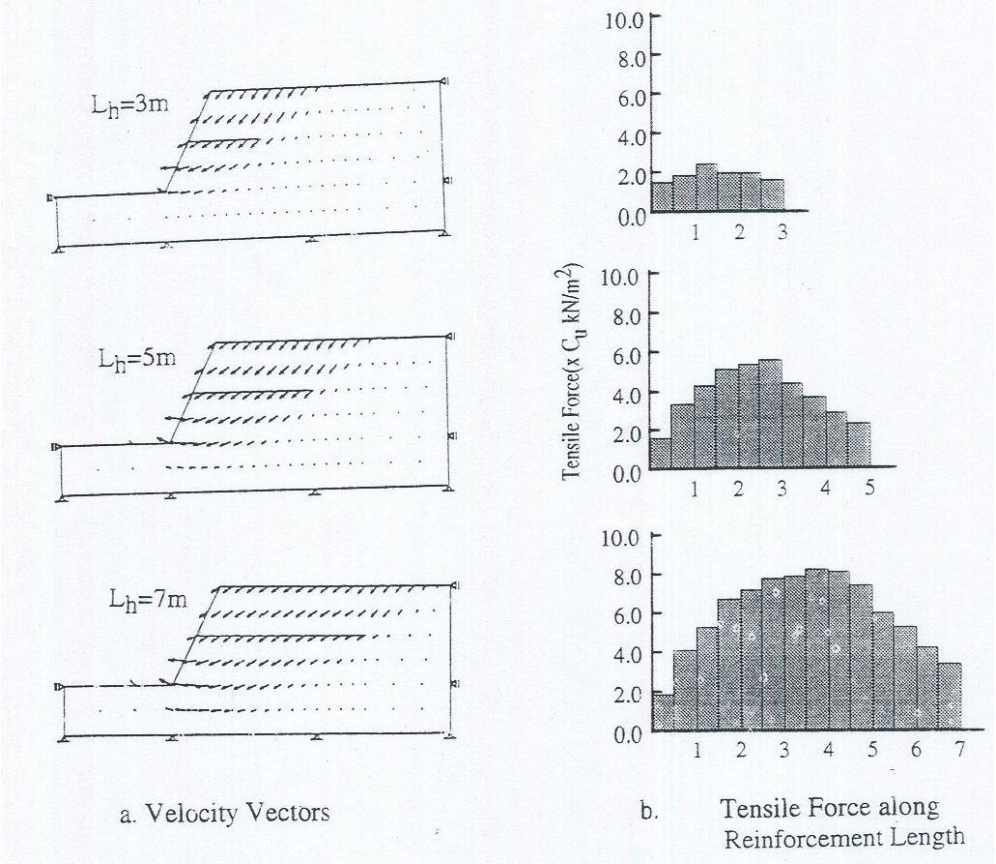

Figure 3.66 Effect of reinforcement lengths on velocity vectors and the tensile force along a reinforcement. (Asaoka *et al.*, 1994)

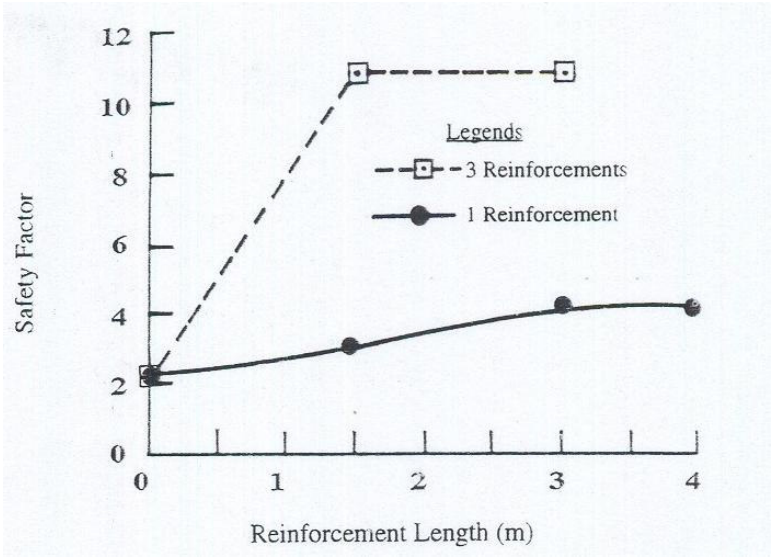

Figure 3.67 The computed factor of safety versus reinforcement length in slope stability problem with c-Ø material. (Asaoka *et al.*, 1994)

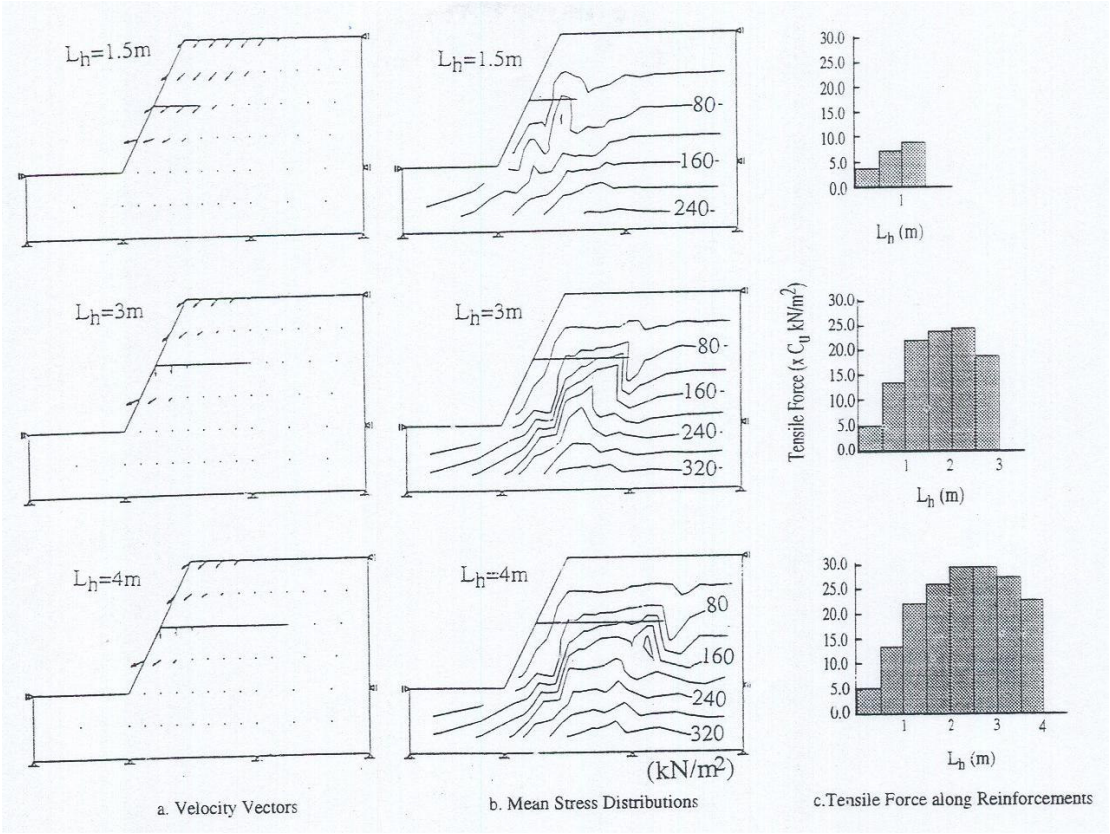

Figure 3.68 Velocity vectors, mean stress distributions and tensile force along reinforcements of different lengths in case of c-Ø soil (Asaoka *et al.*, 1994)

3.2.2. Dynamic Analysis Methods.

Seismic design of earth structures is conducted routinely using a pseudo-static limit equilibrium approach, also referred to as the seismic coefficient method. The earthquake inertia force is considered to act at the centre of gravity of a potential failure soil mass. This method was proposed by Sano, (1916), and they implemented by Mononobe, (1924) and Okabe, (1924) for lateral earth pressure calculation. Design based on pseudo-static analysis is considered conservative since the momentary earthquake acceleration is assumed to act permanently as a static force in the structure. This Conservatism may, however, compensate for possible acceleration amplification that is not implicitly considered in the design.

If the pseudo-static analysis results in an excessively long geosynthetic, a permanent displacement limit can be adopted as a design criterion. In practice, a limited construction space may prevent adequate geosynthetic length from being used, so that direct sliding may be primary source of instability. For the reasons above, in last years deformation based seismic design analysis methods are developed.
There will be discussed some of the pseudo-static analyses and deformation based analyses methods in the following studies.

3.2.2.1 H.I.Ling , D.Leshchinsky and E.B.Perry (1997)

Design procedures, based on pseudo-static analysis, have been developed to determine the required strength and length of geosynthetic layers used to reinforce soil structures. A permanent displacement limit was introduced. Comparison with several case histories from recent major earthquakes supports the validity of the proposed procedure. On the basis of the results of parametric studies the following conclusions are drawn:
a) Direct sliding governs the bottom geosynthetic length as the slope flattens and seismic acceleration increases.
b) The maximum geosynthetic strength and length to resist compound failure doubles under large seismic excitation (C_s=0.3), compared with static design.
c) A tolerable permanent displacement may introduce in cases where the geosynthetic length required to resist direct sliding is extremely long or because of construction space constraint. This can be conducted by selecting a representative strong ground motion and displacement chart.
The study presented here is limited to horizontal seismic acceleration. The same procedure has been extended to include the vertical component of earthquake acceleration (Ling and Leschinsky, 1998). The effects due to the vertical component may become significant when the seismic intensity is extremely large. The concept as presented here has also been adopted for the seismic design of soil cover of waste containment systems (Ling and Leschinsky, 1997).

3.2.2.2 H.I.Ling and D.Leshchinsky (1998)

The stability and permanent displacement of geosynthetic reinforced soil structures, under the influence of combined horizontal and vertical seismic accelerations, are investigated. The required length and tensile reinforcement of the geosynthetic are determined by considering different possible modes of failure, including tie-back/ compound failure direct sliding and pullout. The analysis is conducted by extending the methodology proposed earlier by the authors. While vertical acceleration in the downward direction results in an increased tensile reinforcement by the geosynthetic, acceleration in an upward direction requires a large geosynthetic length to resist direct sliding and tie-back failure. The vertical acceleration has a greater effect on the required tensile reinforcement of the geosynthetic in stabilizing a steep slope when compared to a flatter slope. When the horizontal seismic coefficient exceeds 0-2, the effect of vertical acceleration on the required geosynthetic length becomes significant and is recommended to be included in design. The proposed methodology of design is verified with the performance of a geosynthetic-reinforced soil retaining wall during the Hanshin earthquake. Effects of seismic coefficients on permanent displacements are illustrated through several selected major earthquake records.

It should be noted that seismic design for reinforced soil structures can be conducted rationally using a horizontal seismic coefficient as presented by Ling, (1997), which has been verified by means of several case histories. Procedures incorporating vertical acceleration should be used for important structures sited on subsoil susceptible to large ground surface acceleration, where the effects of vertical acceleration will be considerable.

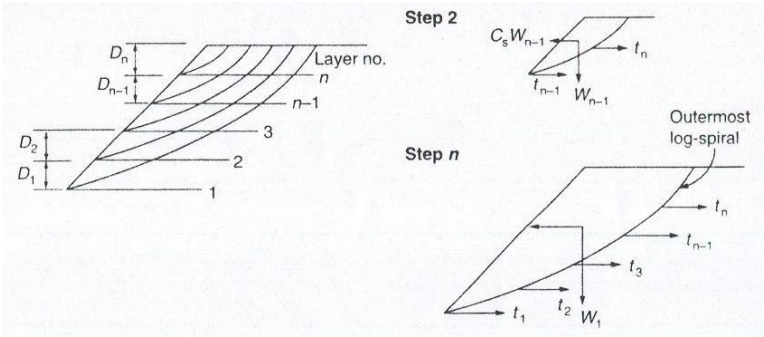

Figure 3.69 Tieback failure analysis (Ling *et al.*,1997)

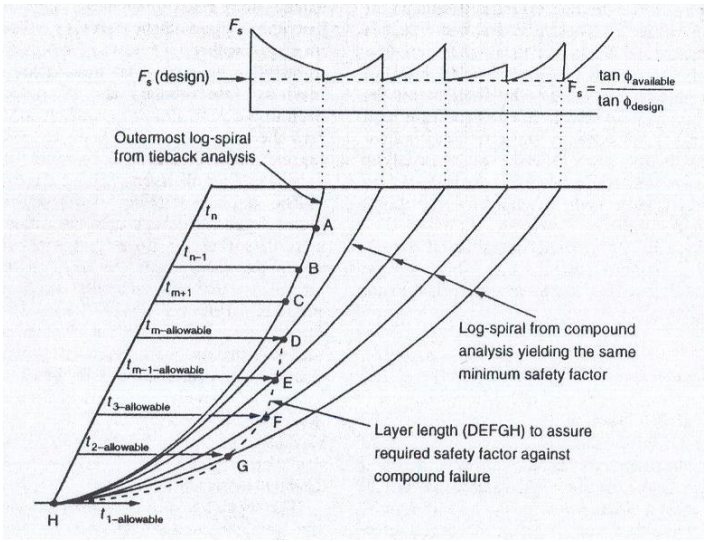

Figure 3.70 Compound failure analysis. (Ling *et al.*,1997)

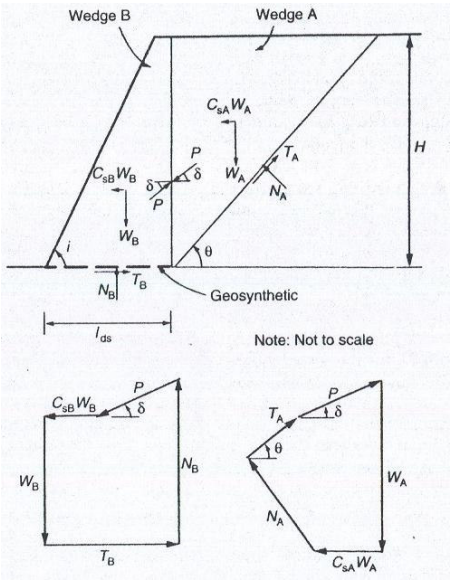

Figure 3.71 Direct sliding analysis. (Ling *et al.*,1997)

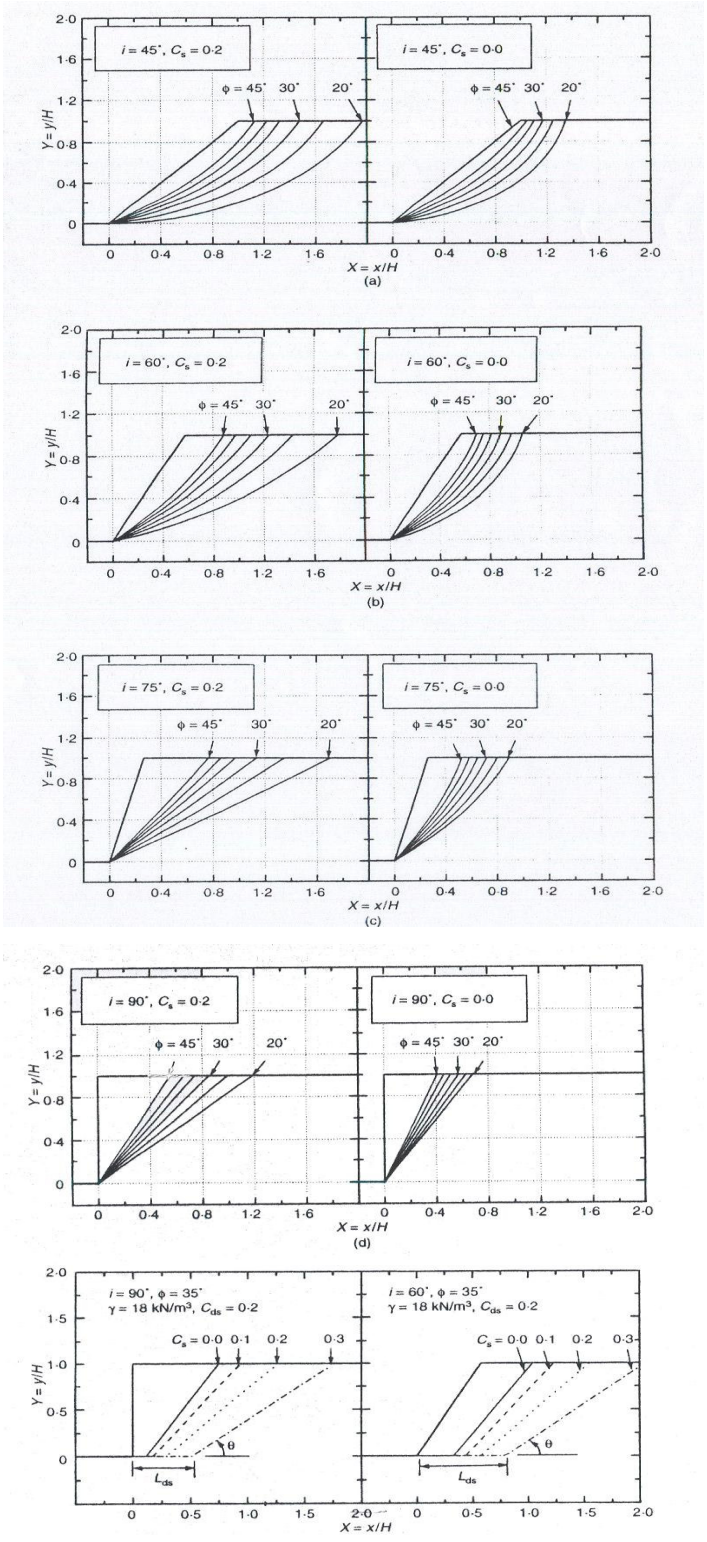

Figure 3.72 Failure surfaces: (a)tieback failure, *i*=45º; (b) tieback failure, *i*=60º; (c) tieback failure, *i*=75º; (d) tieback failure, *i*=90º; € direct sliding, *i*=60º and 90º . (Ling *et al.*,1997)

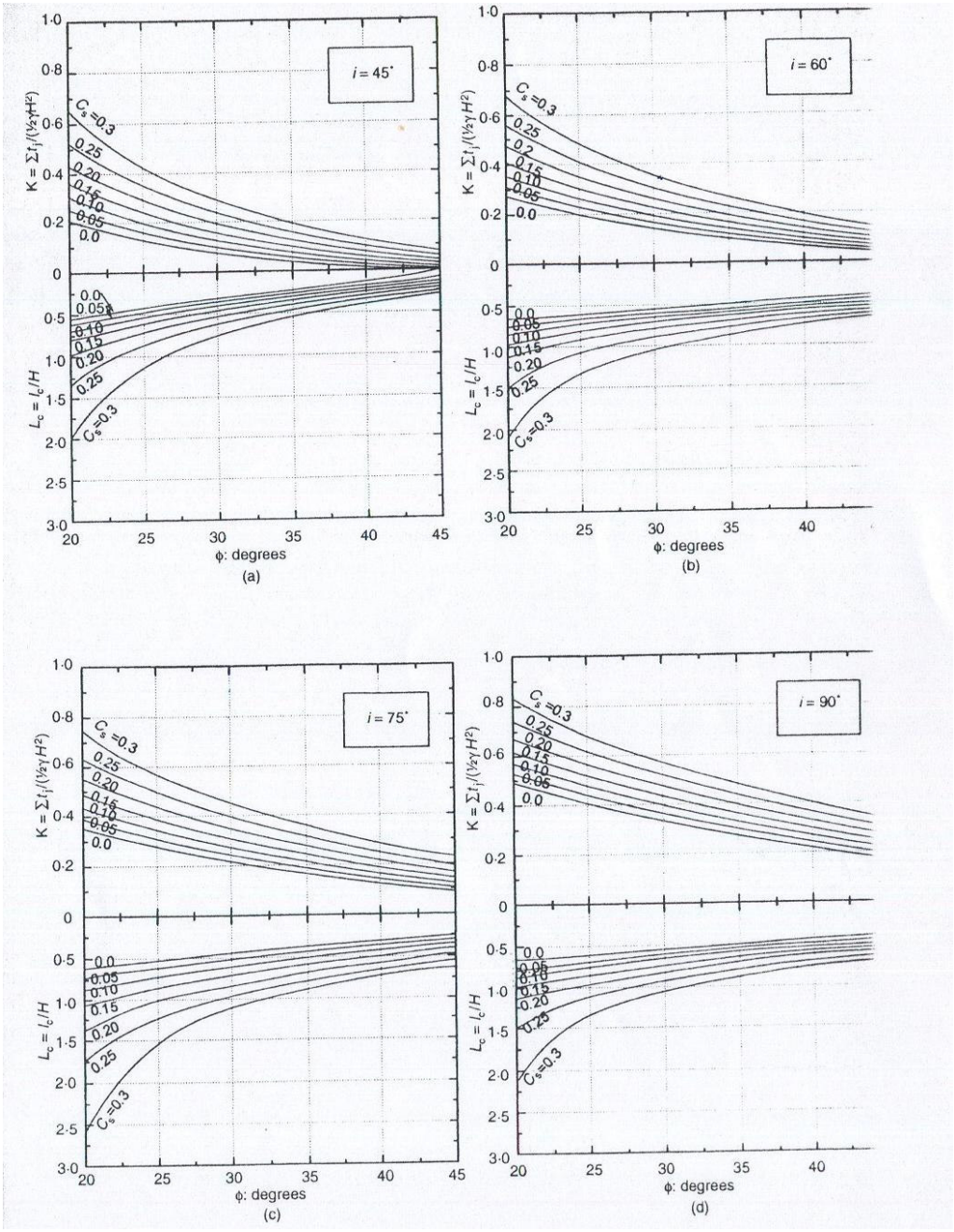

Figure 3.73 Required geosynthetic force and length (tieback/compound failure): (a) *i*=45º ; (b) *i*=60º ; (c) *i*=75º ; (d) *i*=90º . (Ling *et al.*,1997)

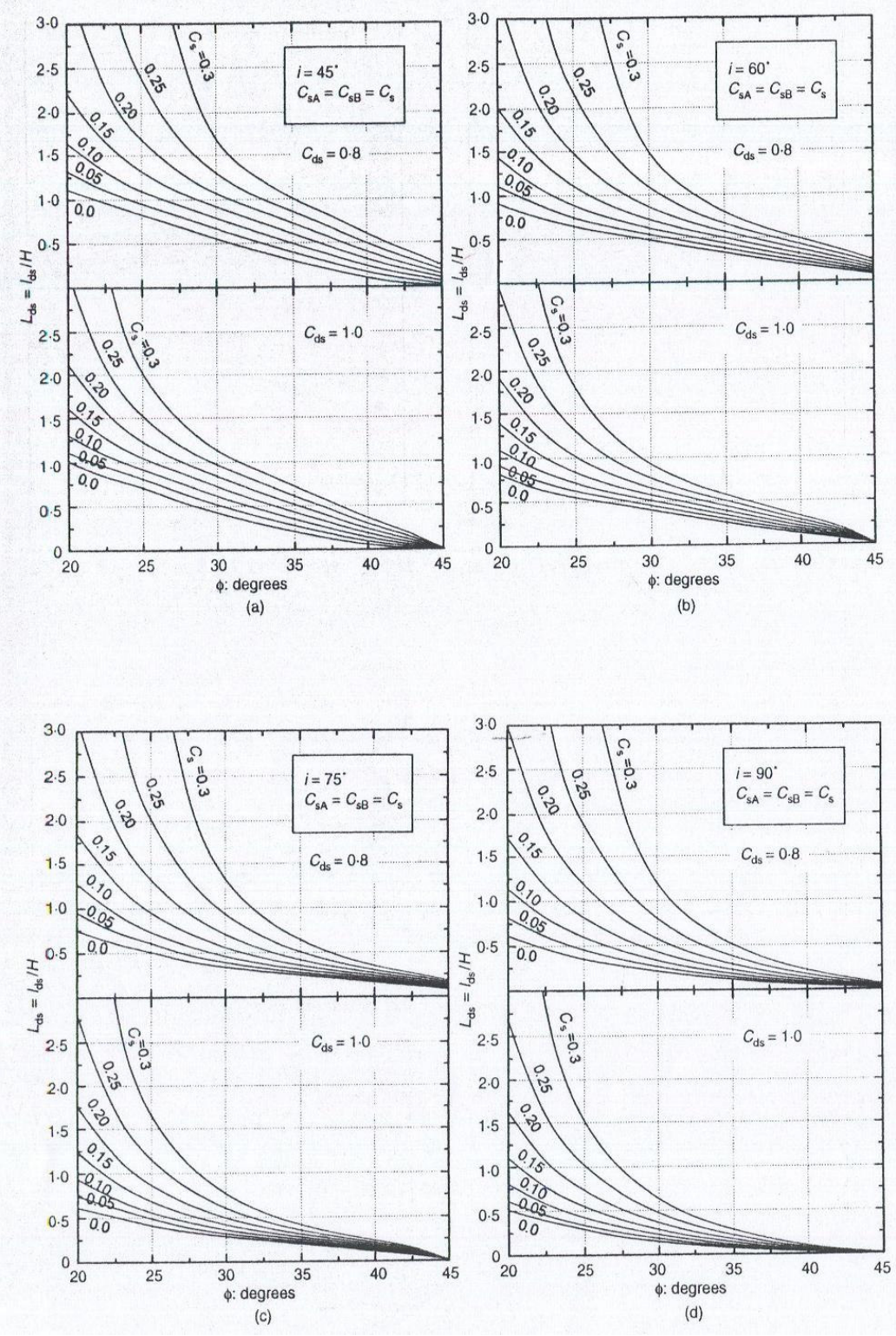

Figure 3.74 Required geosynthetic length to resist direct sliding : (a) *i*=45º ; (b) *i*=60º ; (c) *i*=75º ; (d) *i*=90º . (Ling *et al.*,1997)

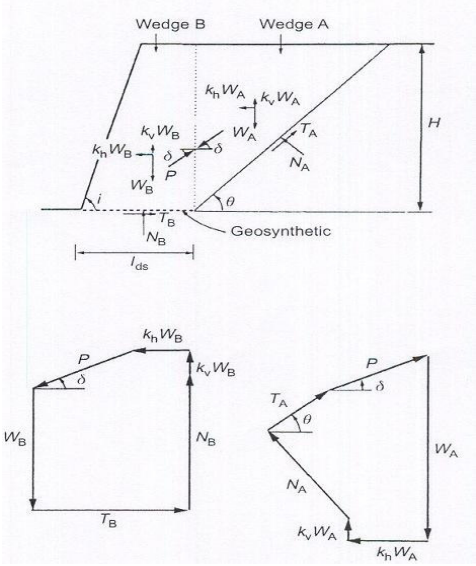

Figure 3.75 Two-part wedge mechansim in sesimic direct sliding analysis.(Ling and Leshchinsky, 1998)

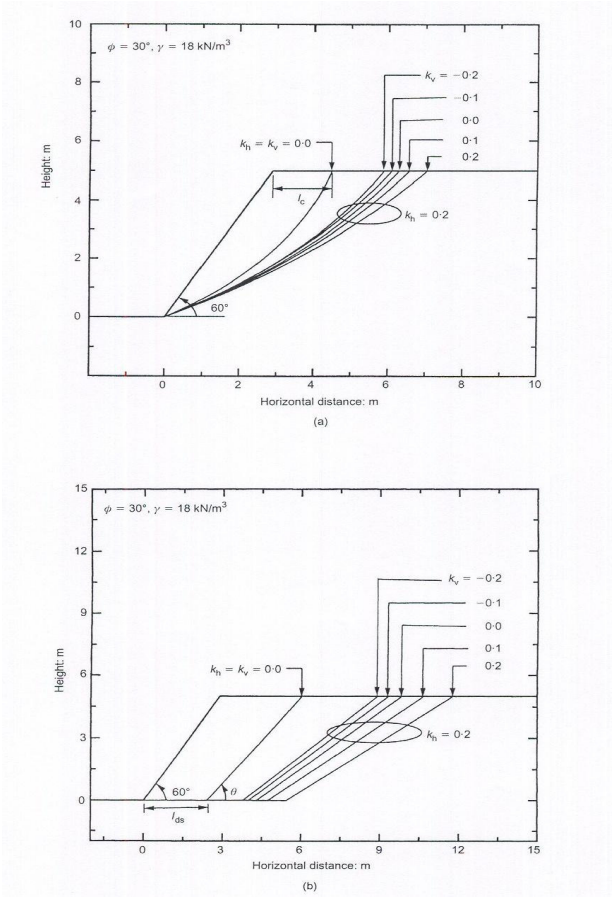

Figure 3.76 Failure surfaces in statically and pseudo-statically designed slopes (a) tie-back analysis; (b) direct shear analysis.(Ling and Leshchinsky, 1998)

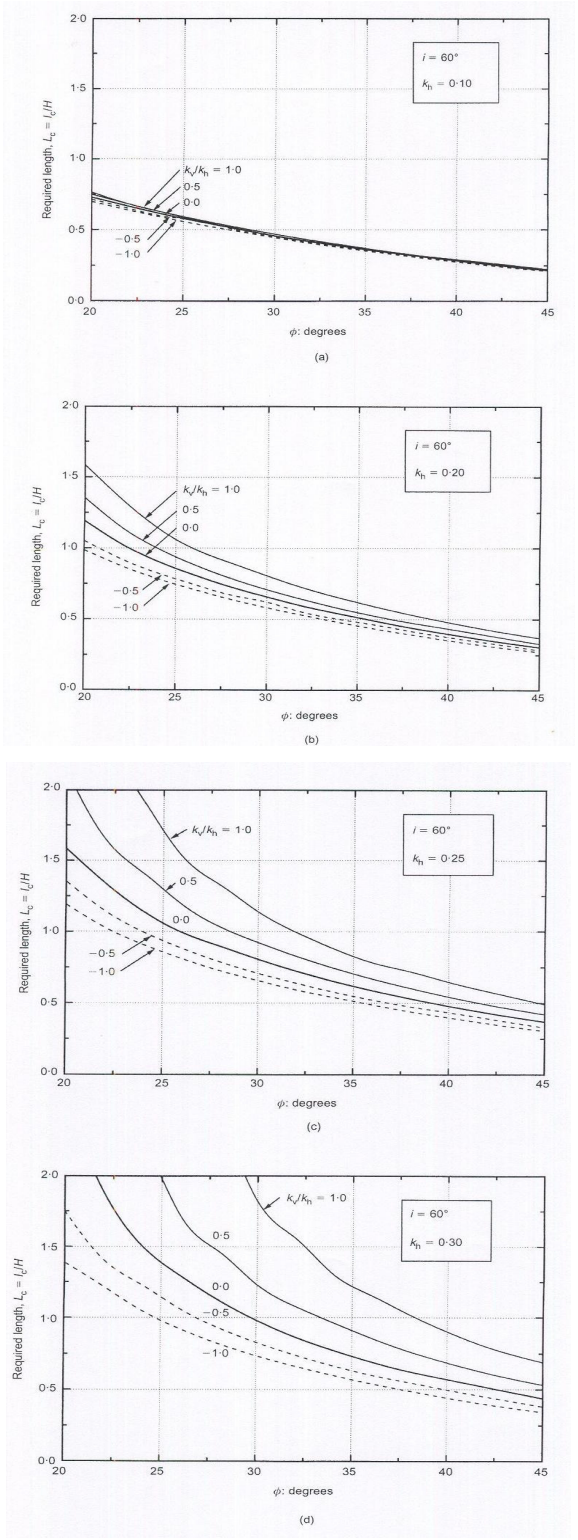

Figure 3.77 Required geosynthetic length (L_c) versus soil friction angle at different sesimic coefficients for slope angle of 60º: (a) k_h=0,1 ; (b) k_h=0,2 ; (c) k_h=0,25 ; (d) k_h=0,3 .(Ling and Leshchinsky, 1998)

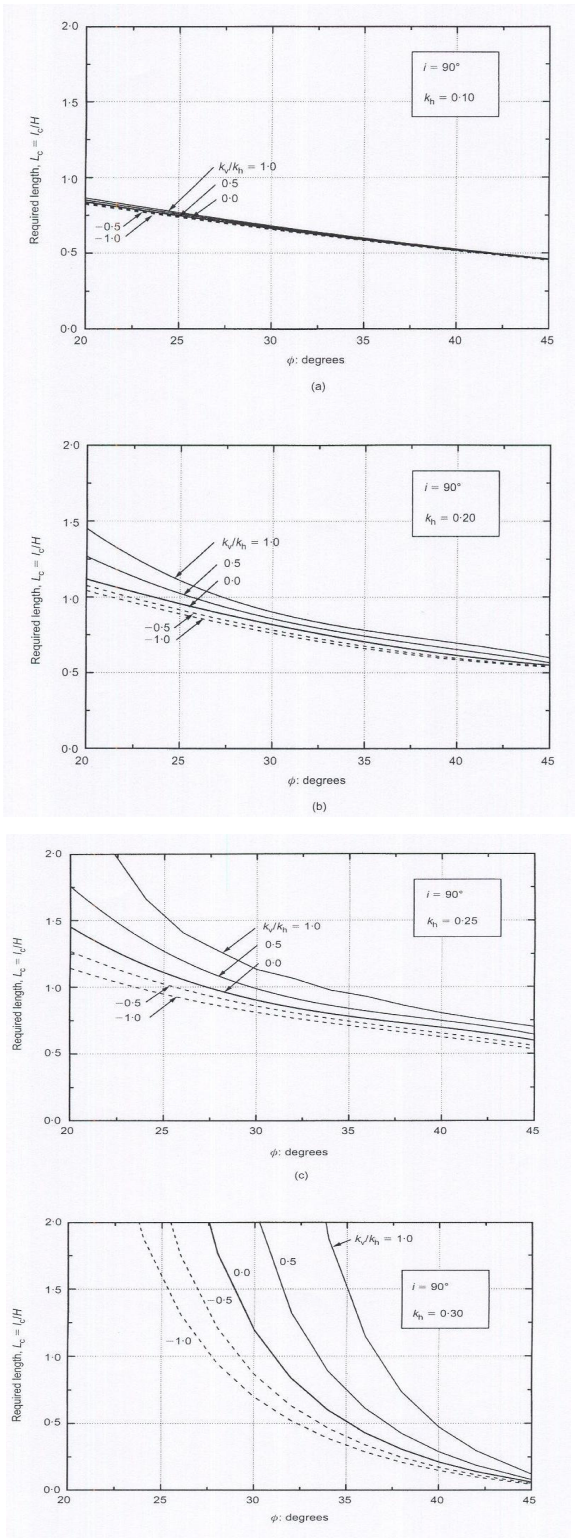

Figure 3.78 Required geosynthetic length (L_c) versus soil friction angle at different sesimic coefficients for slope angle of 90º: (a) k_h=0,1 ; (b) k_h=0,2 ; (c) k_h=0,25 ; (d) k_h=0,3 .(Ling and Leshchinsky, 1998)

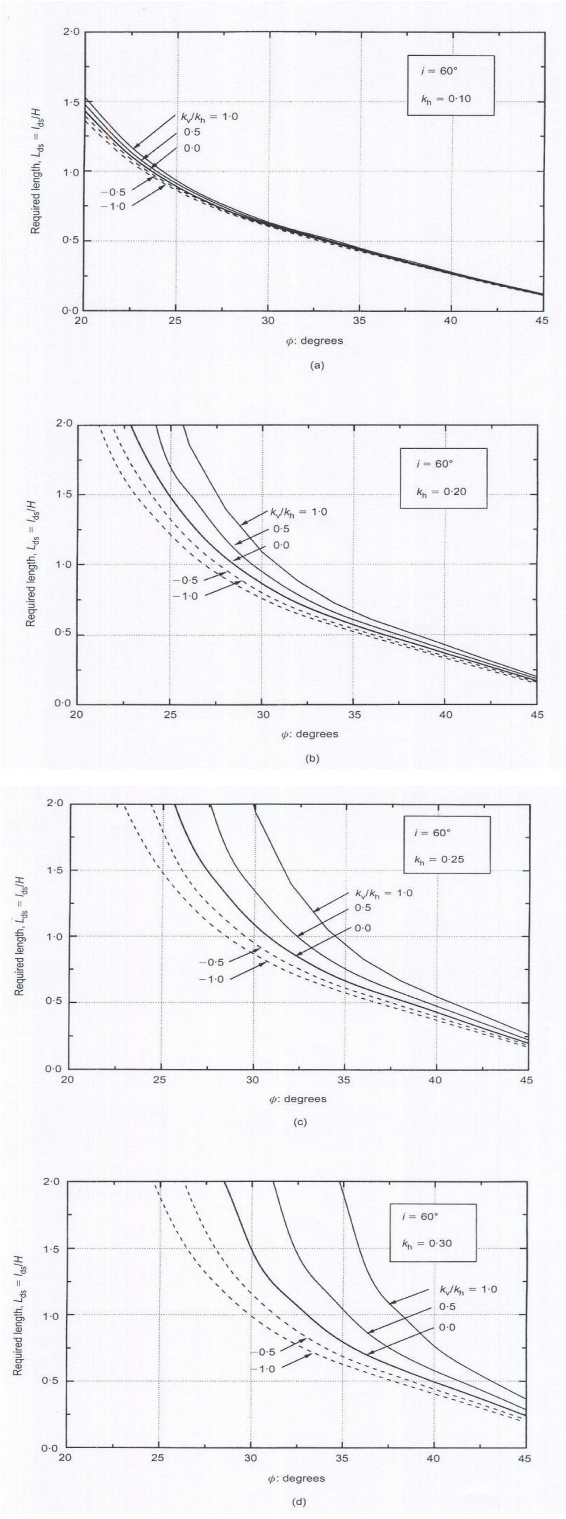

Figure 3.79 Required geosynthetic length for direct sliding (L_{ds}) versus soil friction angle at different sesimic coefficients for slope angle of 60º: (a) k_h=0,1 ; (b) k_h=0,2 ; (c) k_h=0,25 ; (d) k_h=0,3 .(Ling and Leshchinsky, 1998)

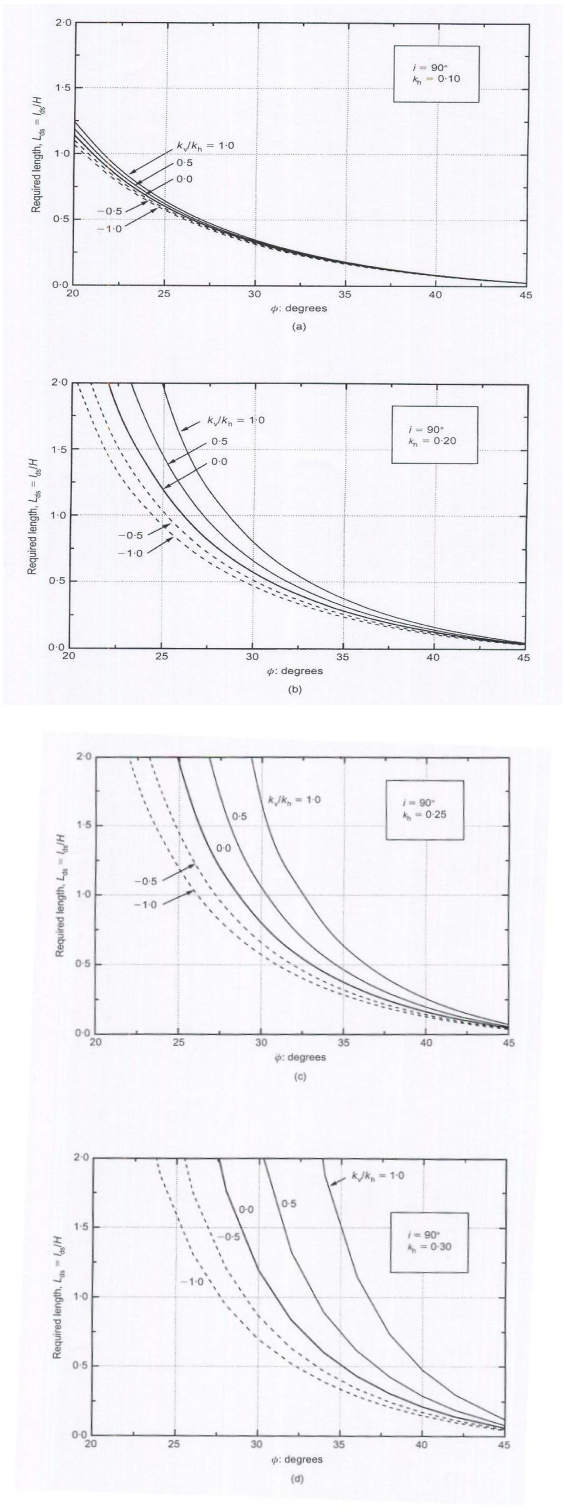

Figure 3.80 Required geosynthetic length for direct sliding (L_{ds}) versus soil friction angle at different sesimic coefficients for slope angle of 90º: (a) k_h=0,1 ; (b) k_h=0,2 ; (c) k_h=0,25 ; (d) k_h=0,3 .(Ling and Leshchinsky, 1998)

3.2.2.3 R.L.Michalowski and L.You (2000)

The researchers studied that the prediction of displacements of reinforced slopes subjected to seismic loads and how they can be used to reduce the reinforcement length.

The kinematic approach of limit analysis is used to calculate critical accelerations for reinforced slopes, followed by an analysis of displacements. The reinforcement length criterion for slopes may be associated with the overall rotational collapse or with the direct sliding mechanism. This also appears to be true for seismically loaded slopes. Calculations of permanent displacement for the two mechanisms are different, and a criterion is derived in order to identify which mechanism should be used for specific slopes.

The sliding block method for calculations of displacement of earth structures subjected to seismic loads is based essentially on the rigid-perfectly plastic concept of the systems behavior. It will be assumed in the analysis that the soil behaves as a perfectly plastic solid; i.e., the resistance to sliding does not change with the progression of soil deformation within the shear band. Also, the soil is considered to be not saturated, and no liquefaction of soil is expected to occur during seismic shaking.

It is pointed out that the collapse of reinforced soils happens by the rotational sliding or direct sliding over the bottom layer reinforcement under seismic loads. The trace of the failure surface in a rotational mechanism must be a log spiral, as only then will the rate of dilation along this surface be compatible with the normality flow rule. (Mohr-Coulomb)

Limit analysis was found to be a convenient tool for implementation of this concept. Another method commonly used in displacement-based design is the limit equilibrium techniques (Ling *et al.*, 1997) Researchers prefer limit analysis because of its rigorous compliance with kinematically admissibility of collapse mechanisms and the proof of the solution being an upper bound to active limit loads and the lower bound to the necessary reinforcement strength.

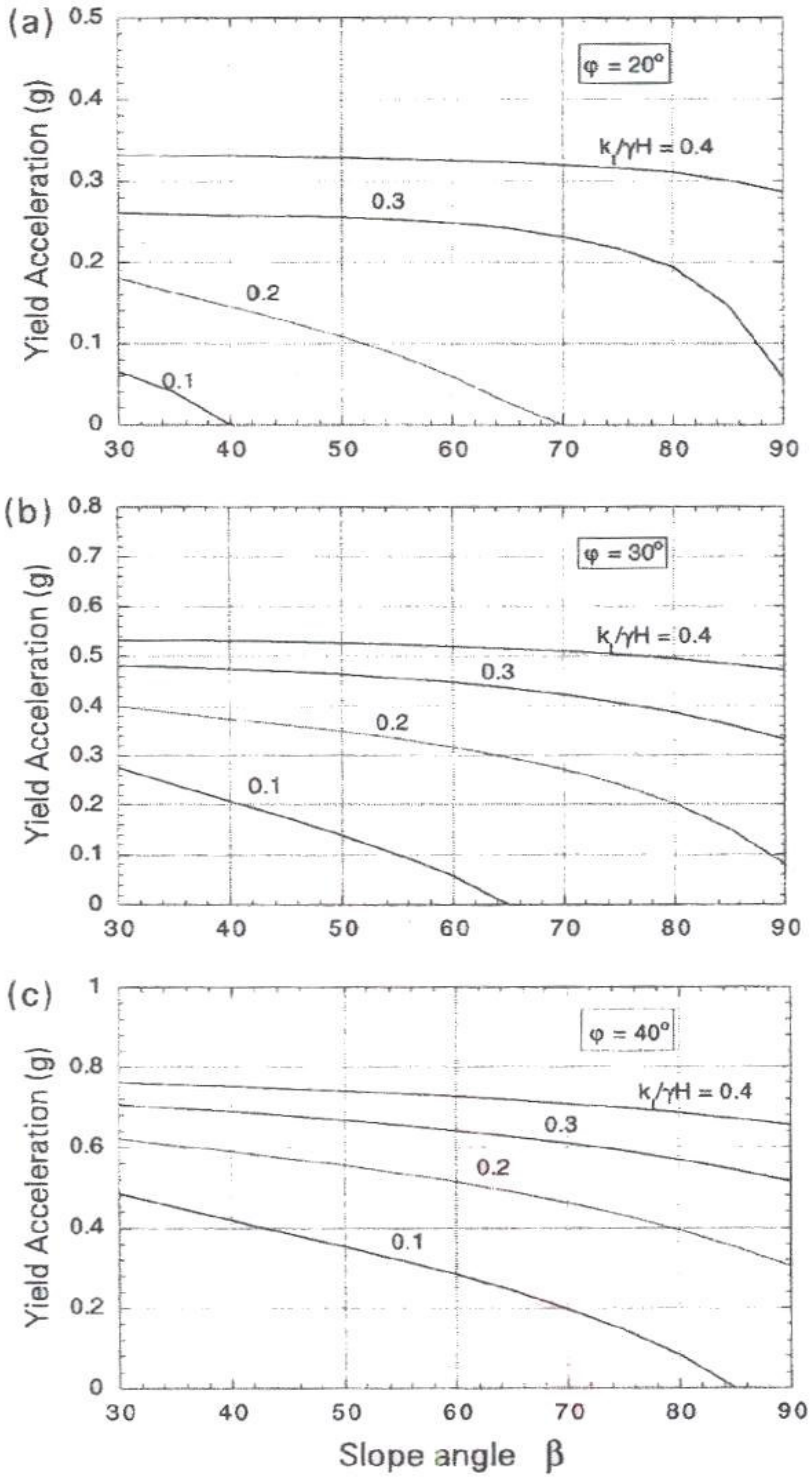

Figure 3.81 Critical acceleration coefficient for reinforced slopes. (Michalowski and Liangzhi, 2000)

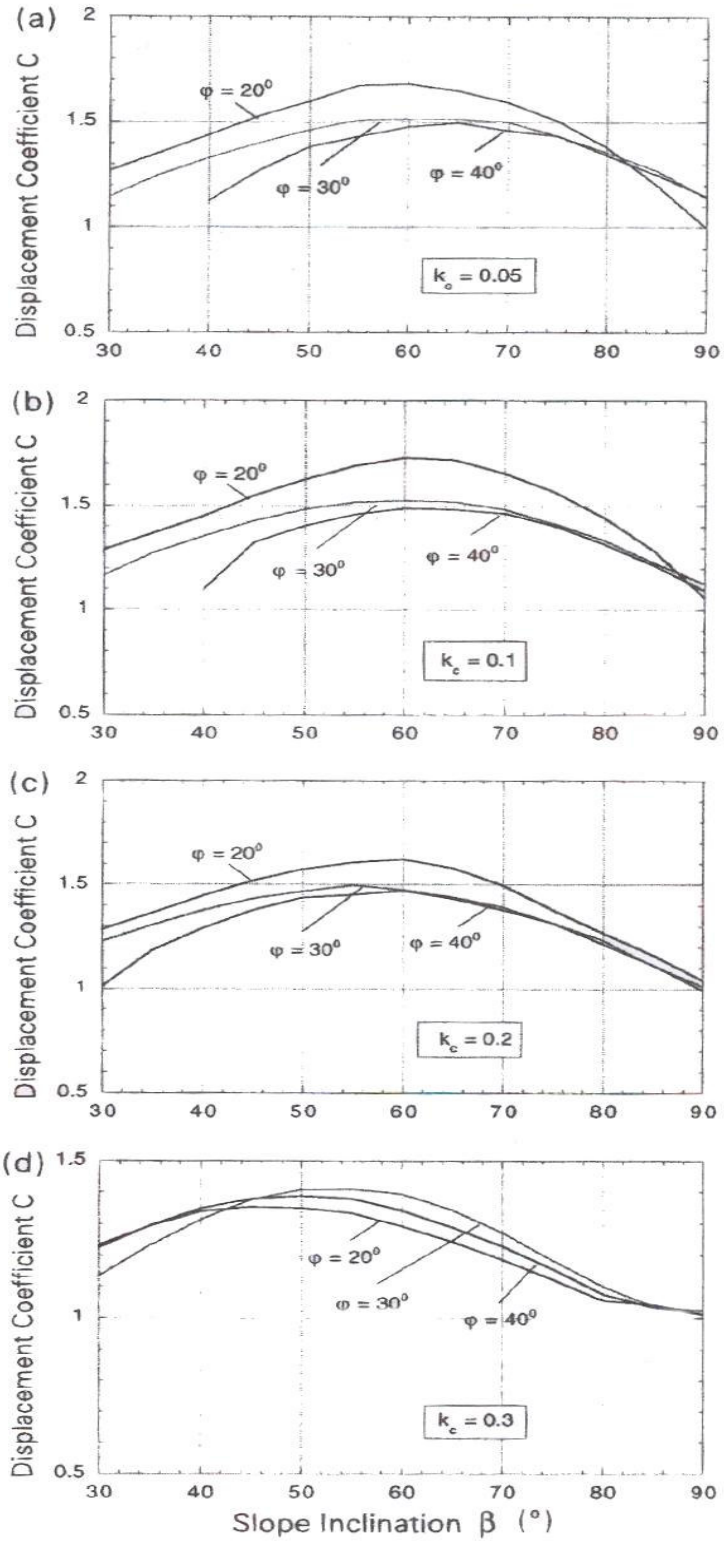

Figure 3.82 Displacement coefficient for rotational failure. (Michalowski and Liangzhi, 2000)

Table 3.9 Coefficient C for direct sliding mechanism. (Michalowski and Liangzhi, 2000)

φ (1)	k_c (2)	Slope Inclination Angle β 30° (3)	40° (4)	50° (5)	60° (6)	70° (7)	80° (8)	90° (9)
25°	0.1	1.073	1.057	1.060	1.122	1.069	0.920	0.951
	0.2	0.979	0.948	0.945	0.940	0.930	0.902	0.922
	0.3	0.826	0.957	0.841	0.836	0.913	0.891	0.941
35°	0.1	1.354	1.138	1.115	1.159	1.303	1.591	1.011
	0.2	1.109	1.025	1.024	1.107	1.260	0.919	0.957
	0.3	0.941	0.936	0.981	0.956	0.839	0.865	0.894
45°	0.1	0.530	1.818	1.342	1.441	1.584	1.530	0.588
	0.2	0.526	1.254	1.162	1.248	1.505	0.985	0.578
	0.3	1.214	0.992	1.026	1.147	1.548	0.898	0.564

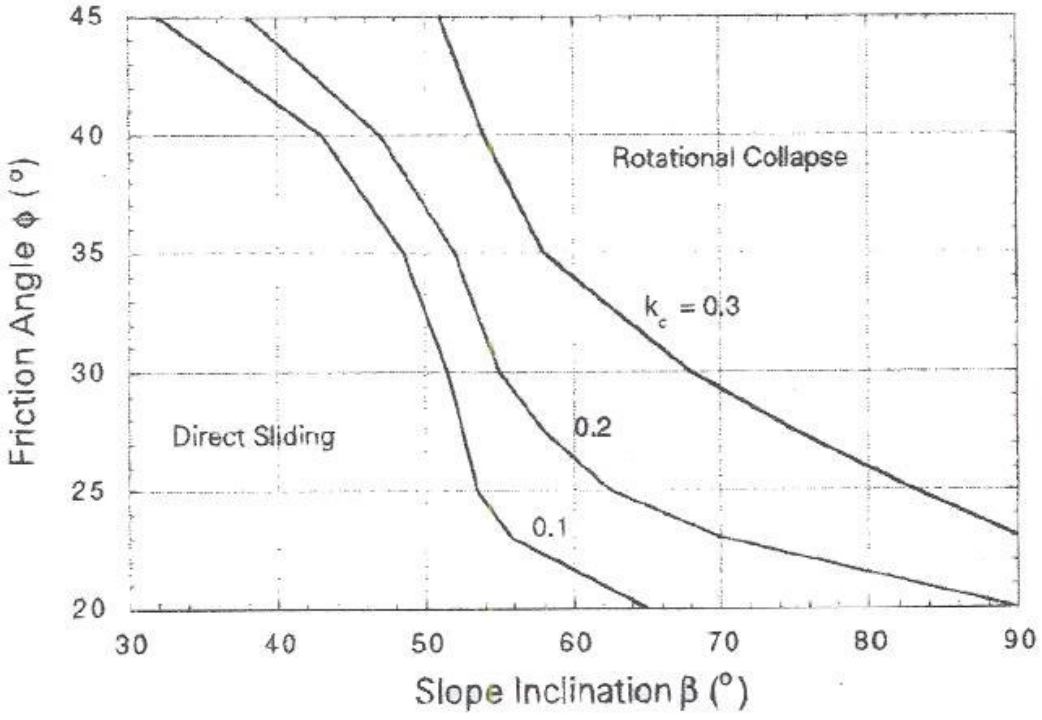

Figure 3.83 Criterion for selecting mechanism for calculations of permanent displacements. (Michalowski and Liangzhi, 2000)

Because of the rigid-plastic nature of the calculated displacements, the issue of possible rupture of reinforcement during the first cycles of shaking in a seismic event was addressed. The viscoelastic properties of most geosynthetics, and opening up of the rupture surfaces into finite thickness layers of intense shear in a real collapse mechanism, provide for accommodation of strains and avoidance of reinforcement rupture during short-term periods when the ground acceleration exceeds the critical acceleration of the structure.

The analysis presented has a common component with other displacement based design techniques in that the acceleration record is twice integrated to arrive at displacements. However, in specific calculations of the limit state of reinforced slopes, it offers an alternative technique to approaches presented recently in the literature.

3.3. Analysis of Geotextile Reinforced Slopes and Retaining Walls

3.3.1. Classical Methods

3.3.1.1 The Analysis of Geotextile Reinforced Retaining Walls

A reinforced soil retaining system basically has three components; Backfill material, reinforcing elements and facing material. In order to provide a sound engineering design, such that the full integrity of these three different elements are maintained, a series of stability and safety investigations should be performed. These investigations may be grouped in two distinct categories as; External and internal stability analyses.

A properly designed volume of reinforced soil forms a coherent mass that can be expected to behave as a unit. The external stability must be evaluated to assure that failure would not occur because of one or more of the following mechanisms; sliding of the reinforced volume on its base or at any level above its base; overturning of the earth wall; bearing capacity failure or loss of serviceability because of excessive settlement of the foundation soil, or possibility of creep of subsoil; and rotational or block sliding failure of the soil behind and beneath earth wall.

The usual methods of soil mechanics and foundation engineering are used to evaluate the factors of safety against these failure modes. The external stability analyses consist of the following failure mechanisms as illustrated in Figure 3.84

1) Overall slope stability-slip failure,
2) Sliding over the base,
3) Overturning,
4) Bearing pressure,
5) Creep of the subsoil.

The internal stability analysis involves determination of lift thickness, fabric length and overlap. To determine the lift thickness, earth pressures are assumed to be linearly distributed using K_0 conditions. This is probably a conservative approach and many designers would use a K_a conditions. Boussinesq elastic theory for live loads on the soil backfill is used. As shown in Figure 3.85, the following earth pressures result:

$\sigma_{hs} = K_0 \gamma z$ (3.1)

$\sigma_{hq} = K_0 q$ (3.2)

$\sigma_{hl} = (P x^2 z) / R^5$ (3.3)

$\sigma_h = \sigma_{hs} + \sigma_{hq} + \sigma_{hl}$ (3.4)

where σ_{hs} = pressure due to soil

$K_0 = 1 - \sin \emptyset$ = coefficient of earth pressure at rest

$\emptyset$ = angle of shearing resistance of soil

γ = unit weight of backfill soil

z = depth from ground surface to layer in question

σ_{hq} = pressure due to surcharge load

$q = \gamma D$ = surcharge load on ground surface

γ = unit weight of surcharge soil

D = depth of surcharge soil

σ_{hl} = pressure due to live load

P = concentrated load

x = horizontal distance load is away from wall

R = radial distance load from point on wall where pressure is being calculated.

The calculations of σ_{hs} and σ_{hq} are quite straight forward, but σ_{hl} presents problems particularly for multiwheeled truck loads where superposition of each wheel must be performed. Figure 3.86 greatly aids in such calculations.

By taking a free body at any depth in the total lateral pressure diagram and then summing the forces in the horizontal direction, one obtains the equation for the lift thickness:

$$\sigma_h S_v = \frac{T_a}{FS} \quad (3.5)$$

$$S_v = \frac{T_a}{\sigma_h FS} \quad (3.6)$$

where S_v = vertical spacing (lift thickness)

T_a = allowable stress in the fabric (sometimes taken as one third of the grab strength)

σ_h = total lateral pressure at depth considered

FS = factor of safety

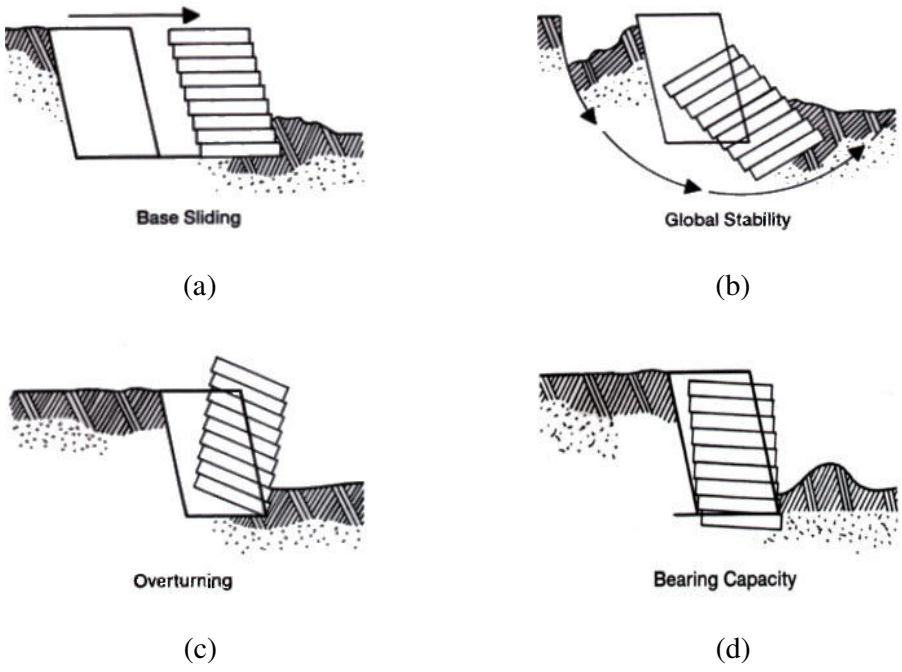

Figure 3.84 External stability considerations for geotextile walls. (a) Base Sliding; (b) Global Stability; (c) Overturning; (d) Bearing Capacity.

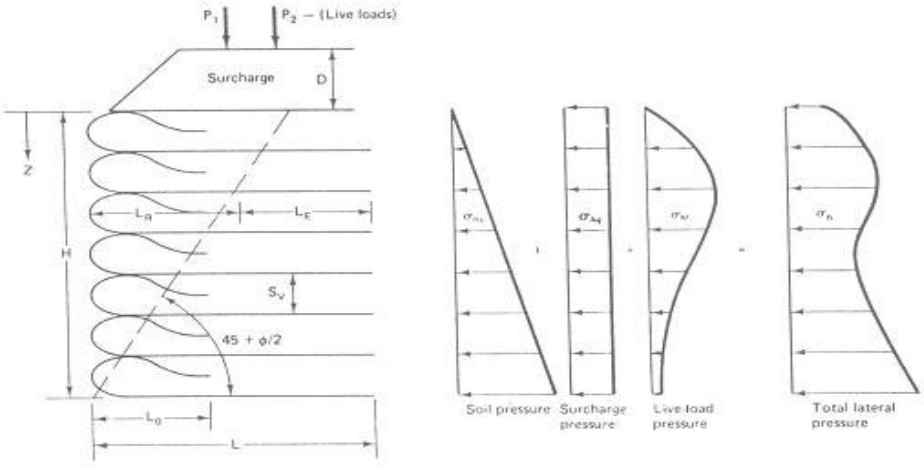

Figure 3.85 Earth pressure concepts and theory for geotextile walls.

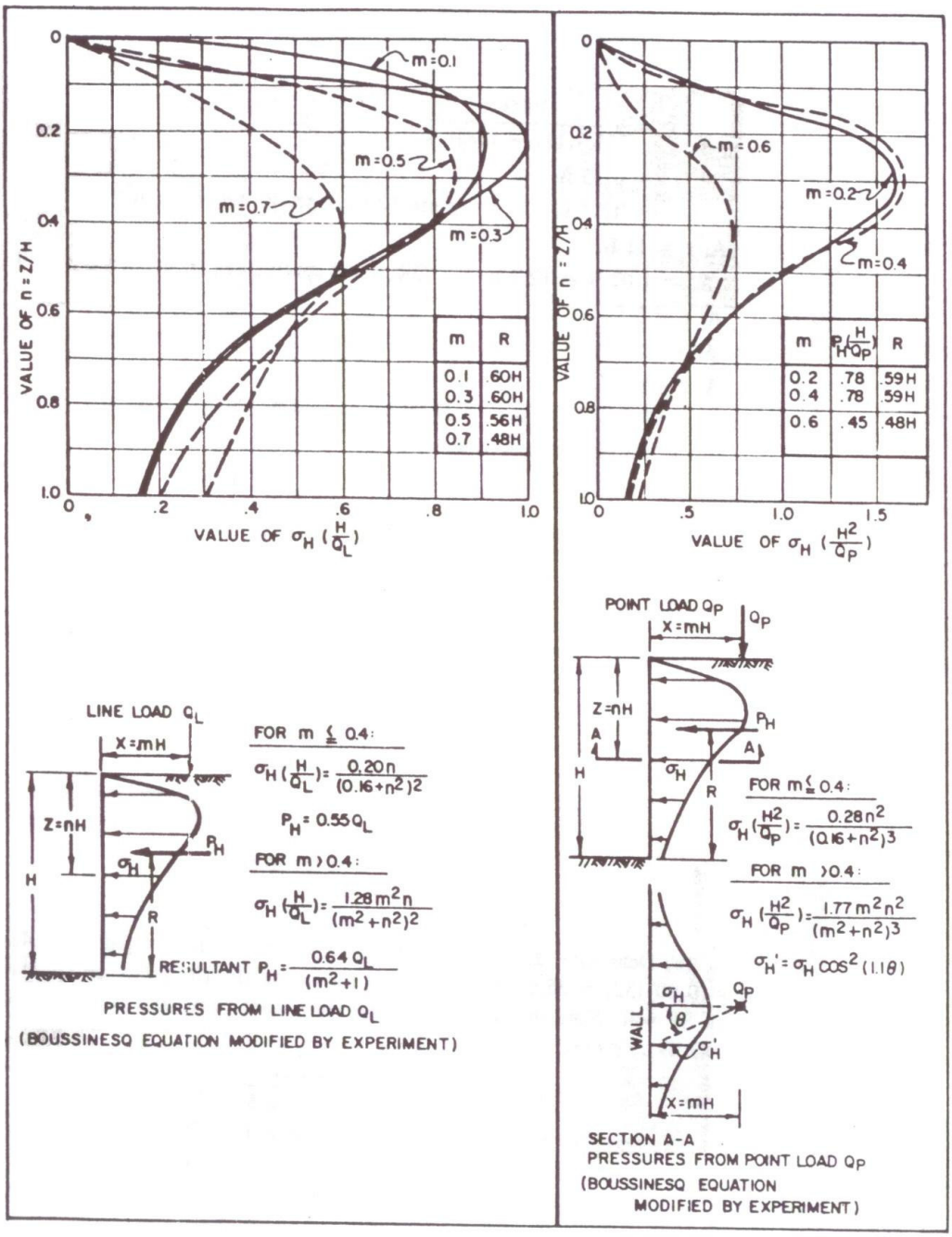

Figure 3.86 Lateral earth pressures due to a surface load.

The same approach can be taken for obtaining the length of embedment of the fabric layers in the same anchorage zone, L_e. These values when obtained must be added to the nonacting lengths (L_R) of fabric behind the failure plane for the total fabric lengths, L , that is,

$$L = L_e + L_R \tag{3.7}$$

where

$$L_R = (H - z)\tan(45 - \frac{\phi}{2}) \tag{3.8}$$

and

$$S_v \sigma_h FS = 2\tau L_e \tag{3.9}$$

$$= 2(c + \sigma_v \tan\delta) L_e \tag{3.10}$$

$$= 2(c + \gamma z \tan\delta) L_e \tag{3.11}$$

$$L_e = \frac{S_v \sigma_h FS}{2(c + \gamma z \tan\delta)} \tag{3.12}$$

where L_e = required embedment length

S_v = vertical spacing

σ_{hl} = total lateral pressure at depth considered

c = soil cohesion

γ = unit weight of backfill soil

z = depth from ground surface

δ = angle of shearing friction between soil and fabric

Finally, the overlap distance L_0 is obtained in a manner similar to that above with a few exceptions; that is , the distance Z should be measured to about the middle of the layer and σ_h is not as large as illustrated in Figure 3.86. It is reasonably well established that the stress in reinforcement elements is maximum near the failure plane and falls off sharply to either side. As an approximation, ½ σ_h will be used, which results in the following equation:

$$L_0 = \frac{S_v \sigma_h FS}{4(c + \gamma z \tan\delta)} \tag{3.13}$$

where L_0 is the required overlap length.

Next, one must consider external stability of geotextile wall, which includes overturning, sliding, and foundation failures. These are illustrated in Figure3.84. These features are

common to all wall systems and can be treated exactly as with gravity or crib walls. They are greatly site specific in so far as calculations are concerned. For overturning, moments are taken about the toe of the wall to form a factor of safety;

$$FS_{ot} = \sum \frac{resisting\ moments}{driving\ moments} \tag{3.14}$$

$$= \frac{w_1 x_1 + w_2 x_2 + P_a \sin\delta(L)}{P_a \cos\delta(R)} \tag{3.15}$$

For sliding, horizontal forces at the bottom of the wall are summed to from another factor of safety;

$$FS_s = \sum \frac{resisting\ forces}{driving\ forces} \tag{3.16}$$

$$= \frac{\left[c_a + (\frac{w_1 + w_2 + P_a \sin\delta}{L}) \tan\delta\right] L}{P_a \cos\delta} \tag{3.17}$$

Finally, check for a foundation failure using shallow foundation bearing capacity theory;

$$P_{ult} = cN_c + qN_q + 0.5\gamma BN_\gamma \tag{3.18}$$

The development of design methodology has been based on limit equilibrium analysis, working stress analysis based on measurements on full-scale and model structures, and the results of finite element analyses. Different assumptions have been made for the failure surface geometry for analyses of different types of reinforcement systems.

3.3.1.2 The Analysis of Geotextile Reinforced Slopes

The usual geotechnical engineering approach to slope stability problems is to use limit equilibrium concepts on an assumed circular arc failure, thereby arriving at an equation for the factor of safety. The resulting equations for total stresses and effective stresses are given below;

$$FS = \frac{\sum_{i=1}^{n} (N_i \tan\phi + c\Delta l_i)R + \sum_{i=1}^{m} T_i y_i}{\sum_{i=1}^{n} (w_1 \sin\theta_i)R} \tag{3.19}$$

$$FS = \frac{\sum_{i=1}^{n} (\overline{N}_i \tan \bar{\phi} + \bar{c}\Delta l_i)R + \sum_{i=1}^{m} T_i y_i}{\sum_{i=1}^{n} (w_1 \sin \theta_i)R} \qquad (3.20)$$

where FS = factor of safety

$N_i = w_i \cos \theta_i$

w_i = weight of slice

θ_i = angle of intersection of horizontal to tangent at center of slice

$\overline{N}_i = N_i - u_i \Delta x_i$

$u_i = h_i \gamma_w$ = pore water pressure

h_i = height of water above base of circle

Δx_i = width of slice

γ_w = unit weight of water

Δl_i = arc length of slice

R = radius of failure circle

$\phi, \bar{\phi}$ = total and effective angles of shearing resistance, respectively

$c, \bar{c}$ = total and effective cohesion, respectively

T_i = allowable geotextile tensile strength

y_i = moment arm for geotextile (in large-deformation situations this moment arm could become equal to R, which is generally a larger value)

n = number of slices

m = number of fabric layers

Use of the total stress analysis (Equation 3.19) is recommended for embankments where water is not involved or when the soil is at less than saturation conditions. The effective stress analysis (Equation 3.20) is for saturated conditions where water is involved and is typical of many delta areas involving fine-grained cohesive soils.

These equations are tedious to solve and when additional consideration is given to finding the minimum factor of safety by varying the radius and coordinates of the origin of the circle, the process becomes unbearable to do by hand. Many computer codes exist which can readily be modified to include the $\Sigma^{m}_{i=1} T_i y_i$ contribution of geotextile reinforcement. When the search is done independent of the computer, the analysis portion easily fits on most personal computers.

For fine-grained cohesive soils whose shear strength can be estimated by undrained conditions the problem becomes much simpler. Here slices need not be taken since the soil strength does not depend on the normal force on the shear plane, which results in the following equation;

$$FS = \frac{cR + \sum_{i=1}^{m} T_i Y_i}{WX}$$

3.3.2. Finite Element Method

In this section finite element analysis will be defined briefly. Plaxis, a program which is used to analyze Geotextile reinforced slopes and retaining walls, is described, material models and parameters used in the analysis are defined. Plaxis is a finite element package specifically intended for the analysis of deformation and stability in geotechnical engineering projects.

To illustrate the results of the technique, Rowe and Soderman [60] evaluated two instrumented test embankments on very soft soils in Holland which were purposely brought to failure. One was without geotextile reinforcement and failed as the height was brought to 1.75 m, and the other was reinforced with geotextile and reached a height of 2.75 m before failure. Using a plane strain nonlinear elastoplastic FEM program with over 1000 triangular elements ,the velocity field and the plastic region continues to a fill height of 1.8 m for the case without reinforcement. Continuous failure was mobilized and at approximately the height when it did indeed fail (i.e.,1.75 m versus 1.8 m). To adapt the FEM to the soil-fabric interface for the reinforced section, the displacement of the soil and fabric were assumed to be compatible until the shear stress reached the limiting shear stress defined by the Mohr-Coulomb failure criterion. Once this shear stress was attained, slip occurred. Note from the FEM-generated plastic zone at a height of 1.8 m, that a continuous plastic region does not yet exist (i.e., the embankment has not yet failed). The plastic zone does begin to be continuous at a height of 2.05 m, and was fully mobilized at a height of 2.66 m. This FEM predicted height of 2.66 m nicely corresponds with the actual failure height of 2.75 m.

Techniques such as this certainly are the way of future geotextile-related designs of large and/or critical situations.

4. NUMERICAL ANALYSIS RESULTS

In this section the results of the geotextile reinforced slopes which are calculated by the finite element method PLAXIS are introduced. Three different slope inclinations, two different backfills and three different foundations are used and eighteen combinations of these are studied in this work. By the help of the results, the slopes, the backfill materials and foundation materials are compared one by one.

In the analyses, slopes similar to the ones studied by San, Leshchinsky and Matsui (1994) are used. The geometry of models is given in the Figure 4.1. All the models have the same wall height, H=5m. Reinforcement spacing is given, S_v= 0.5 m and 10 geotextile layers are used which have different lengths for each model. The reinforcement lengths used are taken from San, Leshchinsky and Matsui (1994)'s model. These reinforcement lengths have been chosen by San, Leshchinsky and Matsui (1994) so that a FS=1 is obtained. For the limit equilibrium analyses they used the limit equilibrium computer code Strata-Slope.

Dense granular backfill material is used in the models D1, D2 and D3 and loose backfill material is used in models L1, L2 and L3. The parameters used in these finite elements analyses are given in Table 4.1. The backfill material is modeled by Hardening soil model and the foundation is modeled by Mohr-Coulomb model.

As it is difficult to properly model the interface between geotextile and the backfill, different coefficients were examined and 0.5 is chosen after a number of calculations.

While modeling the soil, six node triangular elements and plane strain model is considered.

In order to see the effect of the overlap of geotextiles, several analyses were performed. When the overlap was not modeled, the deformations calculated were not the same as in the real construction. So it was concluded that the overlap behaves like a short reinforcement in the model and contribute to the stability.

The stage construction method of Plaxis is used in the model and 50 cm layers were considered during stage construction. Also Phi-c reduction procedure was carried out for the safety analysis.

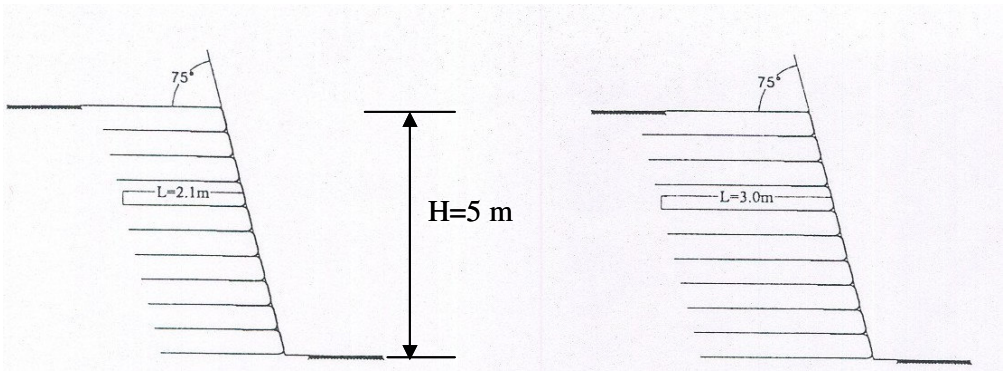

(a) Model D1 (d) Model L1

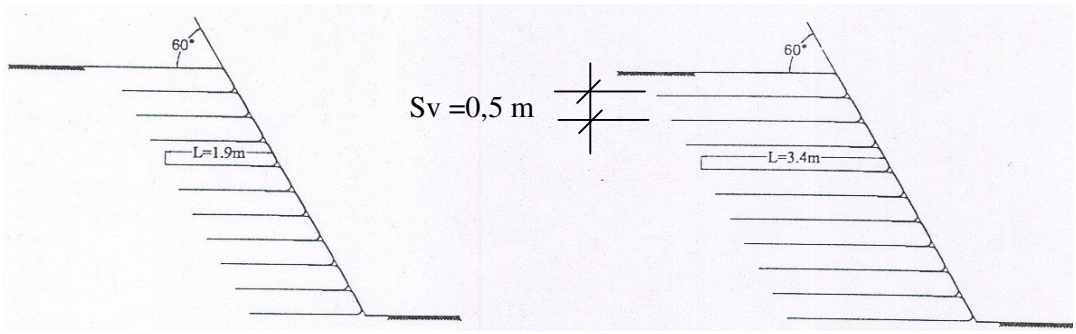

(b) Model D2 (e) Model L2

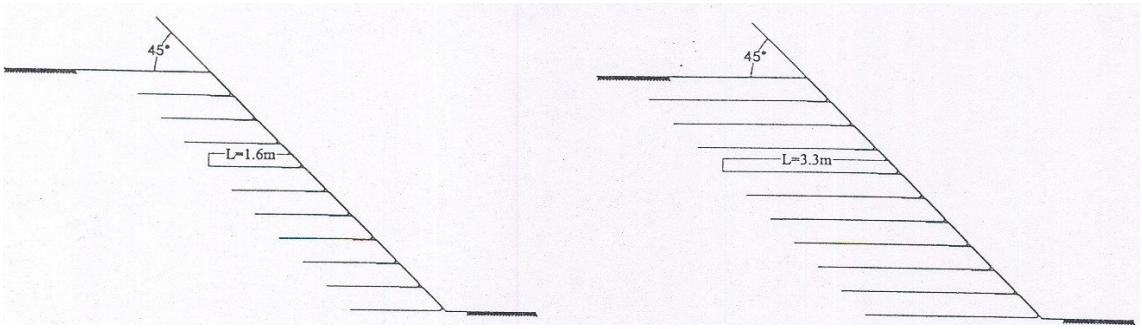

(c) Model D3 (f) Model L3

Figure 4.1 The geometry of the models.

Table 4.1 The parameters used in the analysis

BACKFILL	Model	H(m)	ß°	γ(kN/m^3)	Ø°	c(kN/m^3)	E_{50}^{ref}	E_{ur}^{ref}	R_f	M	S.C.	GEOTEXTILE REINFORCEMENT PROPERTIES		
												EA(kN/m)	S_v(m)	L(m)
DENSE GRANULER	D1	5*	75*	20*	35*	1	100.000	212.000	0.91	0.54	0.5	205	0.5*	2.1*
	D2	5*	60*	20*	35*	1	100.000	212.000	0.91	0.54	0.5	205	0.5*	1.9*
	D3	5*	45*	20*	35*	1	100.000	212.000	0.91	0.54	0.5	205	0.5*	1.6*
LOOSE GRANULAR	L1	5*	75*	20*	20*	3*	14.750	109.000	0.90	0.65	0.5	205	0.5*	3.0*
	L2	5*	60*	20*	20*	3*	14.750	109.000	0.90	0.65	0.5	205	0.5*	3.4*
	L3	5*	45*	20*	20*	3*	14.750	109.000	0.90	0.65	0.5	205	0.5*	3.3*
FOUNDATION														
ROCK	R	-	-	24	37,5	1	500.000	-	-	-	-	-	-	-
SAND	S	-	-	20	30	1	100.000	-	-	-	-	-	-	-
SOFT CLAY	C	-	-	15	20	3	14.750	-	-	-	-	-	-	-

H: Reinforced wall height

ß: Slope angle

γ: Unit weight

m: Bulk modulus exponent

Ø: Friction angle

c: Cohesion

EA: Geotextile reinforcement axis stiffness

S_v: Vertical spacing

L: Geotextile reinforcement length

E_{50}^{ref}: Starting reference Secant modulus

E_{ur}^{ref}: Unload-reload reference Secant modulus

S.C.: Spacing coefficient

$E_{50}^{ref}=0.5(Kp^{ref})$

$E_{ur}^{ref}=K_{ur}p^{ref}$

p^{ref}: Reference pressure

K, K_{ur}: Hyperbolic stress-strain parameters

* Values are taken from K.San, D.Leschinsky and T.Matsui (1994) et al.

.

After the finite element analyses, the total displacements, horizontal displacements, vertical displacements, shear strains, and relative shear stresses were obtained. These are given in the Appendix in graphical format.

The failure planes for dense granular backfill on rock foundation can be seen in Figure 4.2. When the model D1 with 75º slope inclination is examined it is seen that critical failure surface starts from the toe of the slope and cuts the surface far from the crest of the slope. In model D2 with slope inclination of 60º the critical failure surface crosses from the end point of the geotextile reinforcement in 2.50 m height and goes to top. In model D3 with slope inclination of 45º the critical failure surface can be observed as almost aligned with the endpoints of the geotextile reinforcements and very close to the face of the slope. The total displacements in dense backfill on rock foundation models D1, D2 and D3 are 161 mm, 132 mm and 35 mm respectively as seen in Table 4.2. Because of the load distribution of the structure on foundation, displacements are less in 45º slope angled model.

The critical failure surfaces in dense backfill on sand foundation models are given in Figure 4.3. The models with sand foundation show nearly the same reactions as the models with rock foundation. In dense backfill on sand foundation models, the total displacement increases 17 per cent in 45º, 34 per cent in 60º and 30 per cent in 75º slope inclinations when compared to dense backfilled models on rock foundation.

Table 4.2 Total displacements in Dense Granular backfilled models

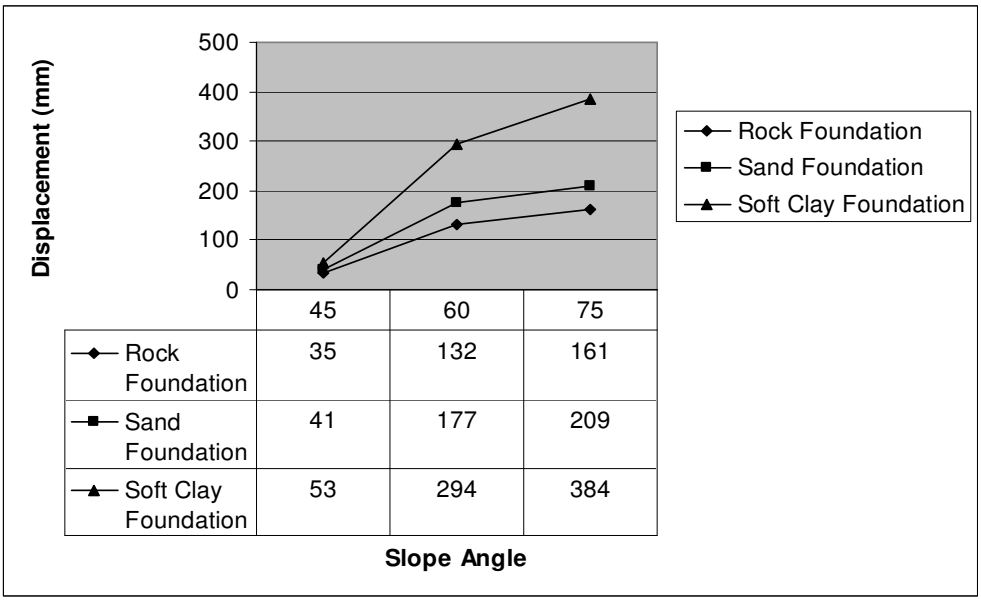

	45	60	75
Rock Foundation	35	132	161
Sand Foundation	41	177	209
Soft Clay Foundation	53	294	384

The slope with an inclination of 75º has a failure surface that starts from the toe and after cutting through a few reinforcements extends well beyond the crest of the slope. In the model with 60º slope inclination the critical failure surface crosses the line of the end points of geotextile at 2,0 m height from the toe. In the model D3 which has the slope angle of 45º with sand foundation and dense backfill, the failure surface can be seen along the end point of the geotextile reinforcements which is very close to the slope face.

In the dense backfill on soft clay foundation models, almost 75 per cent of the total displacements occur in the foundations (Figure 4.4). The total deformation in soft clay foundation and dense backfilled models increases 29 per cent in 45º slope inclination, 66 per cent in 60º slope inclination and 84 per cent in 75º slope inclination. These extreme deformation increase in soft clay foundation especially in 60º and 75º slope inclinations points out the importance of the load distribution on the foundation. When the structure has a slope angle of 45º or less, the loads on the foundation and the deformations decrease proportionally. The total displacements can be seen in Table 4.2. The critical failure surfaces of dense backfill on soft clay foundation models are shown in Figure 4.5. The model with 75º slope inclination has the critical failure surface which starts from the toe and goes up to the top from very behind the slope face. As the inclination angle decreases the critical failure surface line moves forward towards the slope face. This displacement affects the slip stability of the structure negatively.

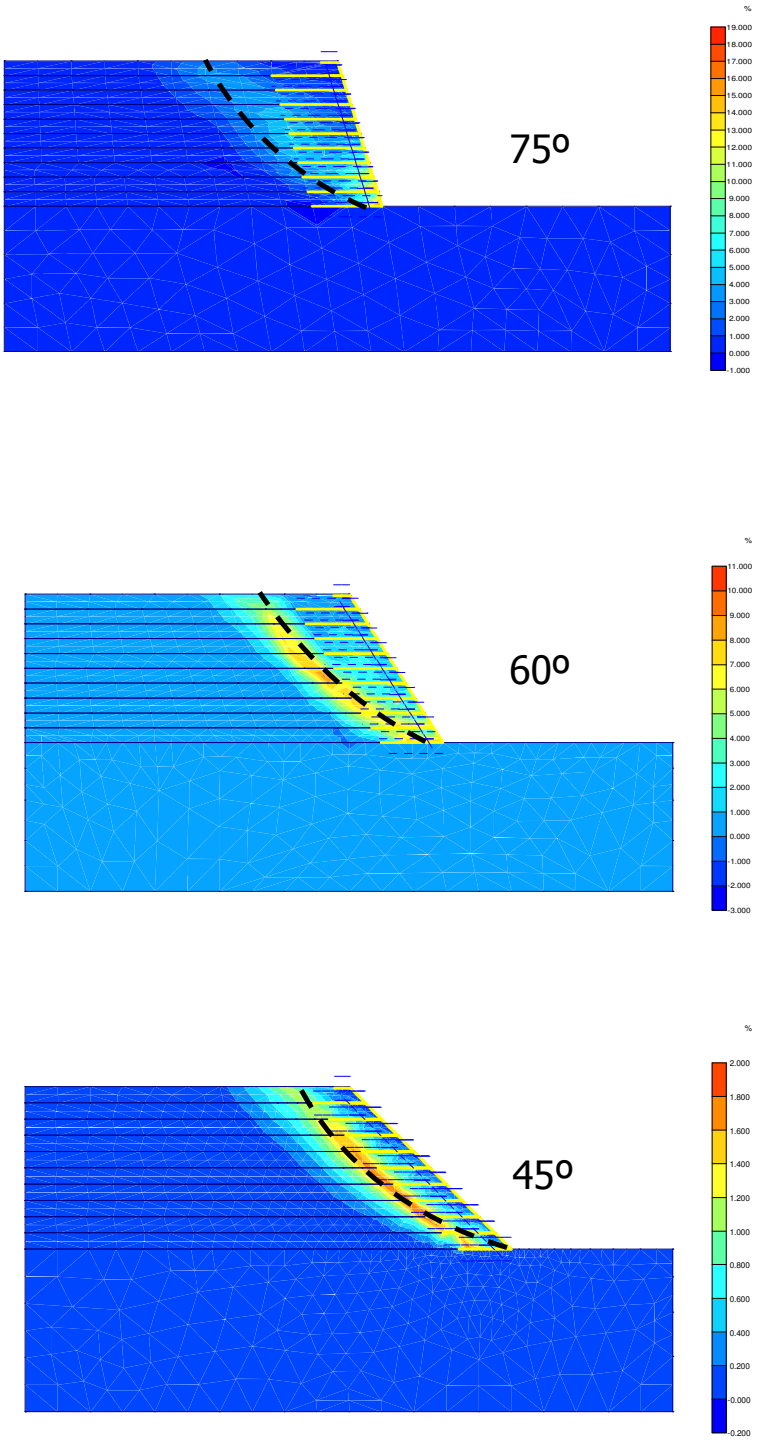

Figure 4.2 Critical failure surfaces of Rock Foundation with Dense Granular Backfilled models, Slope angles; 75º, 60º,45º (Shear strain graphs)

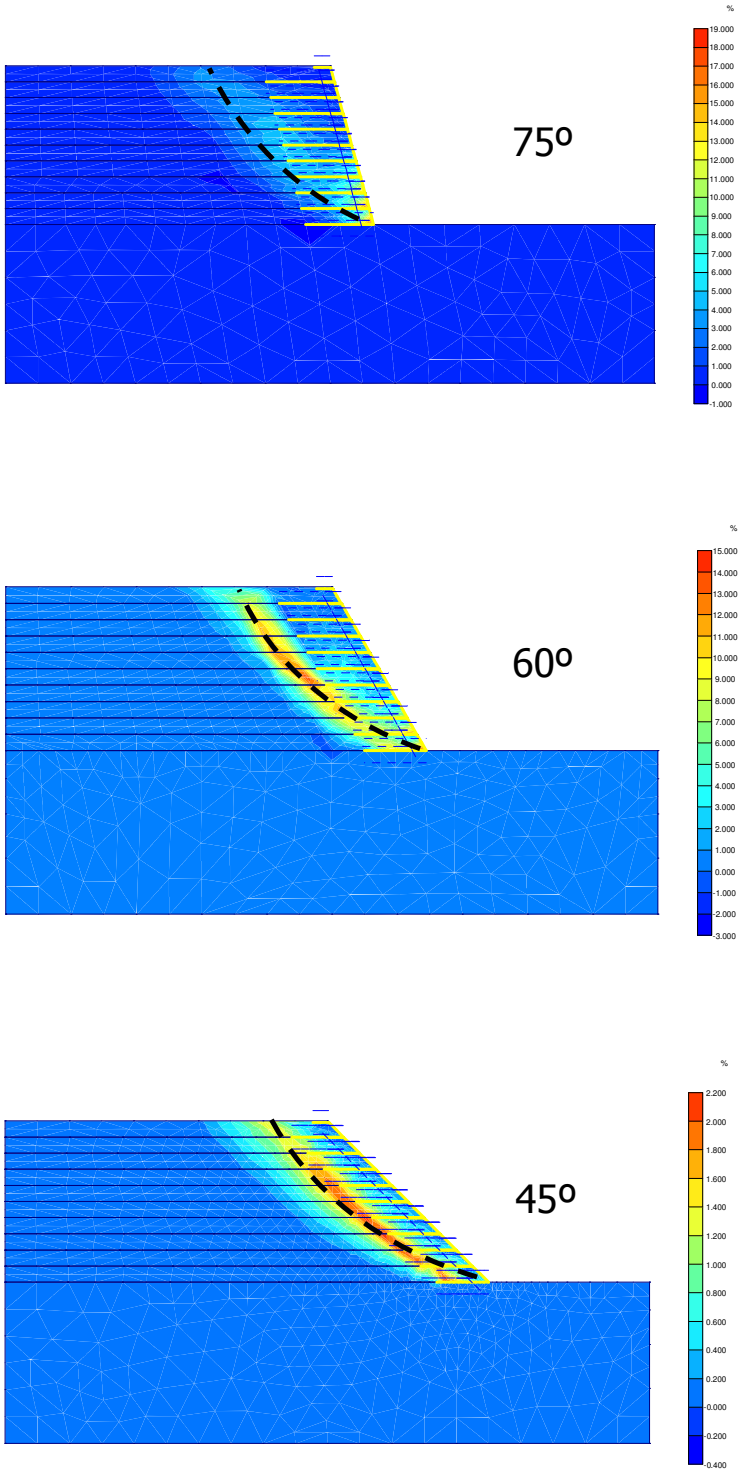

Figure 4.3 Critical failure surfaces of Sand Foundation with Dense Granular Backfilled models, Slope angles; 75º, 60º, 45º (Shear strain graphs)

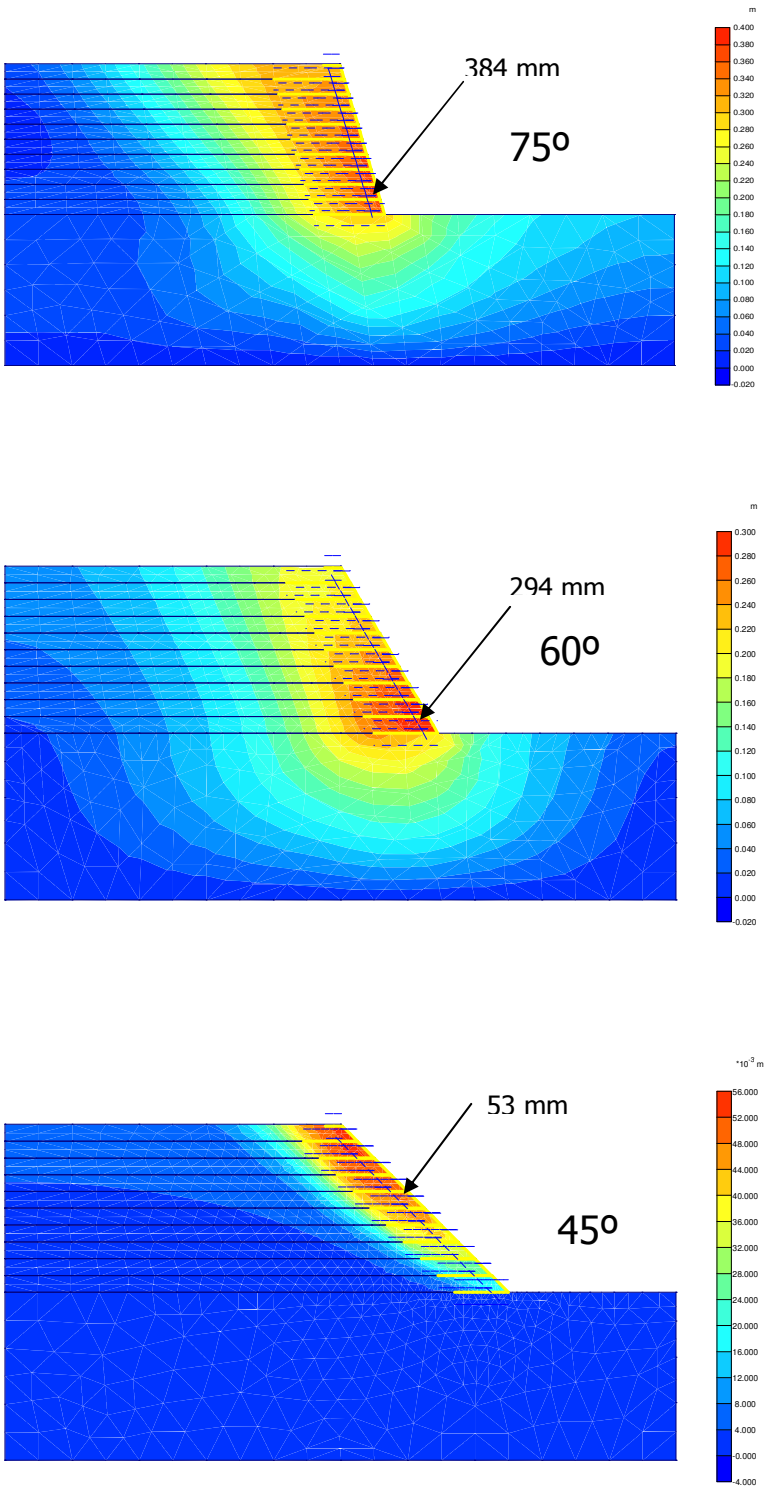

Figure 4.4 Total displacements in Soft Clay foundationed and Dense Granular backfilled models

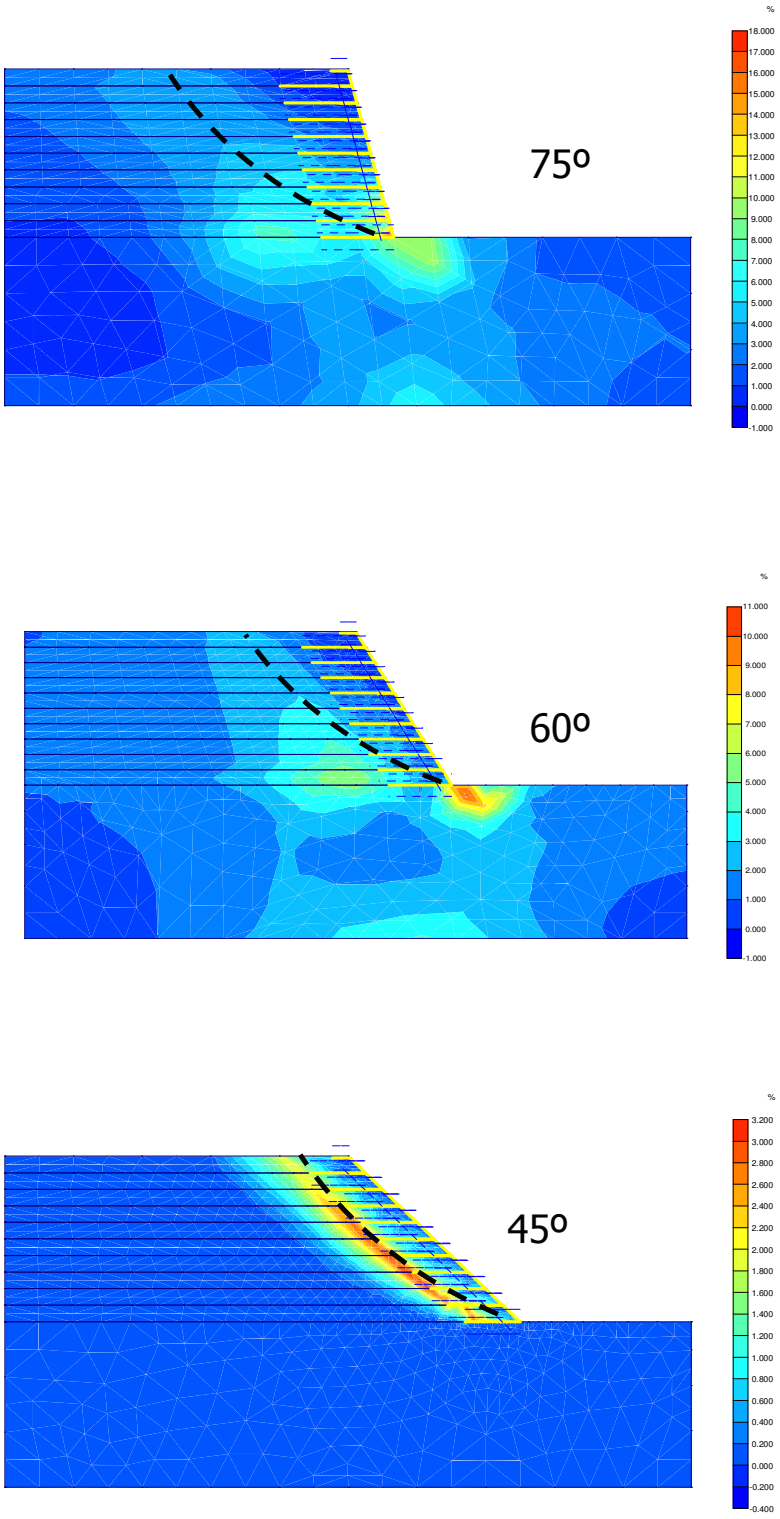

Figure 4.5 Critical failure surfaces of Soft Clay Foundation with Dense Granular Backfilled models, Slope angles; 75º, 60º, 45º (Shear strain graphs)

In the loose backfilled model L1 with rock foundation which has a slope angle of 75º it is observed that more than 90 per cent of the total displacement occurs because of the loose backfill (Figure 4.6). Not only in 75º slope inclinationed model but also in 60º and 45º slope inclinations, the displacement of the backfill happen the same percentage, as 90 per cent of the total displacement of the structure. As can be expected, displacement values increase proportionally with the slope angle (Table 4.3). The critical failure surface starts from the toe of the slope and goes to the top far from the slope face. In model L2 with slope inclination of 60º the critical failure surface crosses from the end point of the geotextile reinforcement at 2.50 m height and goes to top. As the geotextile reinforcements are longer in loose backfilled models the critical failure surface line passes further back from the crest of the slope. In model L3 with slope inclination of 45º the critical failure surface can be observed as being aligned with the endpoints of the geotextile reinforcements after the third layer of reinforcement in the slope. These critical surfaces can be seen in the Figure 4.7.

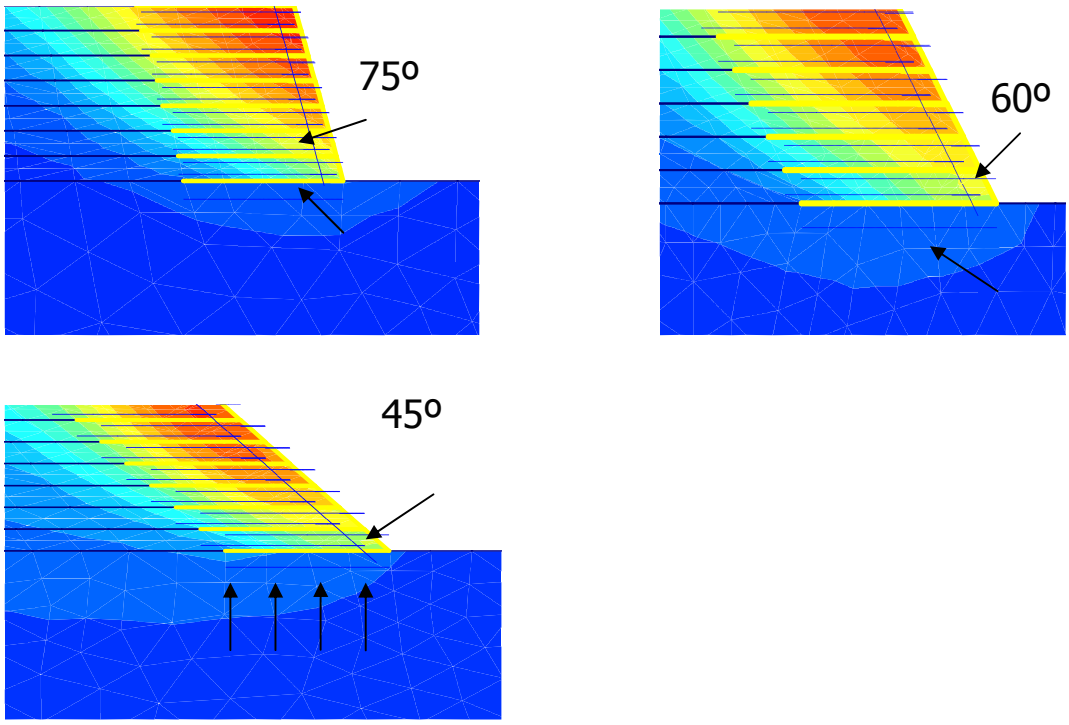

Figure 4.6 Total displacements in Loose Granular backfilled and Rock Foundationed Models.

Table 4.3 Total displacements in Loose Granular backfilled models.

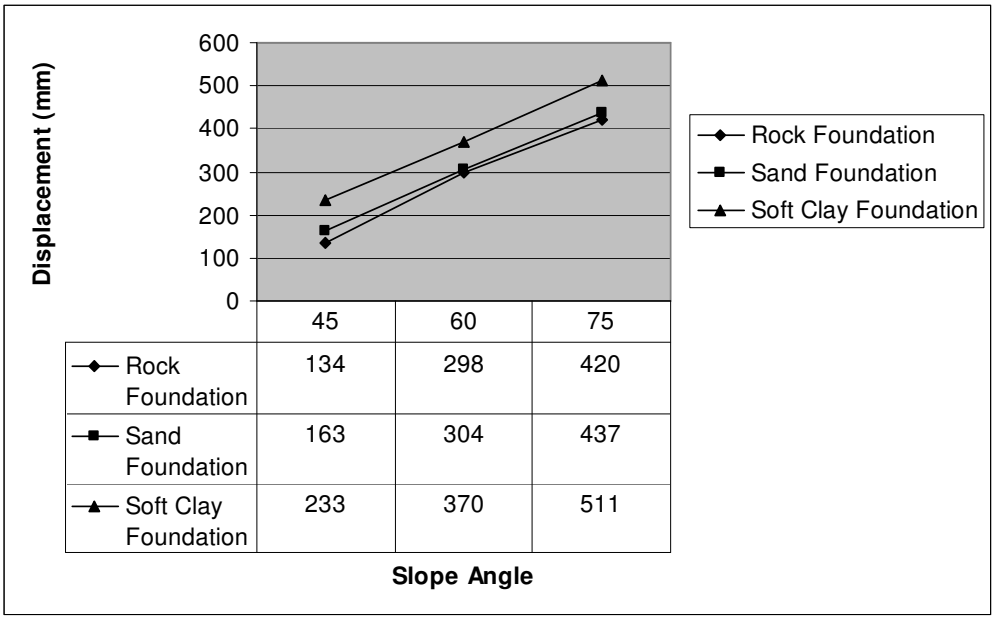

	45	60	75
Rock Foundation	134	298	420
Sand Foundation	163	304	437
Soft Clay Foundation	233	370	511

The total displacements in loose backfill on rock foundation models L1, L2 and L3 are as 420 mm, 298 mm and 134 mm respectively (Table 4.3). Because of the load distribution of the structure on foundation, displacements are smaller in 45º slope inclination than in 60º and 75º slope inclinations.

The same models with sand foundation show nearly the same reactions as rock foundation models. In dense backfill on sand foundation models, the total displacement increases 22 per cent in 45º, 2 per cent in 60º and 4 per cent in 75º slope inclinations according to dense backfill on rock foundation models. The critical failure surface of a 75º slope inclination with loose granular backfill on sand foundation model starts from the toe, passes from the end point of the sixth layer geotextile reinforcement and goes up to the top of the slope. When the loose granular backfill on sand foundation model with 60º slope inclination is investigated, the critical failure surface appears on the line which is very similar to the slope inclination of 75º. In both of these models the critical failure surface ends far from the slope face. The loose granular backfill on sand foundation with an inclination of 45º has the critical failure surface which starts from the toe and passes from the end point of the third layer geotextile reinforcement and goes to the top by following the end points of the geotextile reinforcements.

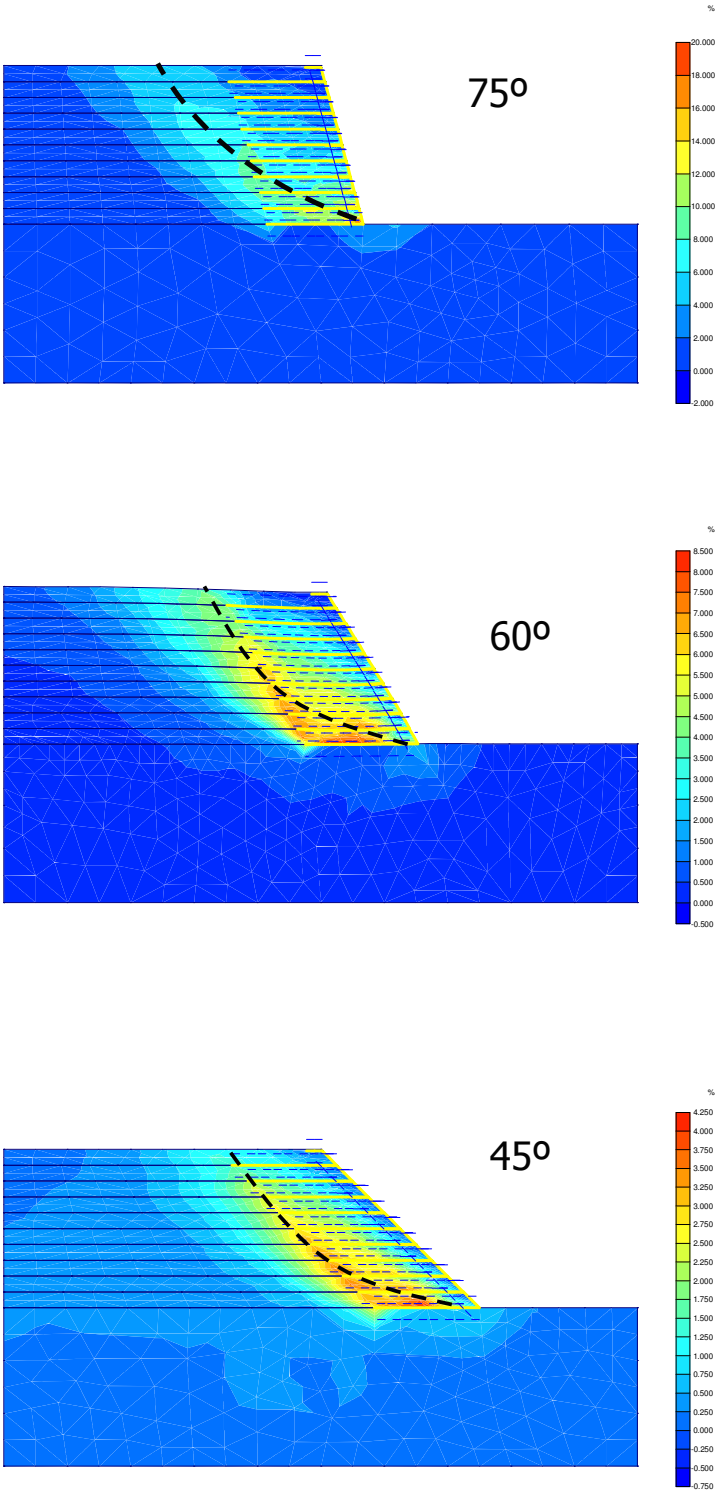

Figure 4.7 Critical failure surfaces of Rock Foundation with Loose Granular Backfilled models, Slope angles; 75º, 60º, 45º (Shear strain graphs)

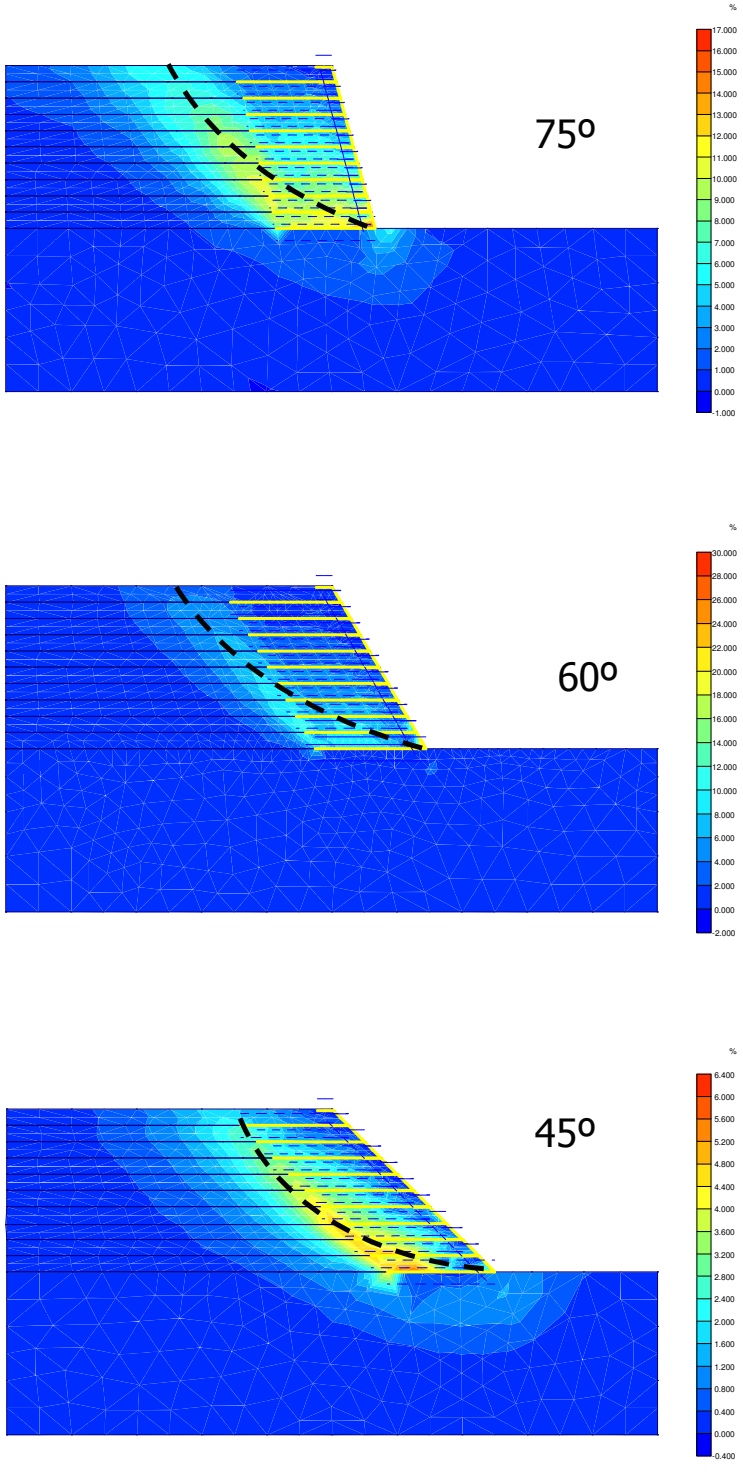

Figure 4.8 Critical failure surfaces of Sand Foundation with Loose Granular Backfilled models, Slope angles; 75º, 60º, 45º (Shear strain graphs)

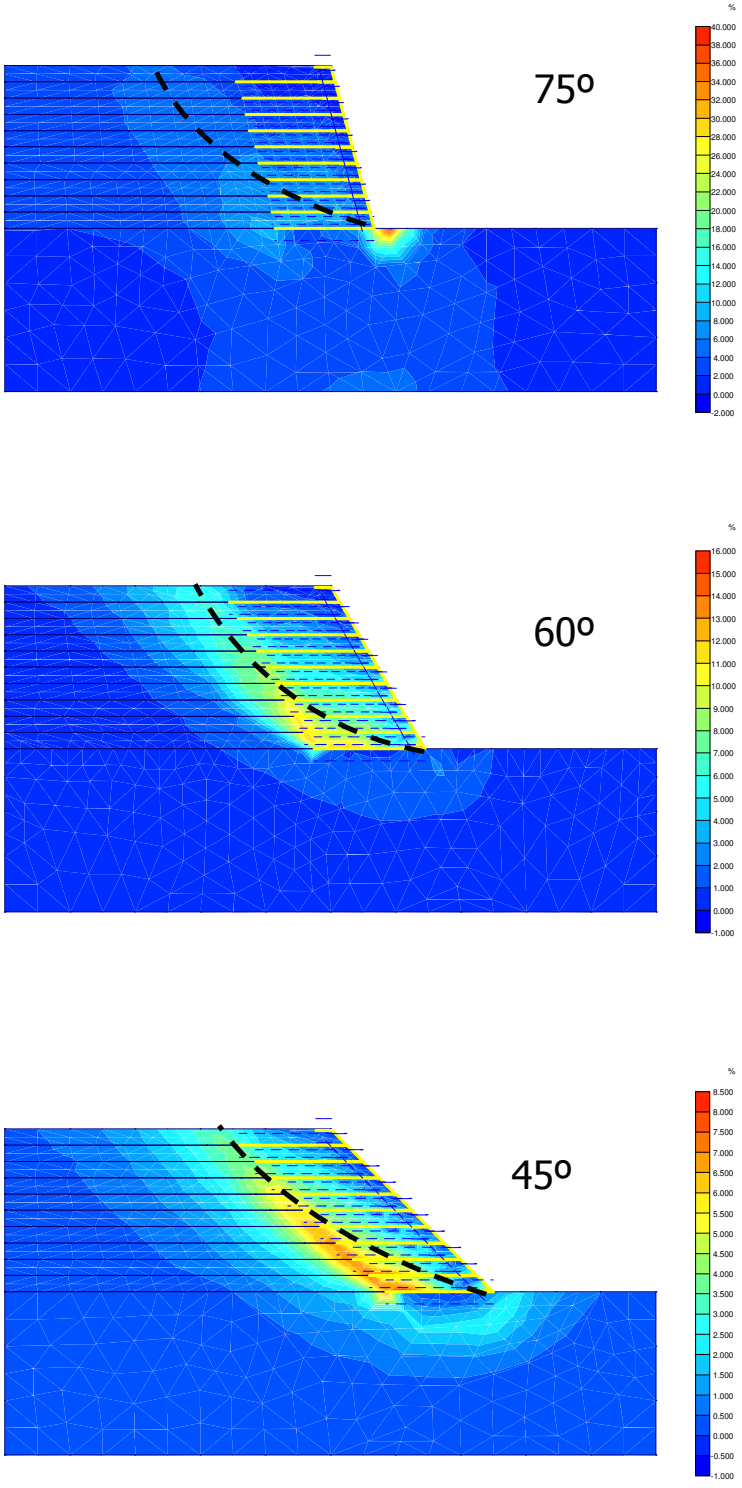

Figure 4.9 Critical failure surfaces of Soft Clay Foundation with Loose Granular Backfilled models, Slope angles; 75º, 60º, 45º (Shear strain graphs)

When the dense and loose backfills are compared, under the same slope inclination and same foundation e.g. rock, vertical displacement increases almost three times when dense backfilled type slope is compared to loose backfilled type (Figure 4.10). Length of the geotextile reinforcement increases the FS values in loose granular backfill against dense granular backfill on rock foundation and sand foundation with 75º slope inclination. FS values are listed in Table 4.4.

In the loose backfill on soft clay foundation models, 50 per cent of the total displacements occur in the foundations. Comparing with the loose backfill on sand foundation models, the total deformation in loose backfill on soft clay foundation models increases 43 per cent in 45º slope inclination, 22 per cent in 60º slope inclination and 17 per cent in 75º slope inclination. While the increment ratios of deformations decrease reverse proportionally with the slope inclination in loose backfilled types, it increases proportionally in dense granular backfilled models. When the structure has the slope angle of 45º or less inclination, the loads on the foundation and the deformations decrease proportionally. The total displacements can be seen in Table 4.3. The critical failure surfaces of loose granular backfill on soft clay foundation models are shown in Figure 4.9. The model with 75º slope inclination with loose granular backfill on soft clay foundation has the critical failure surface that starts from the toe and goes up to the top almost 6.0 m behind the crest of the slope face. As the inclination angle decreases the critical failure surface line moves forward towards the slope face. This displacement affects the slip stability of the structure negatively.

Another important result of the slope inclination effect in loose granular backfilled models on soft clay foundation is the horizontal displacement. The horizontal displacement of 75º slope model is twice of the model with 45º inclination. The extreme difference of horizontal displacement in between these slope angles shows that the geotextile reinforcement helps to improve the stability of the structure and behave like a soil body on the foundation.

The current analysis gives the same results as calculated by the limit equilibrium computer code Strata Slope (San, Leshchinsky and Matsui (1994) et al. In Table 4.4 the factor of safety of these eighteen models are listed. The safety factors are very close to the value 1 except for 75º slope inclinationed and loose granular backfilled models with rock and sand foundations. The length of the reinforcements in these models affects the safety of the structure positively.

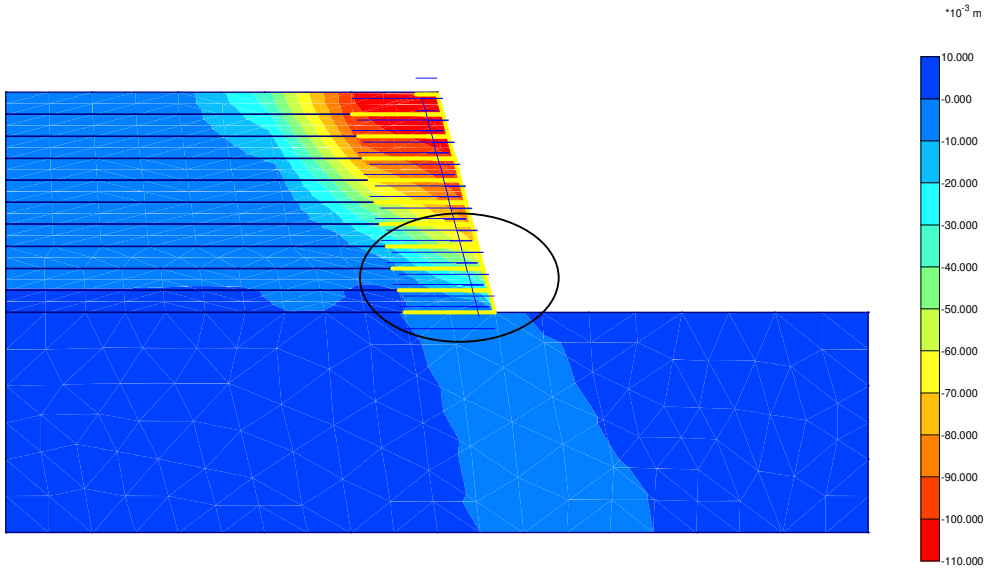

Dense backfill (75º) (D1 Rock)
Displacement : 108 mm

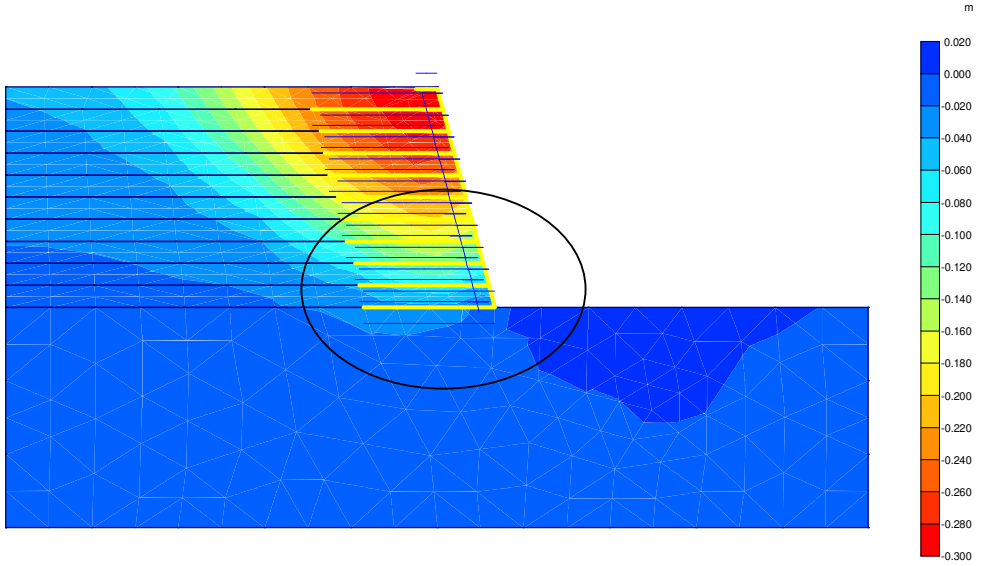

Loose backfill (75º) (L1 Rock)
Displacement : 298 mm

Figure 4.10 Comparison of the backfills by the vertical displacements in rock foundationed models

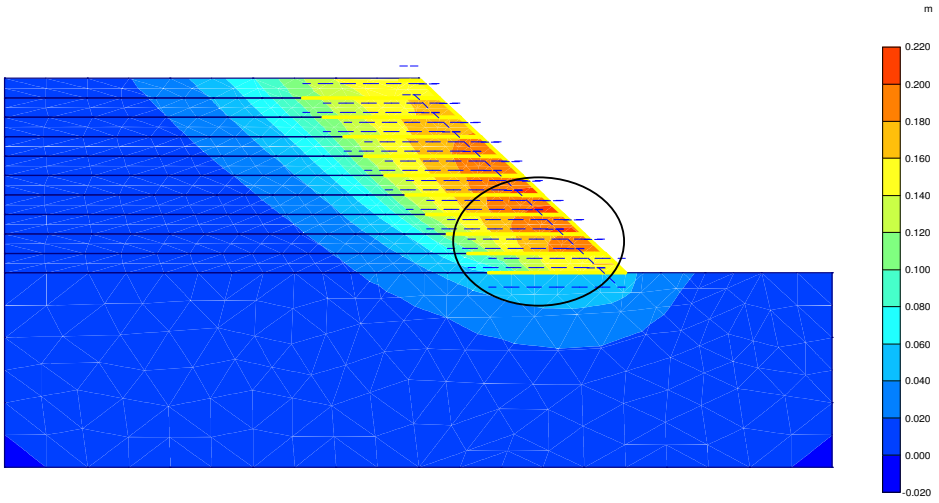

Soft Clay foundation with loose backfill (45º)
Displacement : 207 mm

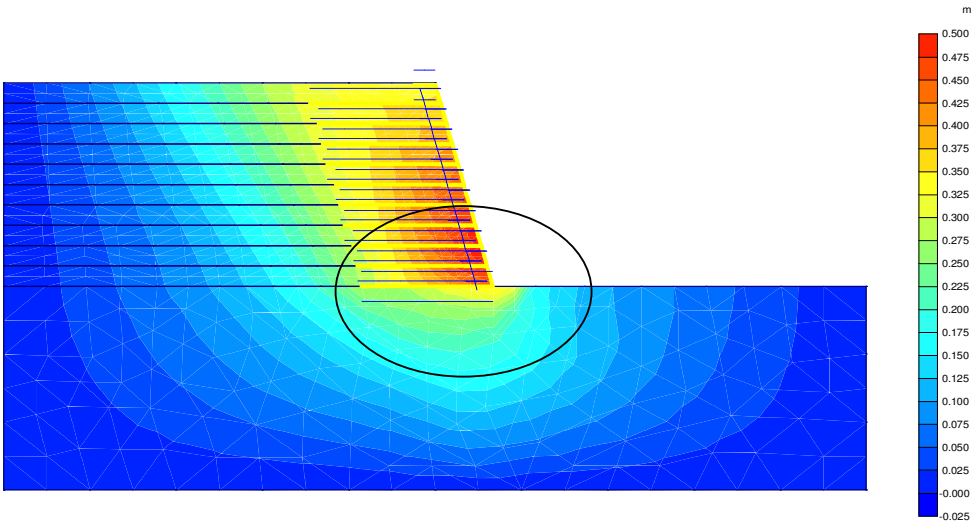

Soft Clay foundation with loose backfill (75º)
Displacement : 492 mm

Figure 4.11 Comparison of the slope angles by the horizontal displacements in soft clay foundationed models

Table 4.4 Factor of safety values calculated by Plaxis Phi-c reduction method.

Backfill Type	Dense Backfill			Loose Backfill		
Slope Angle	75º	60º	45º	75º	60º	45º
Rock Foundation	1,073	1,007	1,008	1,246	1,050	1,101
Sand Foundation	1,010	1,005	1,005	1,225	1,080	1,063
Soft Clay foundation	1,109	1,087	1,010	1,036	1,045	1,084

5. CONCLUSION

5.1. Effect of Front Slope

Referring to these eighteen models, in 45º slope inclination models the critical failure surface appears very close to the slope face. This critical failure surface line moves backwards behind the slope in 60º and 75º inclined slopes. The sudden increase in slope angle makes the load distribution uniform on the foundation. When the slope inclination increase, vertical displacements increase in soft foundations. Slope angle of the structure effects directly the displacements of the foundation. While 75º slope angle causes bearing capacity problems, the lower slope angles such as 45º, the global stability of the system especially in soft foundations becomes more critical.

5.2. Effect of Foundation

Soft foundations effect the safety of superstructure negatively even with the usage of long reinforcement and dense backfills. The critical failure surface appears very close to the slope face in soft foundationed and 45º slope inclinationed models. As the rock and sand foundations show similar behaviors in displacement, extreme deformations occur in soft clay foundations. When the bearing capacity of the foundation increases, the total stability of the structure increases in the same slope inclinations and backfills. Increase in slope angle cause an increase in horizontal displacements in soft foundations such as soft clay. When the slope inclination increase, vertical displacements increase in soft foundations because of the backfills' direct sliding effect on the structure.

5.3. Effect of Backfill

Loose granular backfills always causes big deformations in the structure. In dense backfilled models critical failure surface starts from the toe of the slope and goes vertically far from the slope face to the top of the structure. But in loose backfilled models critical failure surface starts from the toe and goes to the top along the end points of the geotextiles which is very close to the slope face. It can be said that the density of the backfill effects the location of the failure surface. This shows that, there is a correlation between the density of the backfill and failure surface.

Using loose backfills with three different types of foundations and slope inclinations (75°, 60° and 45°), brings extreme displacements with it and does not help the stability of the structures. As the overlap distances of geotextile reinforcements behave like a short reinforcement and help the stability of the structure like in dense granular backfilled models, the lengths of the reinforcements are much longer in loose backfilled models which are not economic in construction.

As a result, geotextile reinforced slope construction in every angle of slope, backfill and foundation is applicable. It is claimed that the soil-geosynthetic interaction coefficient used in finite elements analyses of the structures is very important effect on the outputs and more laboratory models are needed to get a definite coefficient for analyses' sake.
Nevertheless, behavior of the soil structures referring to finite element method analyses may not give the same results during the application because of the ununique construction methods such as manpower or quality of the technical equipment and measurement tools in the site.

APPENDIX: OUTPUTS OF GEOTEXTILE REINFORCED SLOPES ANALYSED BY PLAXIS

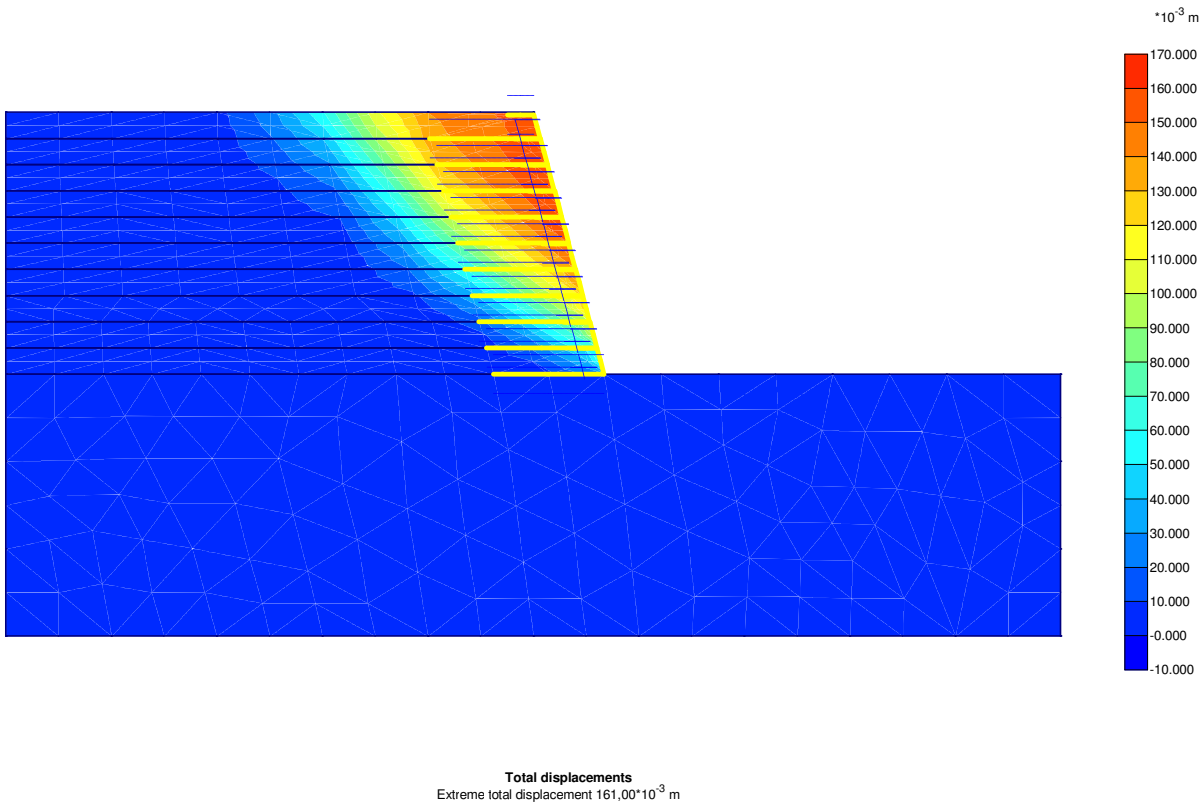

Figure A.1.1 Model D1 with Rock foundation.

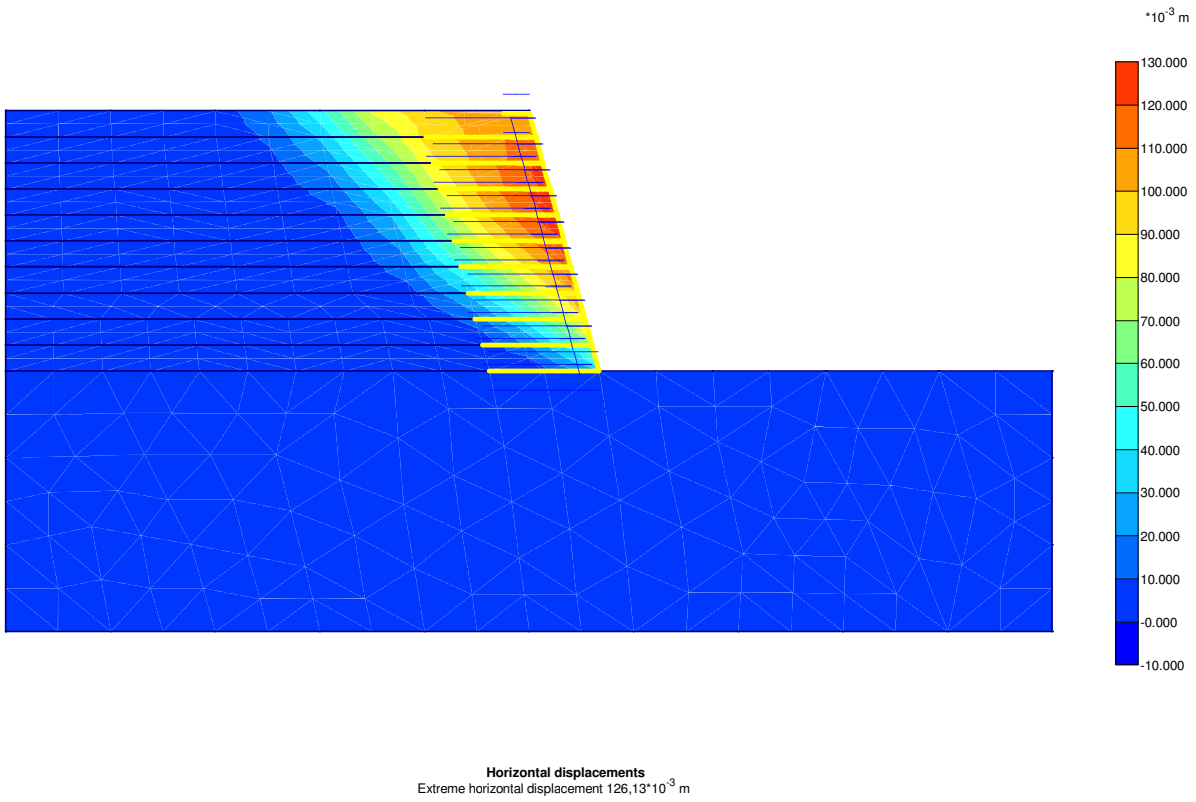

Figure A.1.2 Model D1 with Rock foundation.

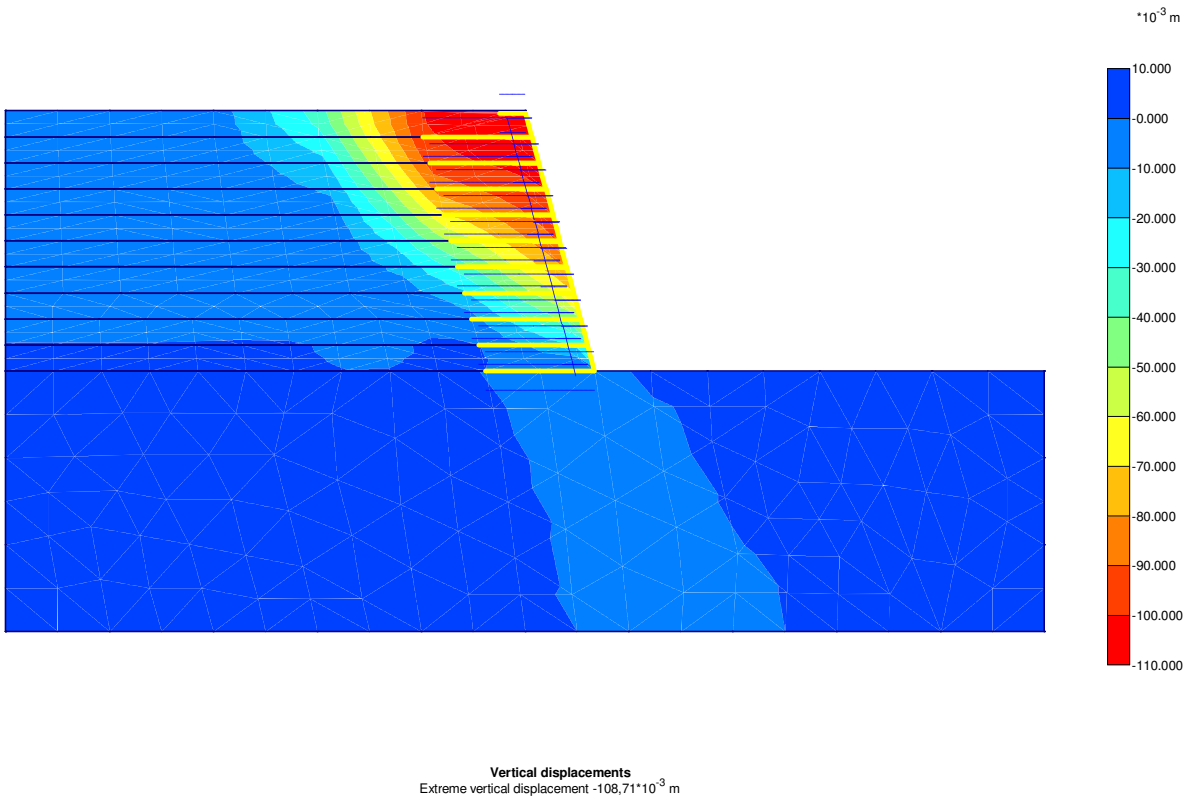

Figure A.1.3 Model D1 with Rock foundation.

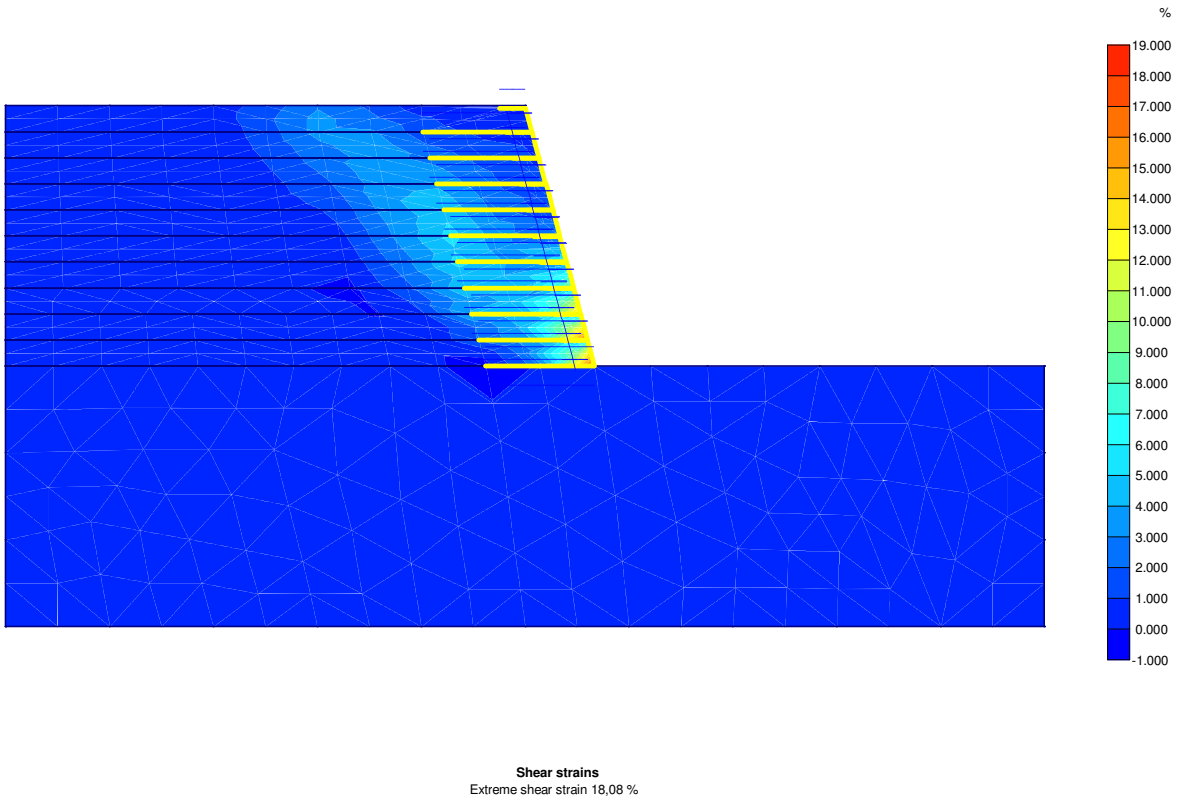

Figure A.1.4 Model D1 with Rock foundation.

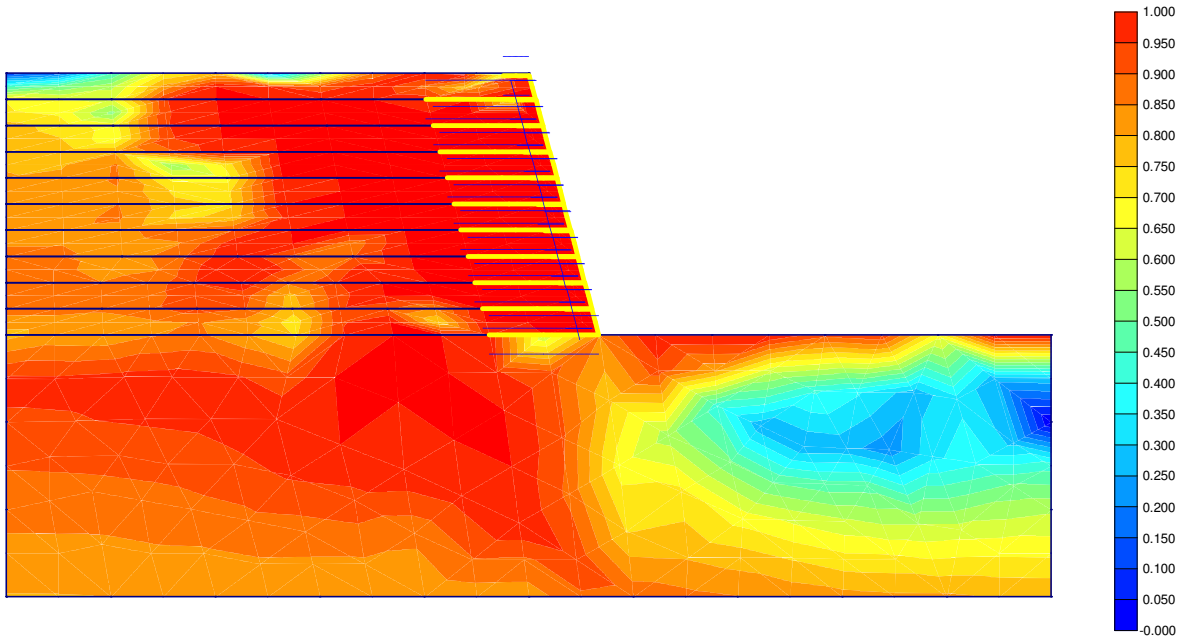

Figure A.1.5 Model D1 with Rock foundation.

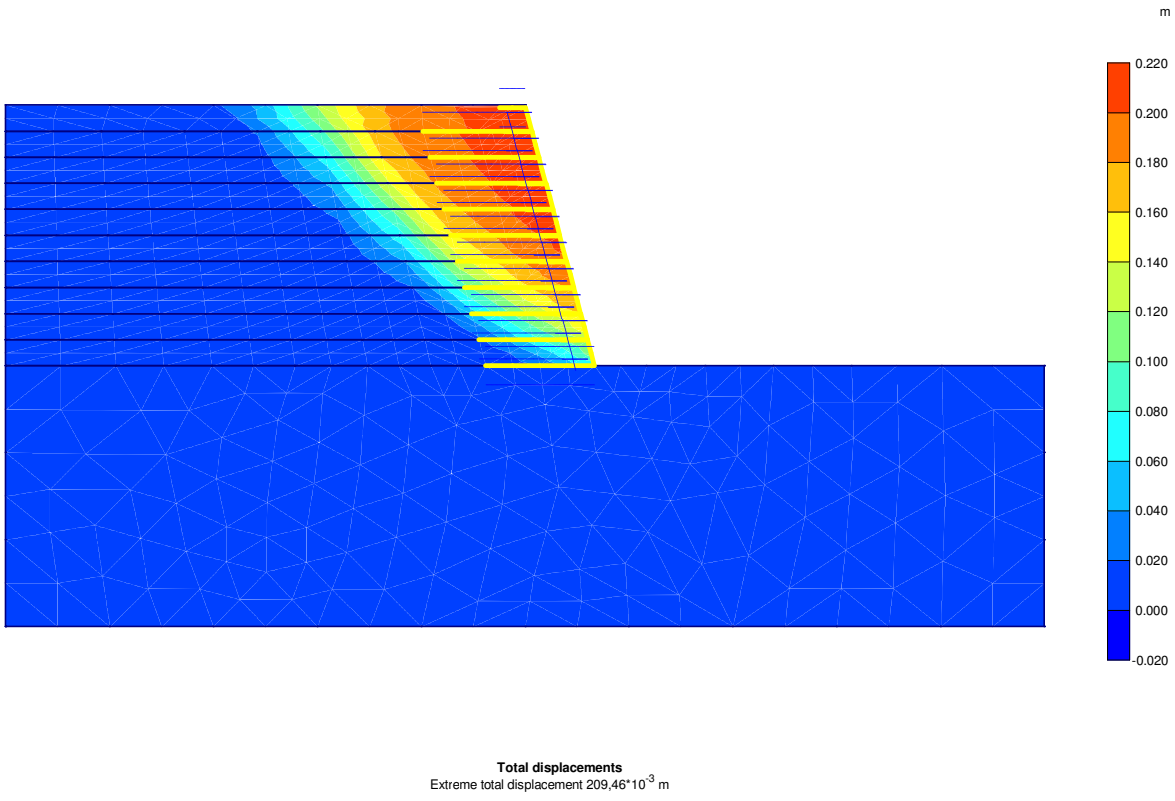

Figure A.2.1 Model D1 with Sand foundation.

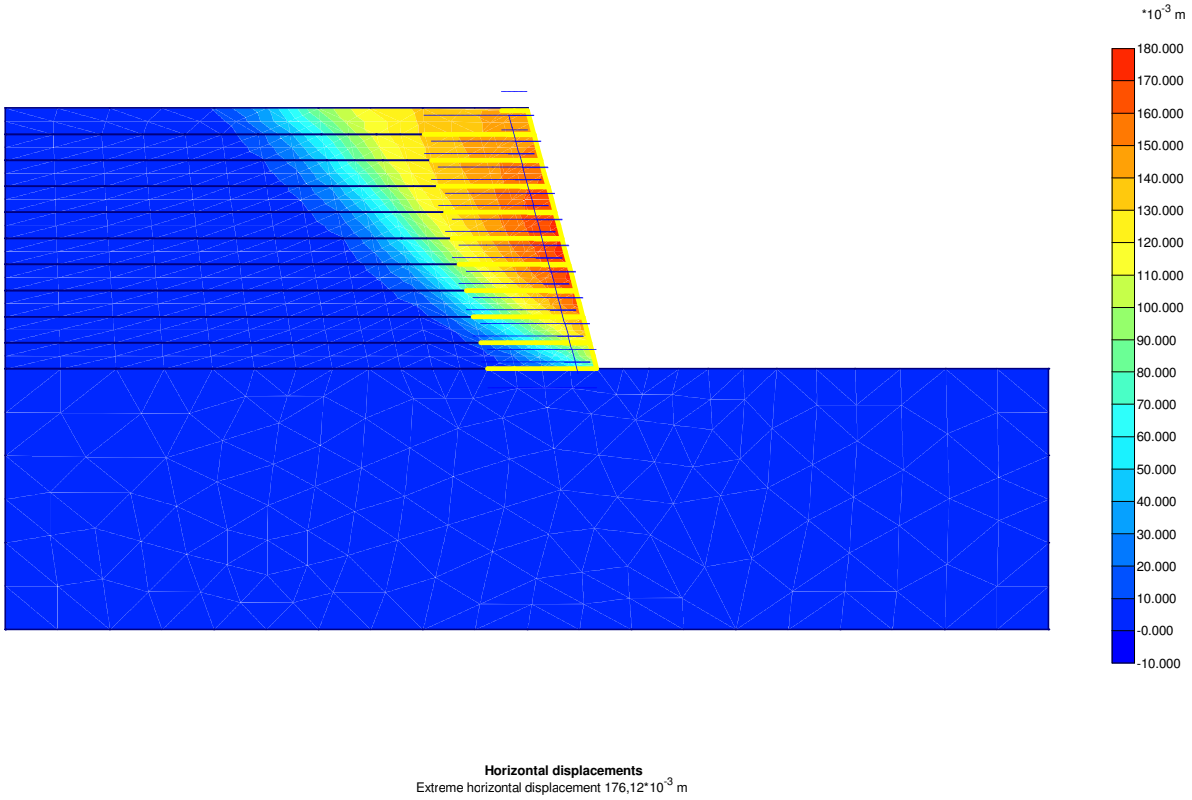

Figure A.2.2 Model D1 with Sand foundation.

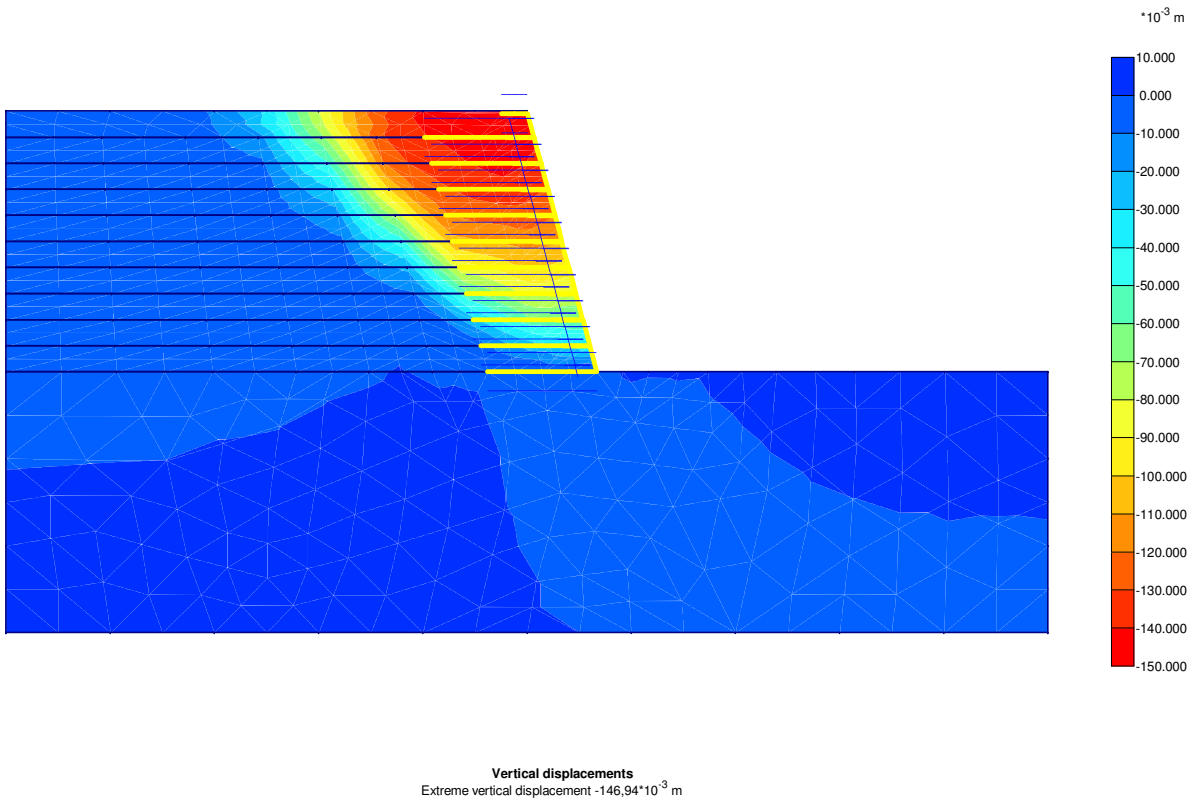

Figure A.2.3 Model D1 with Sand Foundation

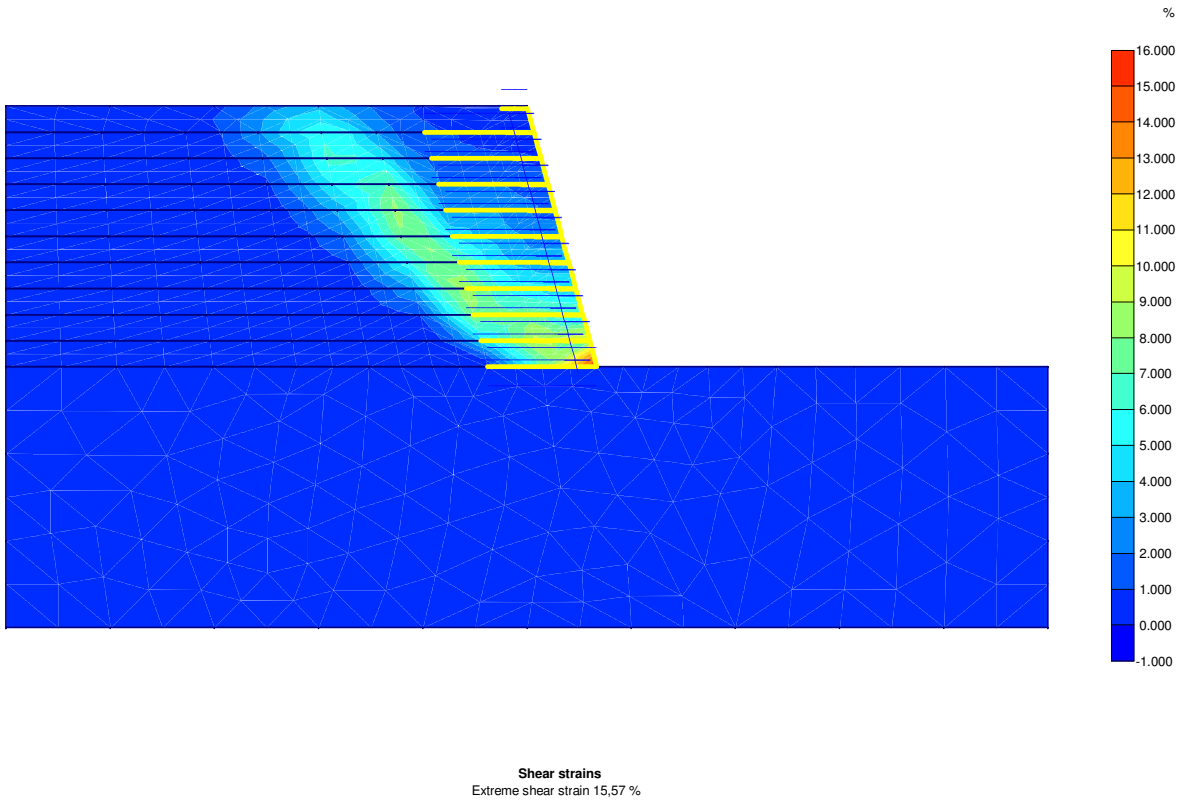

Figure A.2.4 Model D1 with Sand foundation.

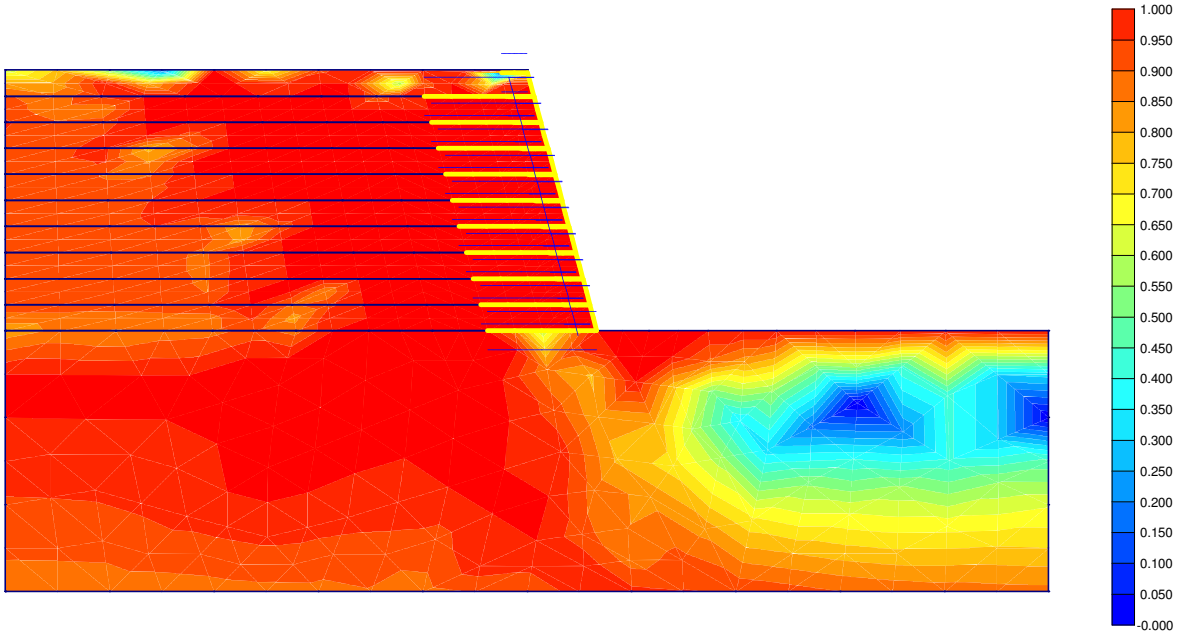

Figure A.2.5 Model D1 with Sand foundation.

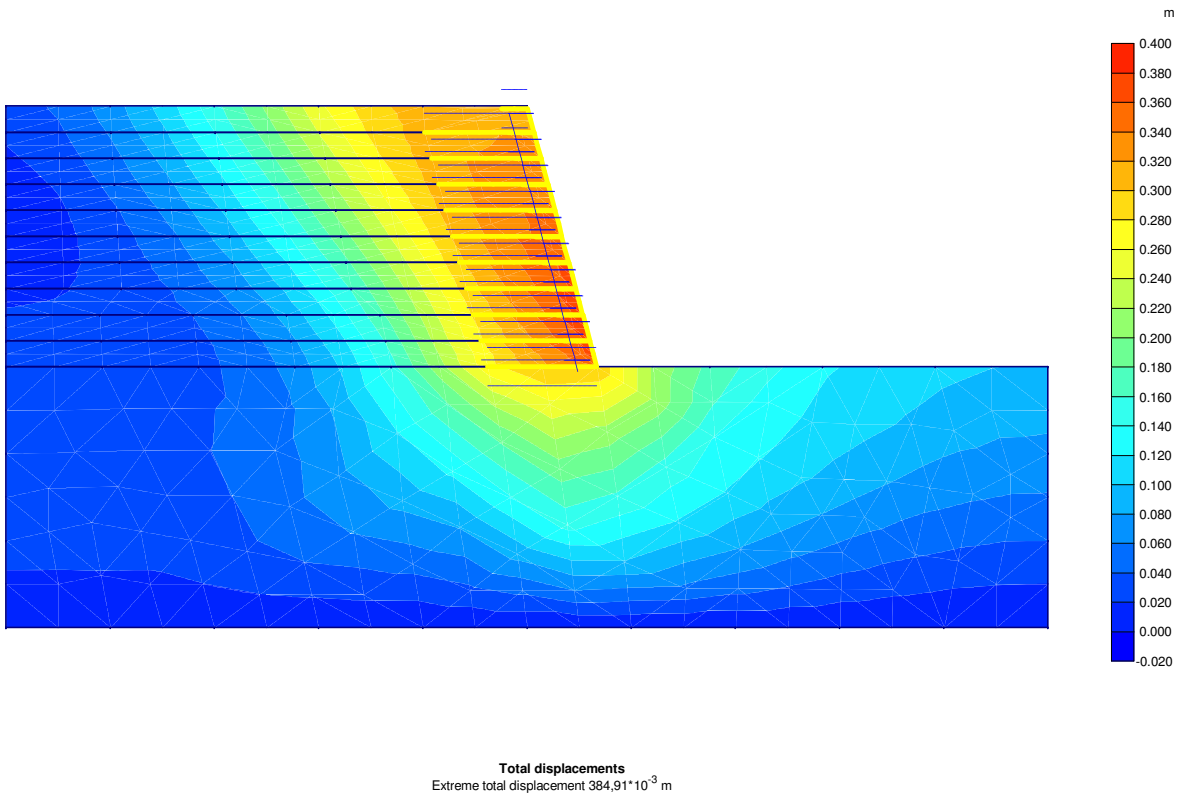

Figure A.3.1 Model D1 with Soft Clay foundation.

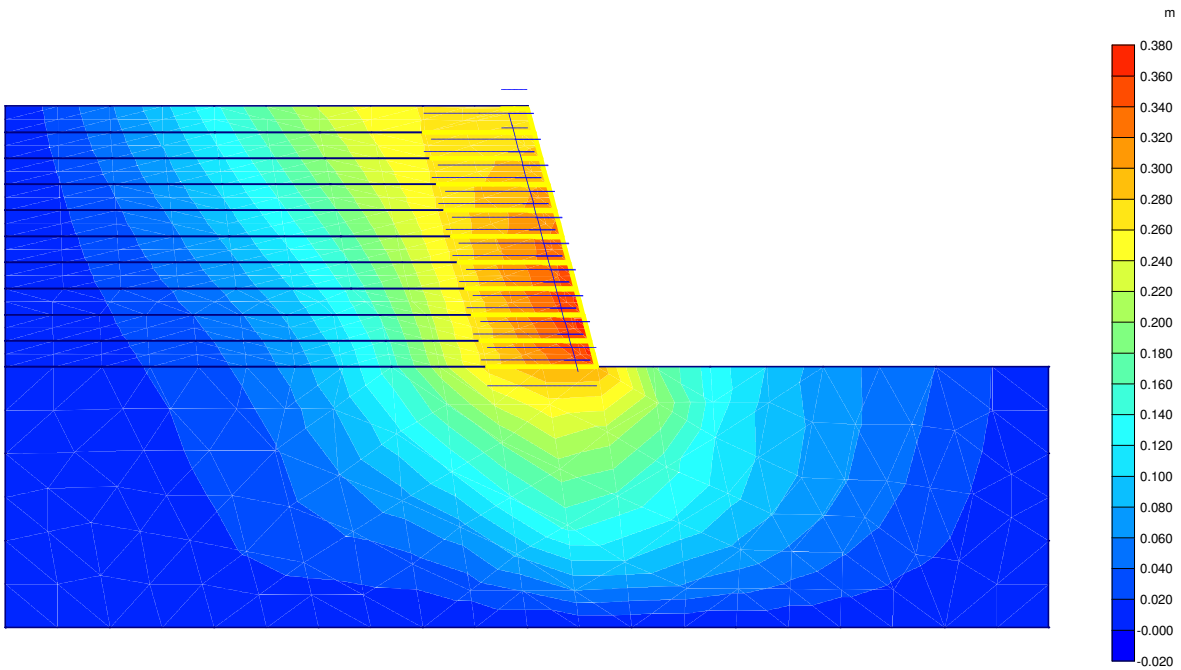

Figure A.3.2 Model D1 with Soft Clay foundation.

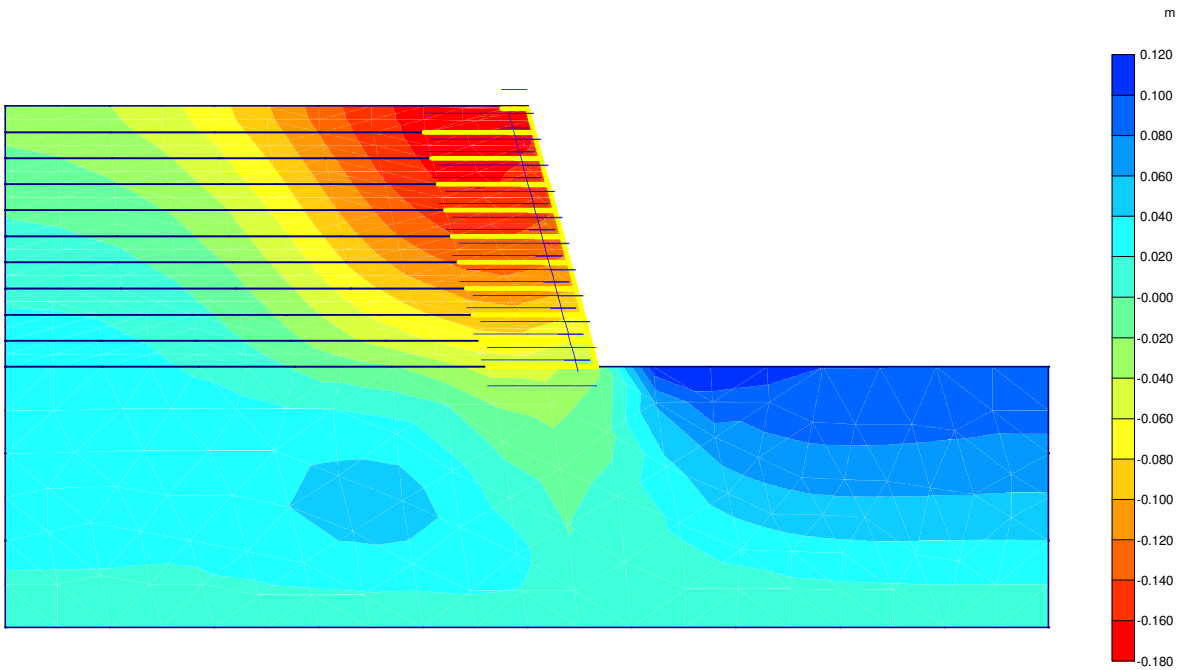

Figure A.3.3 Model D1 with Soft Clay foundation.

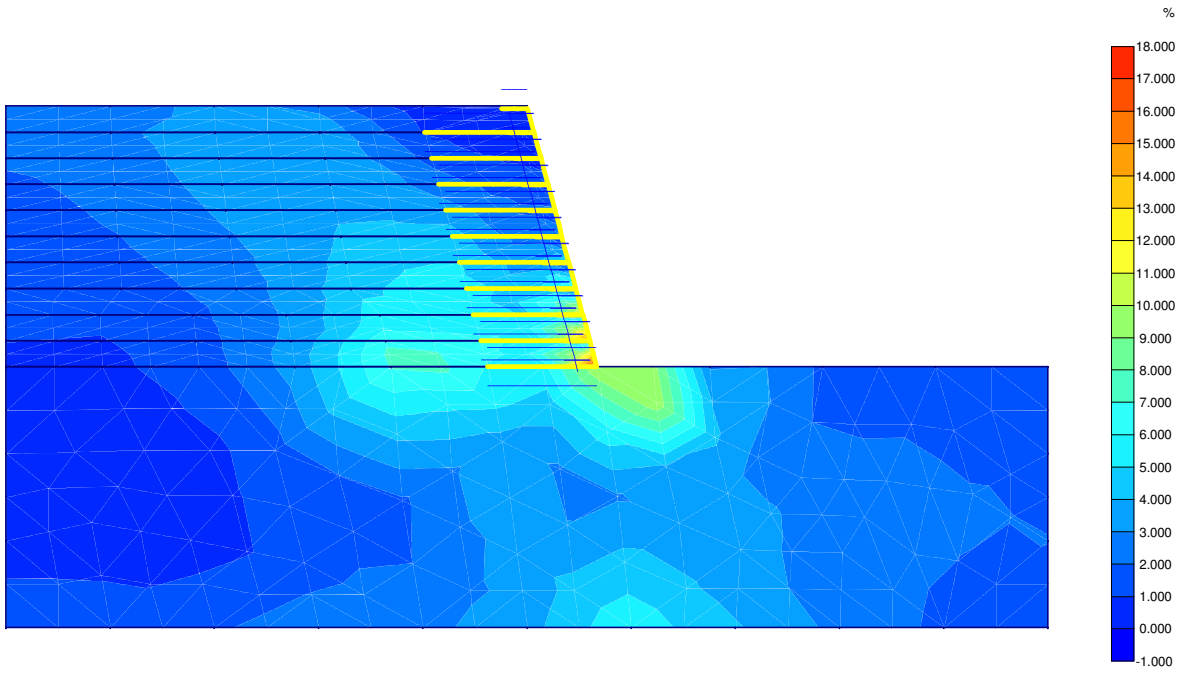

Figure A.3.4 Model D1 with Soft Clay foundation.

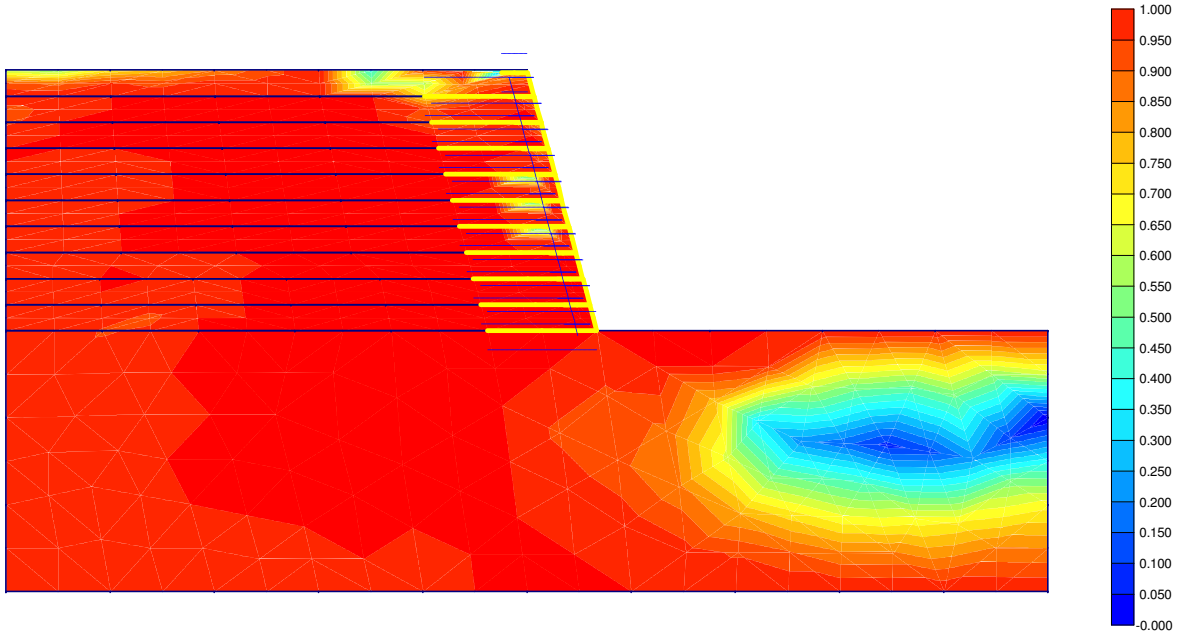

Figure A.3.5 Model D1 with Soft Clay foundation.

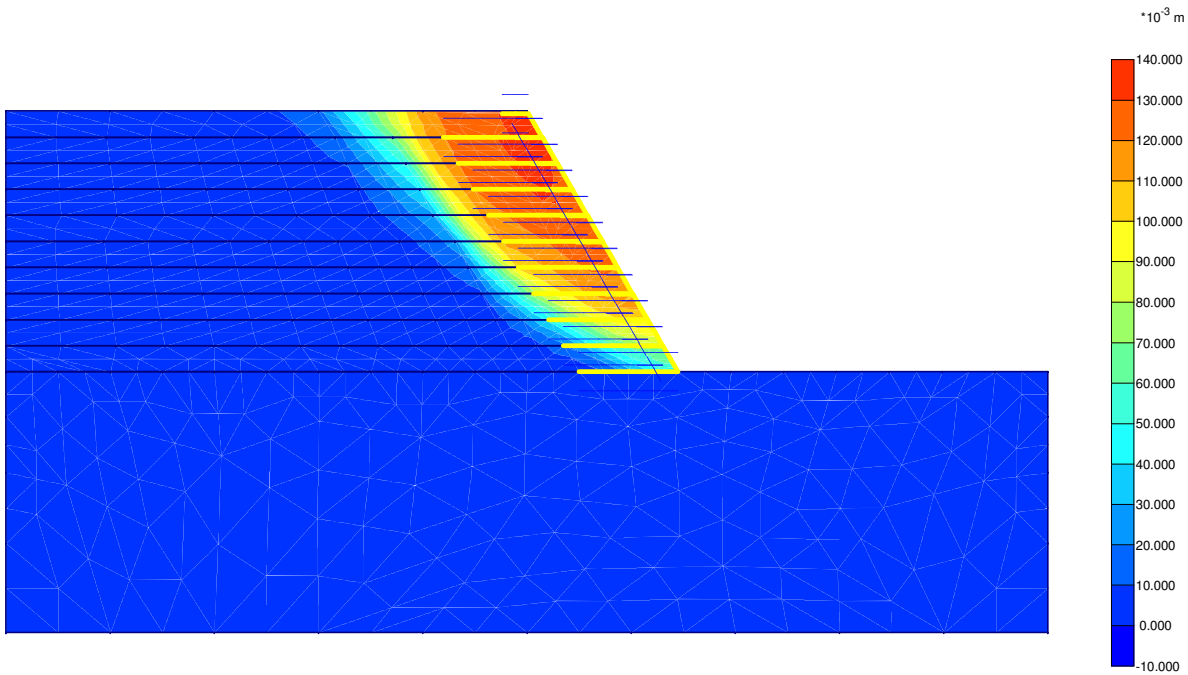

Figure A.4.1 Model D2 with Rock foundation.

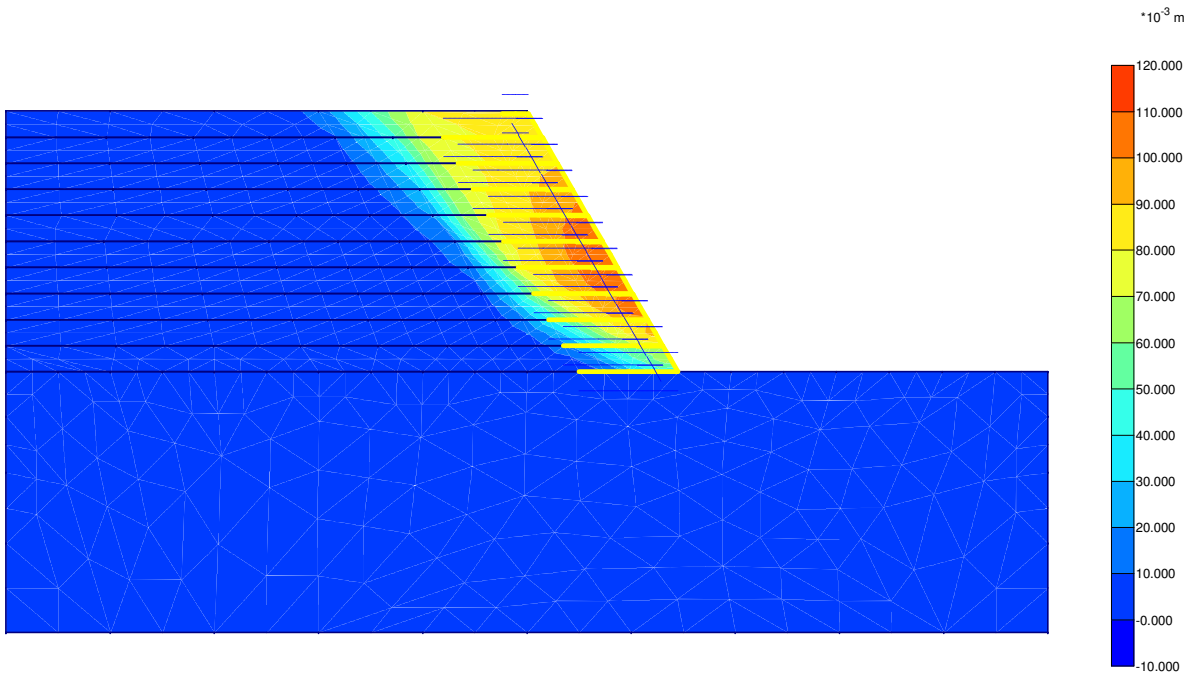

Figure A.4.2 Model D2 with Rock foundation.

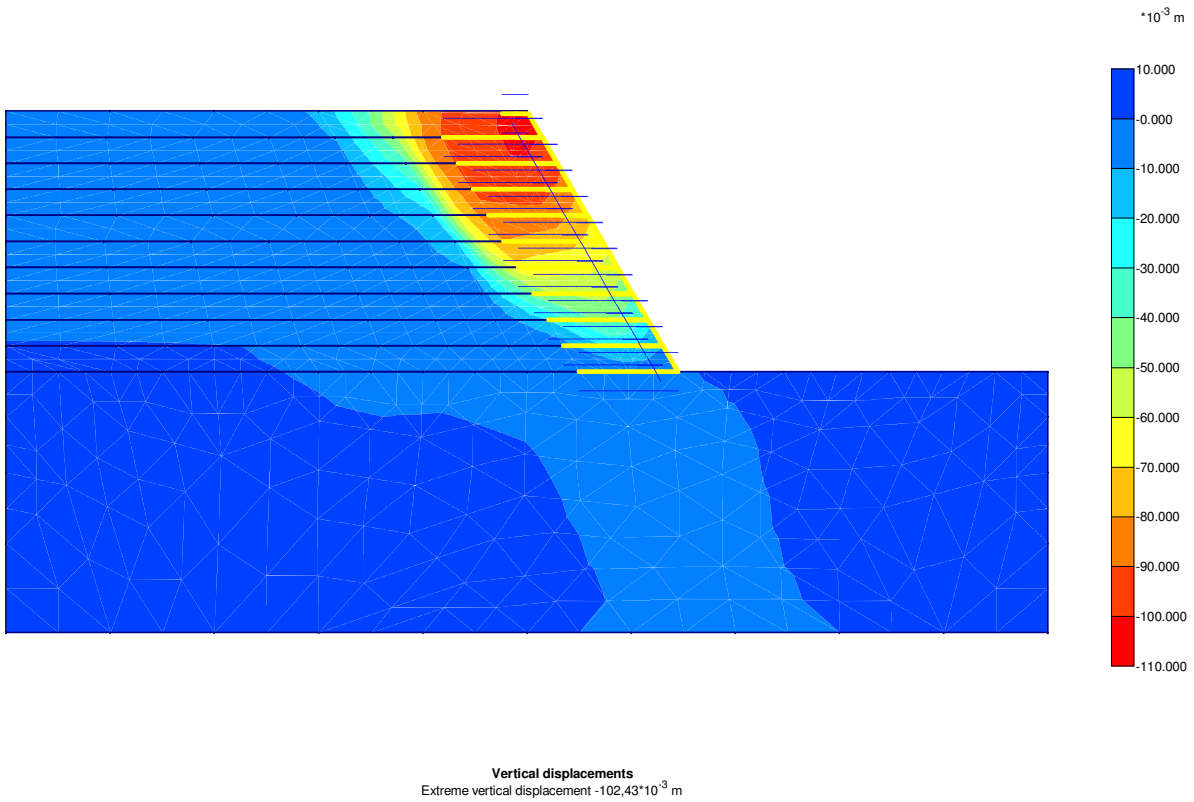

Figure A.4.3 Model D2 with Rock foundation.

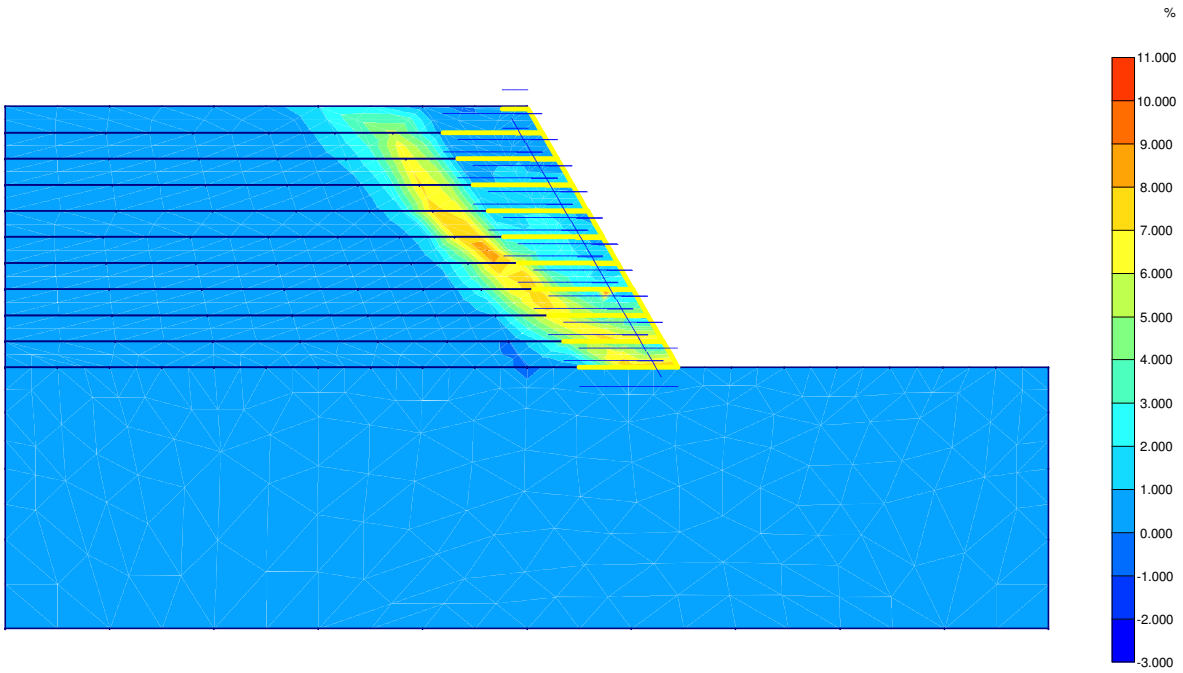

Figure A.4.4 Model D2 with Rock foundation.

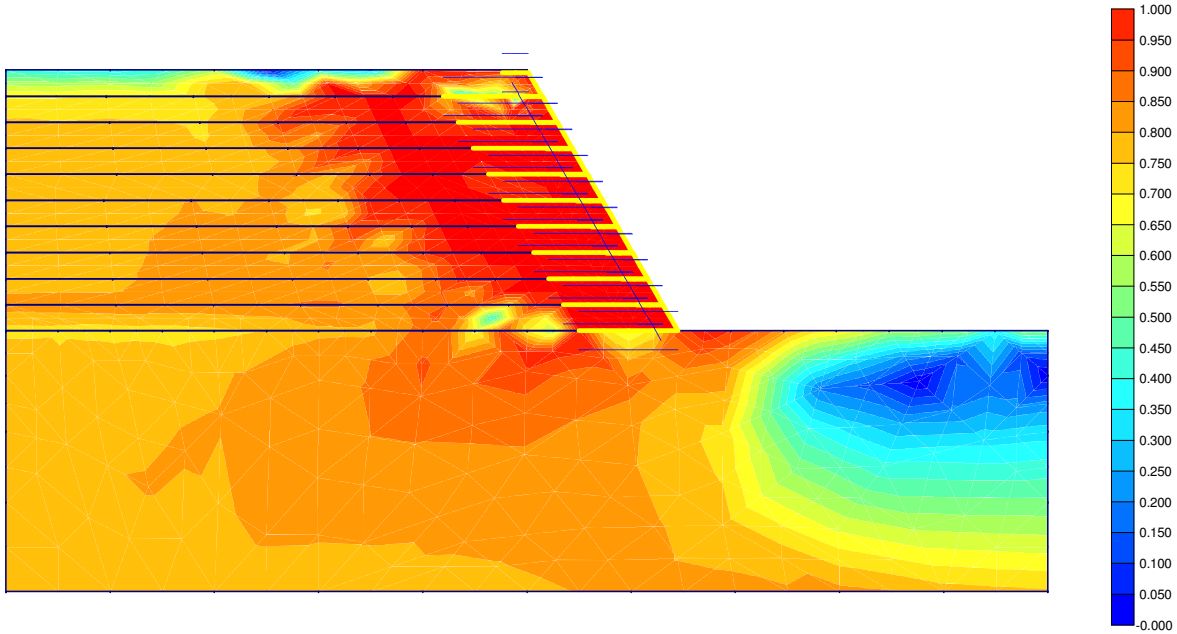

Figure A.4.5 Model D2 with Rock foundation.

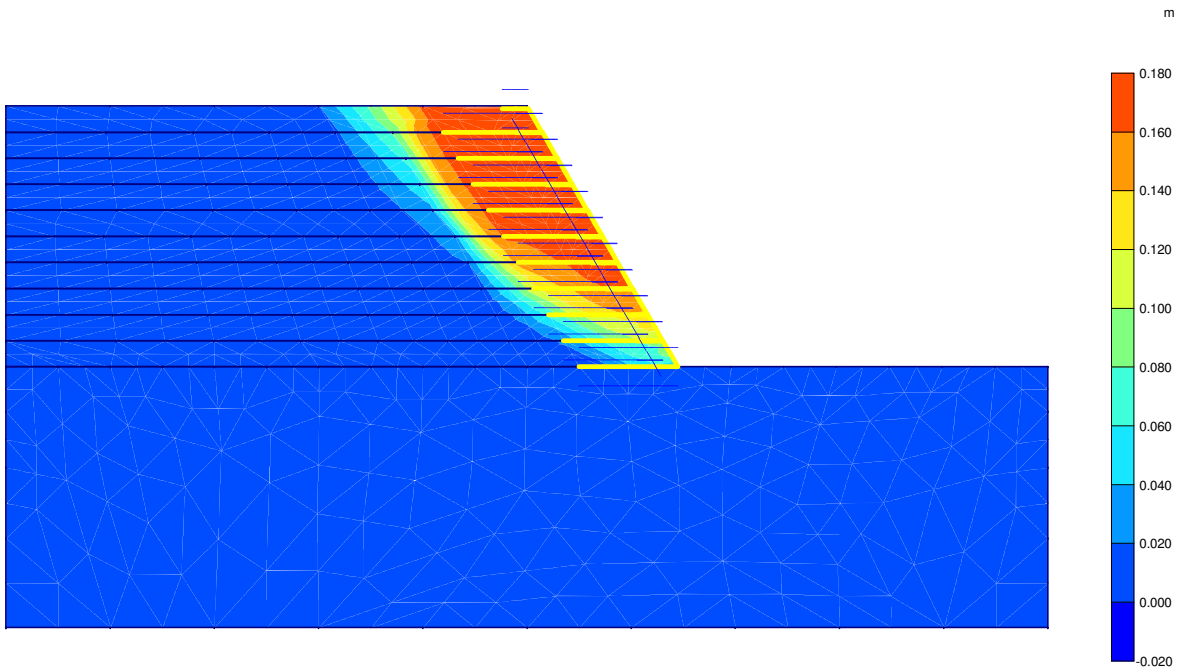

Figure A.5.1 Model D2 with Sand foundation.

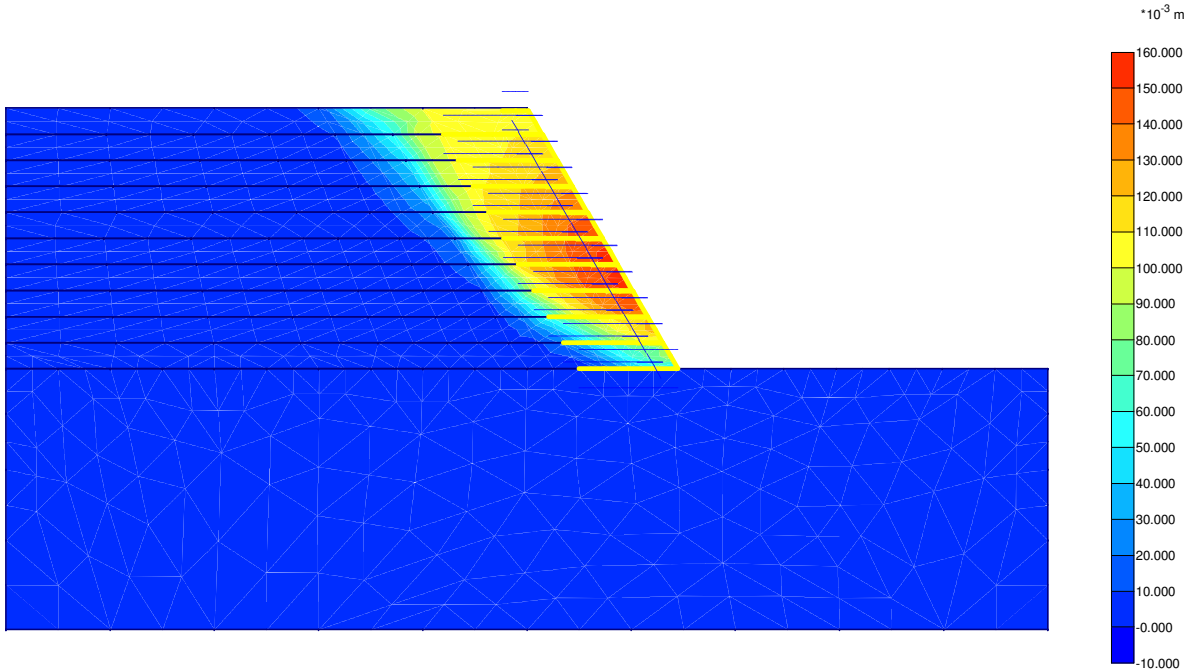

Figure A.5.2 Model D2 with Sand foundation.

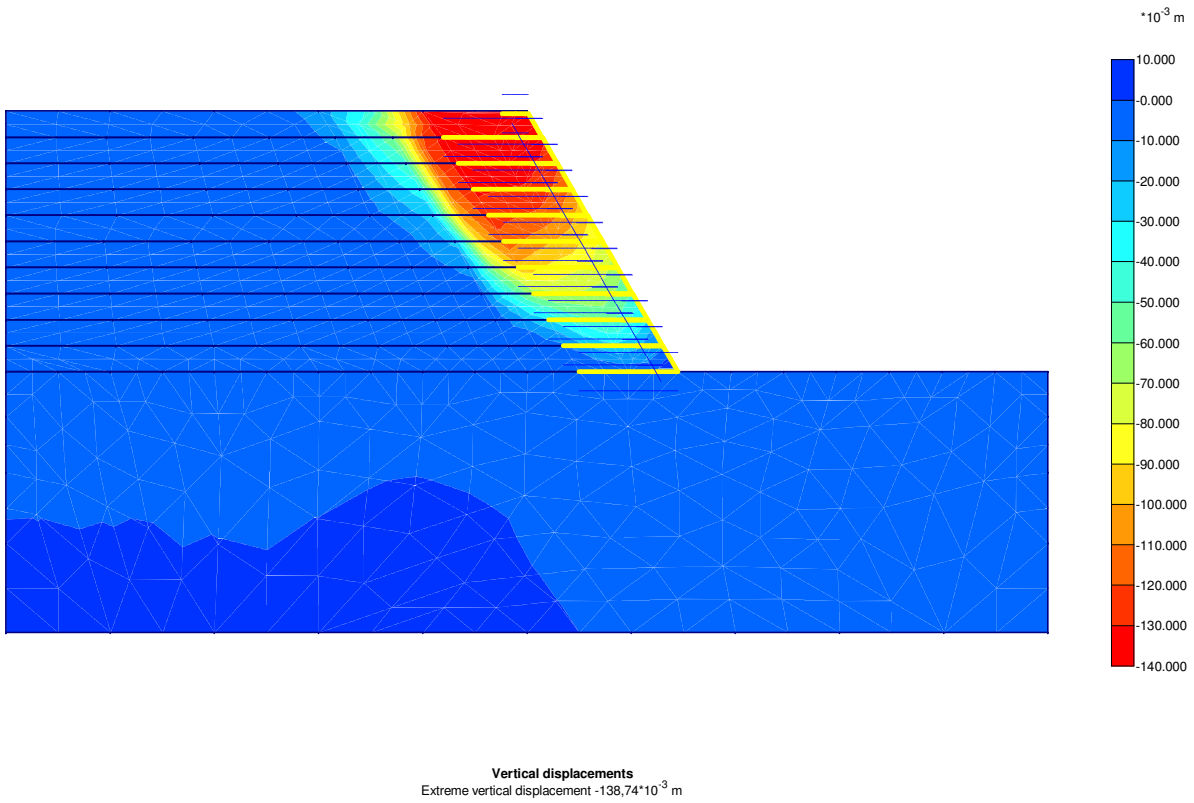

Figure A.5.3 Model D2 with Sand foundation.

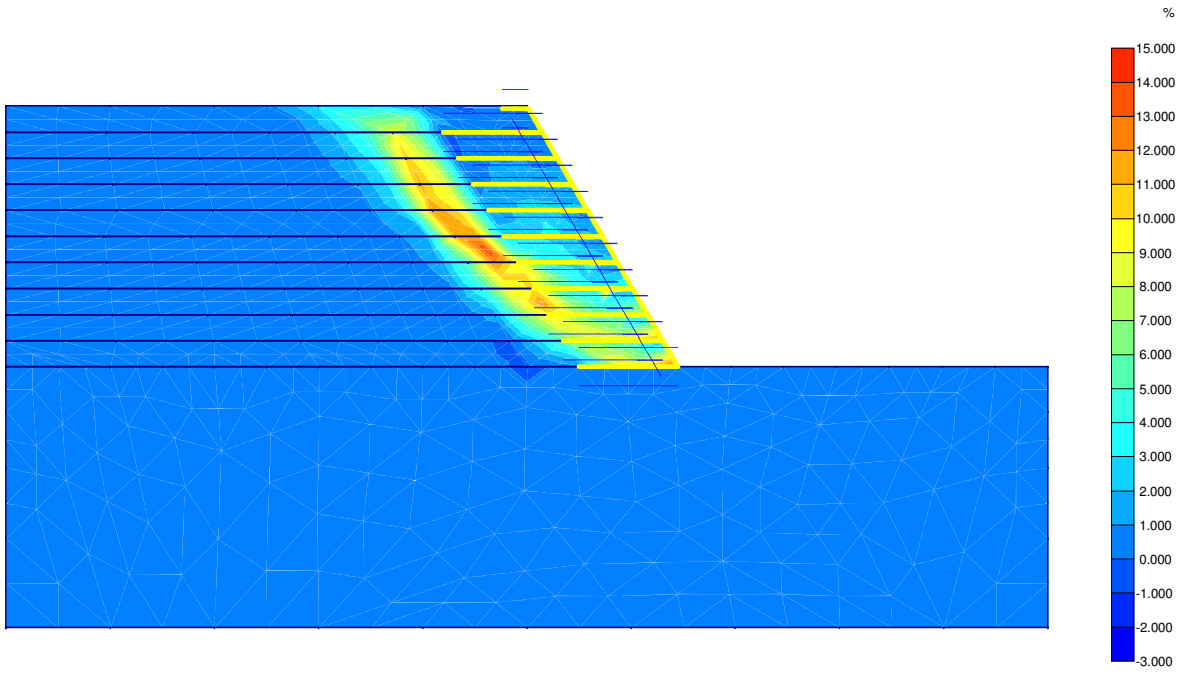

Figure A.5.4 Model D2 with Sand foundation.

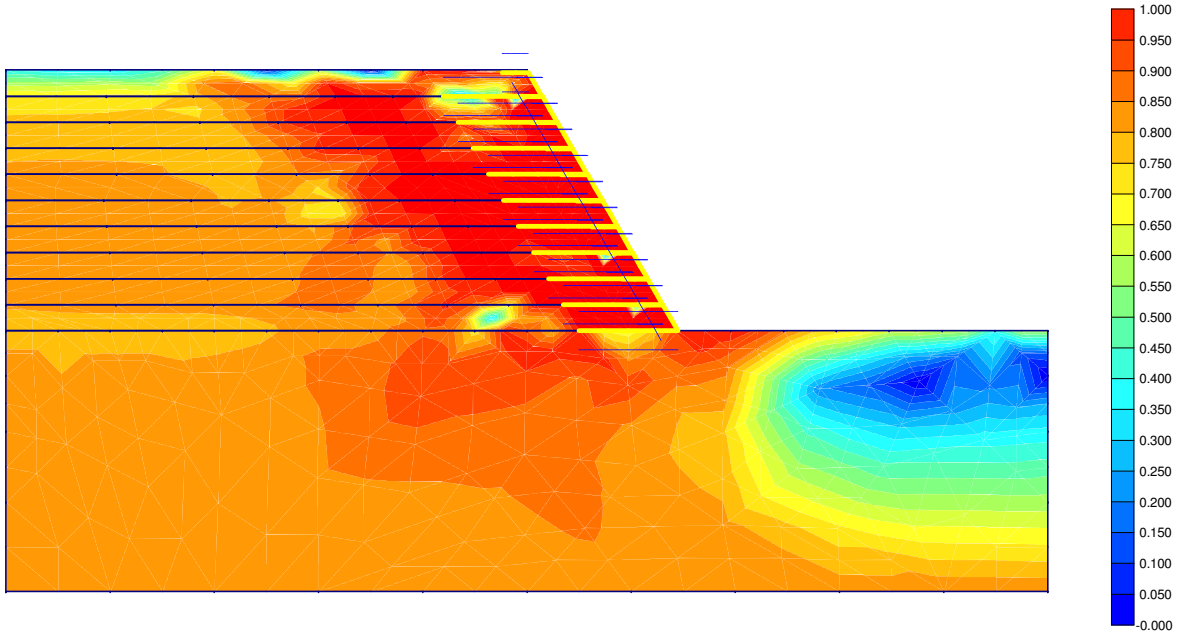

Figure A.5.5 Model D2 with Sand foundation.

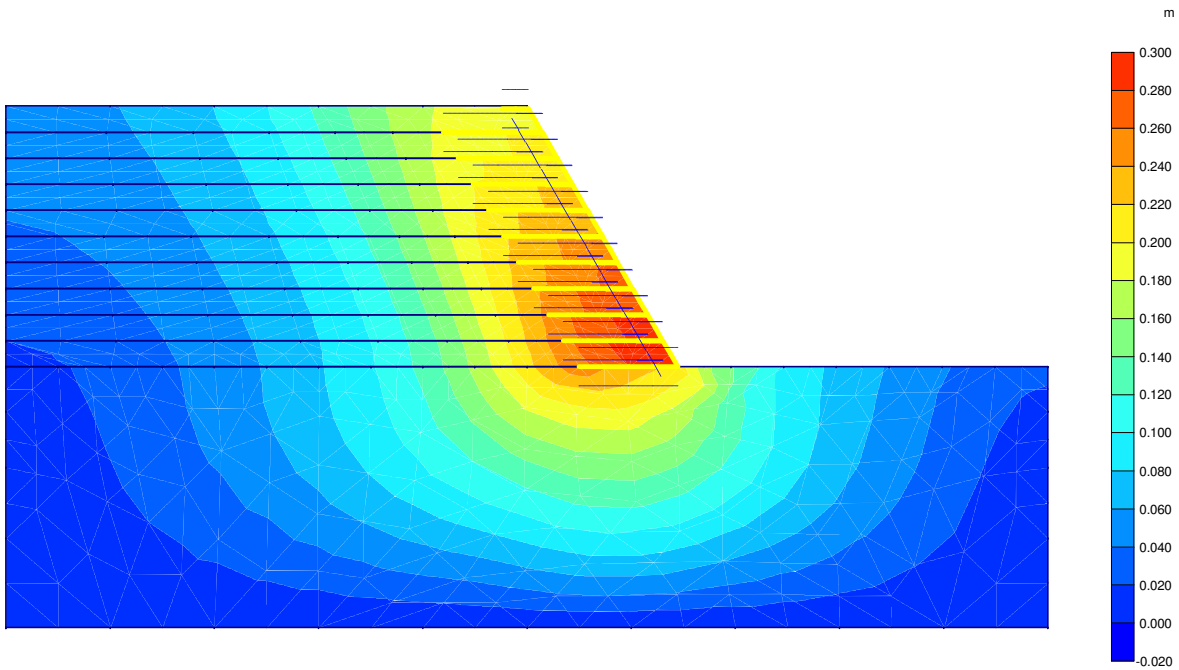

Figure A.6.1 Model D2 with Soft Clay foundation.

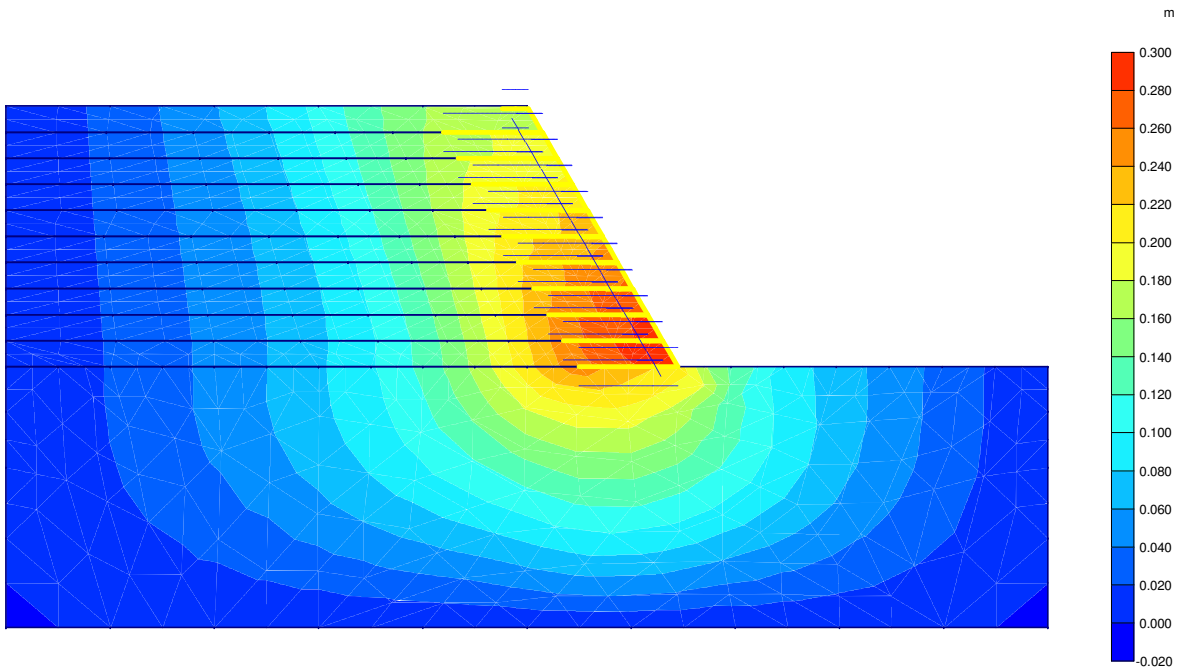

Figure A.6.2 Model D2 with Soft Clay foundation

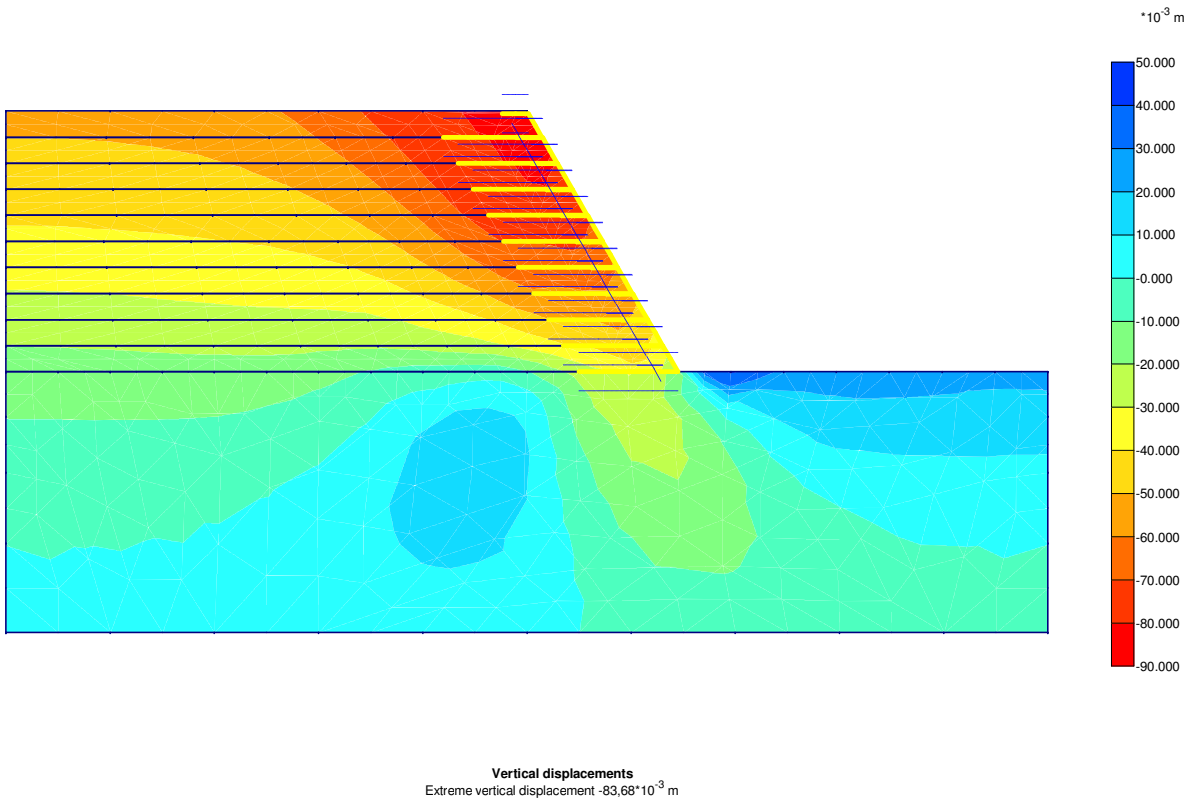

Figure A.6.3 Model D2 with Soft Clay foundation

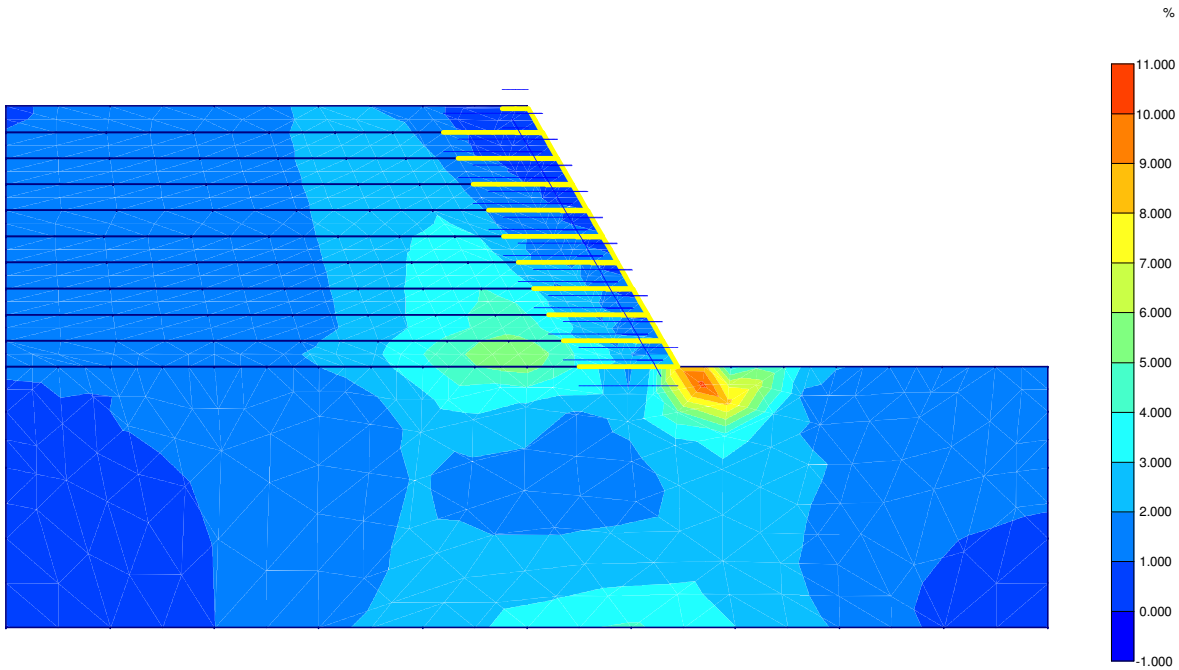

Figure A.6.4 Model D2 with Soft Clay foundation

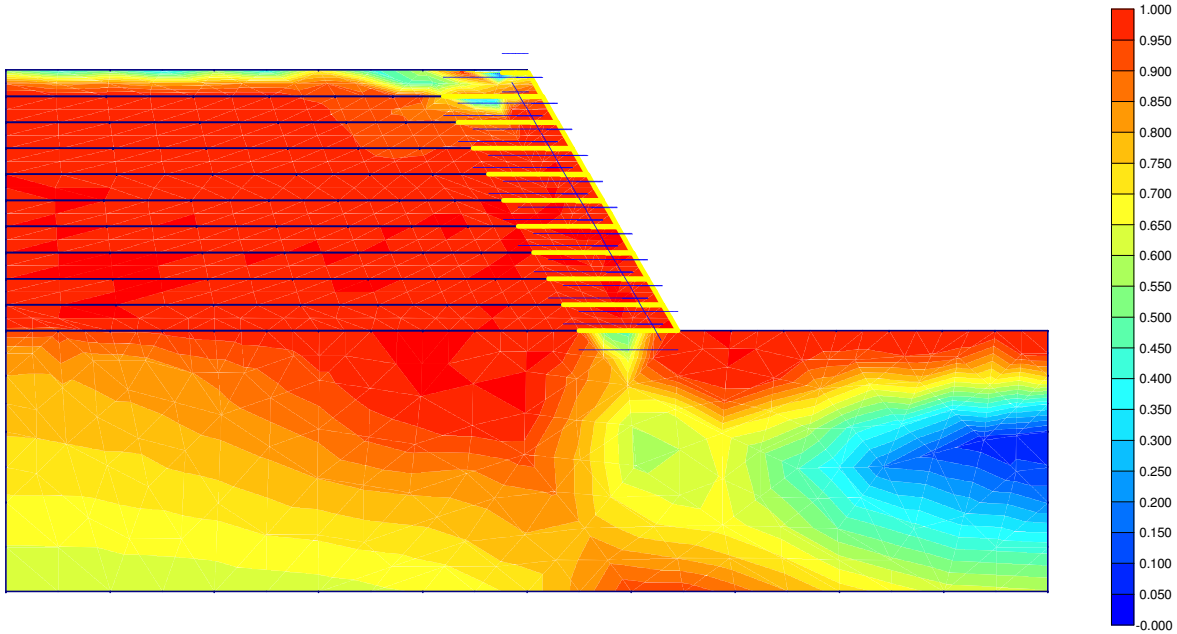

Figure A.6.5 Model D2 with Soft Clay foundation

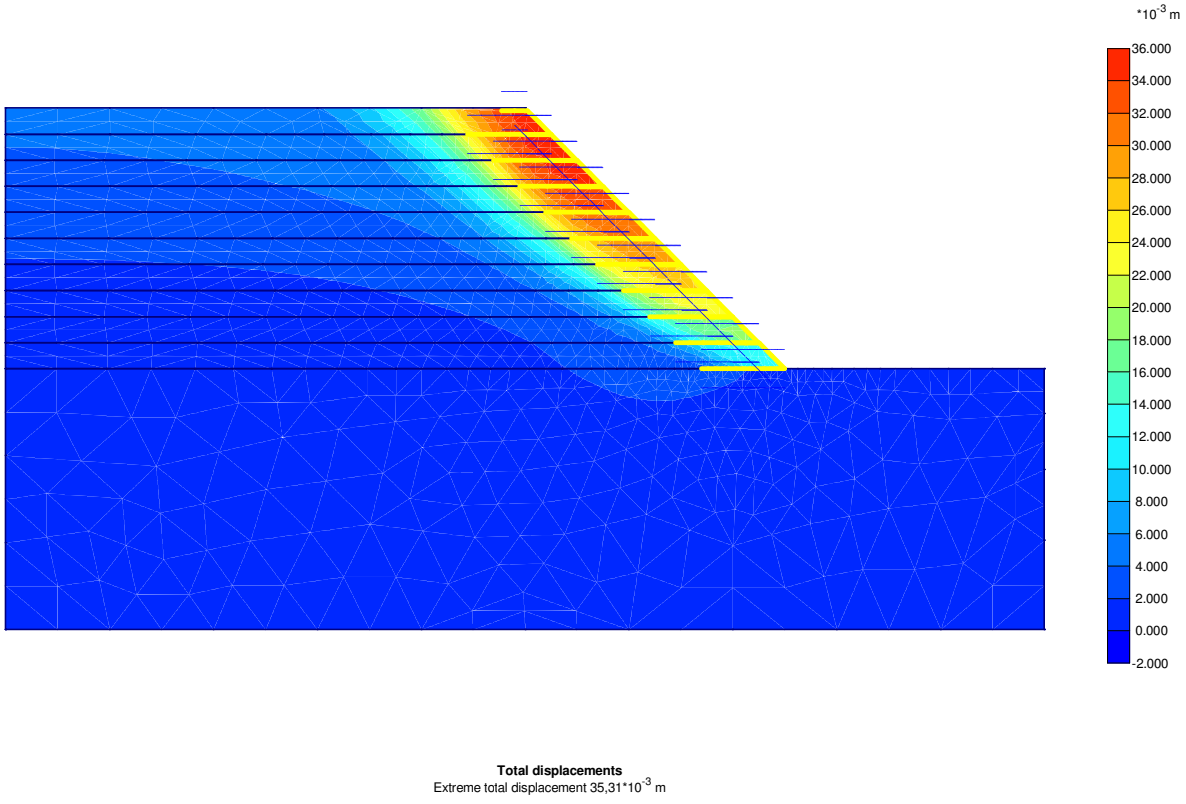

Figure A.7.1 Model D3 with Rock foundation.

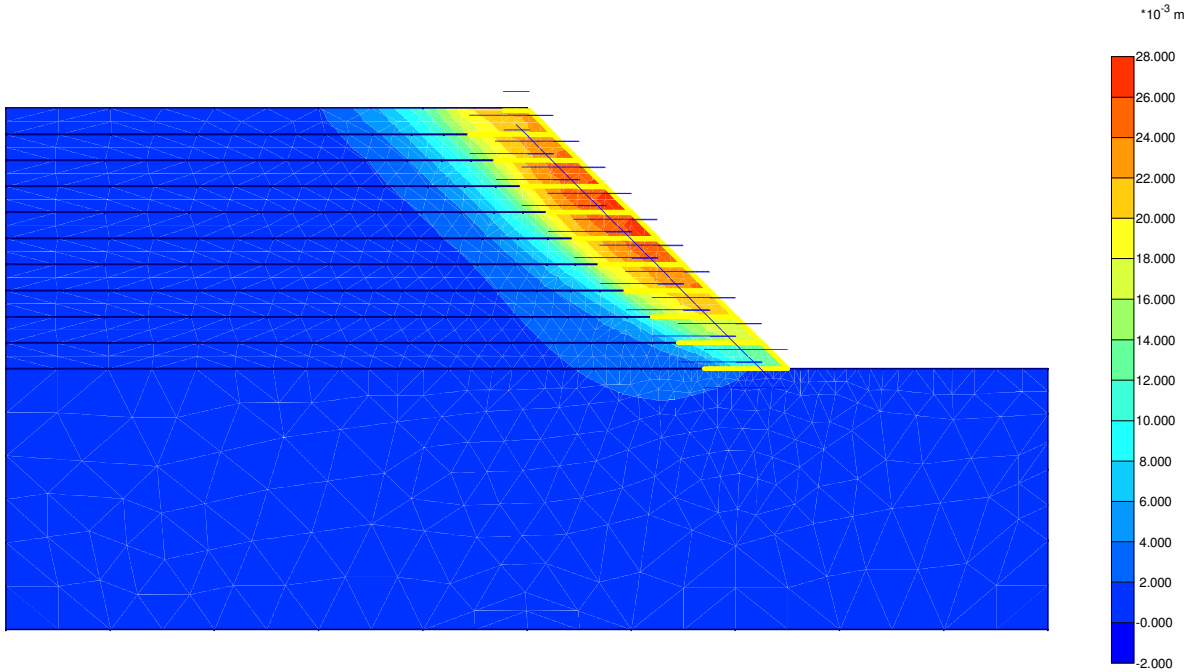

Figure A.7.2 Model D3 with Rock foundation.

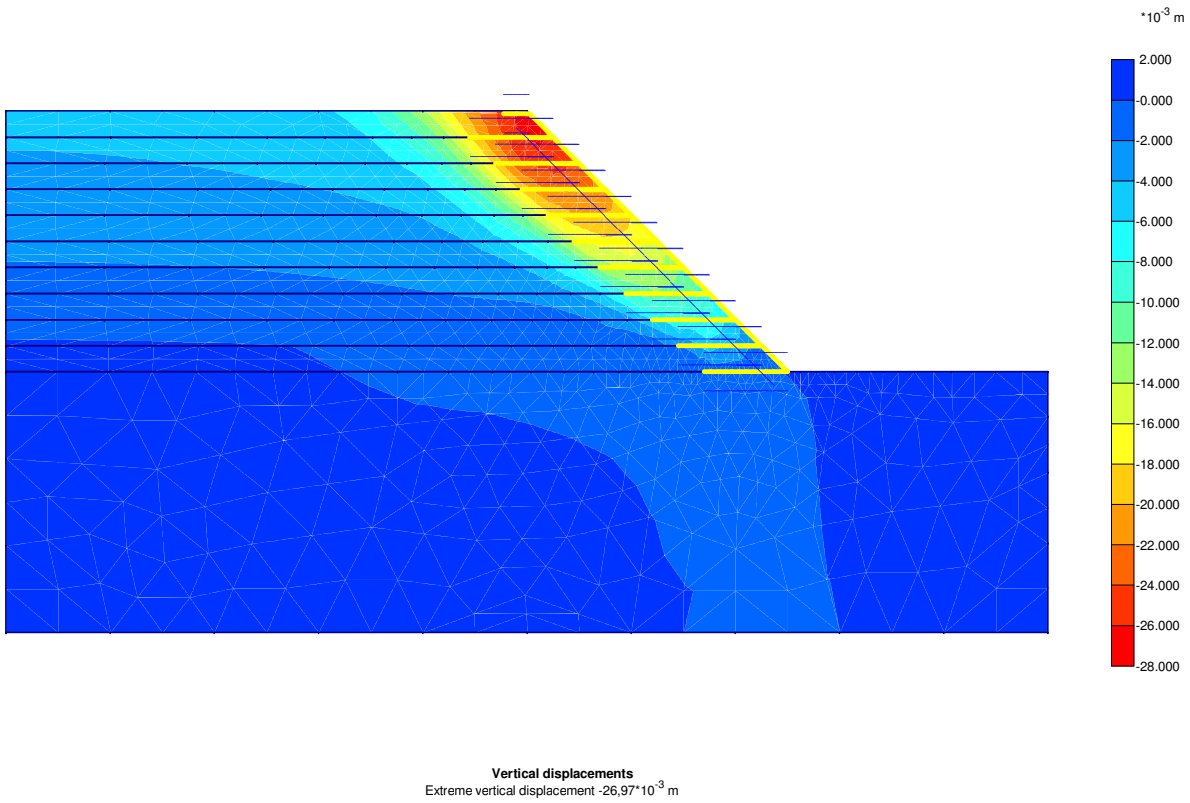

Figure A.7.3 Model D3 with Rock foundation.

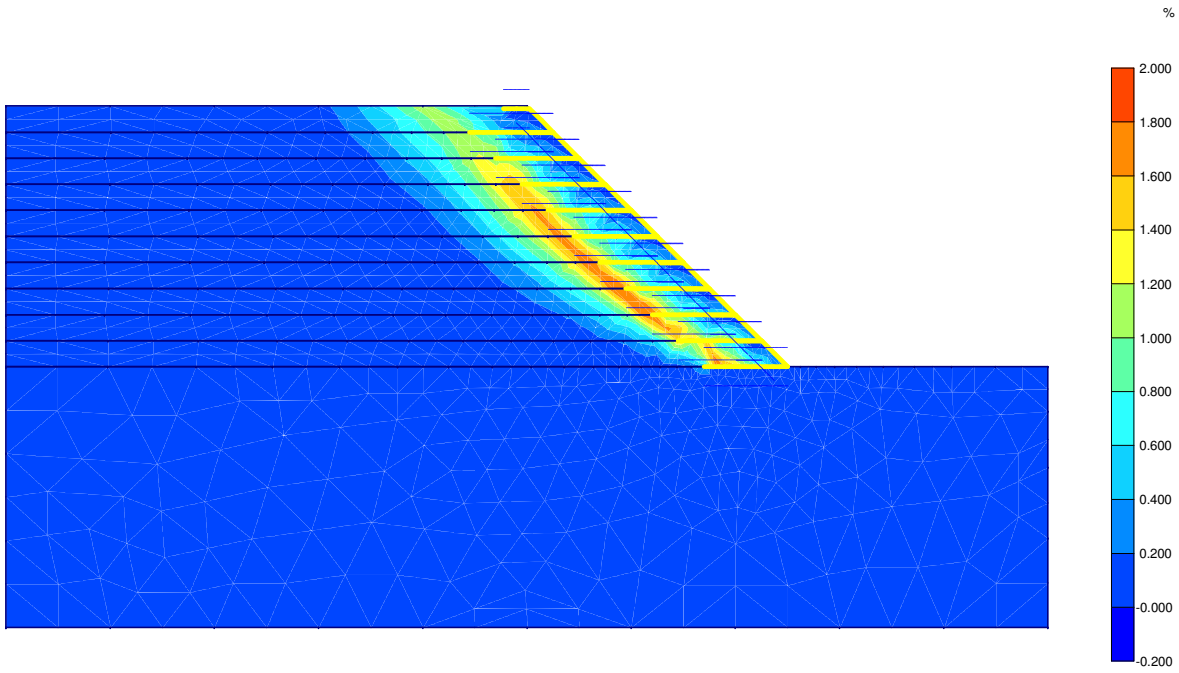

Figure A.7.4 Model D3 with Rock foundation.

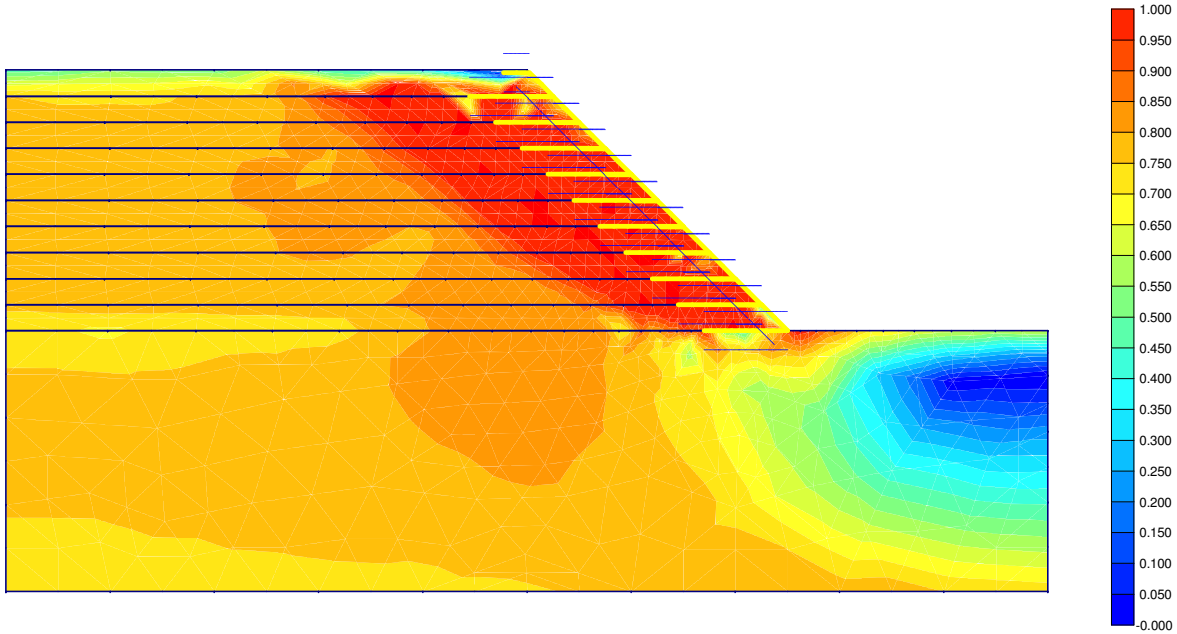

Figure A.7.5 Model D3 with Rock foundation.

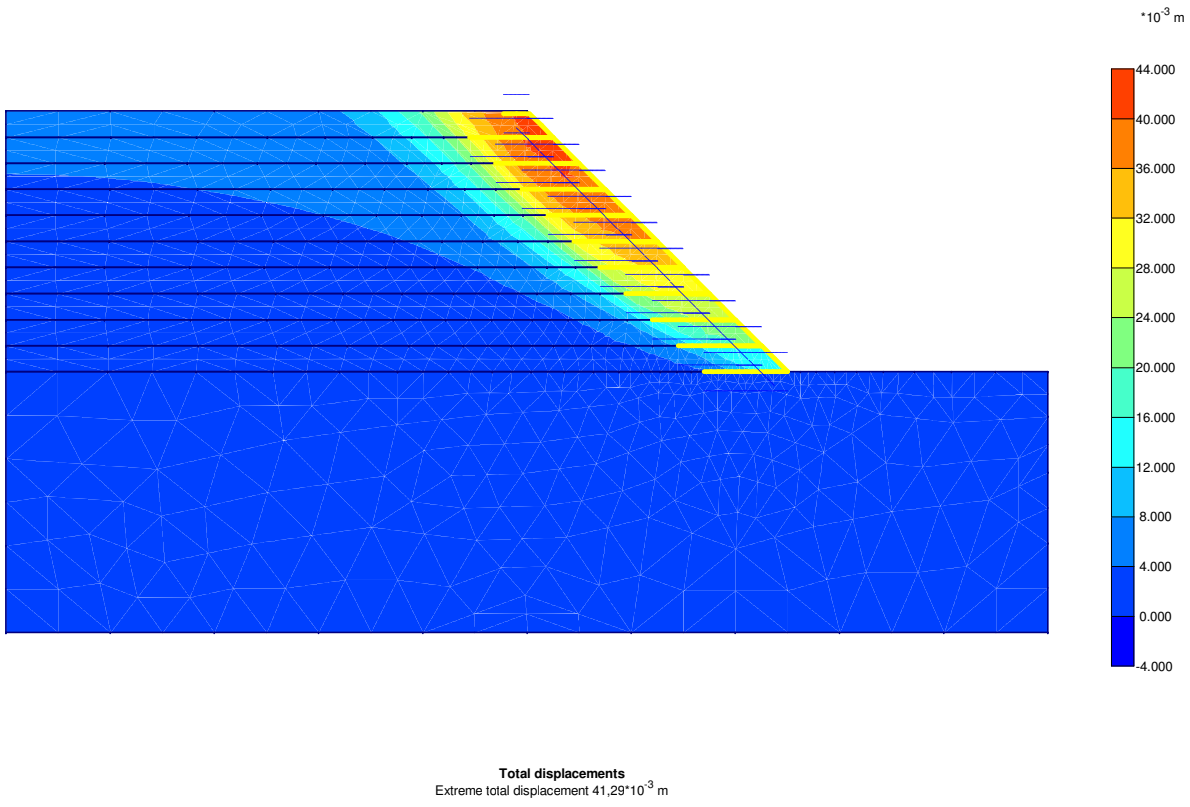

Figure A.8.1 Model D3 with Sand foundation.

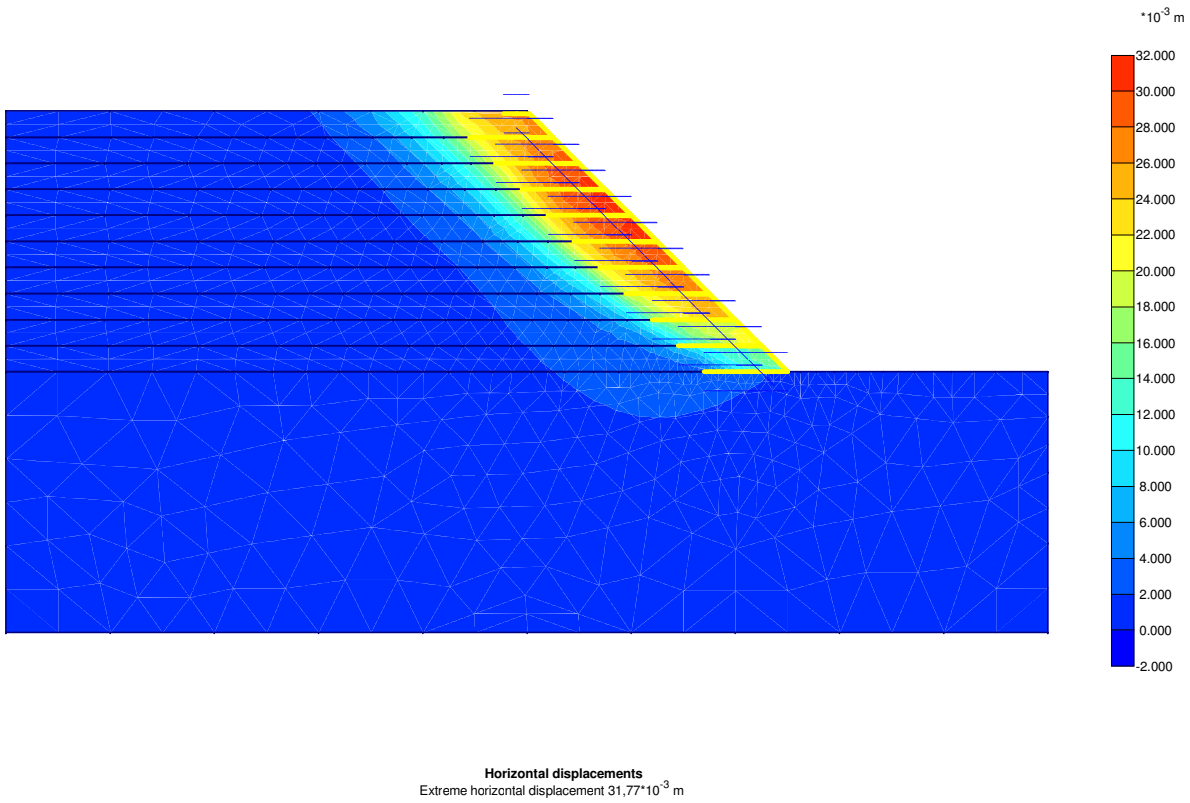

Figure A.8.2 Model D3 with Sand foundation.

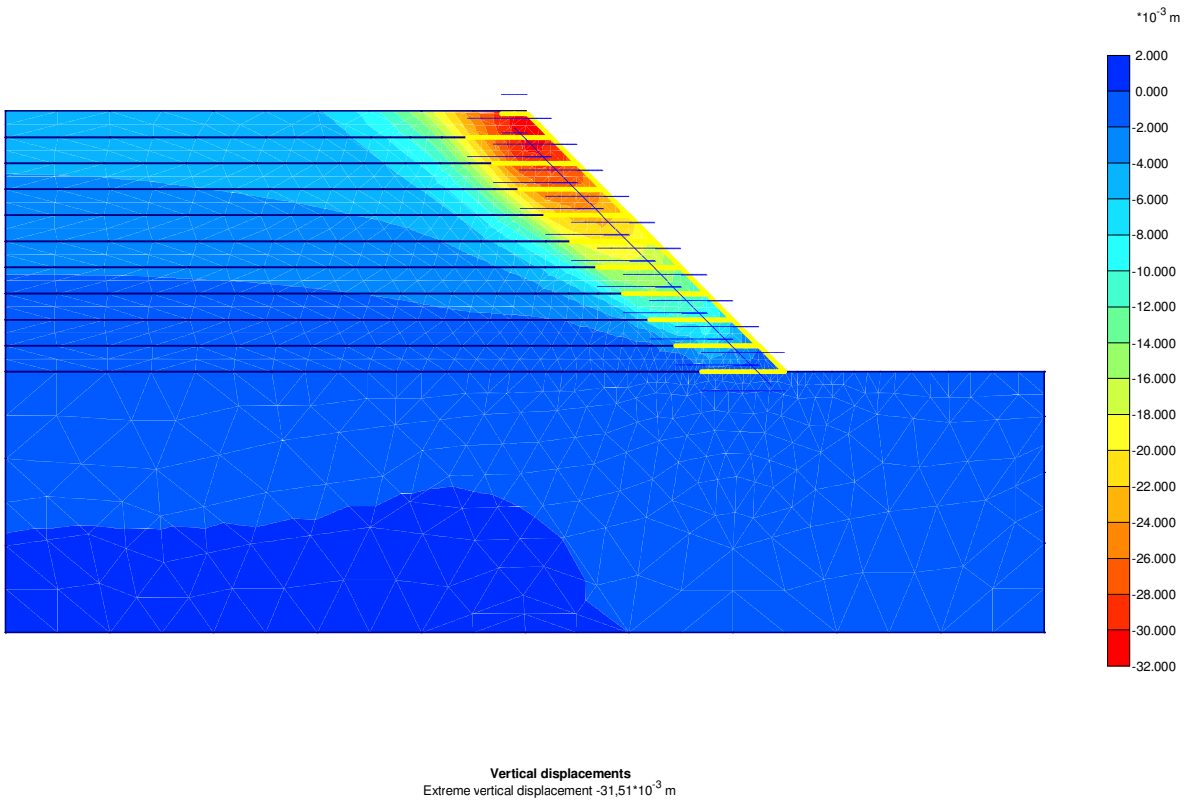

Figure A.8.3 Model D3 with Sand foundation.

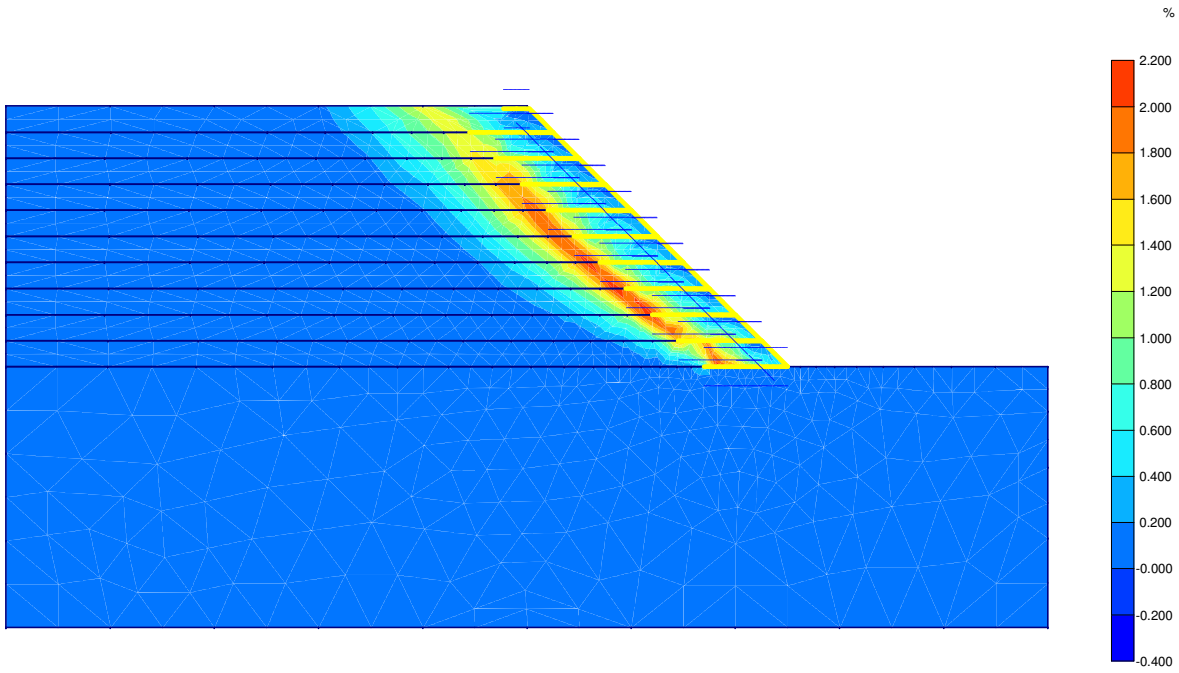

Figure A.8.4 Model D3 with Sand foundation.

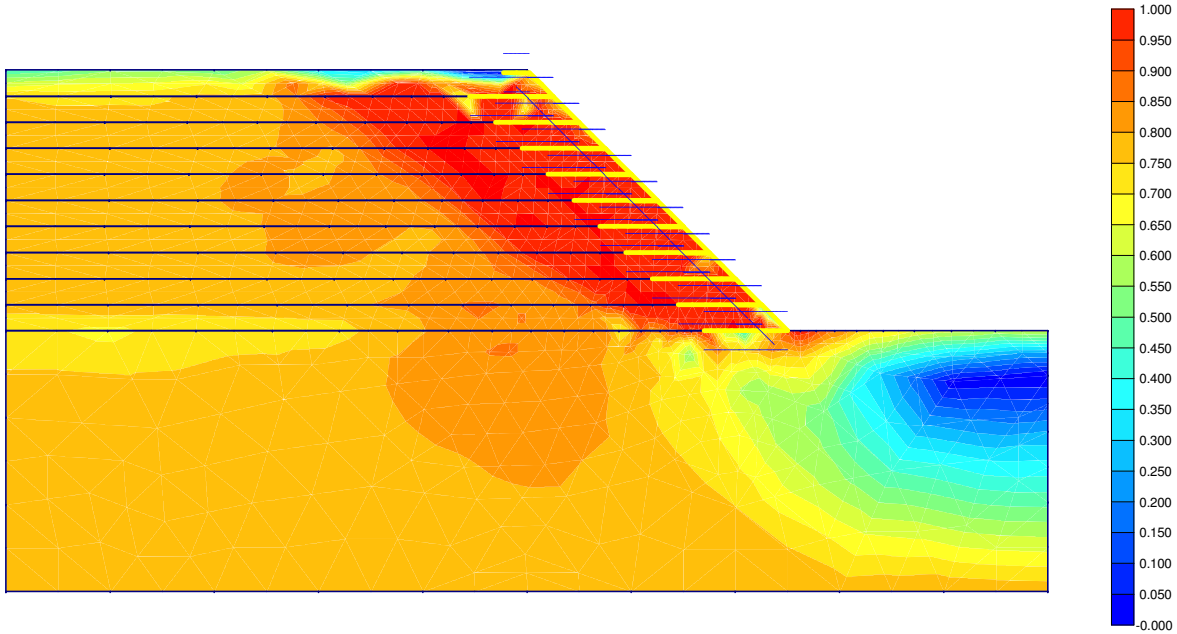

Figure A.8.5 Model D3 with Sand foundation.

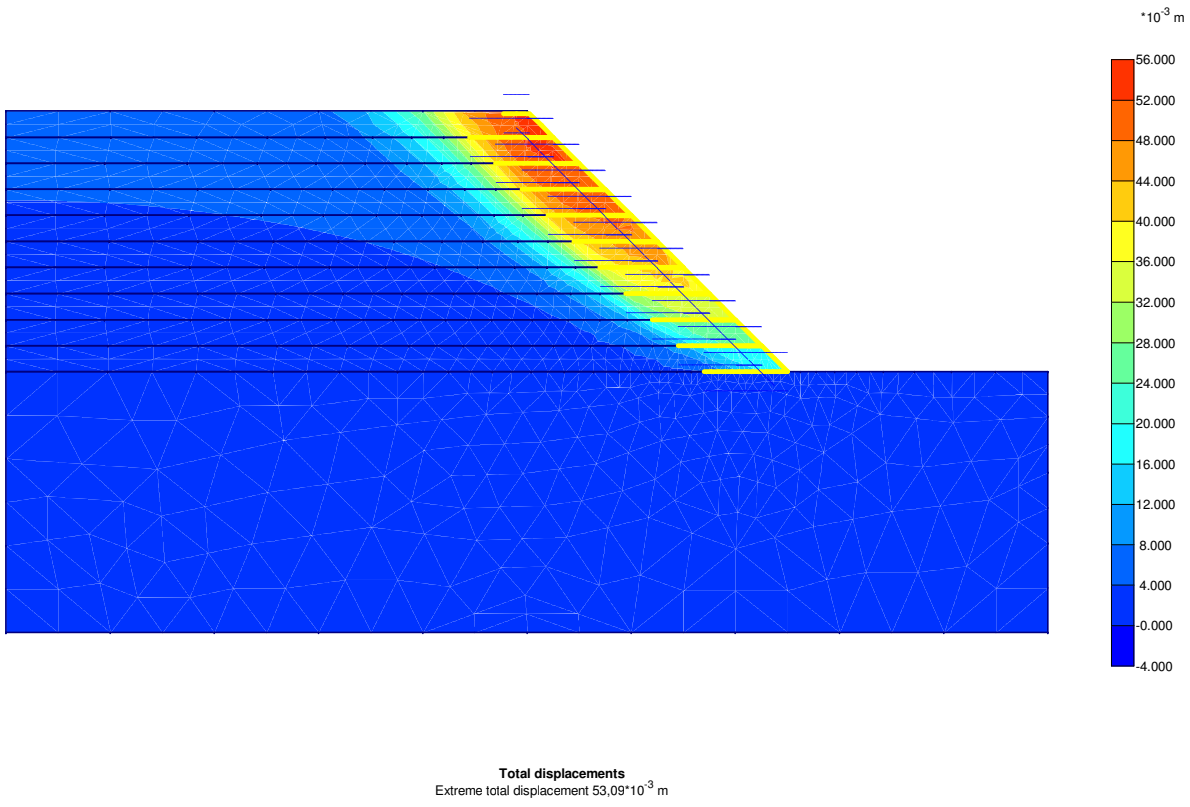

Figure A.9.1 Model D3 with Soft Clay foundation.

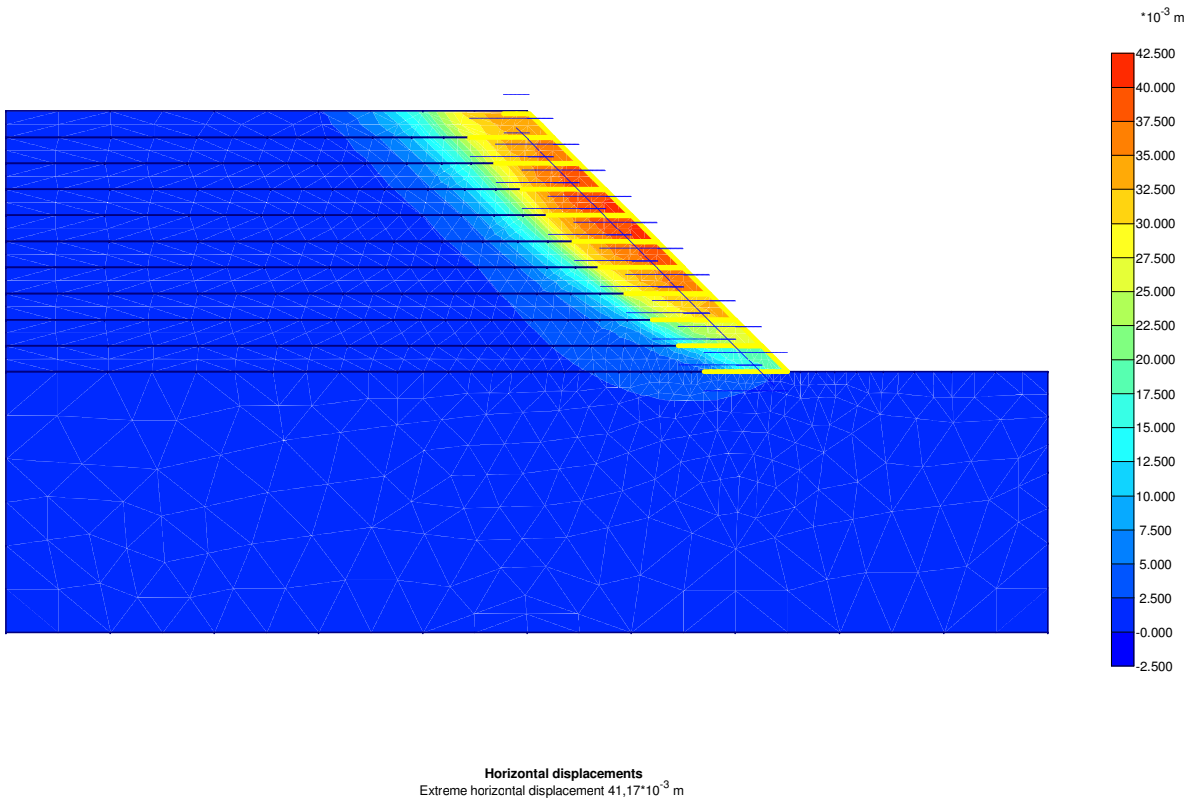

Figure A.9.2 Model D3 with Soft Clay foundation.

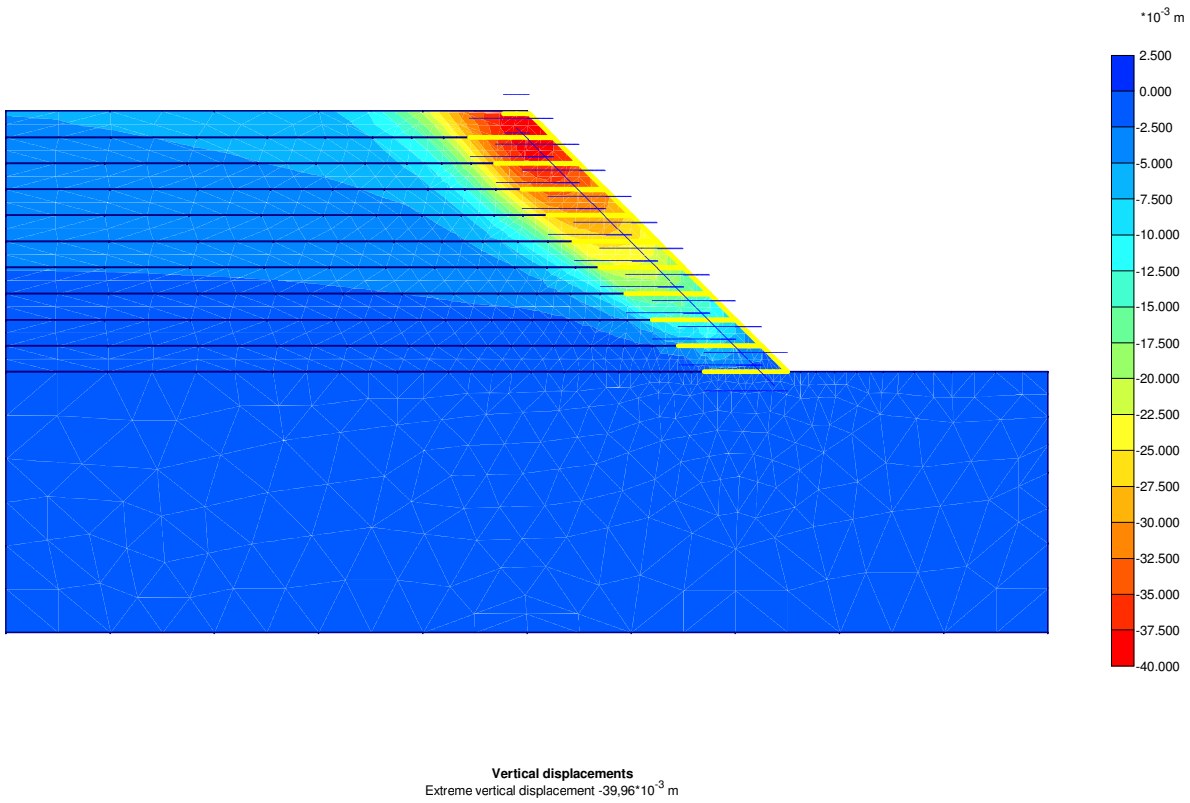

Figure A.9.3 Model D3 with Soft Clay foundation.

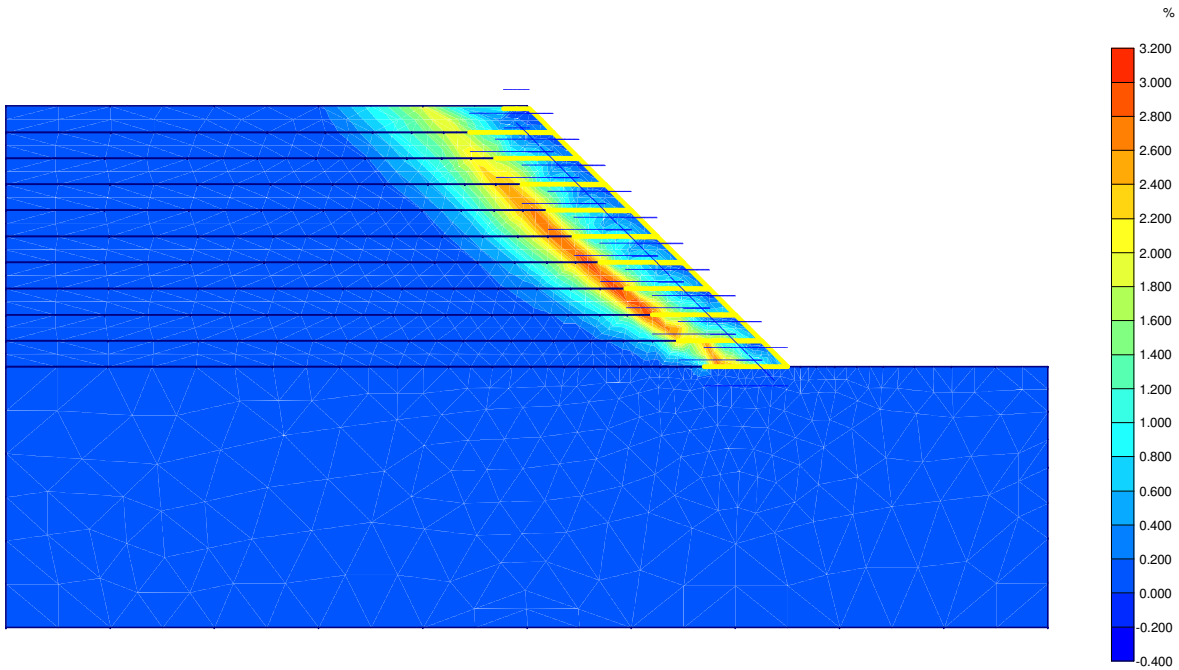

Figure A.9.4 Model D3 with Soft Clay foundation.

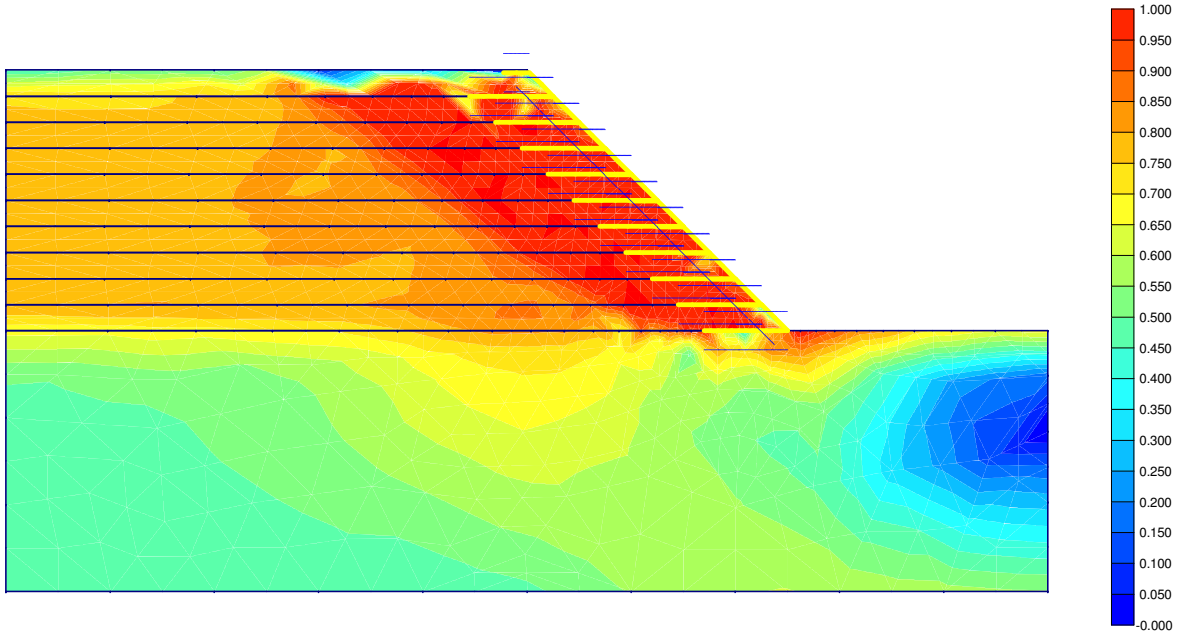

Figure A.9.5 Model D3 with Soft Clay foundation.

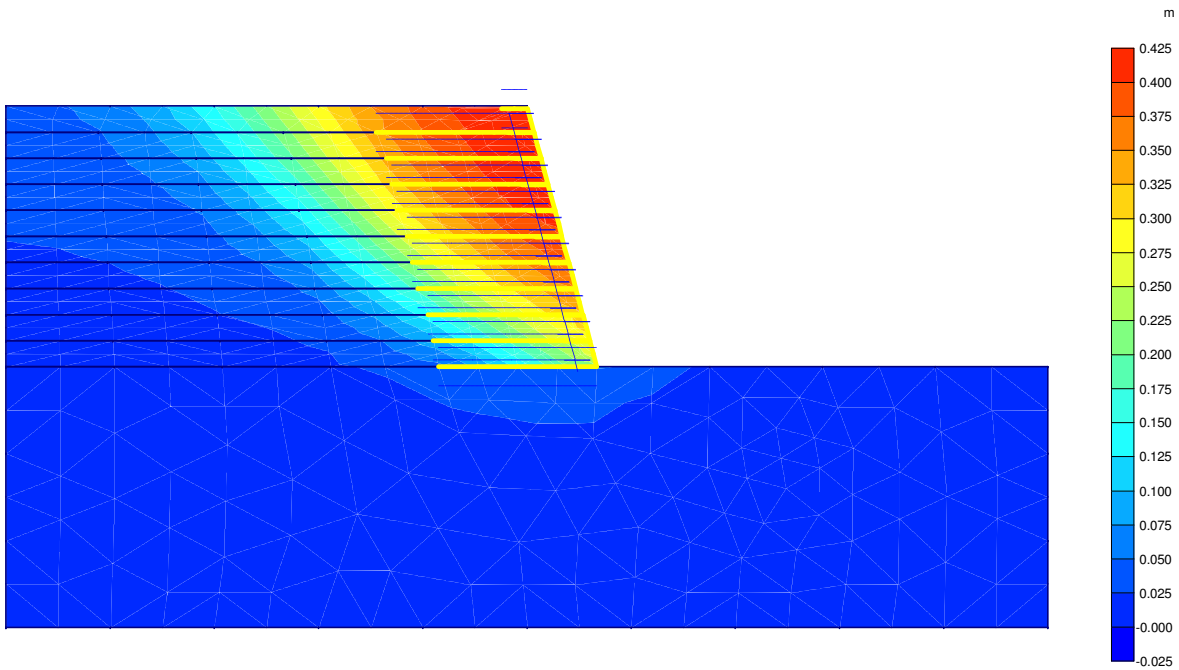

Figure A.10.1 Model L1 with Rock foundation

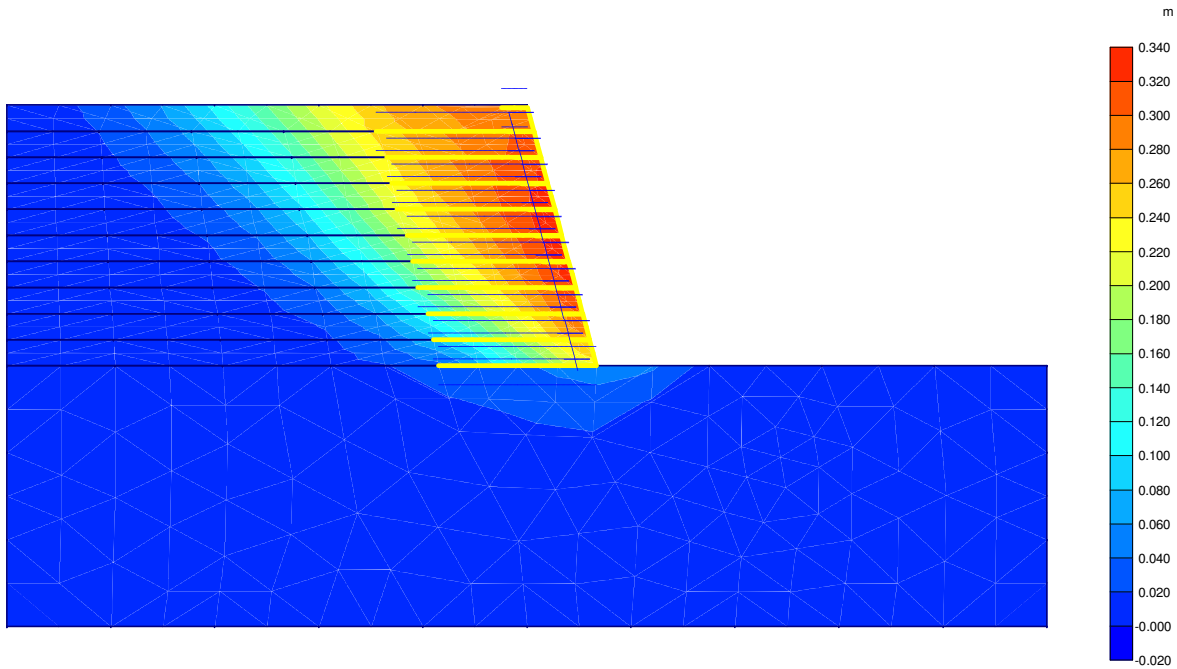

Figure A.10.2 Model L1 with Rock foundation

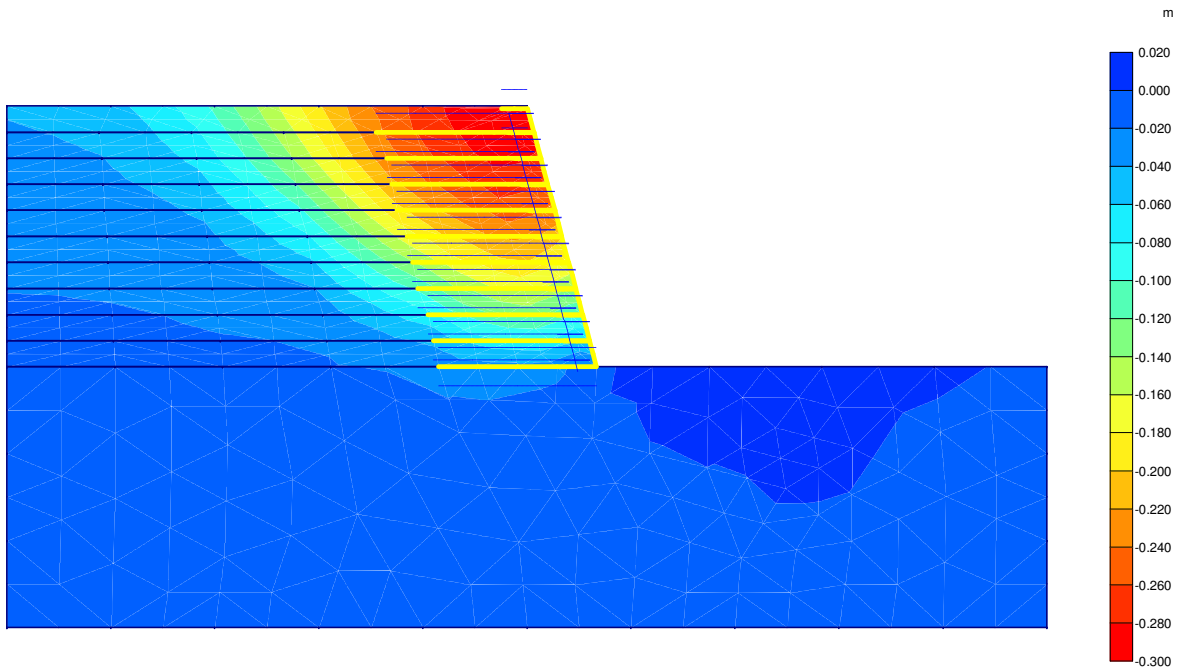

Figure A.10.3 Model L1 with Rock foundation

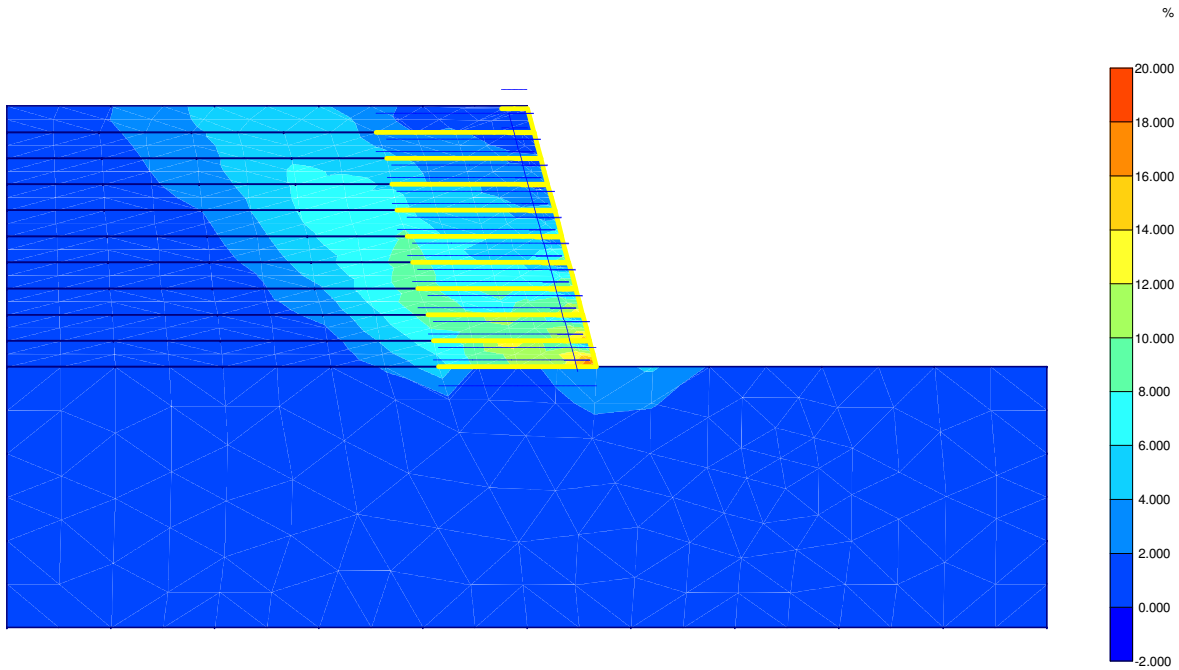

Figure A.10.4 Model L1 with Rock foundation

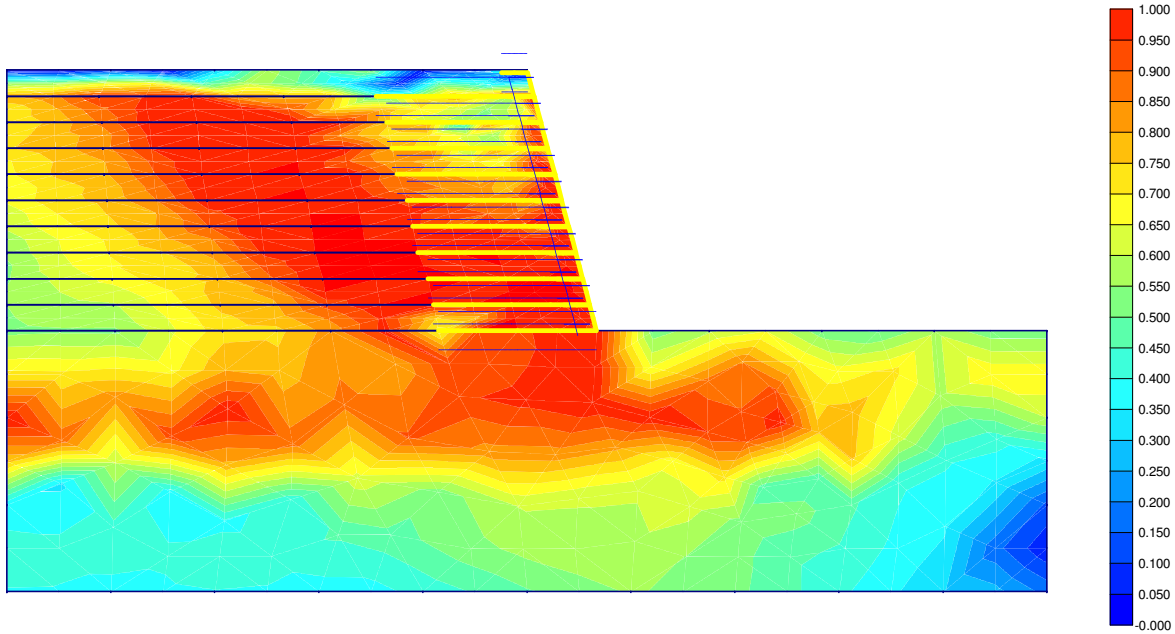

Figure A.10.5 Model L1 with Rock foundation

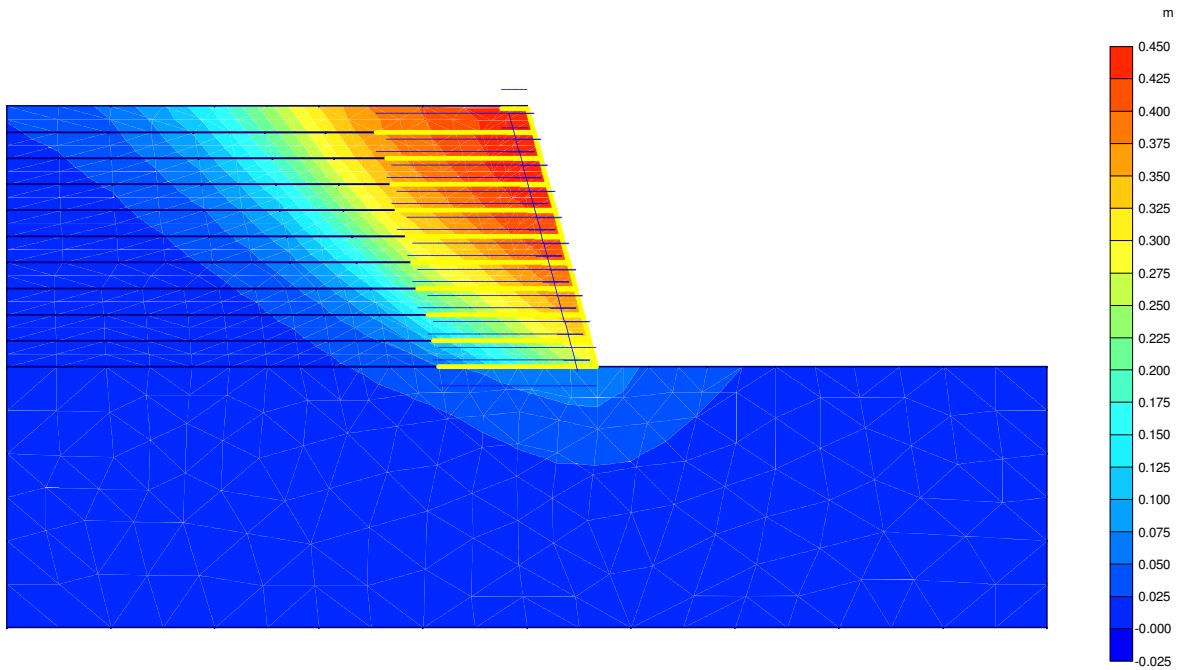

Figure A.11.1 Model L1 with Sand foundation

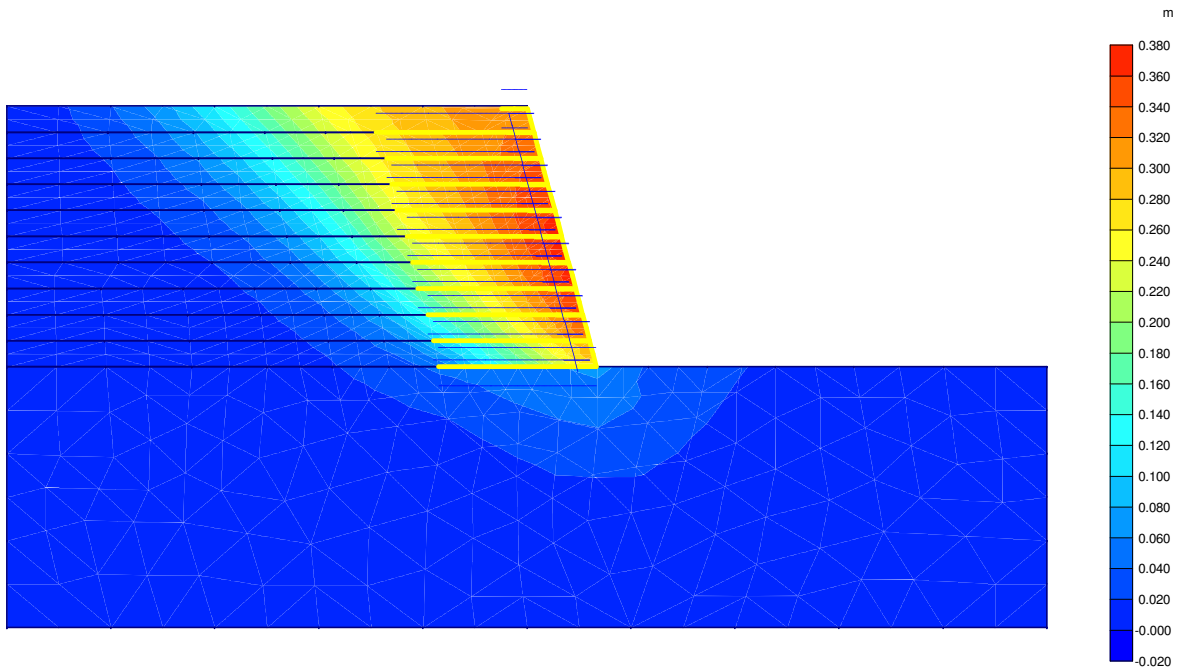

Figure A.11.2 Model L1 with Sand foundation

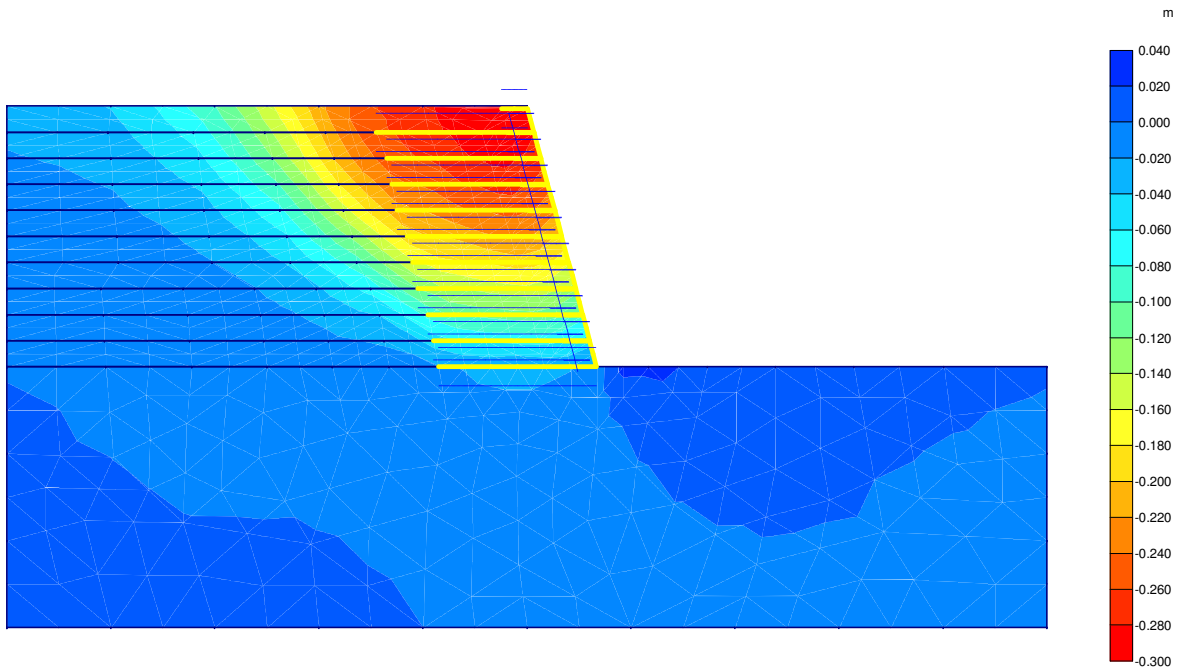

Figure A.11.3 Model L1 with Sand foundation

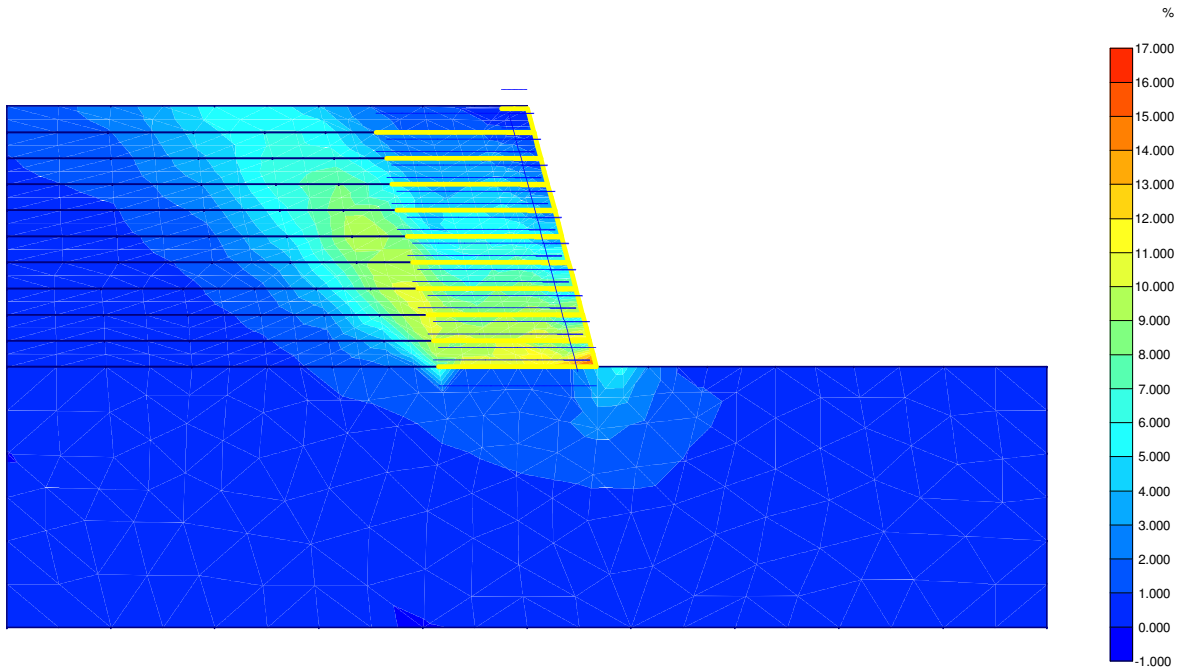

Figure A11.4 Model L1 with Sand foundation

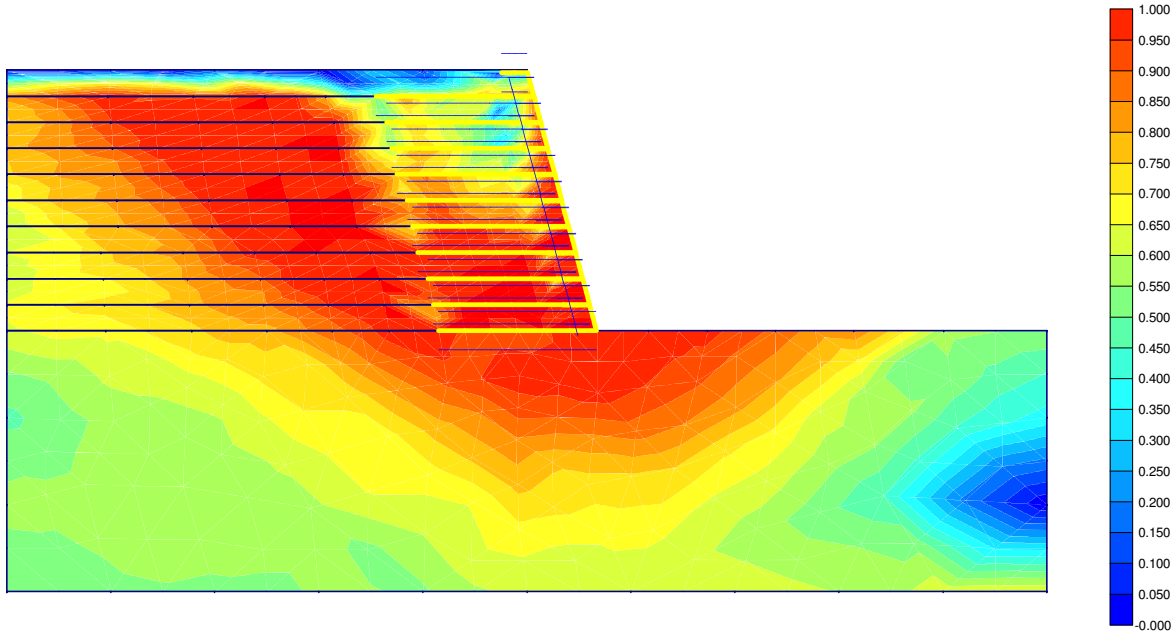

Figure A.11.5 Model L1 with Sand foundation

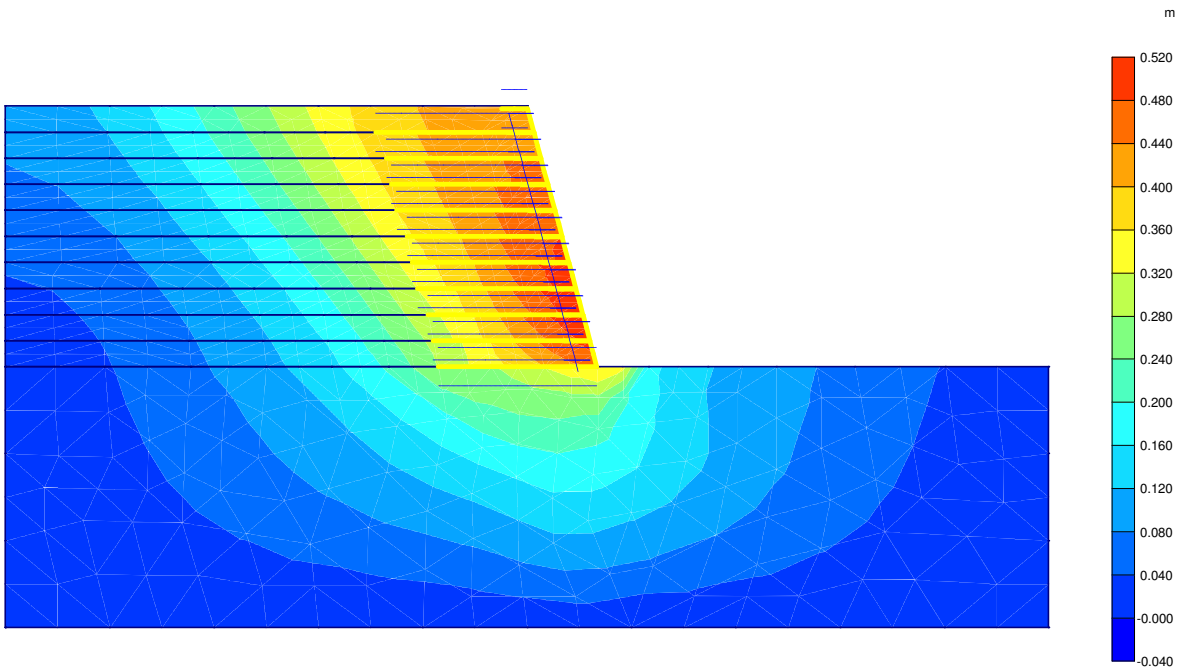

Figure A.12.1 Model L1 with Soft Clay foundation

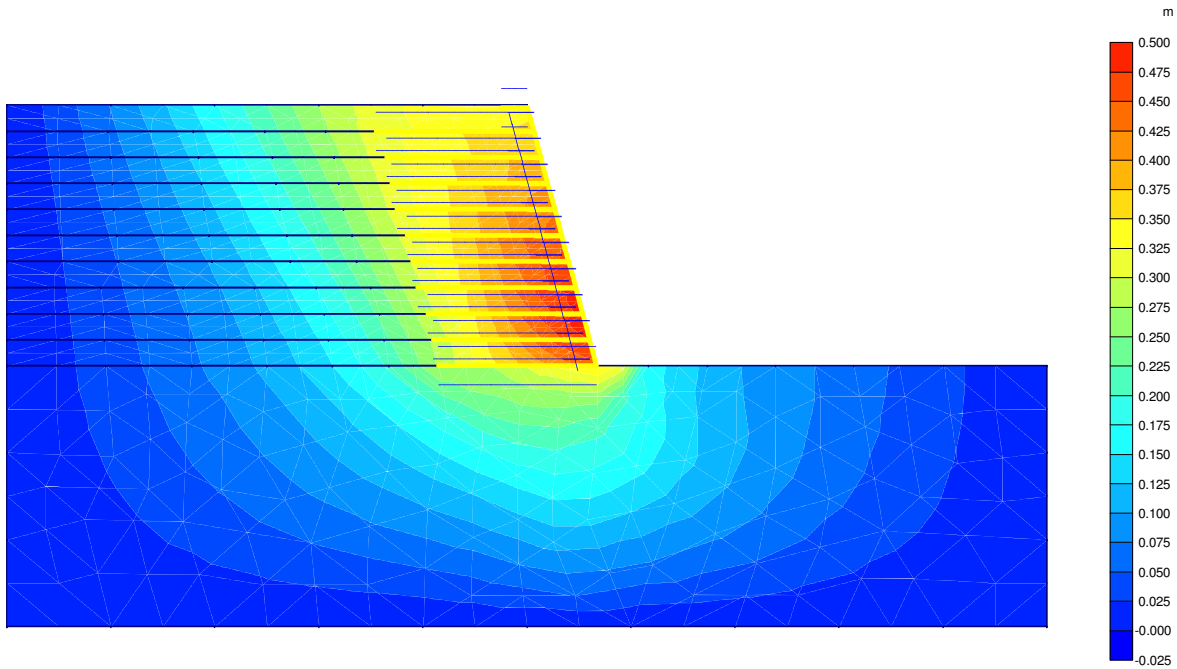

Figure A.12.2 Model L1 with Soft Clay foundation

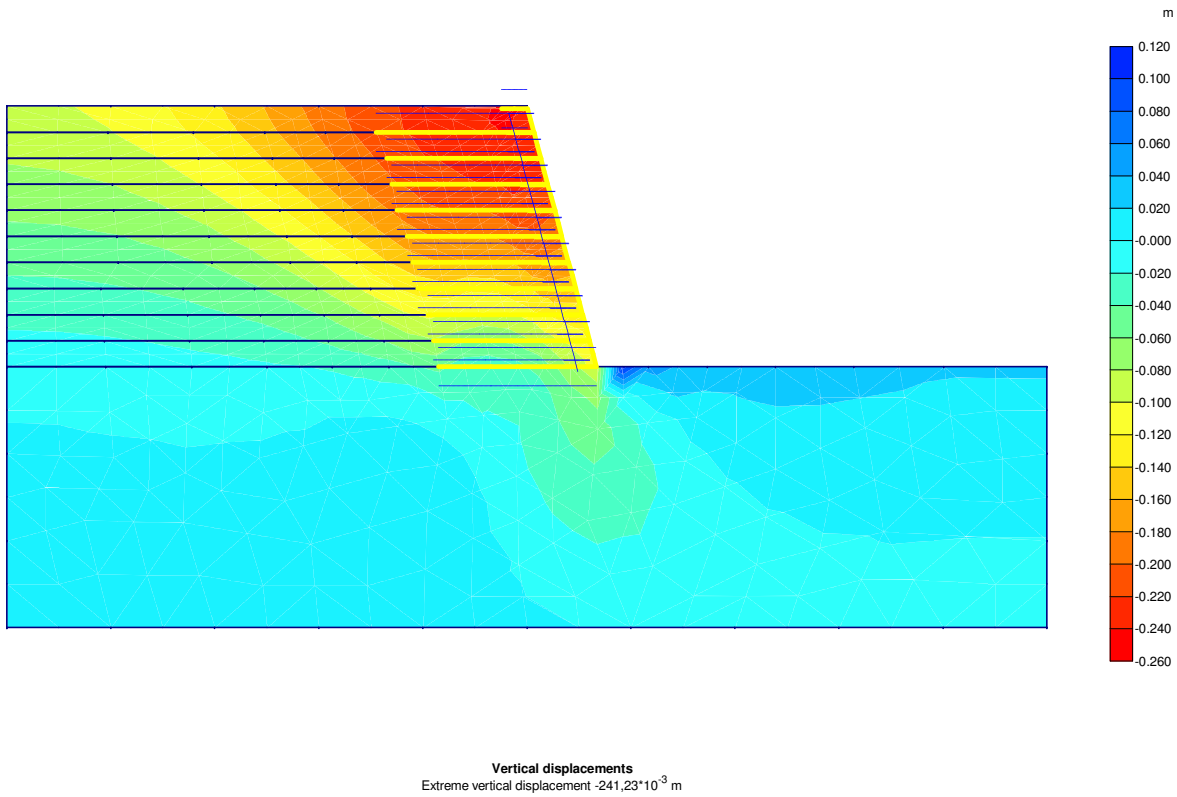

Figure A.12.3 Model L1 with Soft Clay foundation

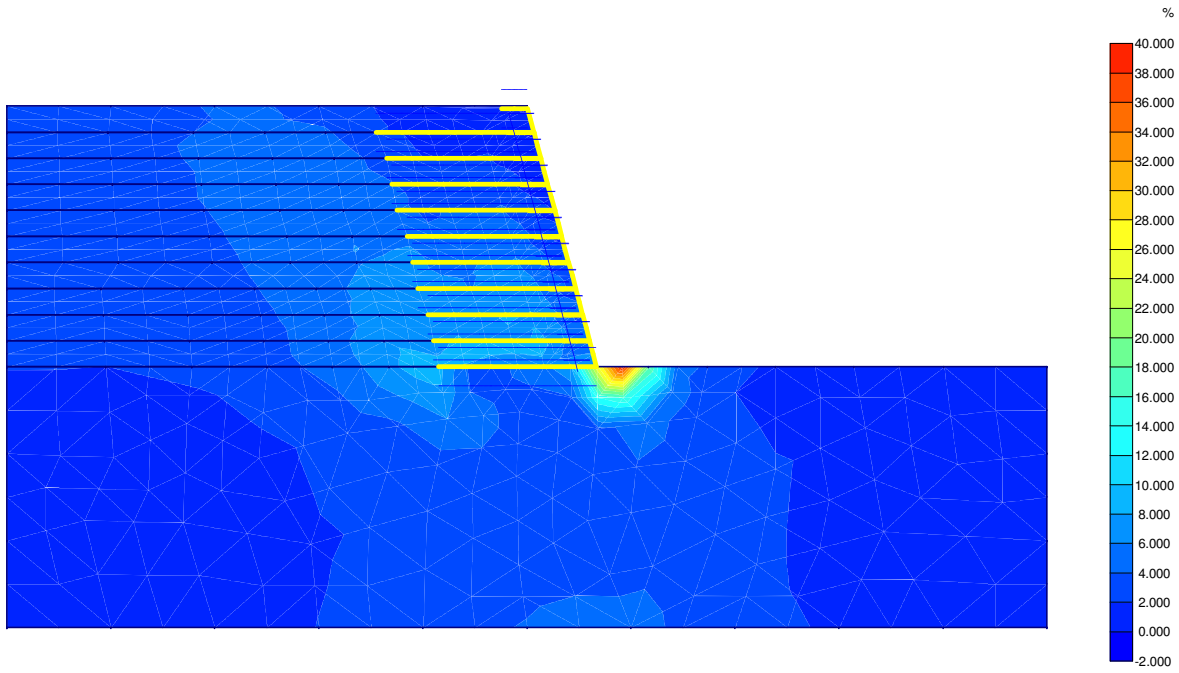

Figure A.12.4 Model L1 with Soft Clay foundation

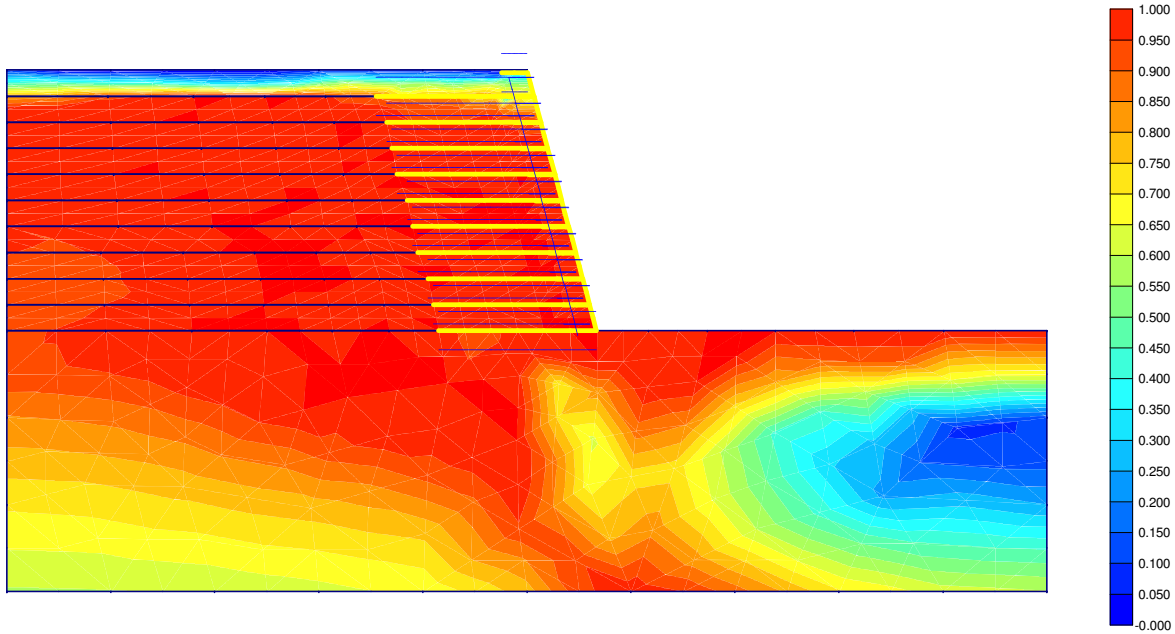

Figure A.12.5 Model L1 with Soft Clay foundation

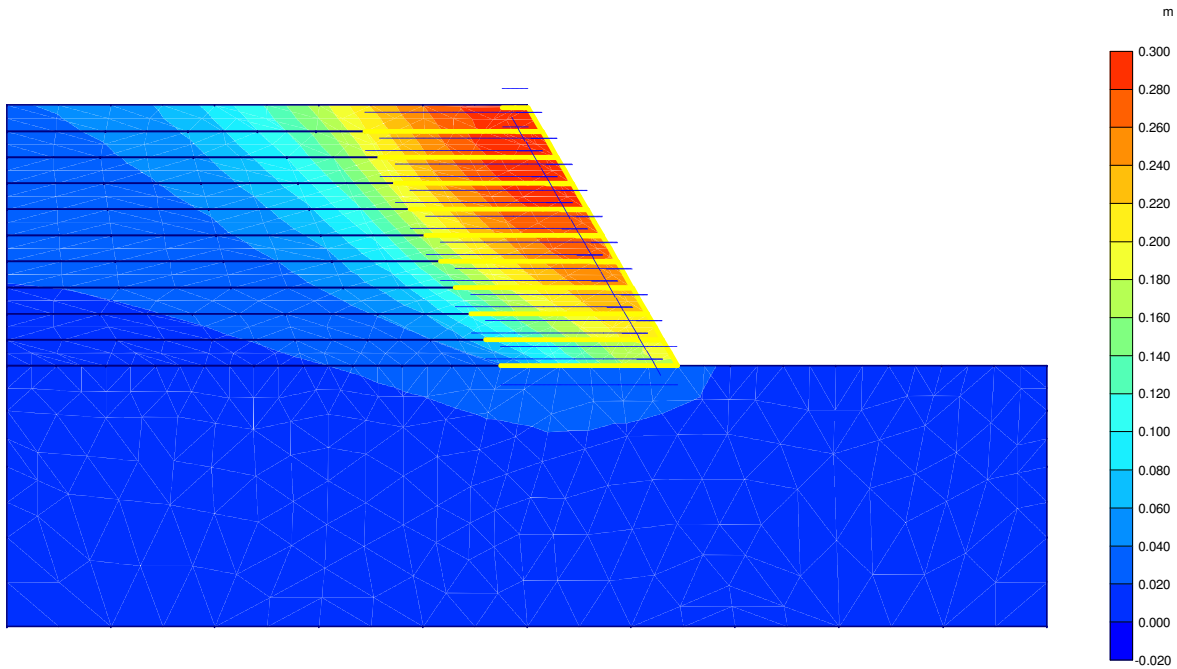

Figure A.13.1 Model L2 with Rock foundation

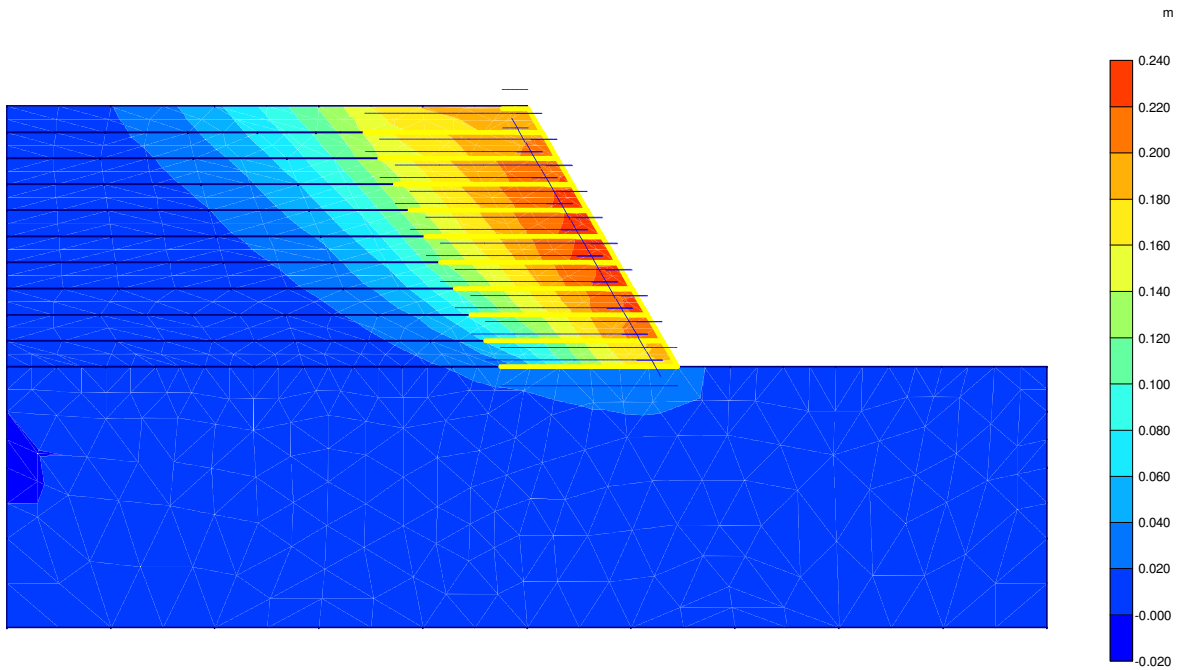

Figure A.13.2 Model L2 with Rock foundation

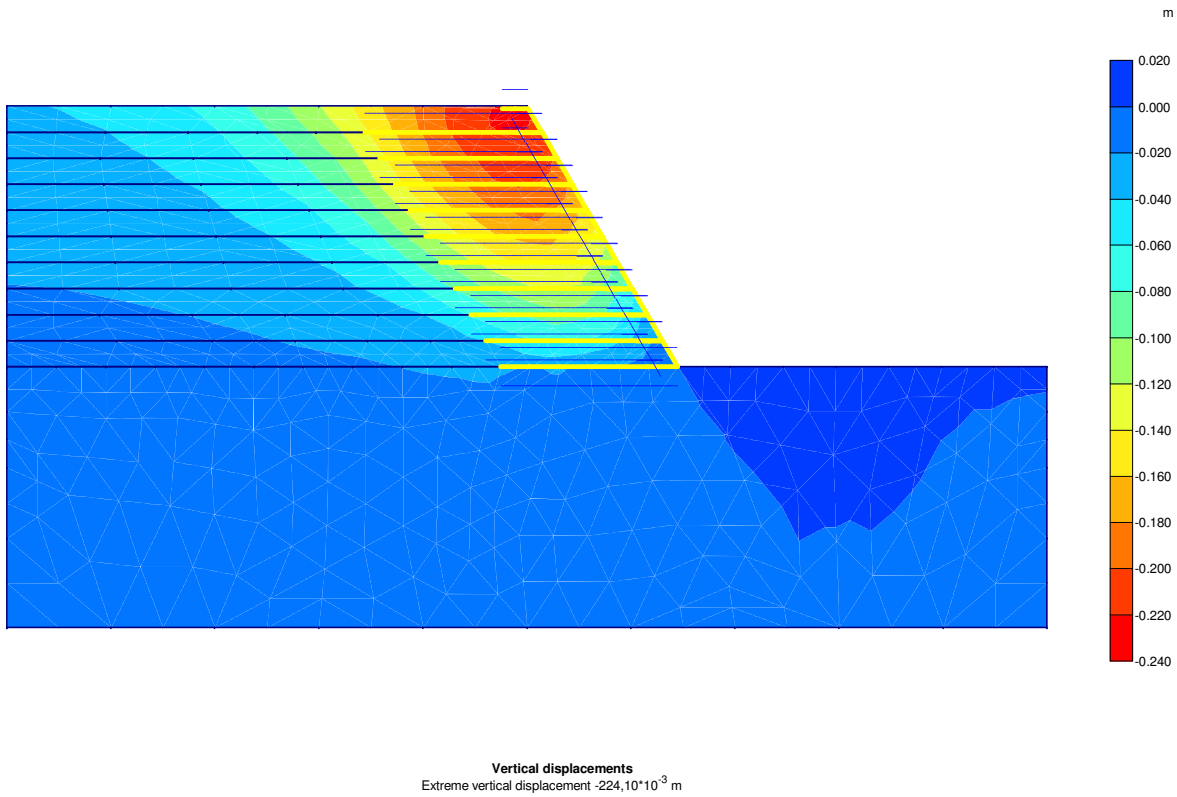

Figure A.13.3 Model L2 with Rock foundation

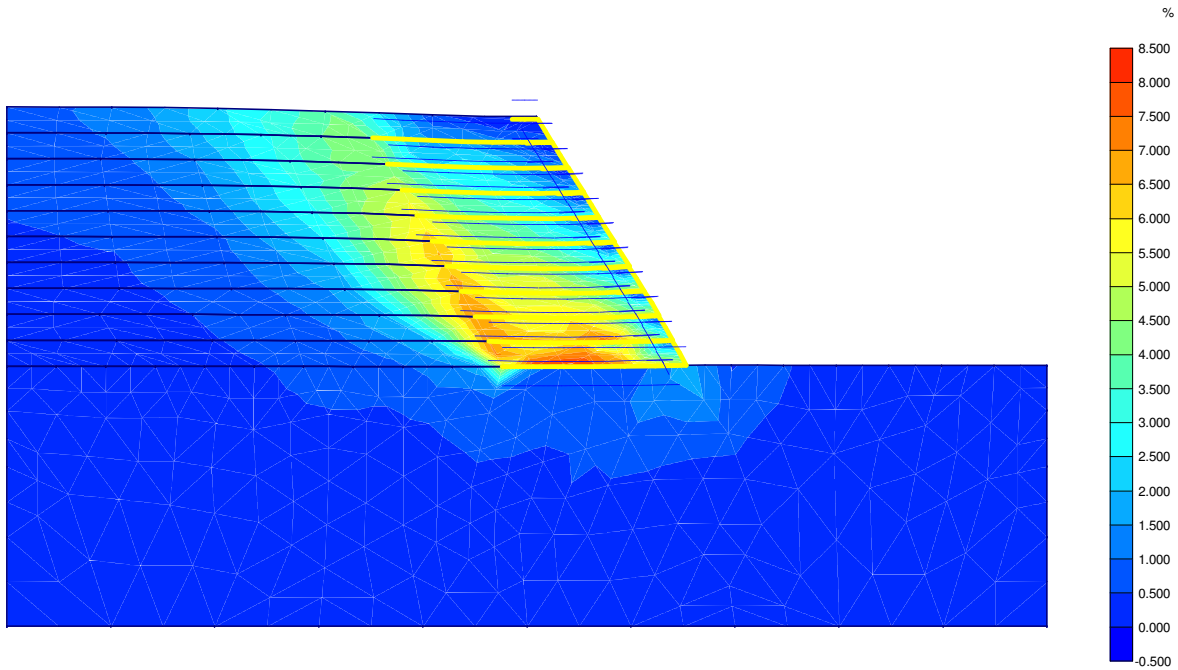

Figure A.13.4 Model L2 with Rock foundation

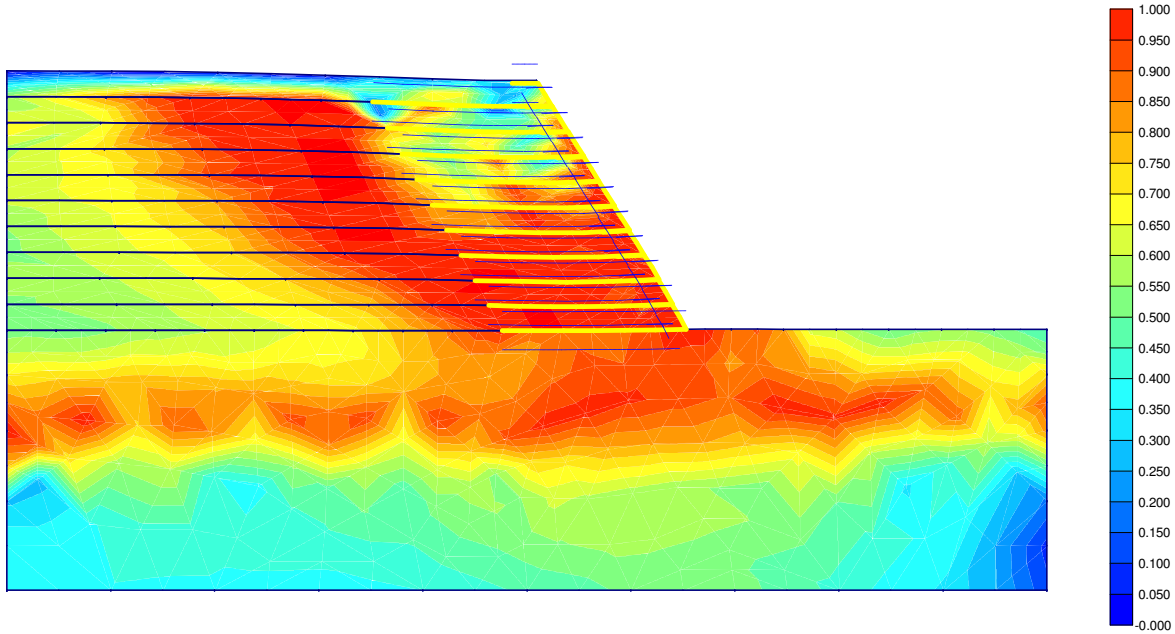

Figure A.13.5 Model L2 with Rock foundation

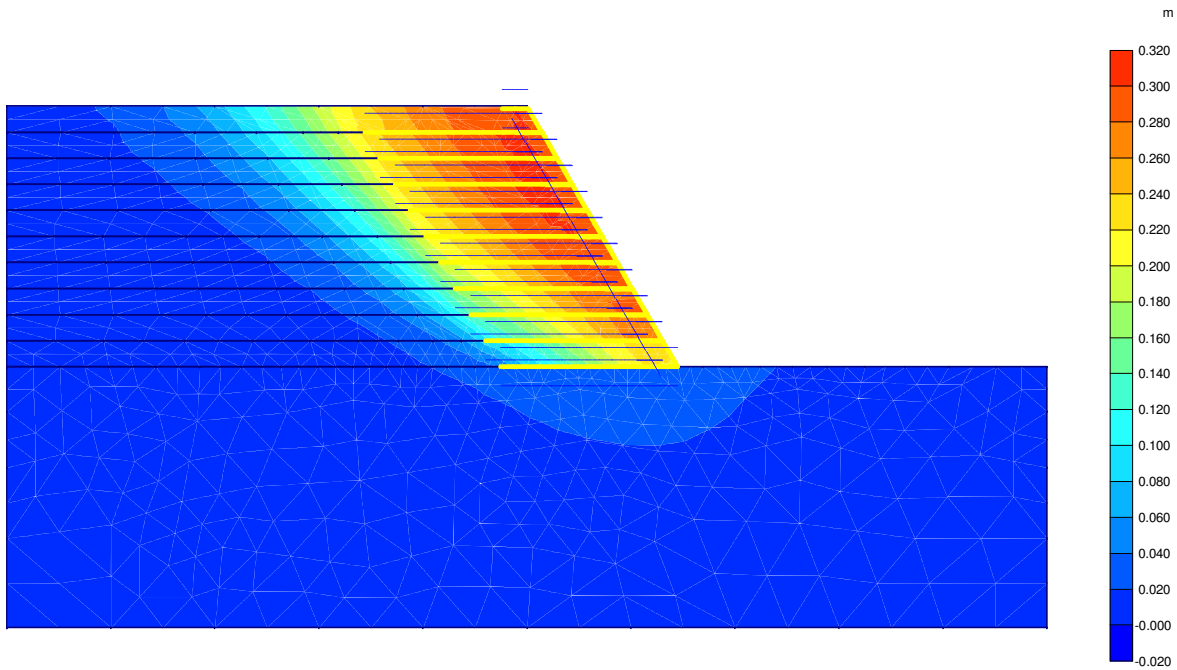

Figure A.14.1 Model L2 with Sand foundation

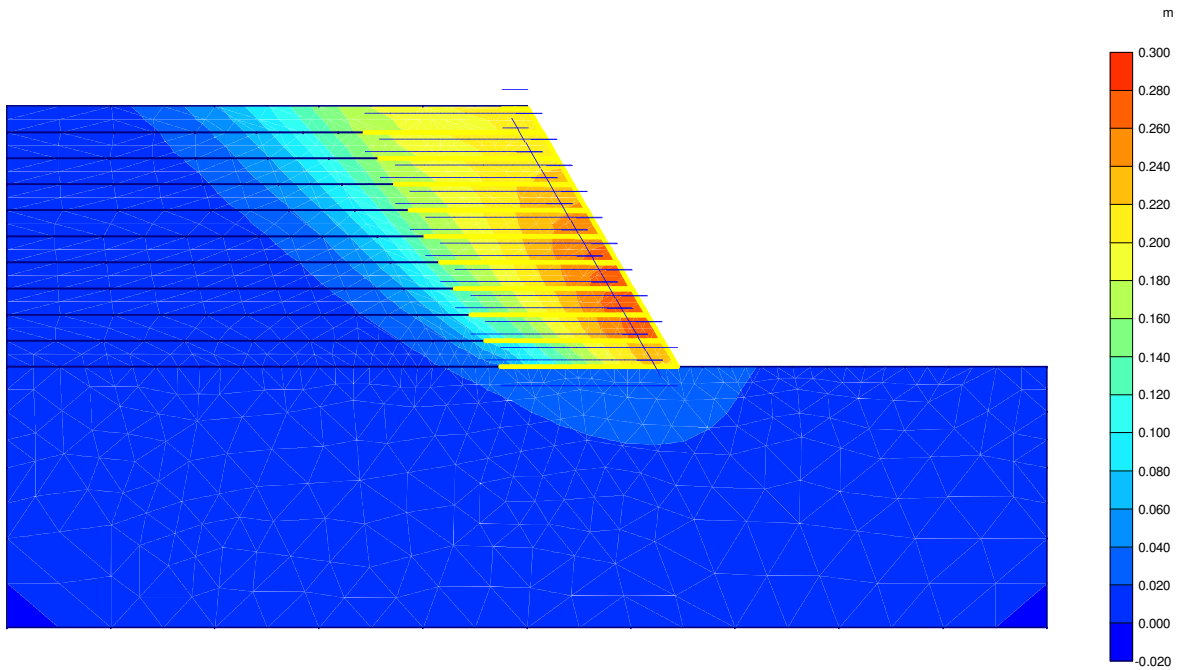

Figure A.14.2 Model L2 with Sand foundation

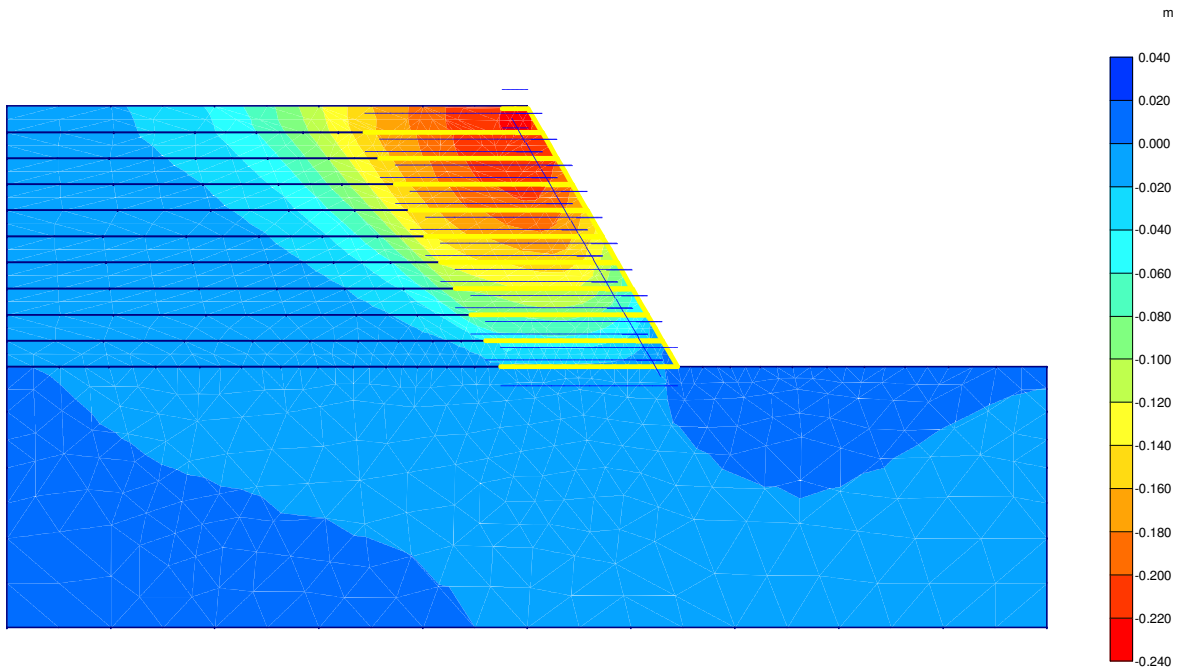

Figure A.14.3 Model L2 with Sand foundation

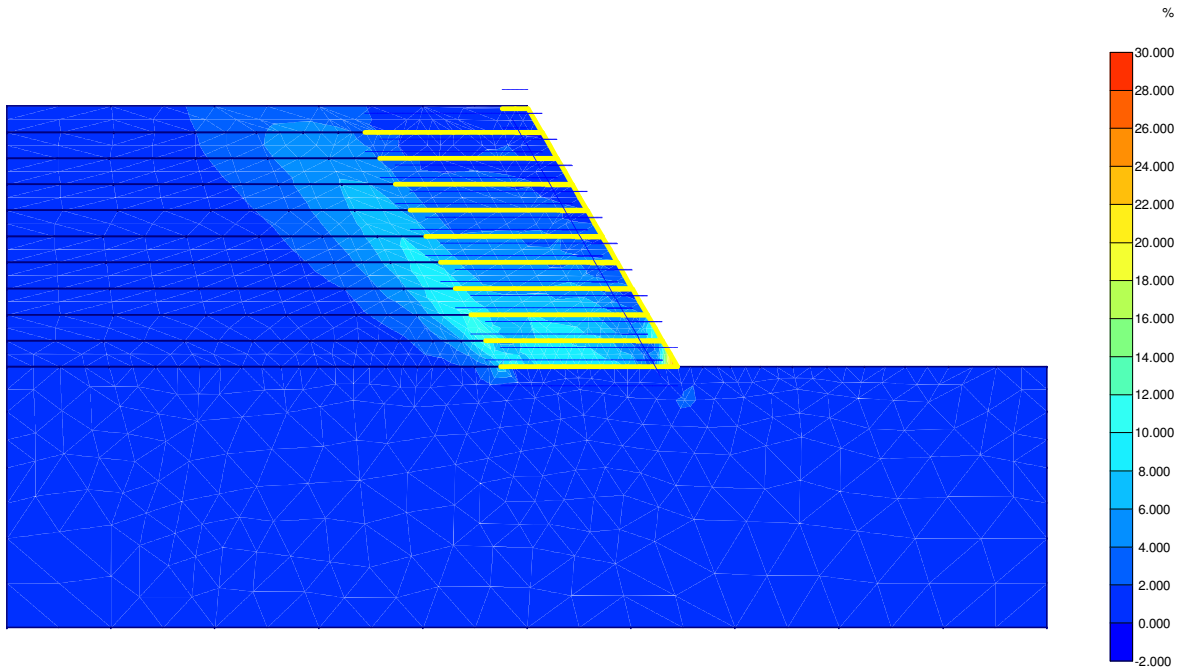

Figure A.14.4 Model L2 with Sand foundation

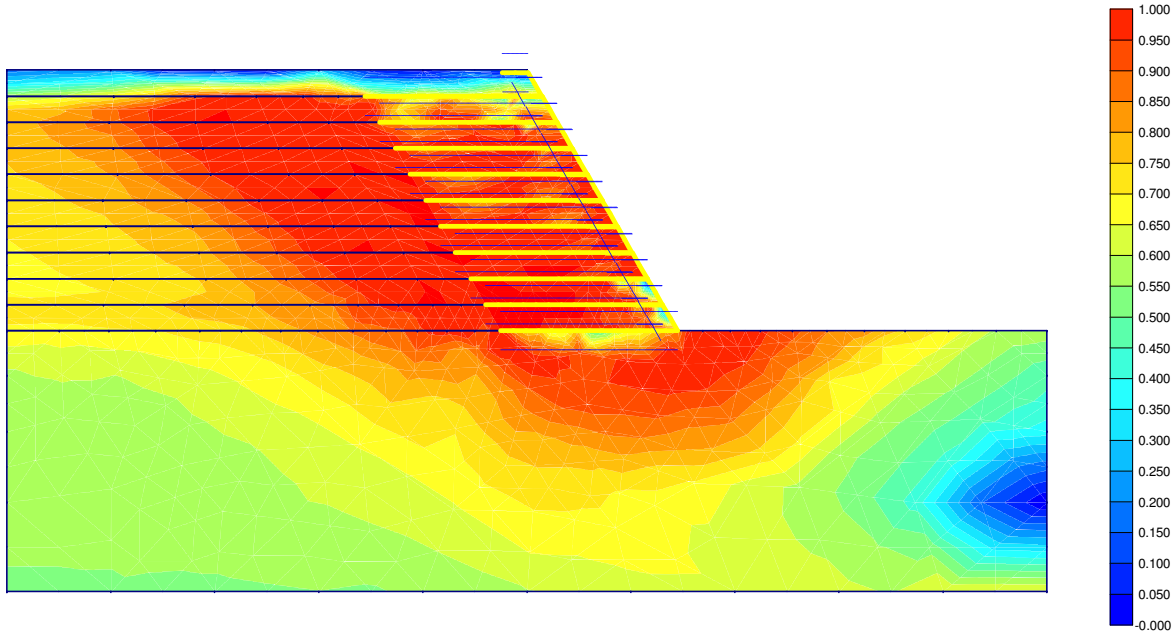

Figure A.14.5 Model L2 with Sand foundation

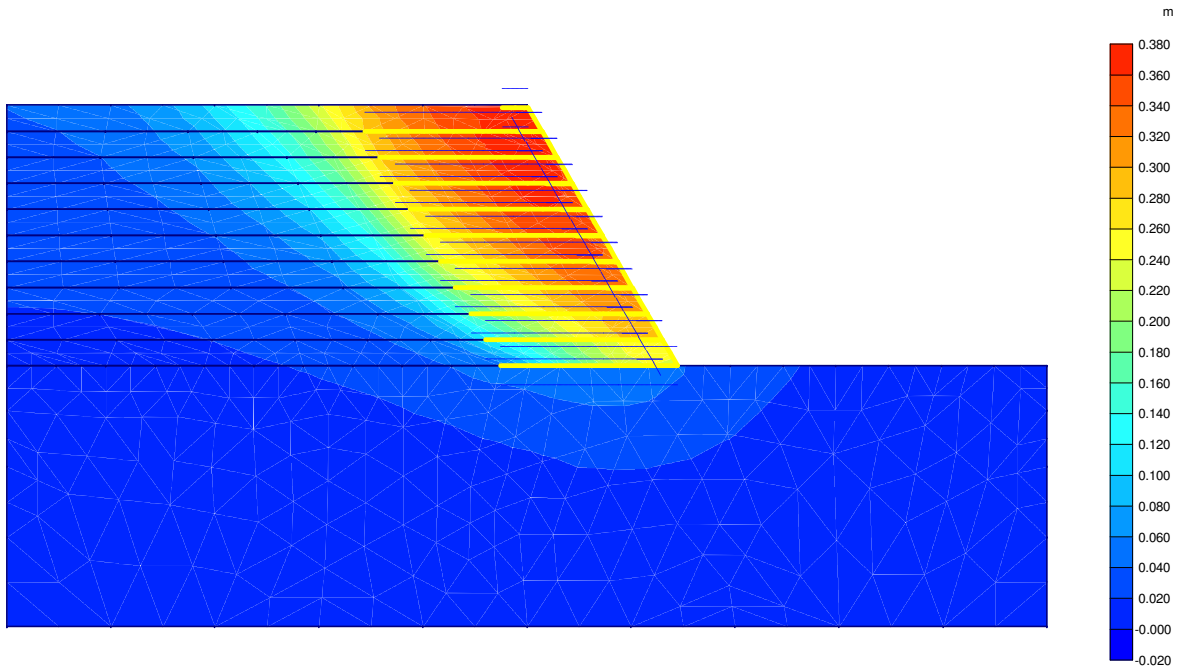

Figure A.15.1 Model L2 with Soft Clay foundation

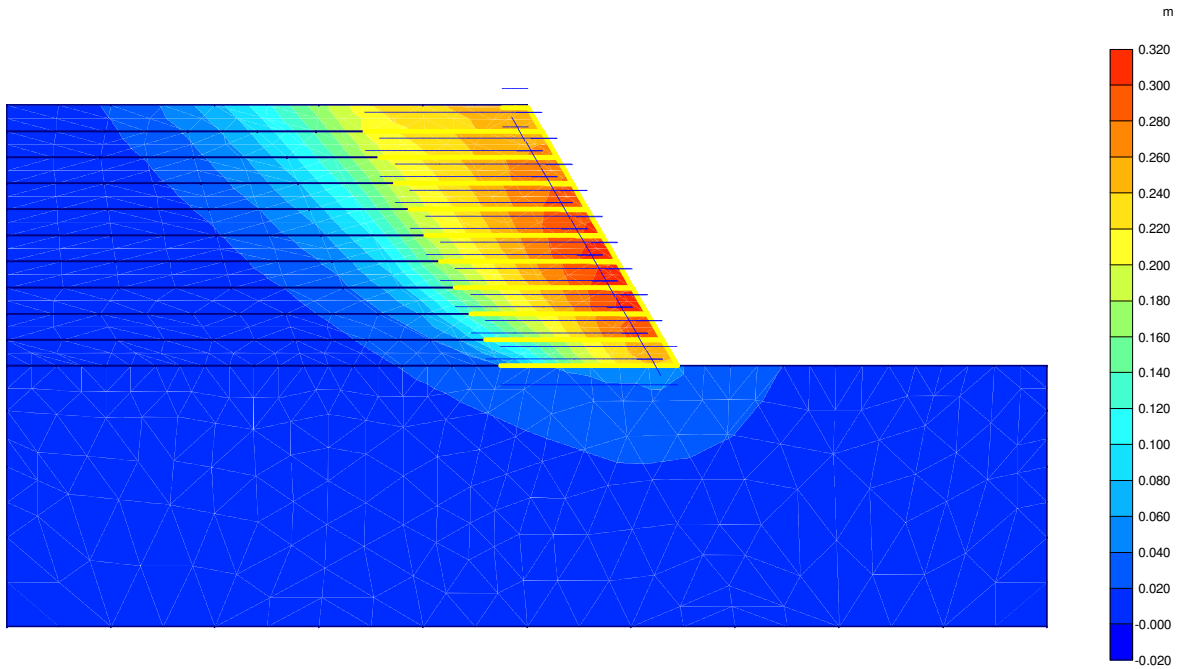

Figure A.15.2 Model L2 with Soft Clay foundation

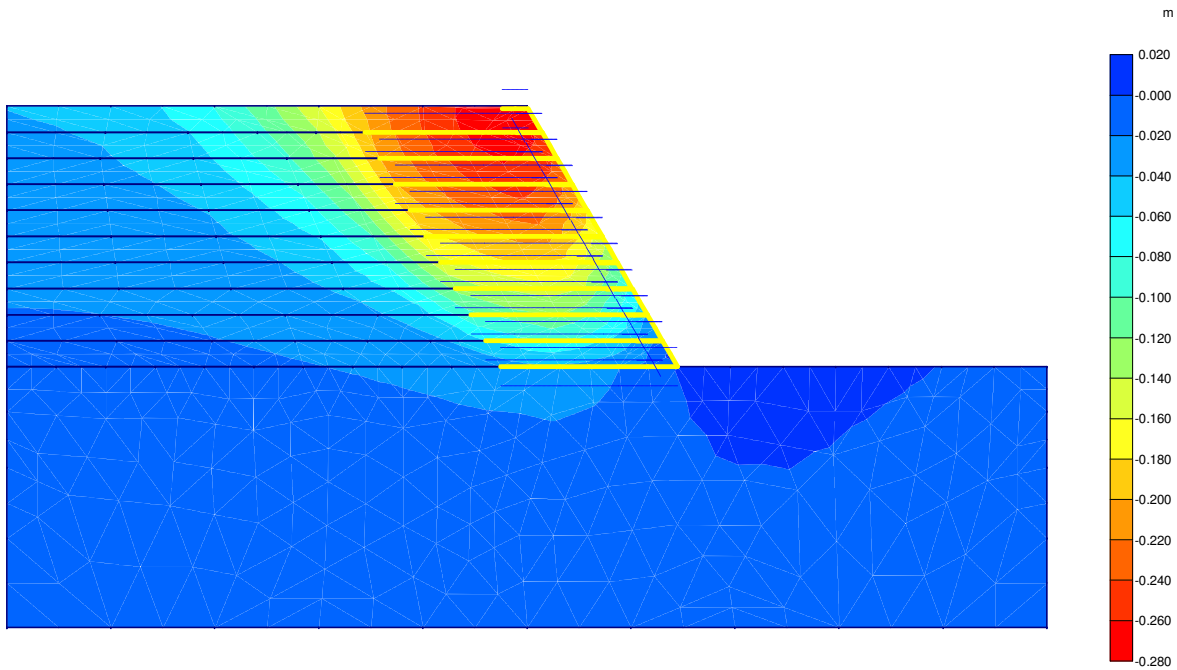

Figure A.15.3 Model L2 with Soft Clay foundation

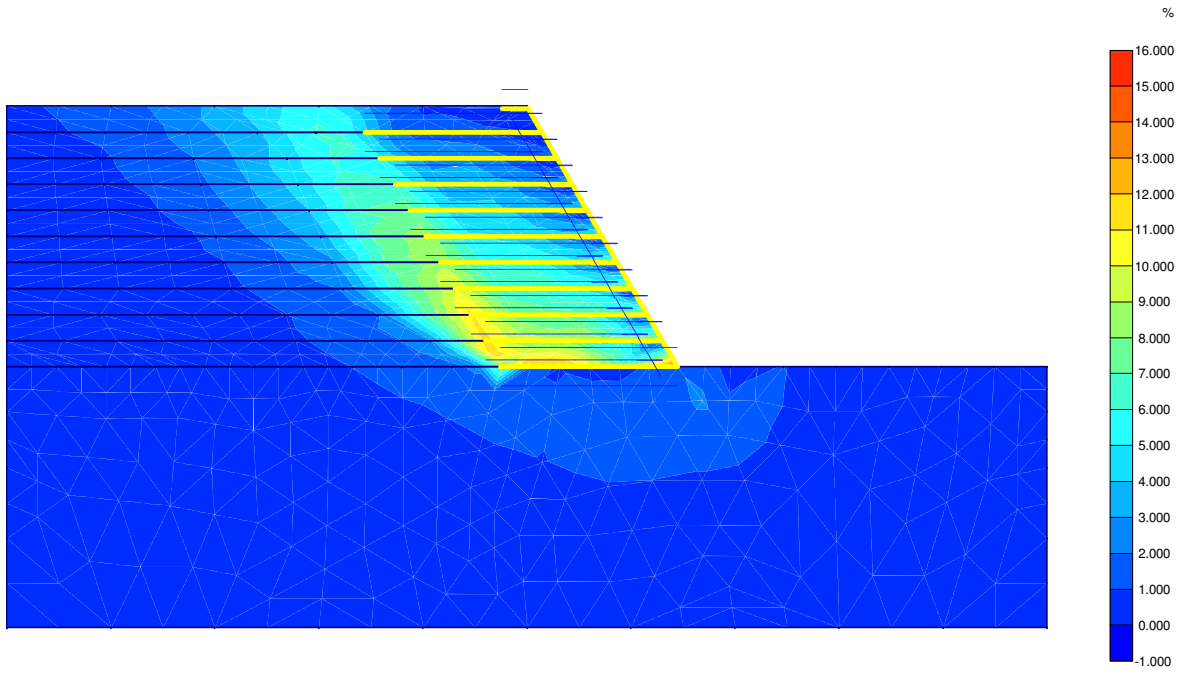

Figure A.15.4 Model L2 with Soft Clay foundation

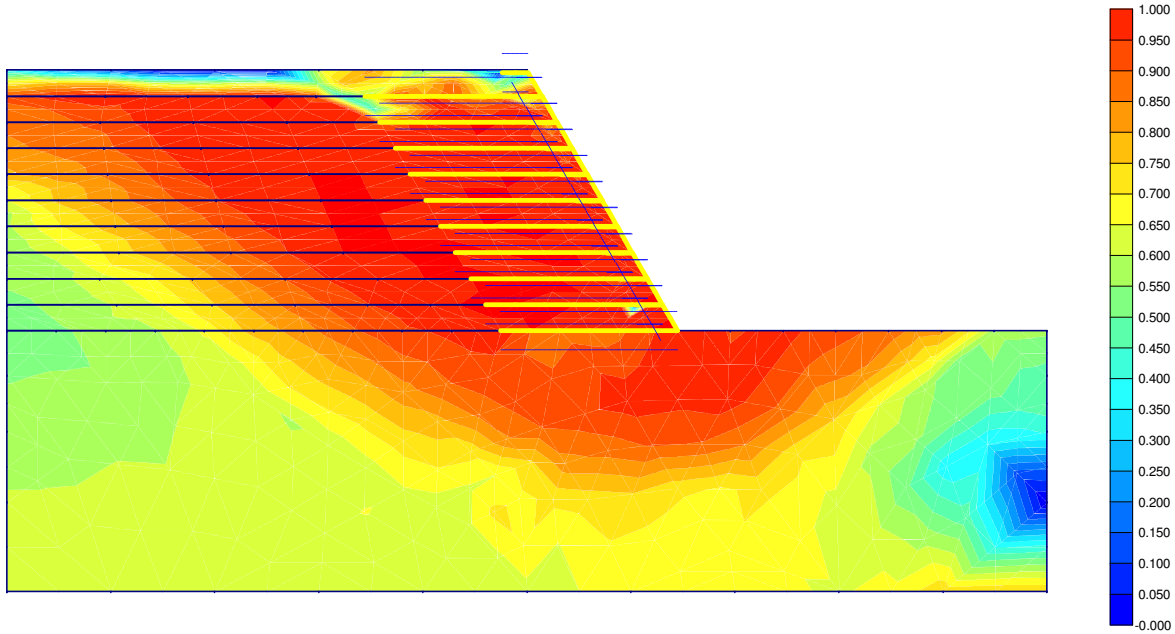

Figure A.15.5 Model L2 with Soft Clay foundation

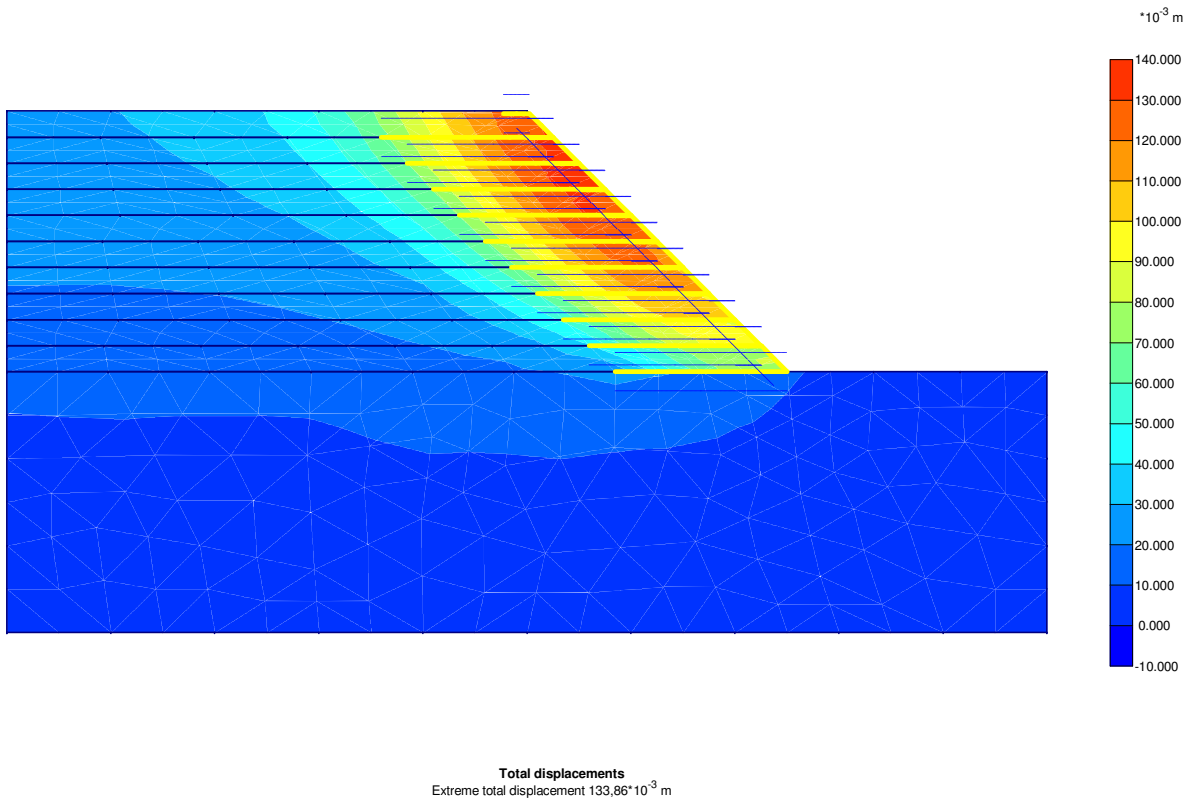

Figure A.16.1 Model L3 with Rock foundation

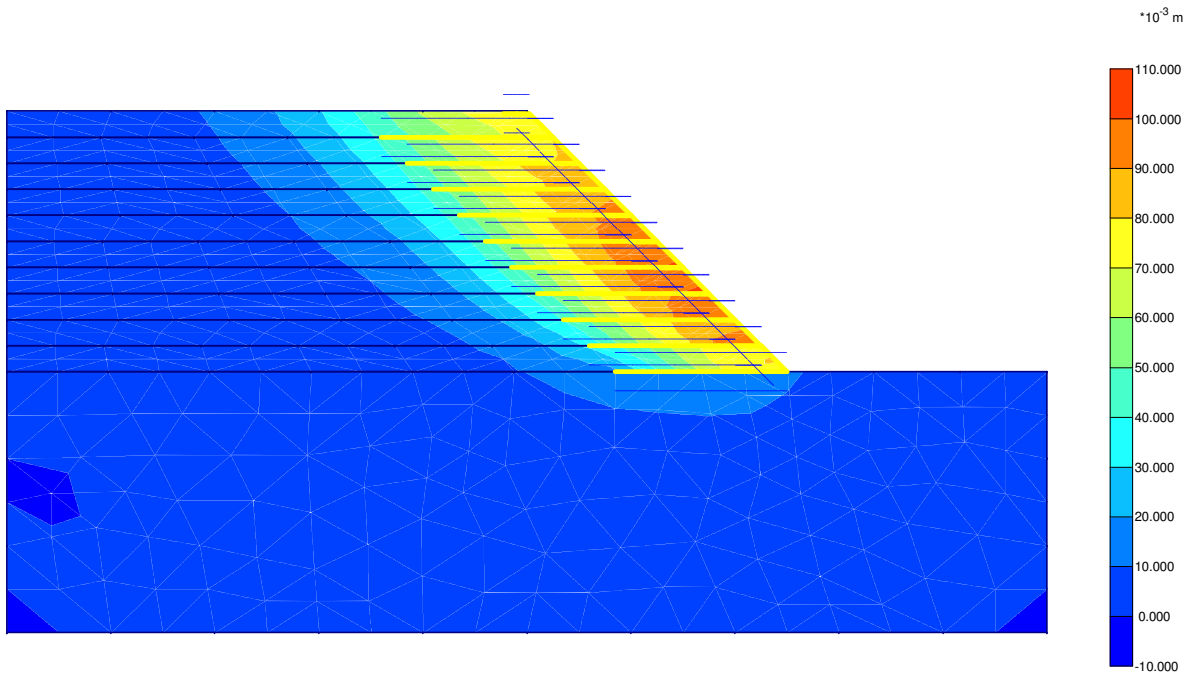

Figure A.16.2 Model L3 with Rock foundation

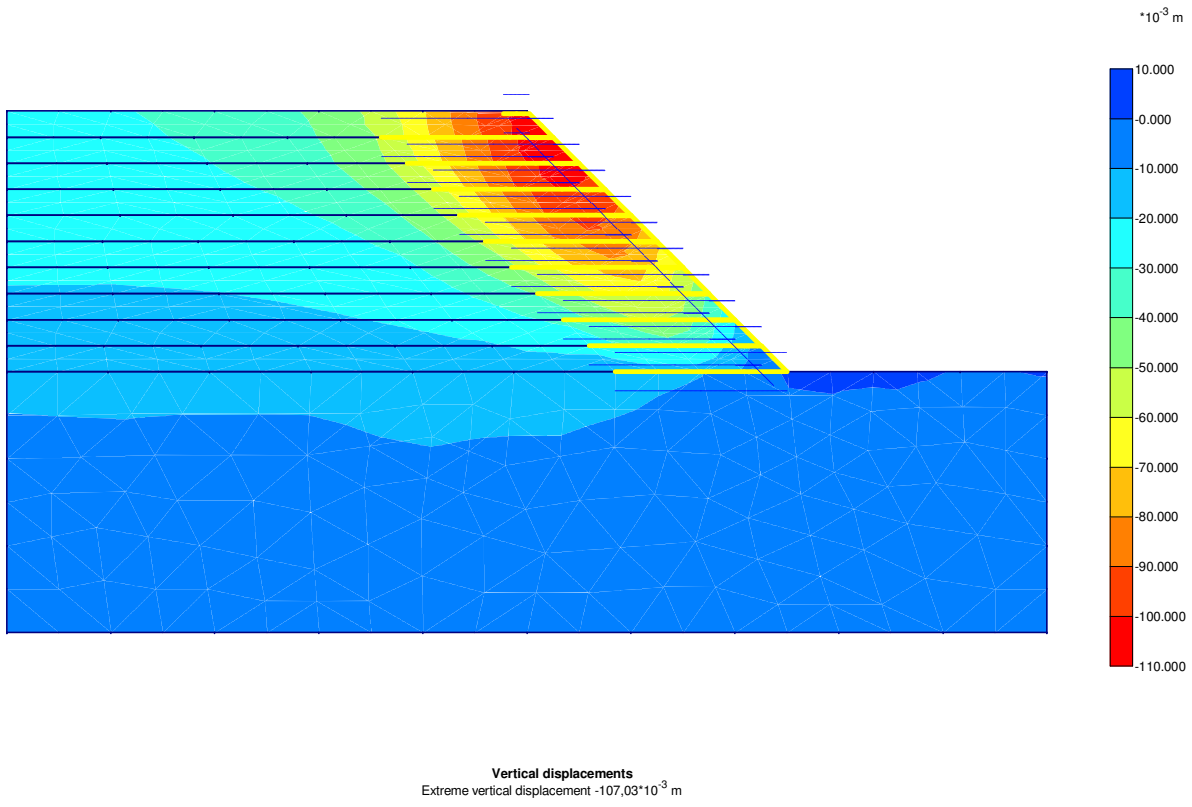

Figure A.16.3 Model L3 with Rock foundation

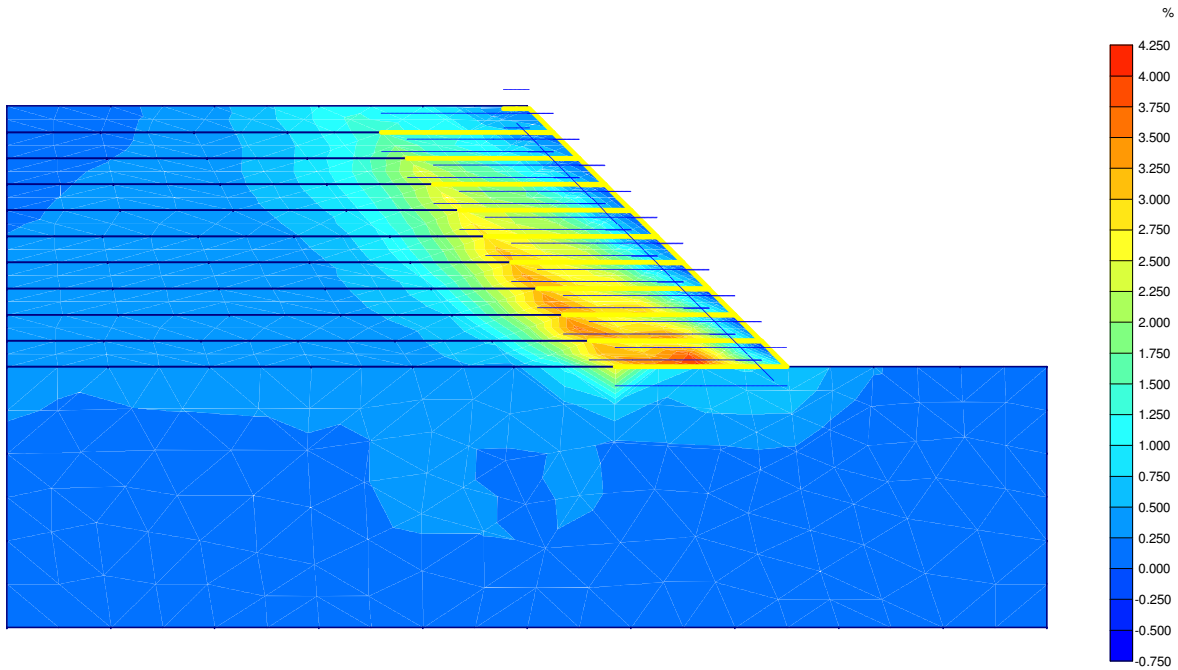

Figure A.16.4 Model L3 with Rock foundation

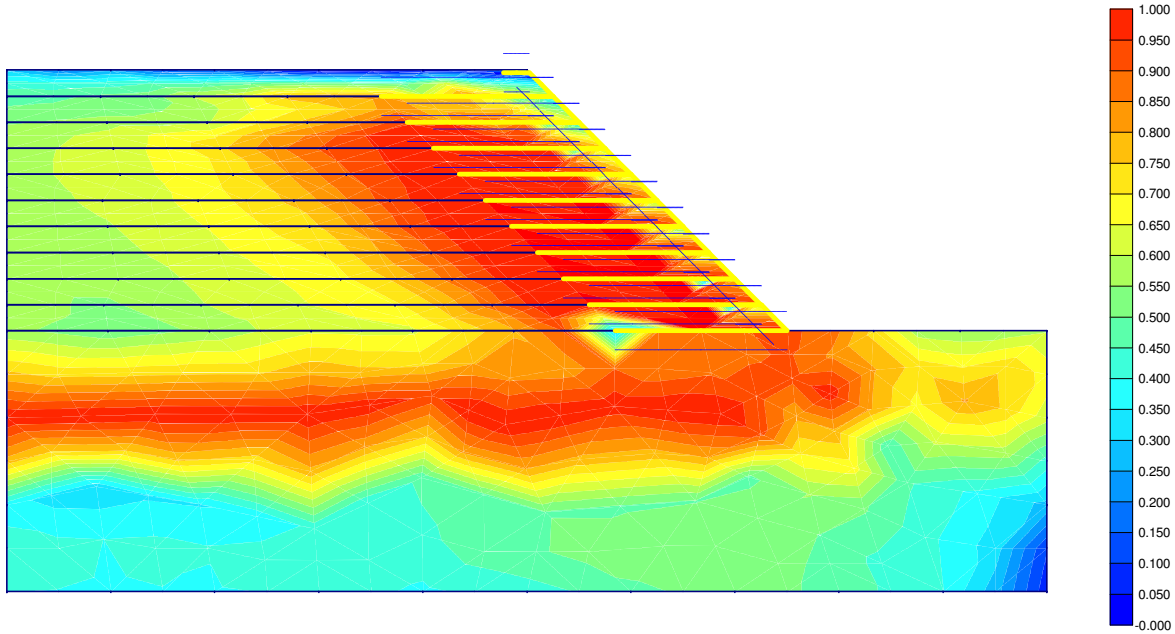

Figure A.16.5 Model L3 with Rock foundation

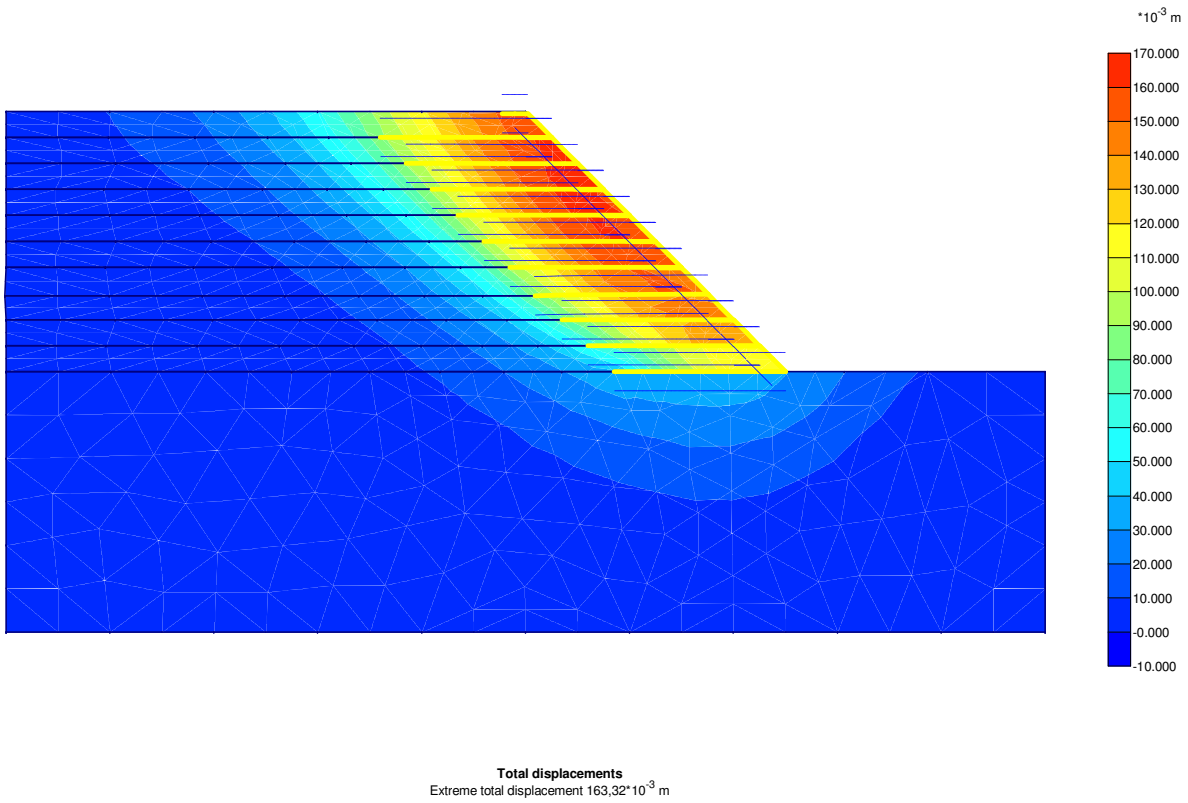

Figure A.17.1 Model L3 with Sand foundation

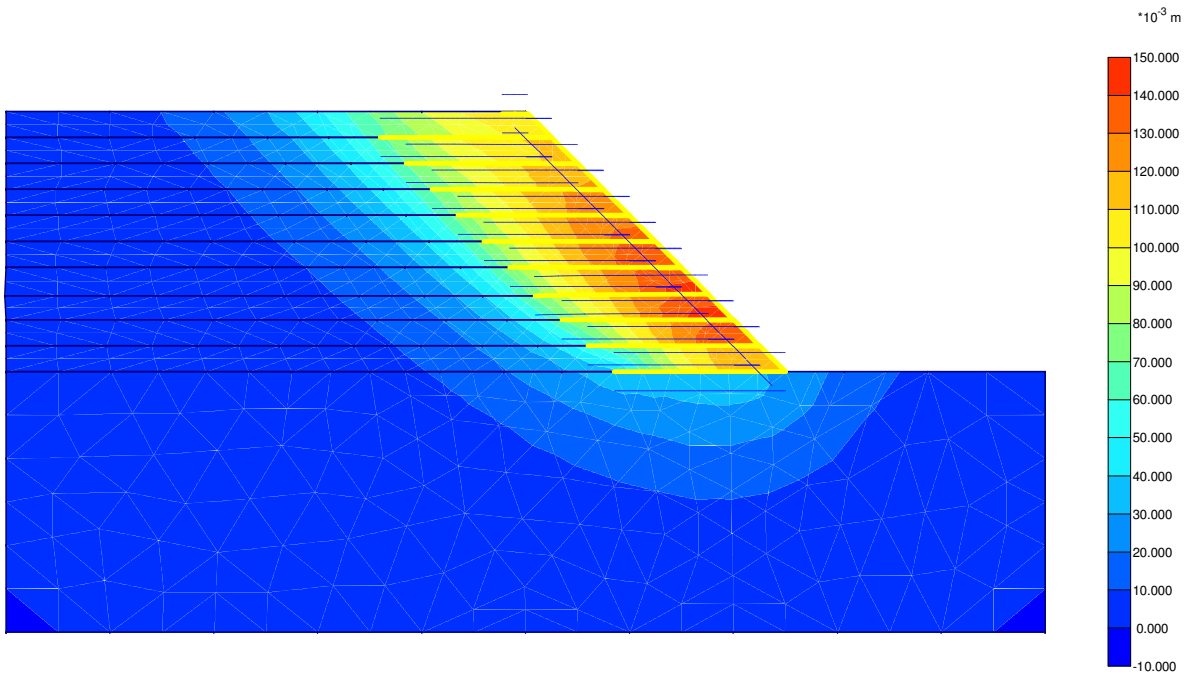

Figure A.17.2 Model L3 with Sand foundation

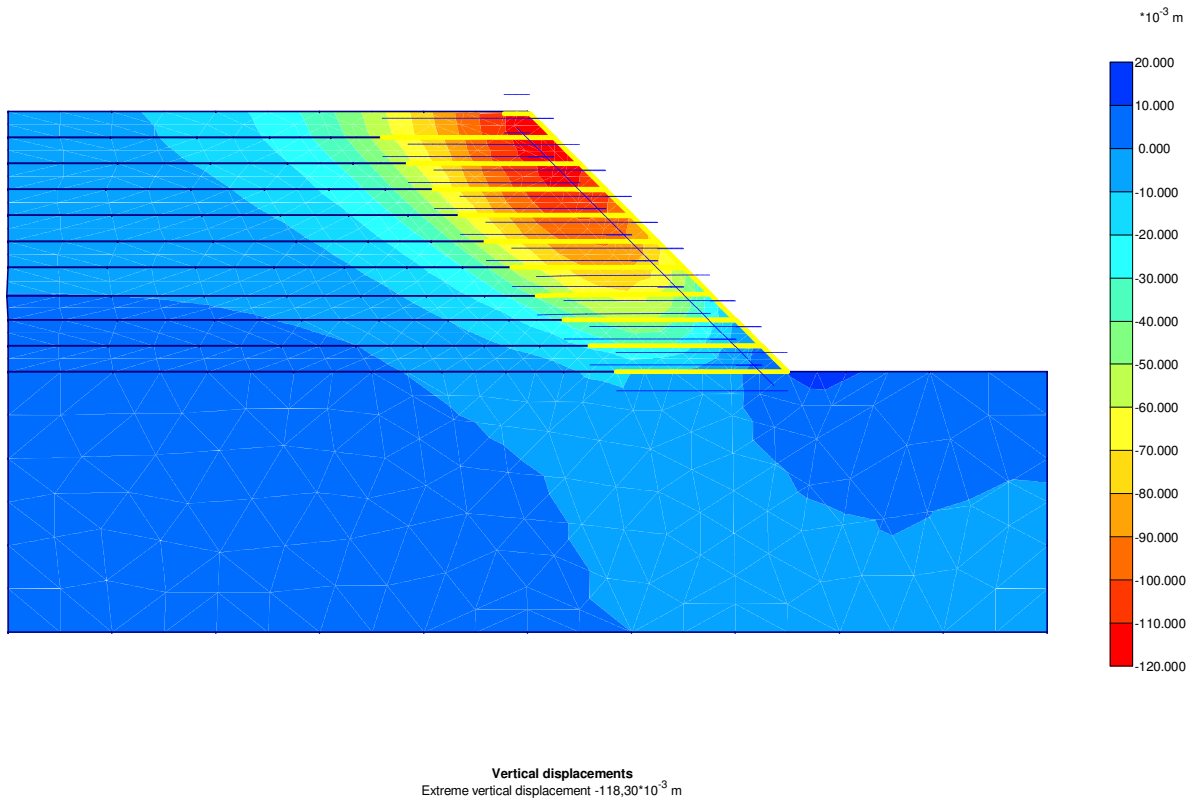

Figure A.17.3 Model L3 with Sand foundation

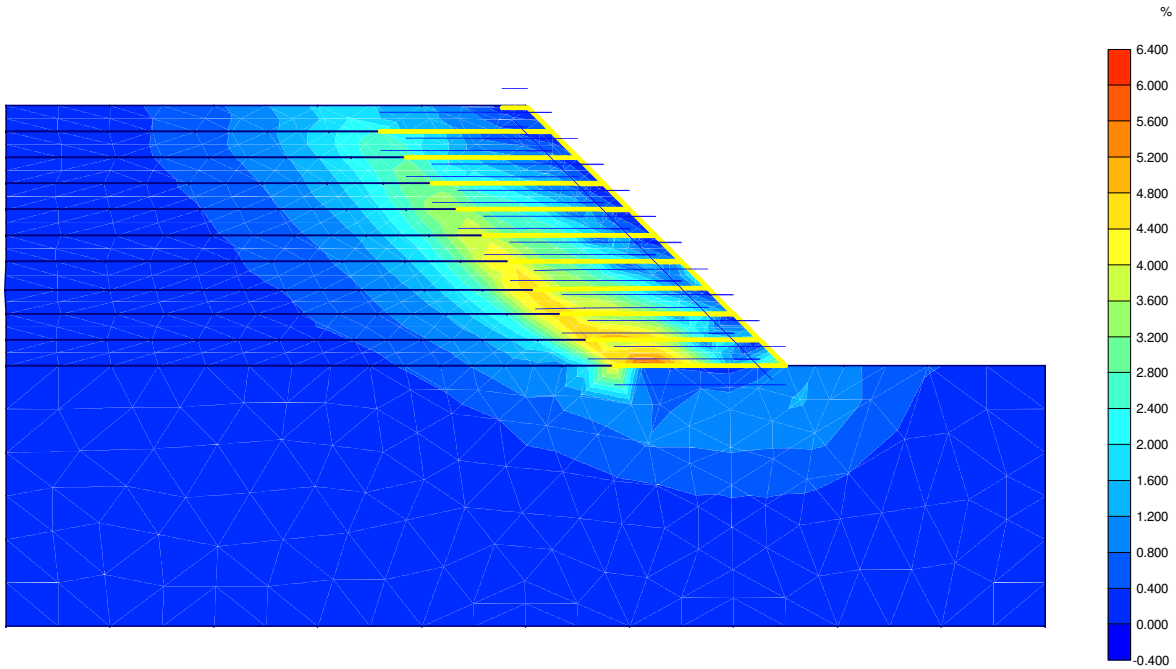

Figure A.17.4 Model L3 with Sand foundation

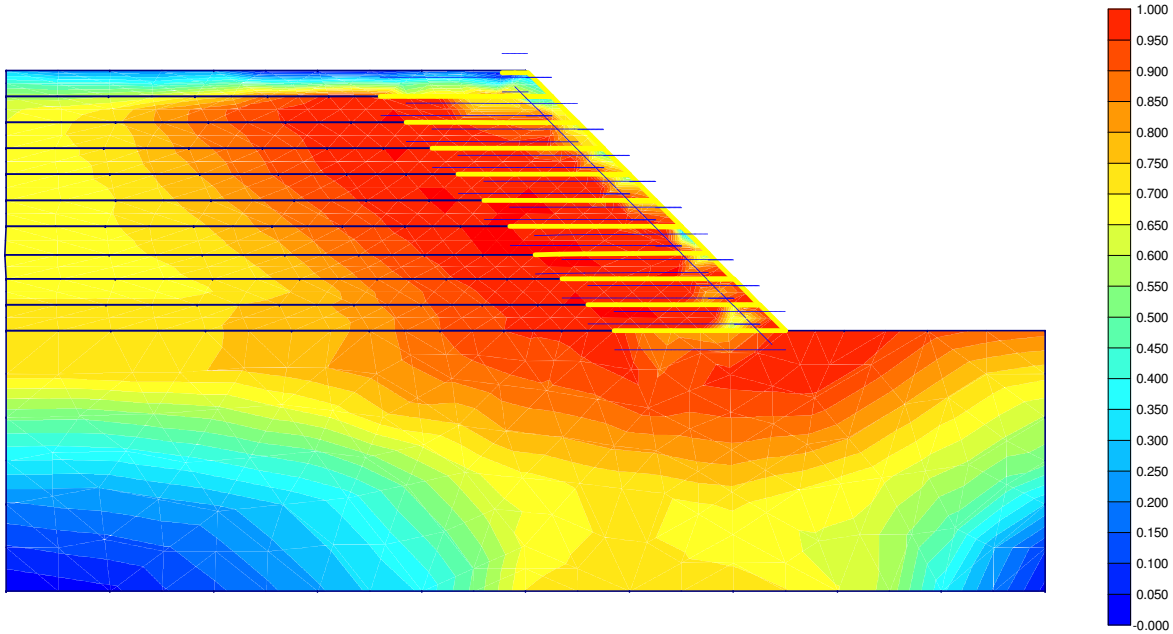

Figure A.17.5 Model L3 with Sand foundation

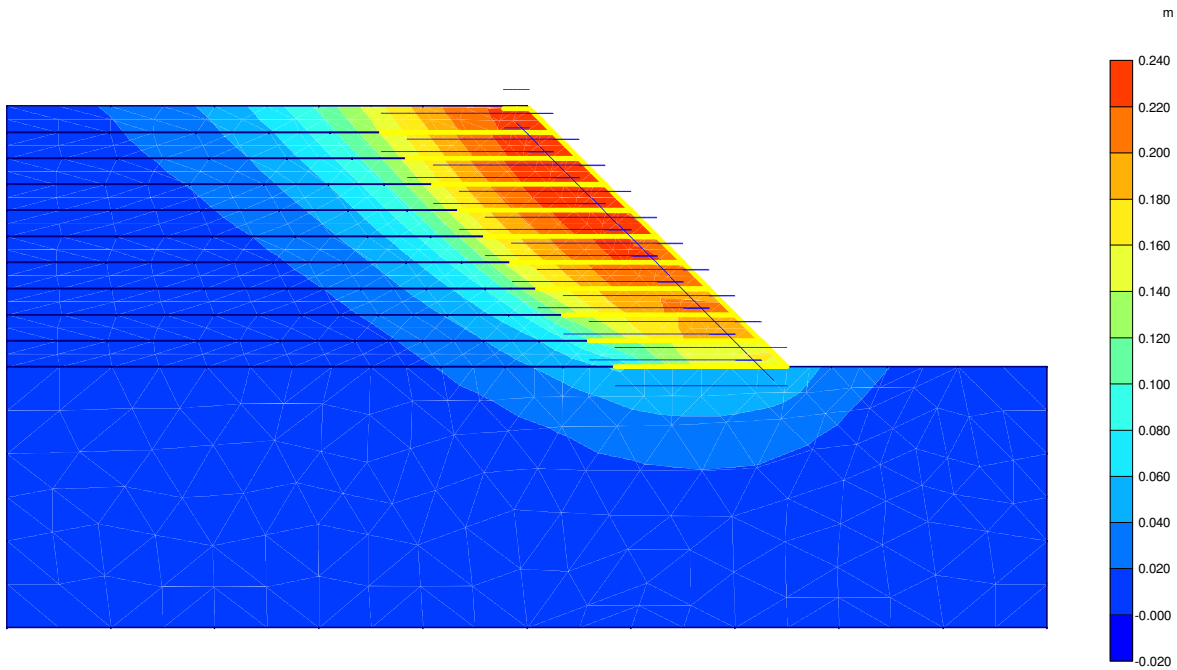

Figure A.18.1 Model L3 with Soft Clay foundation

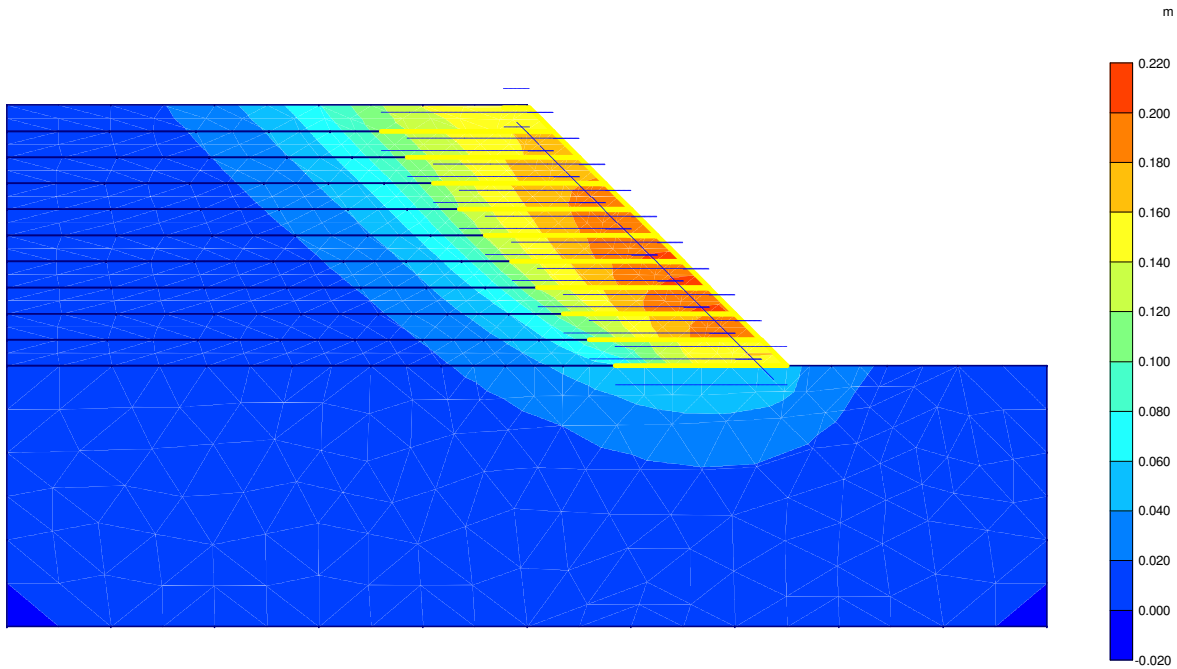

Figure A.18.2 Model L3 with Soft Clay foundation

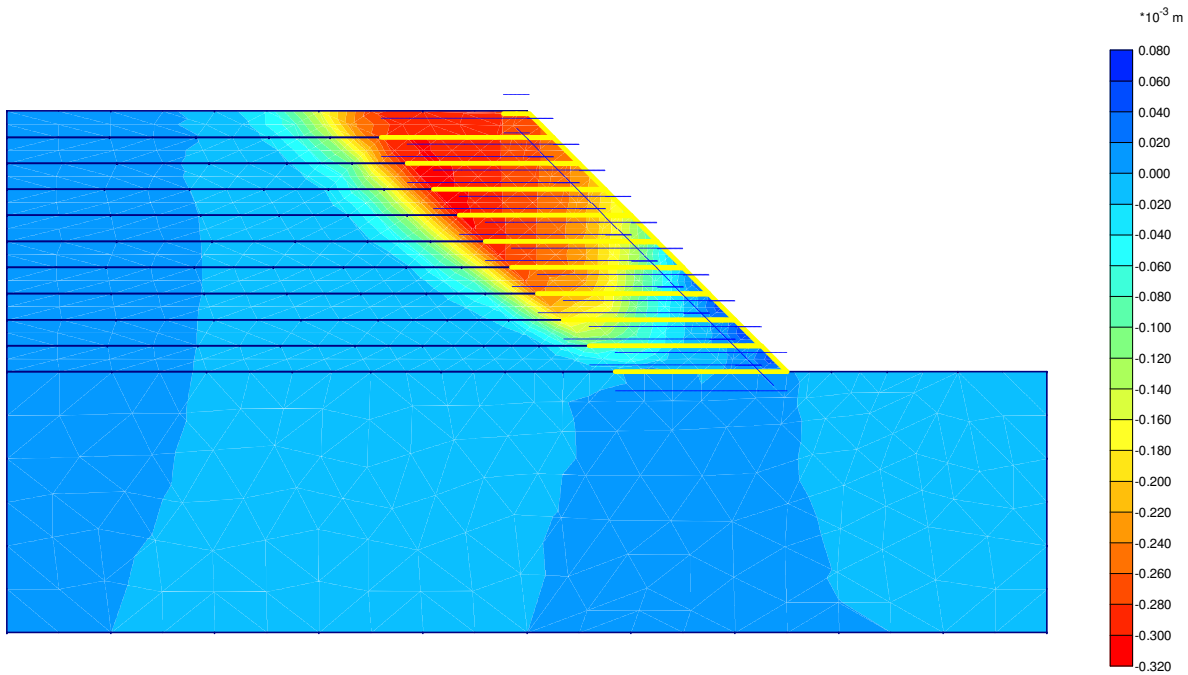

Figure A.18.3 Model L3 with Soft Clay foundation

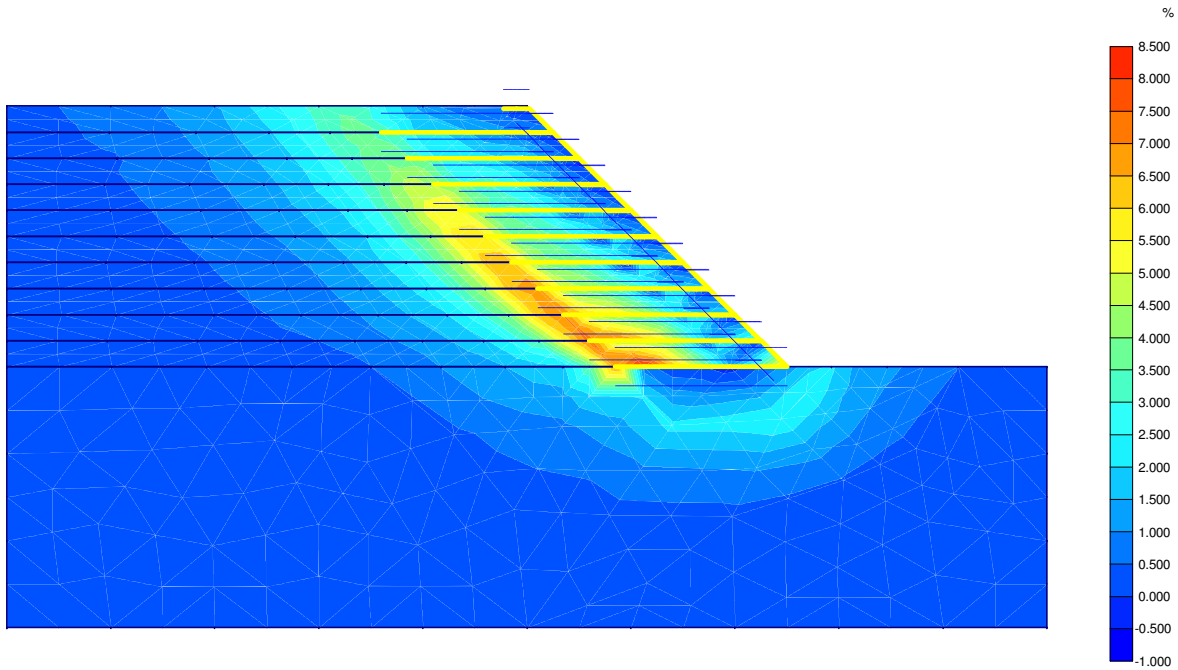

Figure A.18.4 Model L3 with Soft Clay foundation

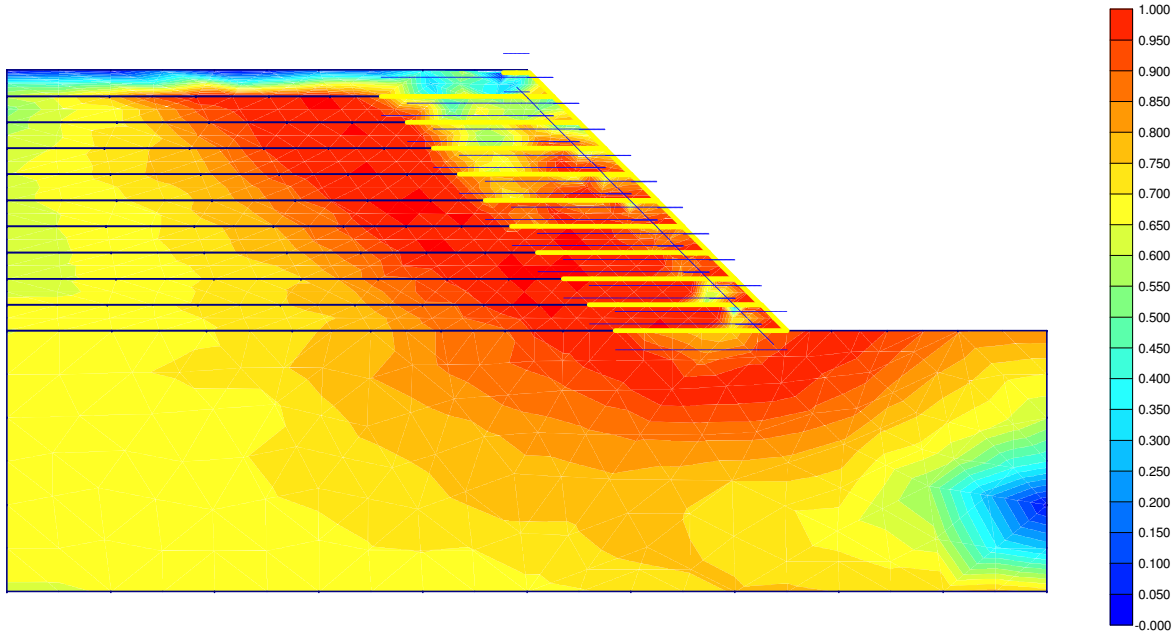

Figure A.18.5 Model L3 with Soft Clay foundation

REFERENCES

Alfaro, M.C., S. Hayashi, N. Miura and D.T. Bergado, 1997 "Soils and Foundation", *Deformation of Reinforced Soil-Wall–Embankment System On Soft Clay Foundation*, Vol. 37 (4), pp. 33-46.

Asaoka, A., T. Kodaka and G. Pokharel, 1994, "Soils and Foundations", *Stability Analysis of Reinforced Soil Structures Using Rigid Plastic Finite Element Method*, Vol. 34 (1), pp. 107-118.

Barret, B., A. Ruckman and G. Richardson, 1998, "Geotechnical Fabrics Report", Geotextile-Reinforced Retaining Walls Using Granular Backfills, March.

Cai, Z. and R.J. Bathurst, 1996, "Canadian Geotechnical Journal", Seismic-Induced Permanent Displacement of Geosynthetic- Reinforced Segmental Retaining Walls, Vol. 33, pp. 937-955.

Chai, J. and D.T. Bergado, 1993, "Soils and Foundation", *Performance of Reinforced Embankment on Muar Clay Deposit*, Vol. 33(4), pp. 1-17.

Genske, D.D., T. Adachi and M. Sugito, 1991, "Soils and Foundation", *Reliability Analysis of Reinforced Earth Retaining Structures Subjected to Earthquake Loading*, Vol. 31(4), pp. 48-60.

Gurung, N. and Y. Iwao, 1999, "Canadian Geotechnical Journal", *Numerical Solution of Pullout Response for Planar Soil Reinforcements*, Vol. 36, pp. 455-466.

Indraratna, B., A.S. Balasubramaniam and S. Balachandran, 1992, "Journal of Geotechnical Engineering", *Performance of Test Embankment Constructed To Failure On Soft Marine Clay*, Vol. 118(1), pp. 12-33.

John, N.W.M., 1986, "Geotextile Reinforced Soil Walls in a Tidal Environment", *Third International Conference On Geotextiles*, pp. 331-336, Vienna.

Juran, I. and B. Christopher, 1989, "Journal of Geotechnical Engineering", *Reinforced Soil Retaining Walls*, Vol. 115(7), pp. 905-925.

Koerner, R.M., 1986, "Designing With Geosynthetics", Prentice-Hall: Eaglewood Cliffs, N.J.

Leschinsky, D., 2000, "Journal of Geotechnical and Geoenvironmental Engineering ", *Discussion: Performance of Geosynthetic Reinforced Slopes at Failure*, pp. 281-283, March.

Ling, H.I., D. Leschinsky and E.B. Perry, 1997, "Geotechnique", *Seismic Design and Performance of Geosynthetic- Reinforced Soil Structures*, Vol. 47(5), pp. 933-952.

Ling, H.I. and D. Leschinsky, 1998, "Geotechnique", *Effects of Acceleration on Seismic Design of Geosynthetic Reinforced Soil Structures*, Vol. 48(3), pp. 347-373.

Low, B.K. and H.T. Wilson, 1997, "Canadian Geotechnical Journal", *Reliability Analysis of Reinforced Embankments on Soft Ground*, Vol. 34, pp. 672-685.

Plaxis 7.12, 2000, Finite Element Code for Soil Rock Analyses, User Manual.

Porbaha, A., 1998, "Soils and Foundation", *Traces of Slip Surfaces In Reinforced Retaining Structures*, Vol. 38(1), pp. 89-95.

Porbaha, A. and D.J. Goodings, 1996, "Journal of Geotechnical and Geoenvironmental Engineering", *Centrifuge Modeling of Geotextile Reinforced Cohesive Soil Retaining Walls*, Vol. 122(10), pp. 840-848.

Porbaha, A. and D.J. Goodings, 1996, "Canadian Geotechnical Journal", *Centrifuge Modeling of Geotextile- Reinforced Steep Clay Slopes*, Vol. 33, pp. 696-704.

Radaslow, L. and R.L. Michalowski, 1997, "Journal of Geotechnical and Geoenvironmental Engineering", *Stability of Uniformly Reinforced Slopes*, Vol. 123(6), pp. 546-556.

Radaslow, L. and R.L. Michalowski, 1997, "Journal of Geotechnical and Geoenvironmental Engineering", *Displacements of Reinforced Slopes Subjected to Seismic Loads*, Vol. 126(8), pp. 685-694.

Reinforced Earth Company Cataloque, 1986.

Robert, L.S. and X. Dai-Wer, 1992, "Soils and Foundation", *Short Term Stability of Reinforced Embankment on Soft Clay: Modeling of Strain Softening and Reinforcement Extensibility*, Vol. 32 (1), pp. 189-204.

Roessing, L.N. and N. Sitar, (1998), "Third Geotechnical Engineering and Soil Dynamics Conference, Geotechnical Special Publication" *Centrifuge Studies of the Seismic Response of Reinforced Soil Slopes*, Vol. 75, pp. 458-468, ASCE.

Rowe, R.K., and B.L.J. Mylleeville, 1996, "Canadian Geotechnical Journal", *A Geogrid Reinforced Embankment On Peat Over Organic Silt: A Case History*, Vol. 33, pp. 106-122.

Rowe, RK., C.T. Gnanendran, A.O. Landva and A.J. Valsangkar, 1995, "Canadian Geotechnical Journal", *Construction and Performance Of A Full-Scale Geotextile Reinforced Test Embankment*, Vol. 32, pp. 512-534.

San, K.C., D. Leshchinsky and T. Matsui, 1994, "Soils and Foundation", *Geosynthetic Reinforced Slopes: Limit Equilibrium and Finite Element Analyses*, Vol. 34 (2), pp. 79-85.

Springman, S.M., S. Balachandran and C. Jommi, 1997, "Geotechnique", *Modeling Pre-Failure Deformation Behavior of Reinforced Soil Walls*, Vol. 47(3), pp. 653-663.

Zornberg, J.G., N. Sitar and J.K. Mitchell, 1998, "Journal of Geotechnical and Geoenvironmental Engineering", *Limit Equilibrium As Basis for Design of Geosynthetic Reinforced Slopes*, Vol. 124(8), pp. 674-698.

Zornberg, J.G., N. Sitar and J.K. Mitchell, 1998, "Journal of Geotechnical and Geoenviromental Engineering", *Performance of Geosynthetic Reinforced Slopes At Failure*, Vol. 124(8), pp. 670-683.